BMR Bulletin

195

Marine geology of the continental shelf off southeast Australia

P. J. Davies

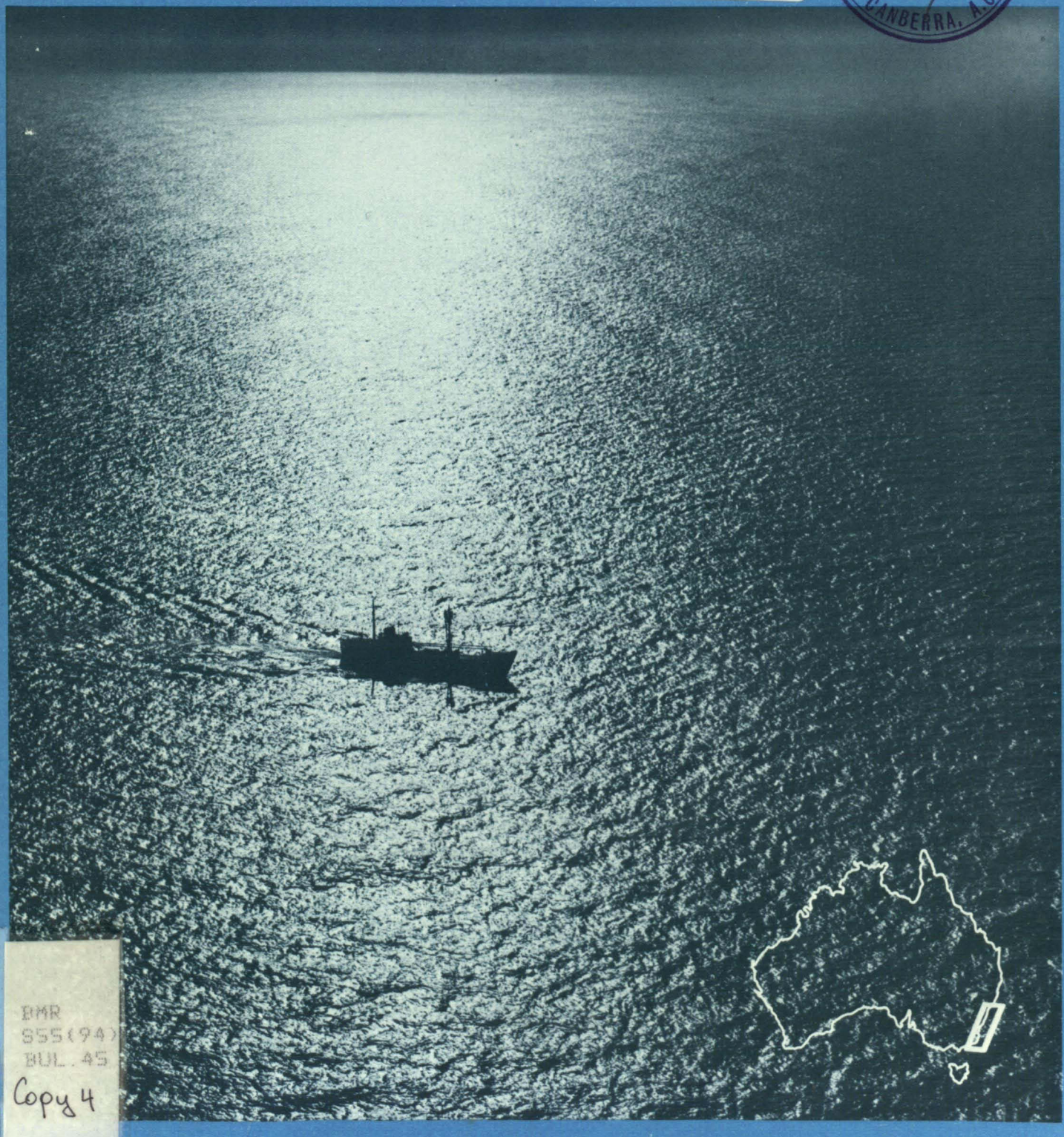

DEPARTMENT OF NATIONAL RESOURCES
BUREAU OF MINERAL RESOURCES, GEOLOGY AND GEOPHYSICS

BULLETIN 195

Marine geology of the continental shelf off southeast Australia

P. J. DAVIES

AUSTRALIAN GOVERNMENT PUBLISHING SERVICE
CANBERRA 1979

DEPARTMENT OF NATIONAL DEVELOPMENT

MINISTER: THE HON. K. E. NEWMAN, M.P.

SECRETARY: A. J. WOODS

BUREAU OF MINERAL RESOURCES, GEOLOGY AND GEOPHYSICS

DIRECTOR: L. C. NOAKES, O.B.E.

ASSISTANT DIRECTOR, GEOLOGICAL BRANCH: J. N. CASEY

ABSTRACT

Over much of the continental shelf of southeast Australia, three distinct morphological zones correspond with three distinct sedimentary zones. Over much of the outer shelf, morphology is basement controlled. Three groups of terrace features occur at depths less than 60 m, between 60 and 120 m, and greater than 120 m. The shelf break varies in depth from 130 to 170 m. A sediment wedge, thickening eastwards, occurs on the mid to inner shelf, and has likely developed as a result of shelf tilting since the Late Cretaceous. The thickest sediment sequence occurs south of Jervis Bay, where the shelf is narrowest. Surface sediments show a dominance of quartz sand on the inner shelf, muds on the mid-shelf, and carbonate sands and gravels on the outer shelf. Present-day sedimentation is limited to the zone 0-15 m. Stable heavy-mineral assemblages mantle the inner shelf, while unstable assemblages occupy the outer shelf.

The principal controls on geochemical differentiation in the shelf sediments are depositional environment, provenance, and effluent input. Nickel, iron, cobalt, and cadmium occur dominantly in mid and outer shelf sediments; carbonate, phosphate, strontium, and arsenic increase with depth; and copper, lead, and zinc occur mainly in mid-shelf muddy sands. Manganese is unusually deficient in all sediments.

Published for the Bureau of Mineral Resources, Geology and Geophysics by the Australian Government Publishing Service

ISBN 0 642 03728 0

MANUSCRIPT RECEIVED: DECEMBER 1975

REVISED MANUSCRIPT RECEIVED: SEPTEMBER 1976

ISSUED: JANUARY 1979

Cover photograph by courtesy of Australian Information Service

Printed by Graphic Services Pty Ltd, 516-518 Grand Junction Road, Northfield, S.A. 5085

CONTENTS

APPENDICES (on microfiche in back pocket)

1. Station data
2. Heavy-mineral values for the continental shelf sediments
3. Modal analysis of shelf sediments
4. Geochemical, X-ray, and granulometric data
5. Q-mode and R-mode factor analysis

TABLES

PLATES

FIGURES

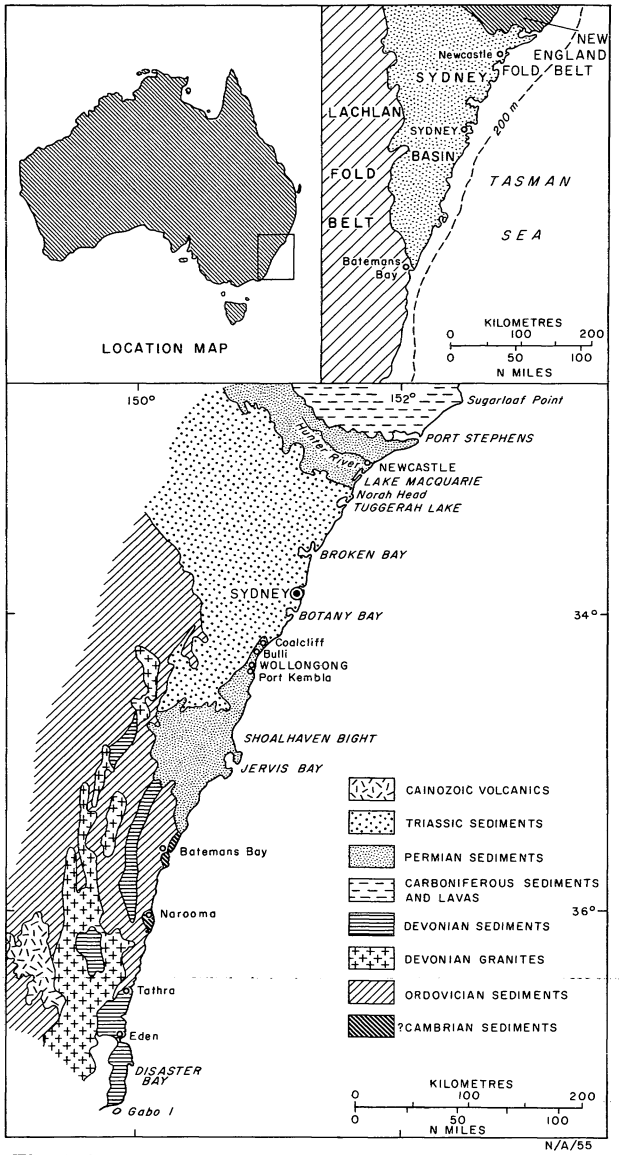

Fig. 1. Simplified coastal geology of southeast Australia.

CORRIGENDUM: In Figure 3 and many of the later maps, *Merimbula* is misspelt *Merrimbula*.

SUMMARY

The continental shelf of southeast Australia between Sugarloaf Point and Gabo Island, New South Wales, varies in width from 72 km east of Newcastle to 17 km east of Montague Island. Over much of this area an inner shelf zone (less than about 60 m water depth), a middle shelf zone (60-130 m), and an outer shelf zone (more than 130 m) can be distinguished by morphology and sediment type. Three groups of terraces are present, shallower than 60 m, between 70 and 110 m, and between 110 and 140 m. The shelf break lies between 130 and 170 m. There is a correlation between the depth of the shelf break and the depth of basement. It is likely that the morphology of the outer shelf is related to morphological variations in basement surface, which is the little-modified Atlantic-type rift scar produced during sea-floor spreading in the Cretaceous. The declivity of the upper continental slope is usually less than 2° to the north of Jervis Bay, but to the south it progressively increases so that slopes steeper than 10° are common. Ten submarine canyons or canyon-like features dissect the slope to the south of Jervis Bay.

A sequence of sediments above acoustic basement (S2), thickening eastwards from the mid-shelf position, is shown in seismic profiles. This sediment wedge is divided into two parts by an unconformity (S1); the lower part is transgressive on S2, and the upper is progradative on S1, and is best seen offshore from the Sydney Basin. Twice as much sediment occurs on the narrow shelf south of Jervis Bay as on the wider shelf to the north. Basement highs crossing the shelf have been identified southeast of Sugarloaf Point and northeast of Jervis Bay; basement lows occur off Newcastle and off Disaster Bay. The probable axis of eastward tilt of the continental shelf in the mid-shelf position has been identified as a basement ridge or step. Tilting and the development of a sediment wedge have probably continued since the Late Cretaceous.

Surface sediments are dominantly terrigenous in water depths shallower than 60 m; eastwards, carbonate components become increasingly dominant with increasing depth. Kaolinitic and chloritic muds occur as discrete zones in the mid-shelf area. Nearly all the shelf sediments are sands, with minor quartz or calcareous gravel occupying the inner and outer shelf areas. Fine to very fine-grained sands have a distribution similar to that of the muds. An unstable amphibole-pyroxene-epidote heavy-mineral suite occurs on the outer shelf, and a stable tourmaline-rutile-zircon suite predominates in water depths less than 60 m. The north-to-south variation in heavy minerals is similar to that in onshore localities, where ilmenite decreases and rutile/zircon increase from south to north. All sediments on the shelf are considered to be relict, with the possible exception of the muds which may be accumulating at present. Sediments between 15 and 60 m were probably deposited during the Holocene transgression; the mid-shelf sands and muds possibly represent a mixed barrier facies, and the outer shelf carbonates probably date back to the end-Wisconsin sea-level low. Sedimentation on the continental shelf at the present day is therefore limited to the zone 0-15 m, and possibly to the muds of the middle shelf.

The principal controls on geochemical differentiation in the shelf sediments are depositional environment, provenance, and effluent input. Nickel, iron, cobalt, and cadmium occur predominantly in the middle and outer shelf sediments; carbonate, phosphate, strontium, and arsenic increase with depth; and copper, lead, and zinc occur principally in the mid-shelf muddy sands. Manganese is unusually deficient in east Australian shelf sediments. Zinc, arsenic, cobalt, and cadmium occur in concentrations considered high when compared with standard rocks and sediments from other continental shelves. This is a result of high input together with minimum dilution by recent sedimentation.

INTRODUCTION

The Bureau of Mineral Resources (BMR) conducted a reconnaissance survey of the continental shelf of southeast Australia between February and May 1972. This Bulletin presents the results obtained from information collected during that cruise, supplemented by data from the BMR multisensor geophysical survey of the continental margin; additional sources of bathymetric data were the recent survey by the Division of National Mapping, and published and unpublished soundings of the RAN Hydrographic Office.

The area studied (Fig. 1) represents about 28 000 km^2 of continental margin between Sugarloaf Point and Gabo Island, a distance of about 700 km. The inshore boundary of the area is the 15-m isobath and the offshore boundary is between the 400 and 500-m isobaths, although sediment sampling was generally restricted to depths less than 300 m. The objectives of the study were to describe the sediments on the continental shelf and upper slope and to map their distribution, and to determine the surface topography and subsurface structure in order to unravel the Late Cainozoic history of the area.

Seaborne activities consisted primarily of sediment sampling and seismic profiling. For this work the motor vessel *San Pedro Strait*, an oil-rig supply vessel, was chartered from San Pedro (Offshore) Pty Ltd. The *San Pedro Strait* was equipped with a Simrad 'Skipper' 38.5 kHz echosounder, a Decca 202 radar unit, and an 'Arkas' automatic pilot. Two portable laboratories owned by BMR were welded to the deck of the vessel, and a large A frame and raised platform were positioned on the stern to facilitate dredging operations.

Bottom samples were collected with a pipe dredge and a box dredge. The box dredge was used only when the bottom was suspected of being rocky, or showed high relief. Samples were collected at intervals ranging from 4 to 18 km. A new hydraulic hydrographic winch was installed on the vessel for use with the pipe dredge and camera cage. The box dredge was operated by one of two winches permanently installed on the vessel using 9.5-mm diameter wire rope with a breaking strength of 3500 kg. These winches, although adequate, were not particularly satisfactory because of the slow rate of recovery. This greatly increased the time at sample sites, leading to inaccuracies in position fixing owing to drift of the vessel.

Photographs of the seabed were obtained with an Edgerton, Germeshausen, & Grier model 205 underwater camera and a model 206 light source. The shutter opening and synchronized flash were triggered by a weight slung 3 m below the frame in which the camera and the light source were mounted. This arrangement gave a field of view of approximately 4 m^2.

The seismic profiling system consisted of a three-electrode Sparkarray sound source, coupled to an E.G. and G. 232A power supply unit, a 2000-Joule capacitor bank type 233, and an E.G. and G. trigger unit model 231. Energy levels of 500, 1000, and 2500 Joules were used. During the early stages of the cruise, the three-electrode Sparkarray was modified for use in shallow water by means of bubble suppressors consisting of rubber hose fitted over the electrodes. During the later stages of the cruise, the suppressors were generally discarded.

Various hydrophone arrays were used. Initially, a 30-element M.P. 7 hydrophone was used in deep water (more than 130 m) and a 7-element Aquatronics hydrophone was used in shallow water. Ultimately, the 30-element hydrophone was discarded in favour of the 7-element Aquatronics for all depths.

Three recording systems were used. In the early stages of the cruise, most of the profiling was carried out with an E.P.C. Graphic Recorder owned by the Geological Survey of New South Wales. The results from this were generally good, but the machine later became unreliable. Throughout most of the cruise, the BMR Ocean Sonics GDR and GDR-T recorders were used. A number of problems arose, including programming difficulties, drying of the recording paper, and rapid deterioration of the belts. An E.G. and G. recorder was tried over the Gascoyne Seamount, but with little success.

Water depth profiles were obtained with the ship's echosounder, which has a straight-line dry paper recorder with a three-range scale to a maximum depth of 1100 m.

Position fixing of sample stations and seismic traverses relied largely on radar, although occasionally it was necessary to use celestial navigation or short dead-reckoning runs. Nearly 80 percent of all samples are considered to be positioned with an accuracy of better than 2 km, while 95 percent are positioned to within 4 km.

Climate and oceanography

The climate of central and southern coastal New South Wales is determined largely by the subtropical high-pressure systems which are centred around latitude

TABLE 1. RAINFALL AND TEMPERATURE STATISTICS FOR SYDNEY
LAT. 33°52′S, LONG. 151°12′E

Month	*Av. daily Max. °C*	*Av. daily Min. °C*	*Av. rainfall (mm)*
January	25.5	18.3	85
February	25.5	18.3	73
March	24.4	17.2	115
April	21.7	14.4	130
May	18.9	11.1	118
June	16.1	8.9	88
July	15.6	7.8	118
August	17.2	8.9	70
September	19.4	10.6	68
October	21.7	13.3	70
November	23.3	15.6	63
December	25.0	17.2	83

Data compiled from information collected between 1859 and 1945 (British Admiralty, 1956).

35°S in the summer, but move north in the winter and are replaced by a low pressure belt associated with southern depressions. The depressions also affect the area periodically in the summer months. The west-to-east passage of depressions determines the climate throughout the year in the southern part of the area (British Admiralty, 1956, 1960).

In winter, winds on the coast and offshore are generally from the west, southwest, or south. From May to July in the open sea, over 10 percent of all wind observations report gales. In summer, especially January to March, winds on the coast vary between north and south, through east, with forces generally between 4 and 5 on the Beaufort Scale. Farther offshore, however, the prevailing winds from these directions may reach force 8. Peculiarities of the summer weather near Sydney are the strong winds (up to 35 knots) and rain associated with the 'black northeaster' and the 'southerly buster' (British Admiralty, 1956, 1960).

Rainfall and temperature statistics for Sydney are given in Table 1.

The water circulation along the east coast of Australia is dominated by the East Australian Current, which sets generally to the southeast (Hamon, 1965, 1968; Boland & Hamon, 1970). North of latitude 32°S, this current is a swift (2 knots) narrow southward flow near the edge of the continental shelf. South of this latitude it breaks up into a number of anticyclonic eddies. Postulated circulation patterns vary considerably from year to year (Fig. 2). During the summer (November to February) a break-up into anticyclonic patterns leads to a dominant strong southerly flow over much of the outer shelf, except for a northerly flow associated with a cyclonic pattern over the southern part of the area. From March through to August, a broad anticyclonic gyre gives rise to a general southerly flow. In September, vortexes result in northerly flow associated with a cyclonic eddy north of Jervis Bay, and an anticyclonic group results in a southerly flow on the southern shelf. The production of vortexes in summer, together with the prevailing wind directions, are probably the causes of the onshore currents reported in the *Australia Pilot*.

Coastal geology and geomorphology

The central and southern New South Wales coast transects three major geological provinces, the Lachlan Fold Belt, the Sydney Basin, and the New England Fold Belt (Fig. 1).

The far south coast between Gabo Island and Tathra is composed of Devonian conglomerate and quartzite; between Tathra and Batemans Bay, Ordovician slate, shale, and greywacke form the coastal cliffs. Supposed Cambrian sediments crop out at Narooma and Batemans Bay. Upper Devonian granite west and south of Eden intrudes Lower and Middle Devonian rhyolite, andesite, and dacite. Throughout this part of southern New South Wales, the sediments of the coastal belt are backed to the west by large tracts of Devonian granite, the whole region forming part of the Lachlan Fold Belt.

The Sydney Basin occupies the area between Batemans Bay and Port Stephens. Permian marine sandstone, shale, and mudstone of the Shoalhaven Group form the southern coast of the Sydney Basin as far north as Shoalhaven Bight, and between this point and Wollongong non-marine shale and mudstone of the Illawarra Coal Measures crop out. The Gerringong Vol-

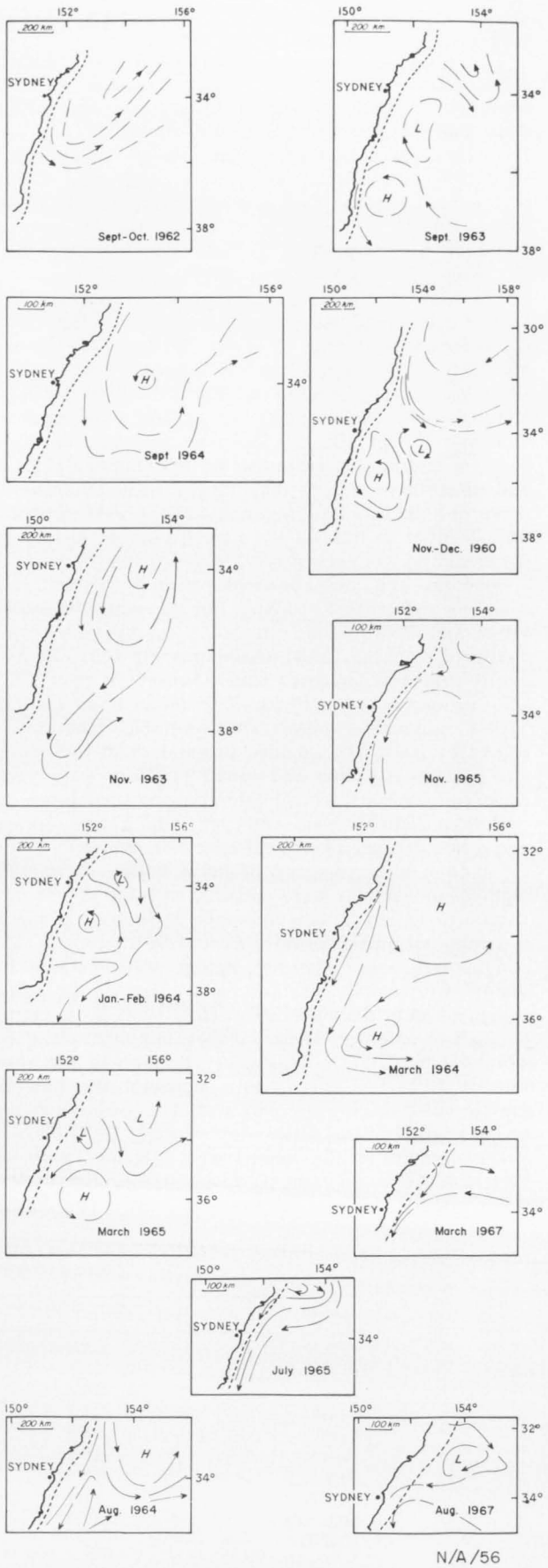

Fig. 2. Ocean circulation patterns off the continental shelf of southeast Australia, after Hamon (1965, 1968) and Boland & Hamon (1970).

canics of Permian age crop out between Port Kembla and Wollongong. These are primarily alkali-rich basaltic marine flows. Triassic sediments and volcanics crop out on the coast between Coalcliff and Lake Macquarie. The two major sedimentary units are the Narrabeen Group, consisting of continental shale and sandstone, and the Hawkesbury Sandstone, mainly composed of massive quartz sandstone, also of continental origin. The Narrabeen Group forms the coast around Coalcliff, and also between Broken Bay and Lake Macquarie. The Hawkesbury Sandstone forms much of the high cliffs between Coalcliff and Broken Bay. In the Newcastle area, the soft conglomerate, sandstone, shale, clay, and coal of the Permian Newcastle Coal Measures crop out on the coast.

North of Port Stephens, resistant Carboniferous sandstone, conglomerate, and lavas form the southern part of the New England Fold Belt. The Carboniferous and Permian rocks are separated along the northern side of the Hunter Valley by the Mooki-Hunter Fault System.

The coast of New South Wales is a drowned embayed coastline, the relief of which is closely controlled by the geology. It can be broadly divided into areas of rugged coastline where the immediate hinterland is mountainous, e.g. the coastline transecting the Lachlan Fold Belt region between Gabo Island and Batemans Bay, and the coast between Bulli and Broken Bay composed primarily of Hawkesbury Sandstone; and areas of subdued coastline where the immediate hinterland has only a few hills and ridges, e.g. the Illawarra Coal Measures section between Shoalhaven Bight and Wollongong, and the Narrabeen Group/Newcastle Coal Measure sections between Broken Bay and Newcastle.

The rugged coastline is characterized by high rocky cliffs and small embayments with bay head beaches; broad beaches and few headlands characterize the subdued coastline. Evidence of the Holocene rise of sea level is clearly seen on both types of coastline. Rias form characteristic features of the rugged coastline (Sydney, Broken Bay). Alluvial fills and delta plains occur on the subdued coasts, where the most conspicuous features are the barrier and lagoon systems; dual sand-barrier systems comprise inner (Pleistocene) and outer (Holocene) components ranging from 20 m to 50 km long and up to 105 m high, especially in the area between Lake Macquarie and Port Stephens. In places, swamps and lakes have formed between the barrier systems (Lake Macquarie, Tuggerah Lake). The outer barrier system has also developed in places along the rugged coasts, as at Disaster Bay.

Previous work

The structure of the offshore Sydney Basin has been described by Kamerling (1966). He concluded that the surface of Permo-Triassic rocks dips eastwards from the coast at an angle of about 1.5° and underlies a sequence of low-velocity ?Tertiary to Pleistocene sediments up to 670 m thick near the edge of the shelf. He also described a depression in the Permo-Triassic surface and an accompanying local thickening of the overlying sediments which he suggested may indicate the Pleistocene course of the Hunter River.

Phipps (1963, 1966, 1967), using echosounder data showing the morphology of the shelf, postulated late Pleistocene tectonic warping of the continental shelf about two structural highs, one east of Sugarloaf Point, and the other east of Jervis Bay. Gill & Hopley (1972) suggested that this indicates that eastern Australia has undergone isostatic readjustment, the movement being of regional significance. Phipps (*in* Thom et al., 1972) later revised his estimate of the age of the warping, and suggested that it could have occurred at any time from the Tertiary to the Pleistocene. Conolly (1969) published a synthesis of marine data outlining the morphological variation on the western Tasman Sea floor, but said little about the continental shelf. Hayes & Ringis (1973) suggested an age of 60-80 m.y. for the opening of the central Tasman Sea; they stated that the greatest thicknesses of sediment occur next to the Australian continental margin, and that the sediment load has aided in the depression and warping of oceanic basement. Symonds (1973), using data gathered during the BMR geophysical survey of the continental margin, supported a tectonic origin for the southeastern margin of Australia, and suggested a two-stage process in the formation of the Tasman Basin.

Shirley (1964) summarized the sediment distribution on the continental shelf between Crowdy Head (lat. 31°50′S) and Batemans Bay.

STRUCTURE

About 3000 km of shallow seismic reflection profiles was run in the area. Sections were obtained along east-west lines spaced 18 km (10 n miles) apart, and along tie-lines parallel to the coast (Fig. 3). In most cases, the depth of penetration was 0.1-0.2 s two-way travel time in shallow water, and 0.4-0.5 s in deeper water on the edge of the continental shelf. Interpretation was made more difficult by multiple reflections, particularly in shallow water. The structure of the area is illustrated by selected profiles (Figs. 4-10).

Reflectors numbered S1 and S2 are seen in most east-west sections (Figs. 4-10). S1 is a major unconformity within the sedimentary sequence. It can be traced from about the mid-shelf position across the outer shelf in each east-west section between Sugarloaf Point and latitude 35°10′S. It is the only major unconformity within the wedge of unconsolidated sediments forming the middle and outer shelf. S2 is a strong reflector in nearly all the sections studied. It can be traced westwards into the coastal cliffs, and probably represents the basement surface on which the shelf sediment sequence has been built. This bedrock surface consists of Permo-Triassic rocks off the Sydney Basin, and older sediments, metamorphics, and intrusives to the south and north.

The S2 reflector

S2 probably represents a marked contrast in acoustic properties between the sediments of the shelf wedge and the underlying consolidated sediments, volcanics, and metamorphics forming the offshore extension of the onshore geology. In most sections examined very little seismic penetration below S2 was achieved; however, a few profiles between Sydney and Port Stephens (Fig. 5B, C) show gentle dips in basement of 2-9°, mostly to the west, with some very gentle folding. This is consistent with the gently dipping Permo-Triassic sediments which crop out onshore. Throughout the rest of the area, the lack of penetration below S2 makes it impossible to determine basement structures.

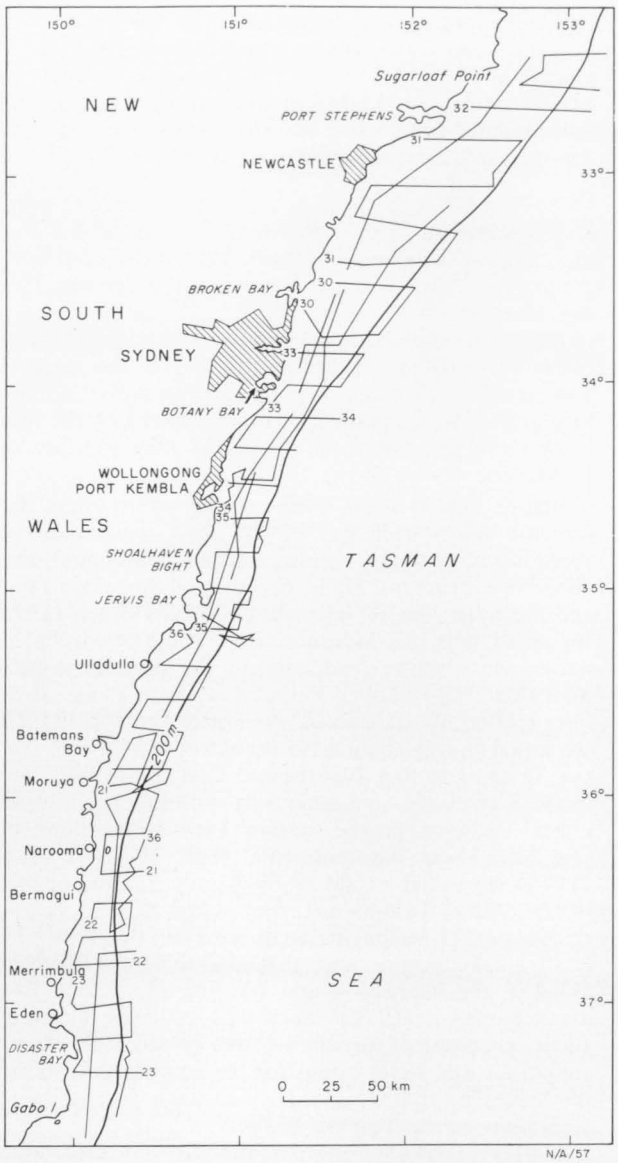

Fig. 3. Track chart of BMR 1972 marine seismic survey.

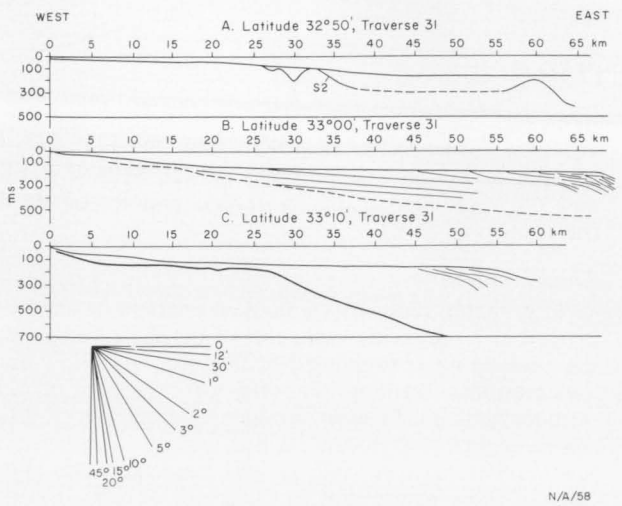

Fig. 4. Interpretation of seismic reflection profiles across the continental shelf between latitudes 32°50′S and 33°10′S. Traverse numbers refer to the track chart (Fig. 3). The horizontal scale along each section shows distance from the coast.

The east-west sections depicted in Figures 4-8 show marked variations in the S2 reflector. In the simplest cases, S2 dips to the east at 0.5-1.0° (Figs. 6D, 9B). In many places, however, a basement ridge or ridges (Figs. 4A, C; 5A, B, C; 6A, C, E; 7A) in about the mid-shelf position separate the inner part of the shelf where basement is very shallow and sediment thin (Fig. 10A, F), from the outer part where the basement dips to the east at up to 2° under a thickening wedge of sediments (Figs. 9B, 10F). Sediments overlying the ridge are thin or absent and water depths range from 100 to 110 m. In other sections there is no basement

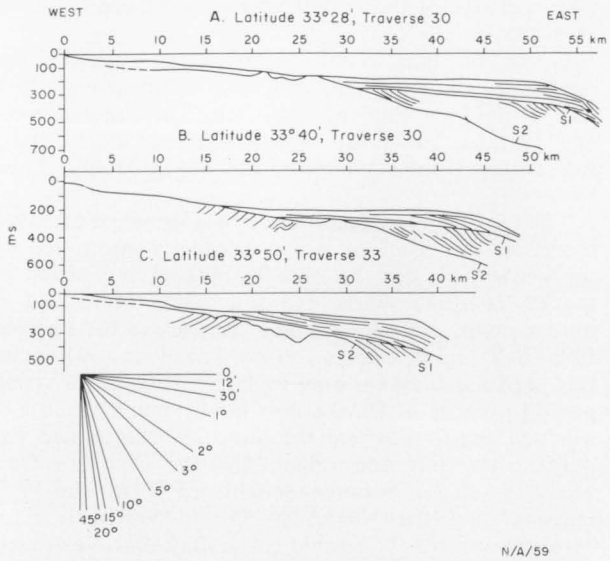

Fig. 5. Interpretation of seismic reflection profiles across the continental shelf between latitudes 33°28′S and 33°50′S. Traverse numbers refer to the track chart (Fig. 3). The horizontal scale along each section shows distance from the coast.

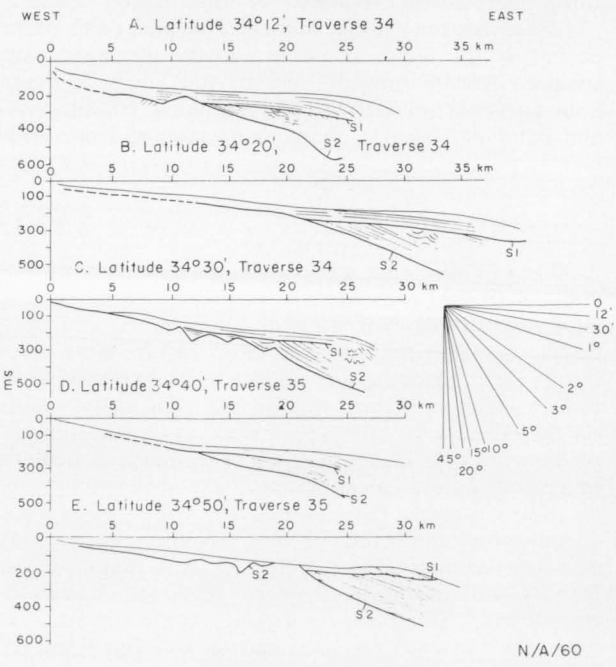

Fig. 6. Interpretation of seismic reflection profiles across the continental shelf between latitudes 34°12′S and 34°50′S. Traverse numbers refer to the track chart (Fig. 3). The horizontal scale along each section shows distance from the coast.

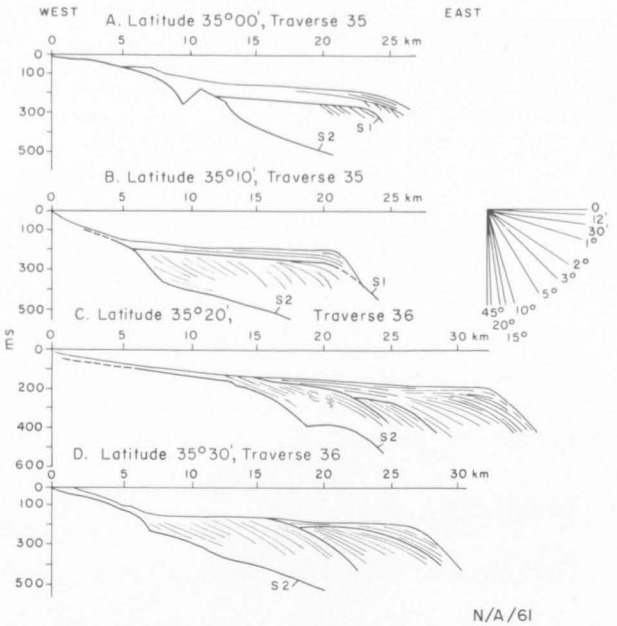

Fig. 7. Interpretation of seismic reflection profiles across the continental shelf between latitudes 35°00′S and 35°30′S. Traverse numbers refer to the track chart (Fig. 3). The horizontal scale along each section shows distance from the coast.

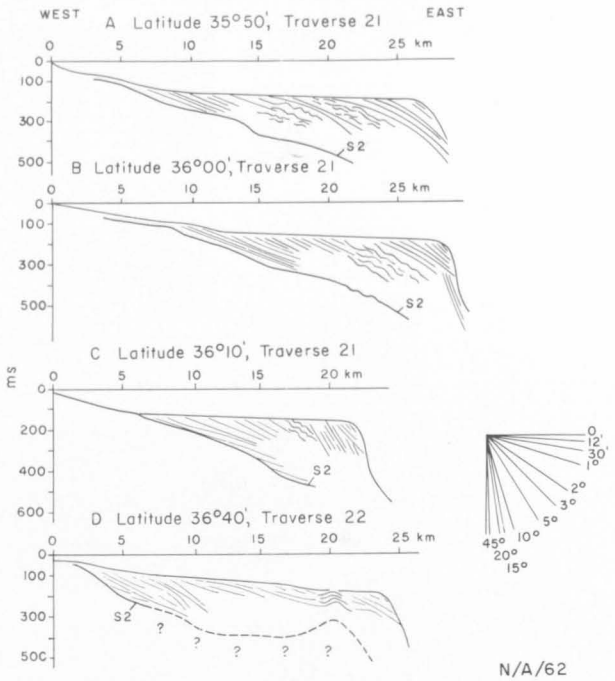

Fig. 8. Interpretation of seismic sections across the continental shelf between latitudes 35°50′S and 36°40′S. Traverse numbers refer to the track chart (Fig. 3). The horizontal scale along each section shows distance from the coast.

ridge, but a basement step occurs in approximately the same position (Fig. 7B, C, D). The step represents a change in slope of up to 10°, and separates the inner part of the shelf where basement is shallow and sediments thin, from the outer shelf where basement depth and sediment thickness increase eastwards. The mid-shelf basement ridges occur only north of latitude 35°10′S, and the mid-shelf step only south of this latitude.

A rise in basement is also present beneath the shelf break in a few sections. Sediments may be thin over the rise (Fig. 4A) or may give marked indications of a basement rise by draping (Fig. 8D).

In most of the shallow seismic sections, basement surface is obscured by multiples below 600 ms reflection time. Depths are indicated by seismic reflection time because of lack of information on formation velocities. In the vicinity of the shelf edge, S2 can be followed in the deep seismic sections of Survey 12 of the BMR geophysical survey of the continental margin. Every section examined showed a major inflection of S2 under the upper continental slope. S2 crops out in places on the continental slope at water depths ranging from 1300 to 1700 m.

The structure contour map (Fig. 11) drawn on S2 shows the broad variations in its attitude, but the contour interval is too great to reveal the middle-shelf features described above. The eastward slope of basement is steeper to the south than to the north of Jervis Bay. Over much of the area between Shoalhaven Bight and Sydney, S2 is at a fairly uniform depth of 500 ms at the shelf edge. Northeast of Sydney, and especially southeast of Port Stephens and Sugarloaf Point, major basement undulations are shown by all contours from 200 to 600 ms. East of Shoalhaven Bight, prominent eastward bulges of the 200 and 300 ms contours coincide with the more general eastward bulge of the 500 ms contour; in this area, basement is shallower on the outer shelf than in areas north and south.

South of Jervis Bay, basement slopes more steeply to the east, and becomes progressively deeper on the outer shelf in a southerly direction. This is especially noticeable south of Montague Island, where basement is deeper closer to the coast than in areas to the north. Southeast of Disaster Bay, a major basement low is indicated by the contour configuration. Isopachs of the sedimentary sequence overlying S2 (Fig. 12) show that the thickest sediments occur in this area, and also that a thick sequence occurs in the basement lows east of Newcastle. Between Jervis Bay and Sydney, the sediments attain a maximum thickness of about 250 m at the outer edge of the shelf.

The mid-shelf basement ridge coincides with the zone of marked sediment thinning shown in Figure 12. Except in the Newcastle area, no isopachs have been drawn west of the basement ridge because of very rapid variations in sediment thickness in the range 0-60 m. The basement step is well shown in Figure 11 by the very close spacing of the 100 to 300 ms contours northeast of Eden. Sections across the close inshore basement step are shown in Figure 10C, D. The distribution of the features described above is shown in Figure 13.

The S1 reflector

The S1 reflector is a prominent unconformity in almost all sections between Sugarloaf Point and latitude 35°10′S (Figs. 5, 6, 7). It is not certain that it is the same unconformity in each section because it cannot be identified in the tie-lines, which are essentially strike sections; however, it displays broadly similar characteristics throughout the area, so it is probably a single event.

S1 truncates the underlying sediments and slopes to the east. In places, it shows a marked downward inflection near the present shelf-break, above a similar downward inflection in basement (Fig. 5A). S1 crops out

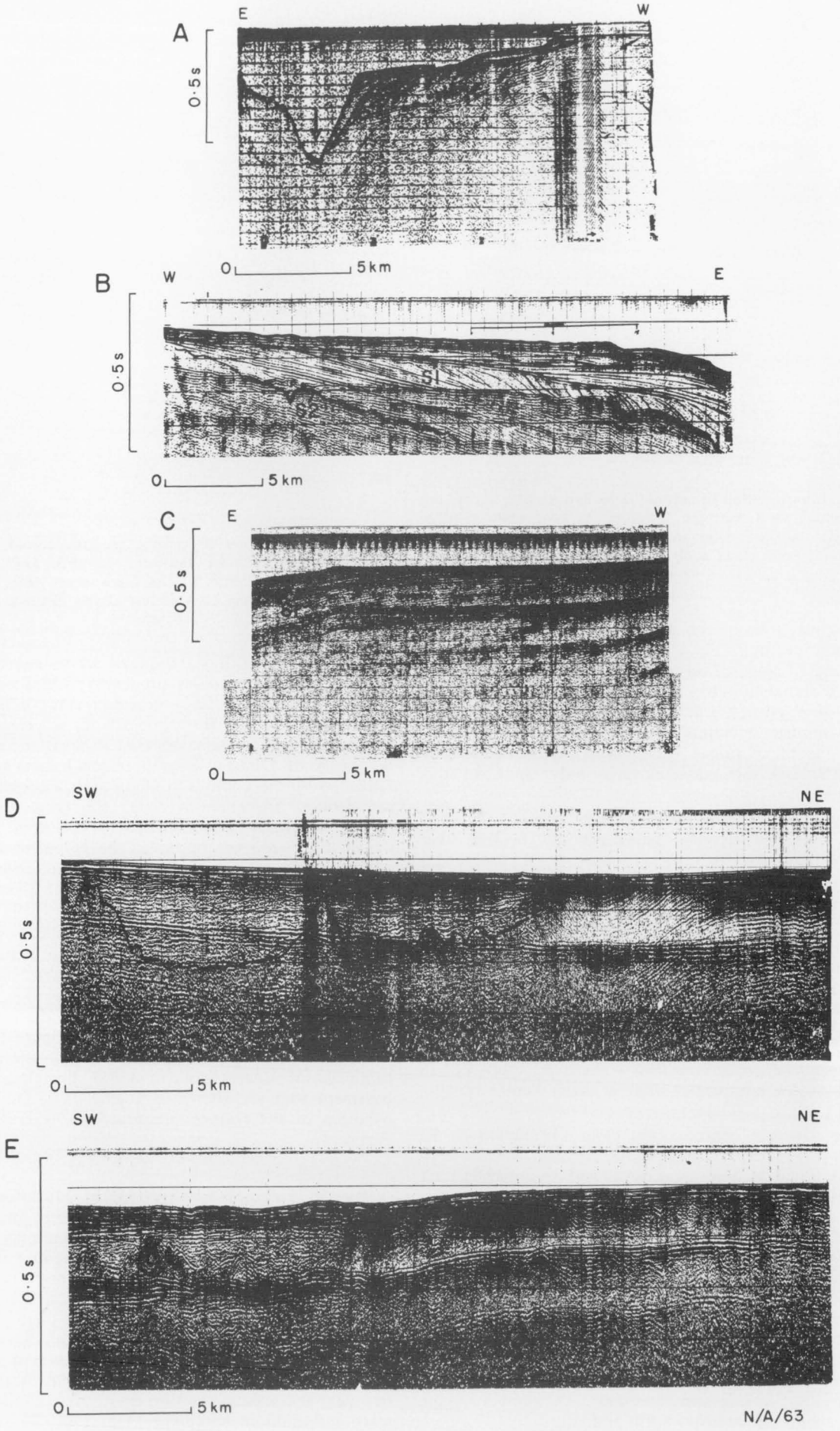
A
E
W
0·5 s
0 5 km
B
W
E
0·5 s
S1
S2
0 5 km
C
E
W
0·5 s
0 5 km
D
SW
NE
0·5 s
0 5 km
E
SW
NE
0·5 s
0 5 km
N/A/63

on the upper slope in one place (Fig. 6E) and it is presumed to do so in others (Figs. 7B, 9C); it is truncated in the middle or inner shelf by the westward-rising basement surface (Figs. 5, 6, 7). S1 divides the sedimentary pile above basement into two distinct sections: structures within the lower part of the lower sequence apear to transgress the basement suface, and those above S1 suggest progradation on S1.

North of the survey area and south of latitude 35°20′S (Figs. 7C, D; 8A, B) more than one reflector showing unconformable relations with underlying reflectors occurs above basement. Which one, if any, correlates with S1 is not known.

Origin of the mid-shelf basement ridge and step

Both the basement ridge and the basement step separate an inner shelf region where sediments are thin (0-60 m), from an outer shelf region where sediments thicken eastwards. The ridge and step could have formed in various ways: they may be the result of erosional processes, and may therefore represent a subaerial surface developed before the continental margin drowned; they may be tectonic features initiated by continental break-up; they may have formed later by differential subsidence of the continental shelf under the combined load of increasing sedimentary thickness and overlying water column; or they may be the result of tectonic modification of a previously eroded surface.

Erosional processes may have affected the formation of the basement ridge system (Figs. 9D, 11). Where major river systems occur onshore, seismic sections show major offshore basement depressions which may be channels representing the eastward extensions of such river systems. Figure 9D shows the feature offshore from Newcastle; the limited number of available sections suggests that the depression trends west-northwest across the basement ridge. The ridge could represent a particularly resistant Triassic sequence, probably sedimentary or volcanic.

There is little evidence on the origin of the basement step system. Both ridge and step may owe their origin to faulting associated with the rifting of the Tasman Basin, or to warping and step-faulting at a later time under the combined load of sediment and water on the outer shelf.

Port Stephens/Sugarloaf Point high and Newcastle lows

Basement lows southeast of Newcastle and southeast of Port Stephens are separated by a basement high, but a more prominent high occurs to the east and east-southeast of Port Stephens (Fig. 11). The larger high is here informally termed the Port Stephens/Sugarloaf Point high, and the lows are termed the Newcastle lows. It is possible that the Port Stephen/Sugarloaf Point high coincides with the southeast extension of the southern part of the New England Fold Belt (Fig. 13), which is bounded on the south by the Mooki-Hunter fault system. Just as the Mooki-Hunter Fault System, utilized by the Hunter River, forms a depression bordering the New England Fold Belt, so offshore a deep basement depression (Newcastle low) borders the Port Stephens/Sugarloaf Point high. The offshore depression aligns with a possible southeast extension of the Mooki-Hunter Fault System.

Shoalhaven/Jervis Bay high

Phipps (1966, 1967) suggested that a basement high trends southeast across the shelf near Jervis Bay. Evidence has already been presented indicating that to the east of Shoalhaven Bight, basement is shallower on the outer shelf than in areas to the north and south. Corroborative evidence is shown by the bathymetry in the Jervis Bay area (Fig. 14), which shows a series of topographic highs trending to the northeast. The sediment distribution map (Pl. 1) shows a linear body of very coarse sand to gravel extending in the same direction along the topographic high.

Disaster Bay low

The structure contour map (Fig. 11) shows a large basement depression southeast of Disaster Bay, which trends southeast. It aligns with the projected extension of the Berridale Fault (Lambert & White, 1965), which according to these authors is 'one of the most significant major structures of the Snowy Mountains of New South Wales' (Fig. 13). In this area, therefore, the basement structure may be related to a major fault system which has been active since the Late Silurian and Early Devonian, during the Tertiary, and possibly in the Holocene (Lambert & White, op. cit.).

Structural development and depositional history

No drilling has been carried out on the continental shelf and there is no direct evidence on the lithology and age of the sedimentary sequence, nor on the nature of the unconformities evident in the seismic profiles and the time intervals that they represent.

Most modern work indicates that continental shelves have undergone some subsidence during their formation. Dietz (1952) and Curray (1969) concluded that the wedge of sediments that form present-day shelves is the result of the close interplay of subsidence and sedimentation. Van Andel & Calvert (1971) and Falvey (1974) invoked subsidence as a major component in the sedimentary development of Atlantic-type shelves, and Falvey (op. cit.) cited the east Australian shelf as a typical example. Rona (1973) advocated episodes of mid-ocean rifting to induce shelf subsidence, but Bloom (1967), Walcott (1972), and Chappell (1974a and b) suggested that isostatic adjustment following Quaternary transgressions has affected shelf subsidence. More specifically, Chappell (op. cit.) stated that as a result of Quaternary transgressions, shelf subsidence will diminish towards the coast, that the axis of tilt should be recognizable, and that between the axis of tilt and the coast a zone of basement depression should occur as the result of movements compensating for the tilting of the outer shelf. He further stated that the hinge-line of tilting would migrate onto the continent wherever continental shelves are narrow.

Fig. 9. Representative seismic profiles. A. Steep continental slope, massive truncation of sediments, and thick sediment pile. Basement is deep, and not visible in the section. East-to-west section south of Jervis Bay. The position of the arrow represents a change of course; it is not a submarine canyon. B. Basement (S2) and disconformity (S1) in a west-to-east section along latitude 32°15′S, northeast of Port Stephens. C. Possible outcrop of S1 on the upper continental slope in an east-to-west direction along latitude 34°20′S. The outcrop occurs outside the picture. D. Folds in the basement along a southwest-to-northeast section southeast of Newcastle. The maximum dip of the beds is about 9°. Note the channel cut into S2. E. Topographic variations in basement in a southwest-to-northeast section in the mid-shelf position, east of Port Stephens.

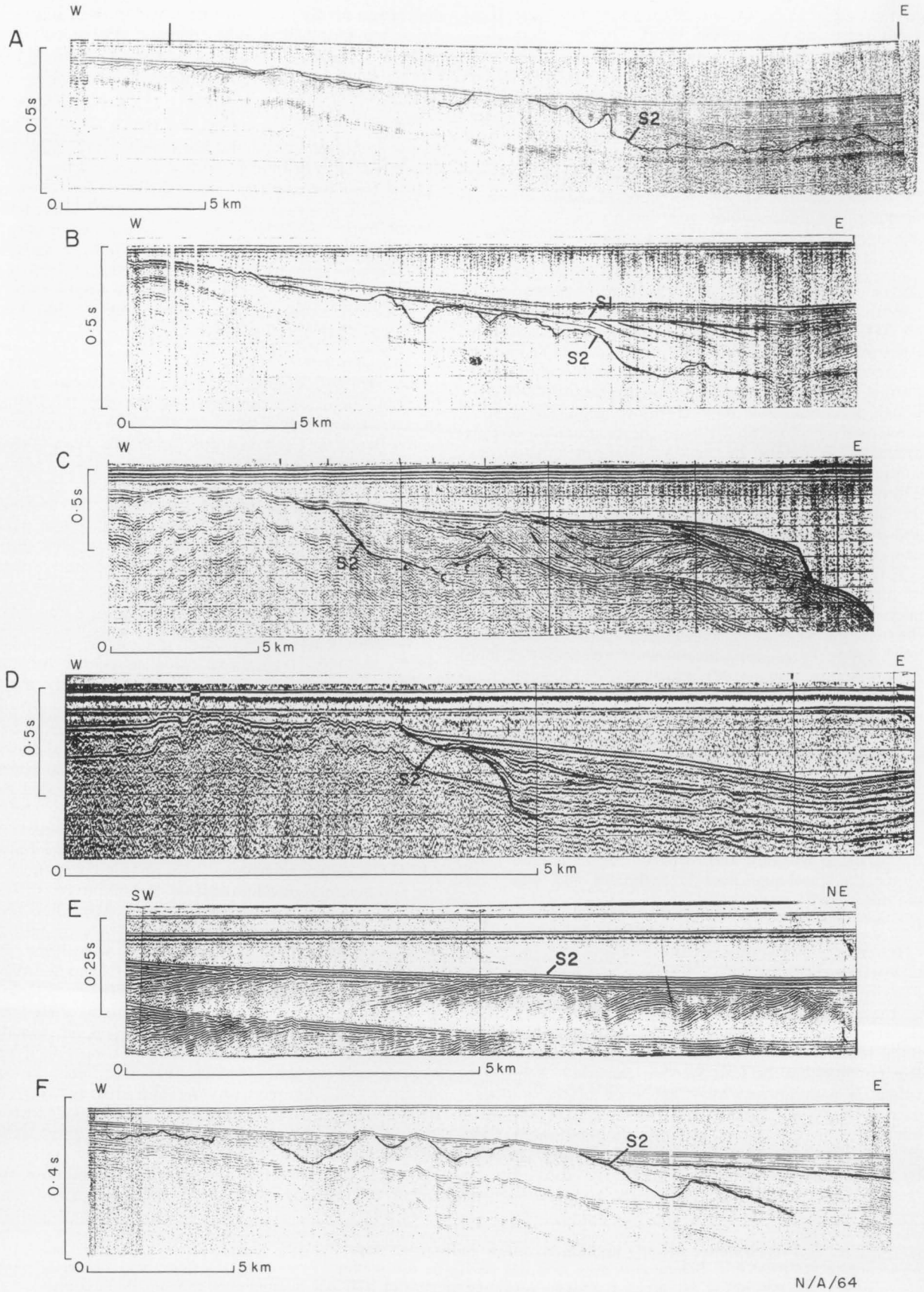

Fig. 10. Representative seismic profiles. A. Basement (S2) variations in a west-to-east section along latitude 33°30′S. B. Basement (S2) variations in a west-to-east section along latitude 34°30′S, east of Port Kembla. C. Step in the basement (S2) in a west-to-east section along latitude 37°20′S, east of Disaster Bay. D. Step in the basement (S2) in a west-to-east section along latitude 37°30′S, northeast of Gabo Island. E. Sub-basement (S2) structure in a southwest-to-northeast section southeast of Broken Bay. F. Basement structure in a section east of Shoalhaven Bight.

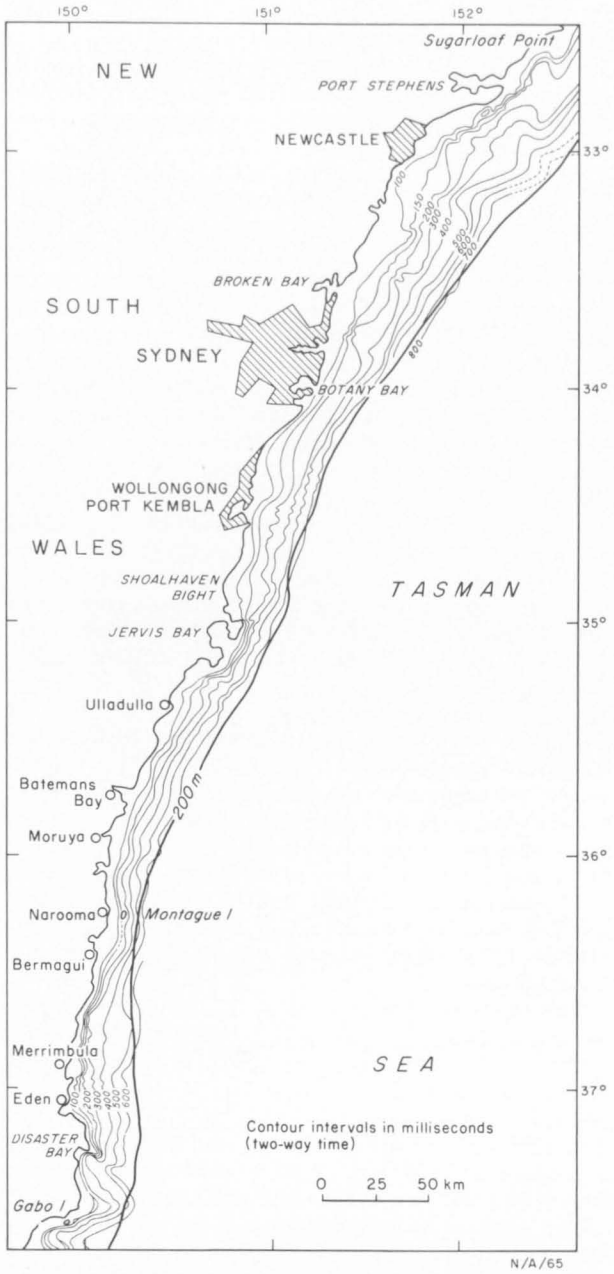

Fig. 11. Structure contours on S2 between Sugarloaf Point and Gabo Island.

Whatever the mechanisms are, most researchers agree that subsidence is an integral part of continental shelf evolution, and that evidence for the process is visible in the attitude of subsurface reflectors. Many features described by the above authors are visible in our seismic sections. These include:

(a) A wedge of sediments thickening seawards is everywhere present.

(b) The basal part of the sediment sequence is transgressive on basement (Figs. 4B, 6E) in the manner described by Van Andel & Calvert (1971) and Falvey (1974).

(c) Above S1, a prograding sequence is recognizable (Figs. 9B, C, 10B), as suggested in the model of Van Andel & Calvert (1971).

(d) A mid-shelf to inner-shelf area where sediments are thin or absent is generally recognizable (Fig. 10A, B, C, D, F); this may correspond with Chappell's (1974b) hinge-line of tilting.

(e) On the widest part of the shelf, basement is deeper in the nearshore zone, where it is overlain by more than 50 m of sediment (Fig. 4C). This area of deeper basement may correspond to Chappell's zone of basement depression immediately behind a hinge-line.

The conclusion follows that on the east Australian shelf, sediment has accumulated on a subsiding basement which hinges about a zone in the mid-shelf to inner-shelf area.

There is no direct evidence of the age of basement or of the overlying sediments. Hayes & Ringis (1973) concluded that the central Tasman Sea formed by a process of sea-floor spreading between 60 and 80 m.y. ago. If this is true, the continental slope probably forms

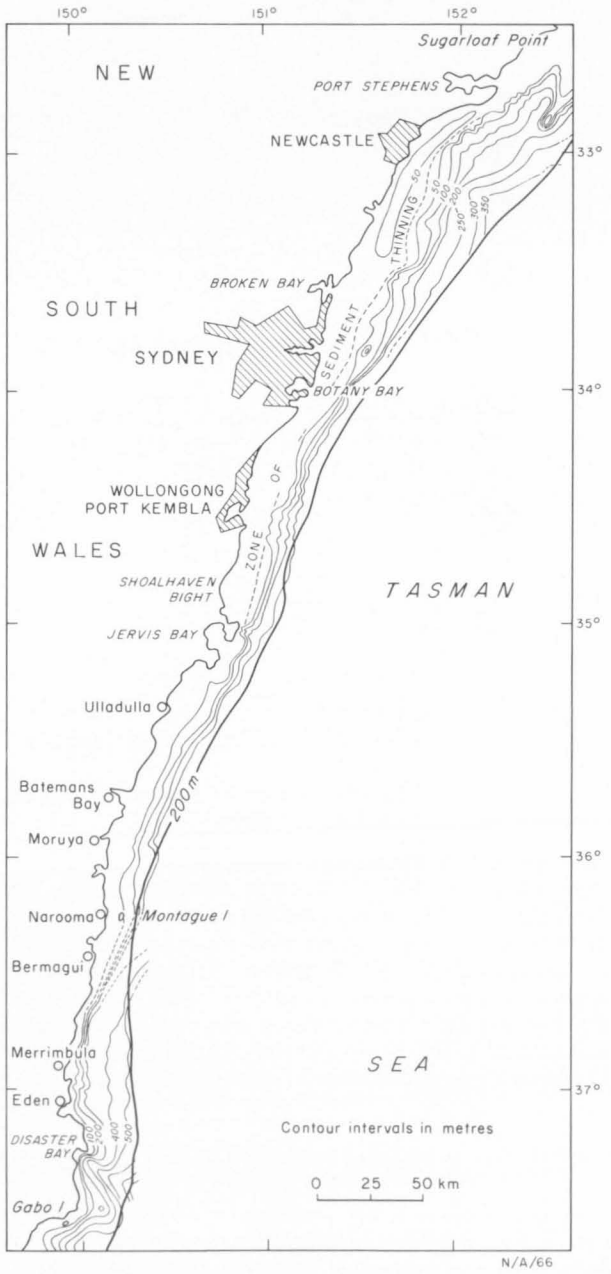

Fig. 12. Isopachs of the sediments resting on S2 between Sugarloaf Point and Gabo Island, assuming sediment velocities of 1.7-1.8 km/s.

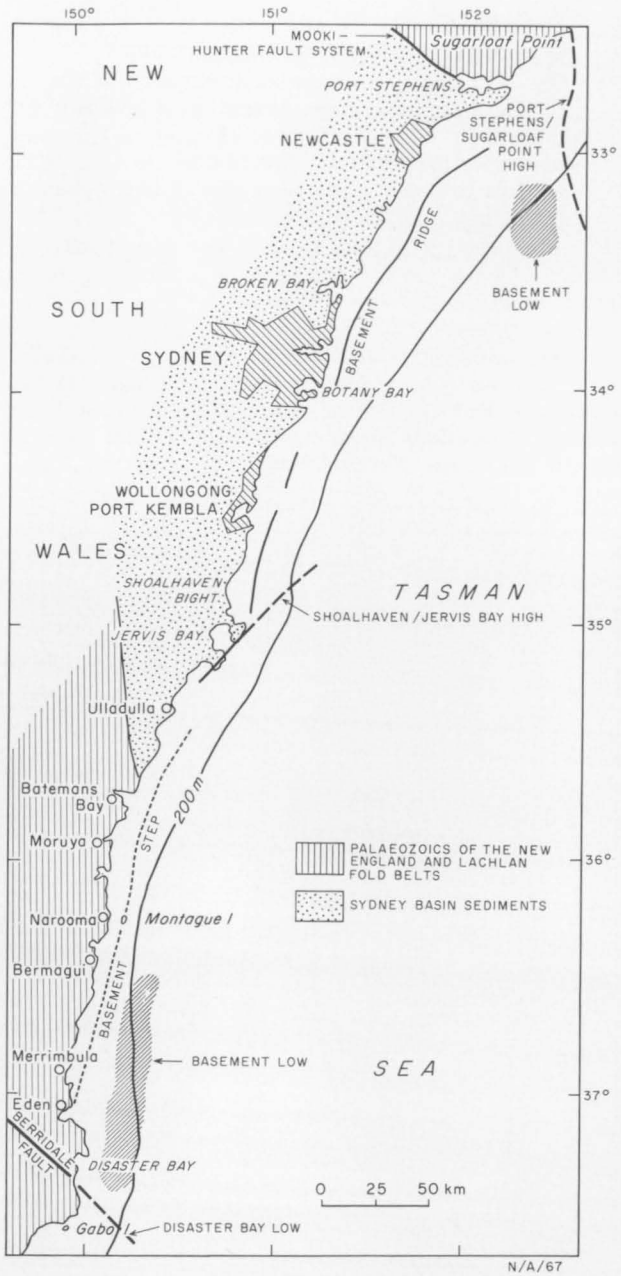

Fig. 13. Major structural features of the continental shelf of southeast Australia.

one side of the original rift, which opened in the Late Cretaceous or Early Tertiary (Jones, Davies, & Marshall, 1975). Rona (1973) calculated average sedimentation rates of 2 cm/1000 years for the shelves of eastern USA and northwest Africa. This value applied to the southeast Australian shelf would place the first marine transgression in the Eocene, but such an estimate must be speculative, particularly in view of the unknown duration of gaps in the succession. Browne (1969) described Eocene uplift of a Cretaceous peneplain in the onshore area of New South Wales. This movement may be contemporary to the general subsidence accompanying rifting and sea-floor spreading, S2 being the offshore representative of the Cretaceous peneplain.

The age of S1 is unknown, but a tentative estimate can be made by comparison with the east Gippsland section where unconformities occur in the Late Cretaceous, Eocene, and early or middle Pliocene. The Eocene unconformity is at a depth of 1500 m in the section, which is about 10 times the depth of S1 in the area studied. Early and middle Pliocene unconformities have been reported at 91 and 61 m in the Bairnsdale No. 1 and Duck Bay No. 1 wells. Taylor (1966) also reported shallowing of the upper Miocene sequence in Gippsland No. 1 well, which implies a possible late Miocene or early Pliocene unconformity, at a depth shallower than 122 m sediment thickness. James & Evans (1971) and Griffith & Hodgson (1971) reported a maximum Pliocene to Holocene sequence of 304 m in the Gippsland Basin. The sediment thickness above S1 at the continental edge in the present study area ranges from 120 to 212 m. These figures place the S1 surface in the same depth range as the early to middle Pliocene unconformity in Gippsland. If S1 is of this age, then the rate of sedimentation above S1 in areas unaffected by the Shoalhaven/Jervis Bay high or the Newcastle lows is 2.0-2.5 cm/1000 years. This is close to the sedimentation rates calculated by Rona (1973) for the whole of the sediment section on the eastern USA and northwest African shelves. It is, however, faster than the rates calculated by Rona for the Quaternary parts of the sections, but is much slower than sedimentation on the continental shelf of New Zealand (Lewis, 1973) where rates of 150-300 cm/1000 years are suggested.

The thickest offshore sediment sequence occurs where the shelf is narrowest (Fig. 12). Rough calculations of the total volume of sediment indicates that between Jervis Bay and Gabo Island, a distance of 240 km, there is about 2200 km^3 of sediment, compared with 1200 km^3 between Jervis Bay and Sugarloaf Point, a distance of 300 km. Further calculations indicate that in the southern area, most sediment on the shelf occurs south of Montague Island. It is clear, therefore, that the southern area has trapped much more sediment than the northern area. This can only be related to the rate and duration of sedimentation on a basement surface which was either originally deep or has subsided rapidly synchronous with deposition. Wellman & McDougall (1974) have shown that major tectonic uplift has affected the onshore, the intensity of which decreases from south to north and from west to east. A corresponding offshore subsidence might ensue, which, together with the opening of the Tasman Sea from the south (Hayes & Ringis, 1973), would result in a thicker sediment sequence in the south than in the north.

ORIGIN OF THE SEDIMENTARY SEQUENCE

Direct evidence is not available on the nature of the subsurface sediments. However, many workers have made suggestions as to the composition and depositional environment of the sediments forming typical continental shelf wedges elsewhere in the world (Dietz, 1963; Curray & Moore, 1964; Knott & Hoskins, 1968; Emery & Milliman, 1969; Rona, 1969; Swift, 1969; Stanley, 1969; Van Andel & Calvert, 1971; du Plessis et al., 1972). Very little evidence has been obtained from cores.

Shelf sediments have been classified as open shelf, slope, deltaic complex, and paralic complex. The deltaic

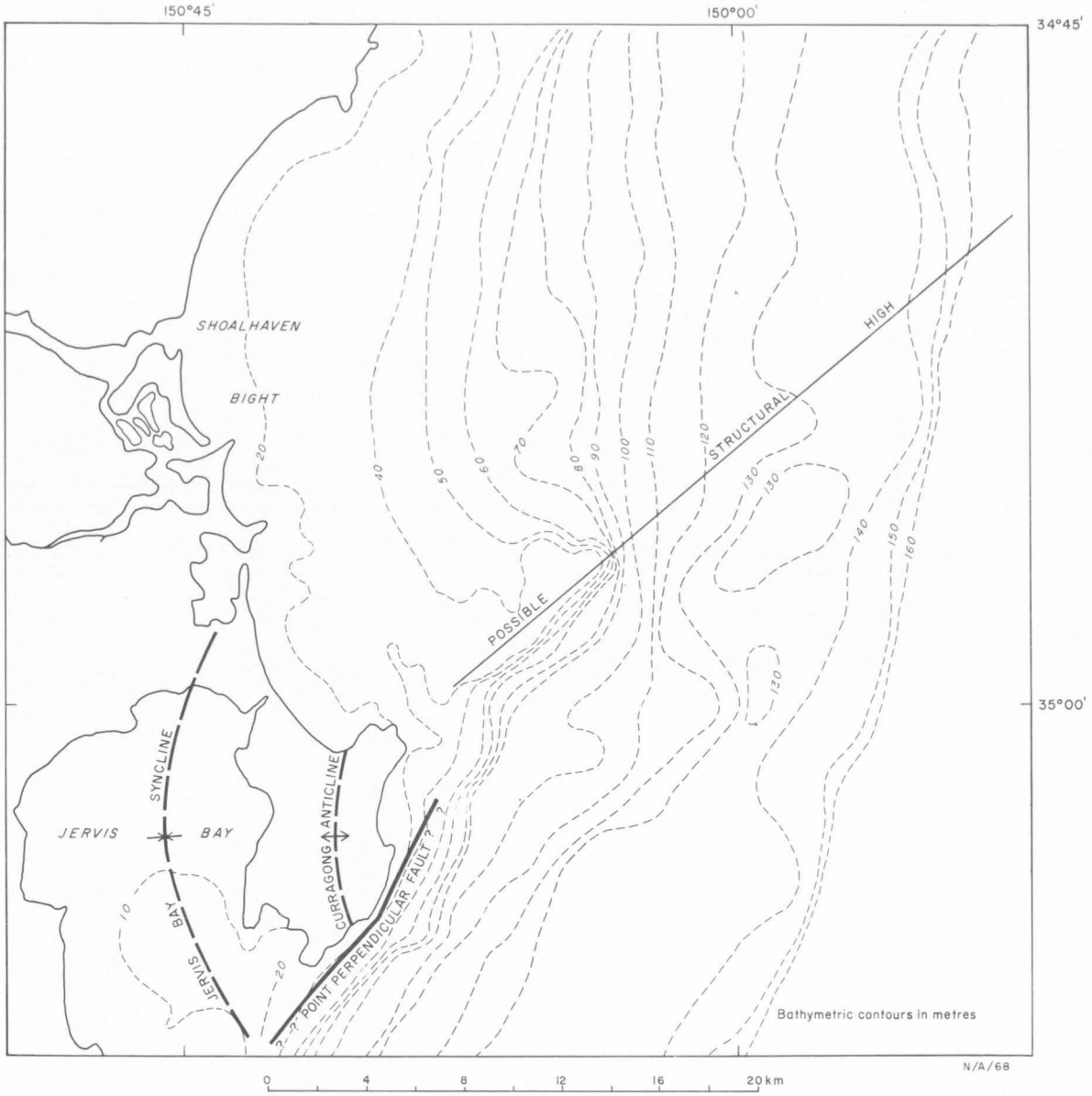

Fig. 14. Bathymetry and structure in the Jervis Bay/Shoalhaven Bight area.

complex may grade landwards into the paralic complex. Each sediment group is characterized by specific features (Table 2), some of which are recognizable in BMR seismic records.

Sediments immediately above basement (S2) generally show transgressive onlapping relations with it (Figs. 4B; 6C, E; 8D). This part of the sequence gives way upwards into one whose attitudes resemble shallow-dipping deltaic sediments. Both concave and convex reflectors are common and are usually truncated by S1 (Figs. 5A, B, C; 6C; 7B). This part probably represents a prograding sequence. The sequence between S1 and S2 therefore represents a transgressive phase followed by a prograding phase. The general parallelism of sediments to the basement step (Figs. 5A, B, C; 6A, B, C), the undulations in the sediments above a major change in basement slope (Figs. 6A, 7C), and the general parallelism of some unconformities to basement steps (Fig. 7C) all suggest some basement control over sediment attitudes. This control may be both syn-depositional and post-depositional. Sediments above S1 are generally prograding on it (Fig. 5B, C). They form regular reflectors which are laterally traceable for many kilometres. The division of the seismic sections into two sequences above and below S1 is visible in most profiles down to and including latitude 35°30′S. Reflector characteristics are similar to those described by Van Andel & Calvert (1971) in their shelf sediment model (Fig. 15A). However, in the east Australian sections, the sequence above S1, characterized by continuity of reflectors, flat bedding, and progradation, resembles previous descriptions (Table 2) of open-shelf sediments, probably climax sediments deposited either during a slowly rising sea level or during a relative rise in sea level where subsidence exceeds sedimentation. It is apparent, however, that this regime was terminated by the late Pleistocene low sea levels. An adaptation of the Van Andel & Calvert (1971) model, with some variations, is shown in Figure 16. In its simplest form (Fig. 16A), S1 separates two prograding units, i.e. the transgressive prograding cycle is not repeated. This suggests that the second transgressive phase was either

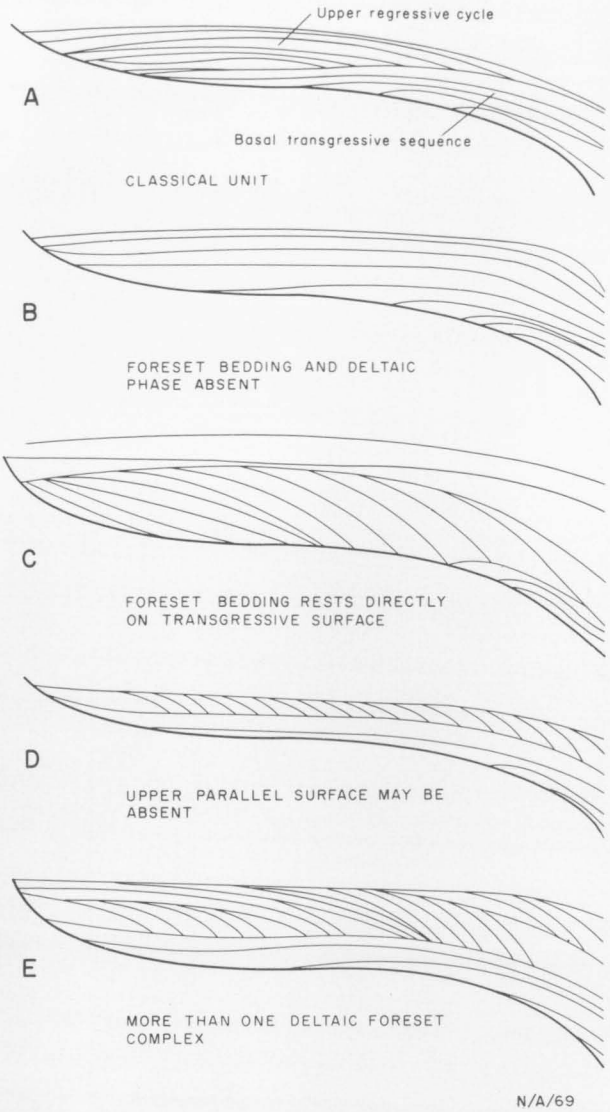

Fig. 15. Shelf sedimentation model of Van Andel & Calvert (1971). The classical sequence: A, shows an upper progradative regression unit resting on a lower basal transgressive unit. Variations on this theme include: B, absence of foresetting in the upper progradative unit; C, dominance of foresetting in the upper progradative unit; D, absence of the upper sequence conformable with the surface; E, the presence of more than one foreset complex in the upper progradative unit.

not deposited, has been removed by erosion, or is not discernible on the sections. It is likely, however, that the erosion giving rise to S1 was followed by rapid subsidence.

TABLE 2. FEATURES CHARACTERISTIC OF PRINCIPAL SEDIMENT COMPONENTS OF CONTINENTAL SHELVES

Open shelf	Even bedding Continuity of bedding Conformity with the present surface
Slope	Dip of 4° Convex upwards May be prograding
Deltaic complex	Dip of 7-9° Foresets are prograding Convex upwards Commonly forms a distinct wedge
Paralic complex	Gently dipping Discontinuous bedding

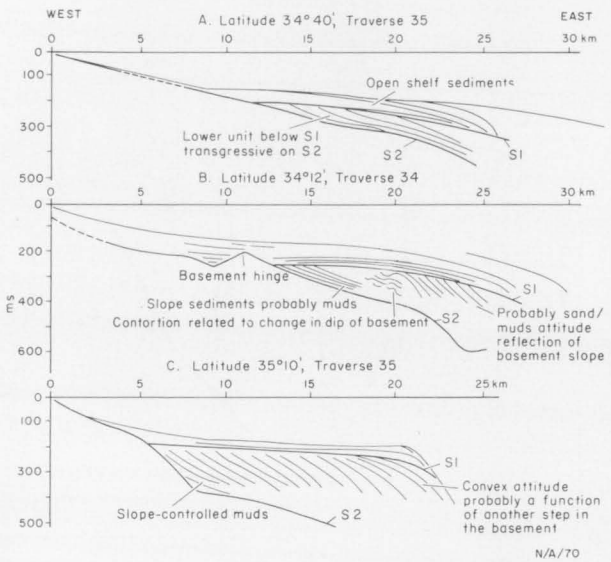

Fig. 16. Sediment sequences on the continental shelf of southeast Australia. Sections A, B, and C show two cycles similar to the Van Andel & Calvert (1971) model. However, in each section the transgressive part of the upper cycle cannot be identified.

MORPHOLOGY

Between Crowdy Head and Sydney, the width of the shelf out to the shelf break at about 165 m varies markedly. East of Port Stephens it is 52 km wide, increasing to 72 km east of Newcastle. Southwards it narrows to 26 km east of Botany Bay, and this trend continues to Montague Island where the shelf is only 17 km wide. From Montague Island to Gabo Island it widens to about 32 km.

General bathymetry

The bathymetry of the area is shown in Plate 1. Data sources for this compilation include RAN hydrographic charts, National Mapping profiles, and profiles obtained during the 1972 BMR cruise.

Phipps (1963) divided the continental shelf of southeastern Australia into two zones, the shore zone, and the outer shelf plain. The present work shows that over much of the area between Sugarloaf Point and Batemans Bay, three morphologic zones may be recognized (Pl. 1): an inner shelf shallower than about 60 m, a middle shelf zone between 60 and 130 m, and an outer shelf zone deeper than 130 m. Some variations in the depth limits of each zone are apparent. North of Swansea, the 40-m isobath separates a gently sloping inner zone from a steeply sloping middle-shelf zone, while south of Swansea the 30-m isobath separates a steeply sloping inner zone and a gently sloping middle-shelf zone. The inner zone is best developed

between Sydney and Montague Island. It ranges in width from 0.5 to 8.0 km, is widest east of Shoalhaven Bight and Wreck Bay, and narrowest east of Botany Bay and Beecroft Peninsula. South of latitude 36°50′S, a marked change in slope occurs at the 20-m isobath.

The middle-shelf zone is best developed north of latitude 36°30′S. It is generally characterized by a steeper slope and prominent terracing. Major breaks of slope occur between 60 and 120 m. This middle shelf zone is 16 km wide east of Wollongong and Shoalhaven Bight, but is only 6 km wide east of Beecroft Peninsula. The steep slope may extend over the depth range 40-120 m, or may be localized between 40 and 50 m, as to the east of Bass Point and Botany Bay. South of latitude 36°30′S, a steep slope extends from 20 to 70 m, after which it flattens out eastwards of the 90-m isobath.

North of Newcastle, the 130-m isobath marks the beginning of a gently eastward-sloping terraced area, termed the outer shelf plain by Phipps (1963). In this northern area, the outer-shelf zone lies between 130 and 140 m and is 16 km wide. Southeast of Port Stephens a large embayment of the 140-m isobath can be correlated with a basement high. Between Newcastle and Norah Head, the major break of slope occurs between 110 and 120 m, but south of Norah Head it coincides once again with the 130-m isobath. In this same area, the outer-shelf zone slopes gently eastward for 6 km, a pronounced change of slope occurring at 140 m. Between Port Jackson and Jervis Bay the outer-shelf zone averages 7-8 km in width and is widest east of Bulli and Shoalhaven Bight. In the south, a marked break of slope occurs between 140 and 160 m but this steepening diminishes northwards. South of Jervis Bay and north of latitude 36°30′S, the outer-shelf zone begins at the 110-120-m isobaths. Slopes are generally gentle between 110 and 140 m, but southeast of Ulladulla steeper slopes occur between 120 and 130 m. South of latitude 37°10′S the outer shelf zone begins at the 90-m isobath.

East of Shoalhaven Bight, a pronounced eastward bulge of the 130-m isobath appears to link up with the ridge trending northeast from Beecroft Peninsula, as shown by the 40-m isobath. A topographic high therefore extends northeast from Beecroft Peninsula to the edge of the shelf.

Terraces

Terraces, nick points, and breaks of slope are common on the shelf of southeast Australia. They are better displayed between Sugarloaf Point and Jervis Bay than south of Jervis Bay (Pl. 2). The frequency distributions of terraces (Fig. 17) indicates three major groupings: shallower than 60 m; between 70 and 110 m; and between 110 and 150 m. The excellent north-south correlation, especially in the offshore Sydney Basin, is in general disagreement with conclusions put forward by Phipps (1966).

Shelf break and upper slope

The shelf break is 'an obvious steepening of the gradient between the continental shelf and the continental slope' (Gary et al., 1972). The configuration of the shelf break along most west-to-east sections is shown in Figures 18 to 21. The shelf break may form a sharp well-defined feature and may coincide with a terrace or a series of terraces. However, over much of the area between Port Jackson and Sugarloaf Point the gradient from the outer shelf to the upper slope gradually increases, so that the position of the shelf break may be identified with less certainty. The north-to-south variations in the depth of the shelf break are shown in Figure 22.

The steepest inclination of the upper continental slope noted in this region is 14°. North of Jervis Bay it is generally less than 2°, except near latitude 34°10′S

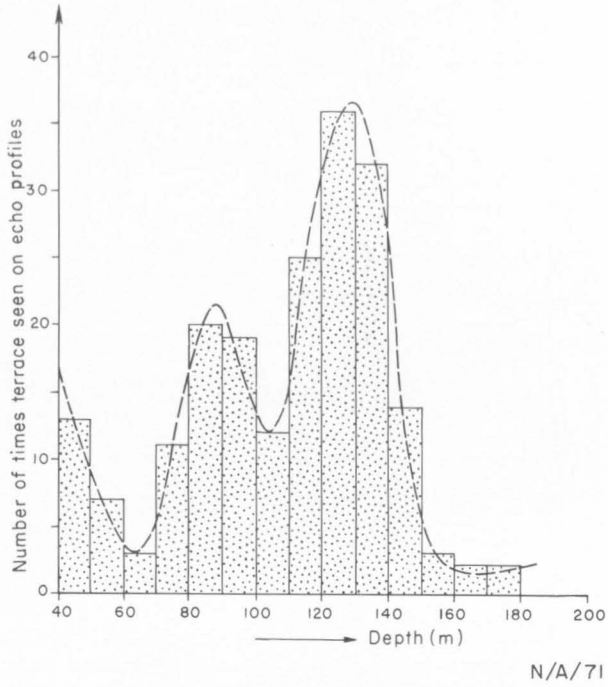

Fig. 17. Frequency of occurrence of terraces on the continental shelf as seen in BMR 1972 echo profiles.

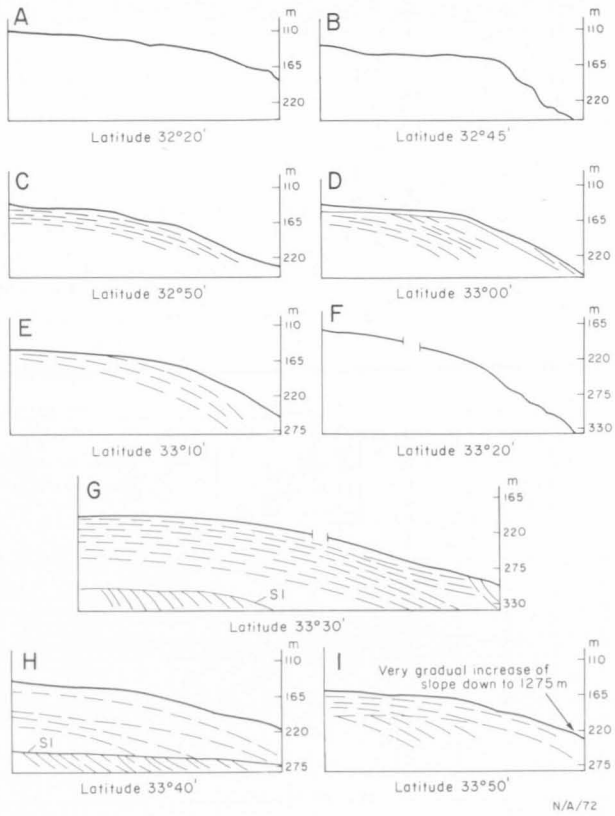

Fig. 18. Seismic profiles across the outer continental shelf between latitudes 32°20′S and 33°50′S. Attitudes of subsurface reflectors are also shown.

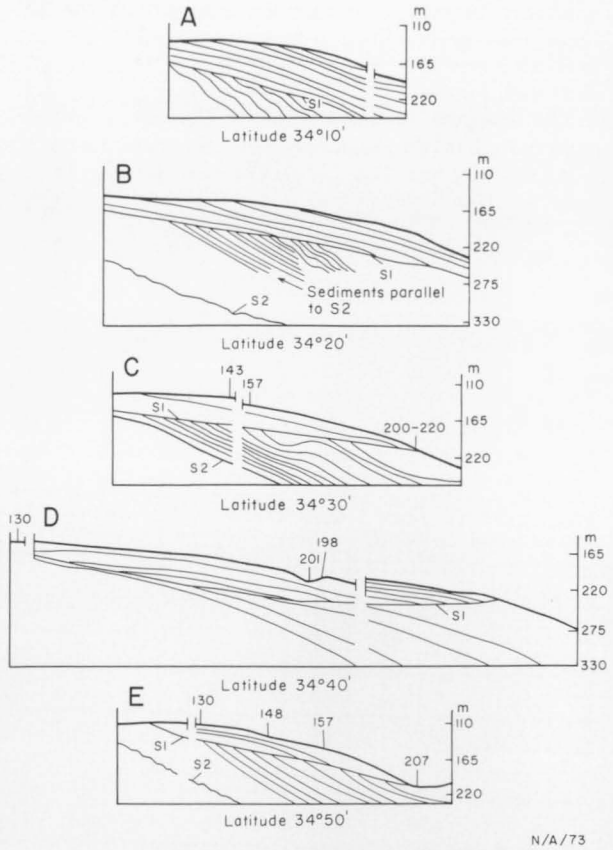

Fig. 19. Seismic profiles across the outer continental shelf between latitudes 34°10′S and 34°50′S. Attitudes of subsurface reflectors are also shown.

where it is more than 4°. The inclination of the slope progressively increases south of Jervis Bay, so that slopes of more than 10° are common, especially south of Montague Island. Terraces or notches on the upper continental slope occur at many depths (Fig. 17).

Submarine canyons

Ten submarine canyons or canyon-like features were identified between Jervis Bay and Bermagui; some may be tributaries of the same canyon system. Their positions are shown in Figure 23. Deep-water bathymetry (Fig. 24) is taken from the general Bathymetric Chart of the Oceans 1:1 000 000 Sheet No. 443. These canyons have been given informal names to facilitate description. Depths described in the text relate to data on the figured profiles.

Canyons east and southeast of Jervis Bay. Three canyons crossed in this area are named informally Beecroft canyon (Fig. 23-1), Perpendicular canyon (Fig. 23-2), and St George canyon (Fig. 23-3) from prominent shoreline features. Echo-sounder profiles across these canyons are shown in Figure 25.

Figure 25 shows a profile across the *Beecroft canyon.* The canyon consists of a wide upper portion, and a V-shaped lower portion from 530-728 m. The two parts are separated by a broad gently inclined terrace on the north side, and a much narrower terrace on the south side at about 550 m.

The profile across *Perpendicular canyon* is shown in Figure 25. Perpendicular canyon is morphologically similar to Beecroft canyon. It is typically V-shaped, and has shoulders at 379 m and 366 m. Its bottom, which is flat-floored, is at 596 m. Some irregular relief is present on the northern shoulder. The canyon is 1.0 km wide across the shoulders, and 0.25 km wide across the floor. It is possible that Beecroft and Perpendicular Canyons form one system and coalesce farther east.

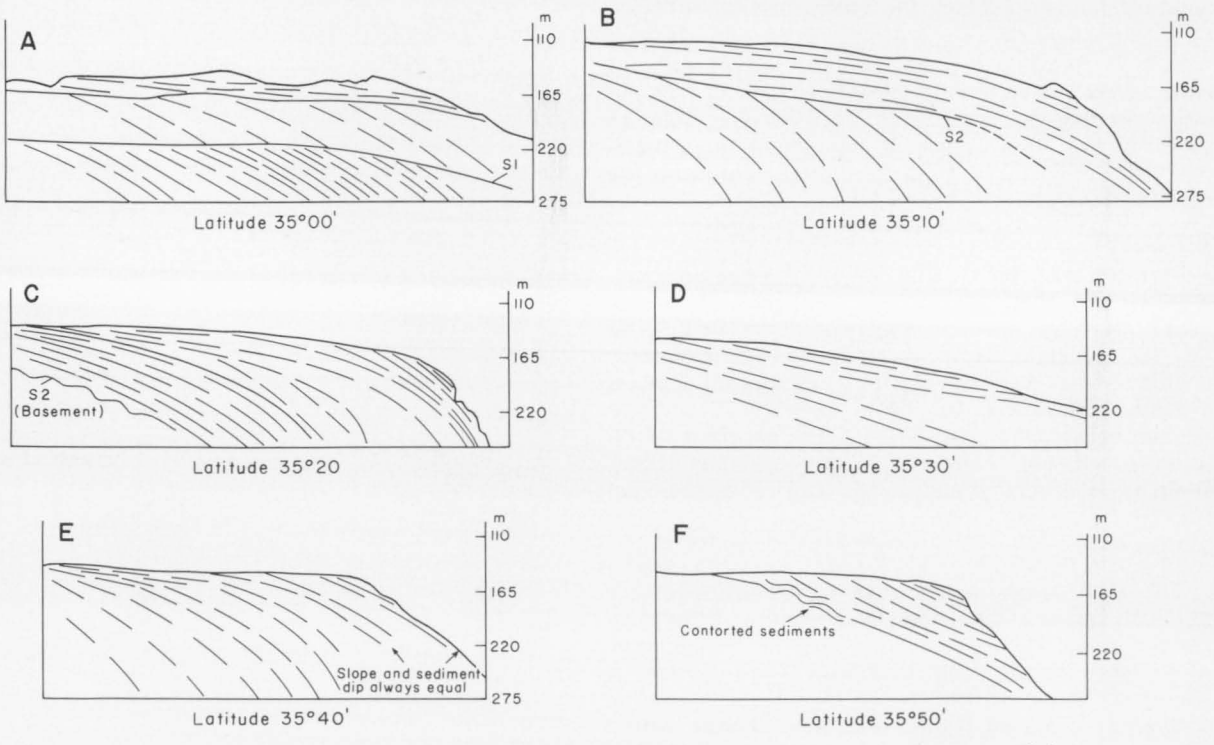

Fig. 20. Seismic profiles across the outer continental shelf between latitudes 35°00′S and 35°50′S. Attitudes of subsurface reflectors are also shown.

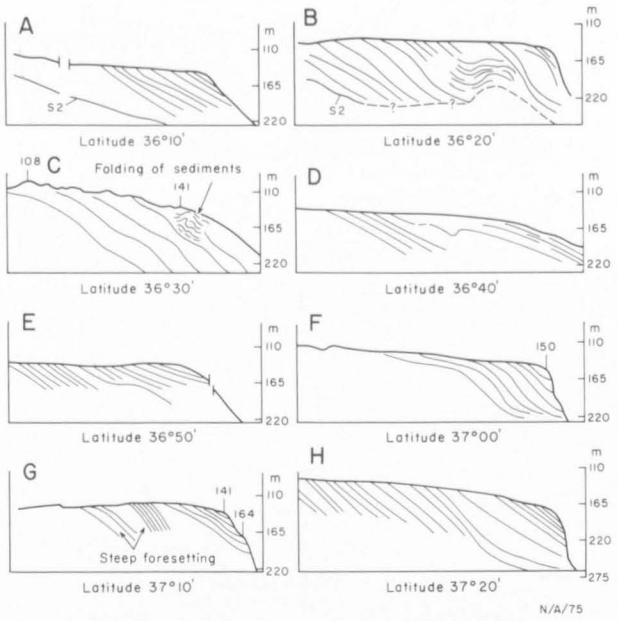

Fig. 21. Seismic profiles across the outer continental shelf between latitudes 36°10′S and 37°20′S. Attitudes of subsurface reflectors are also shown.

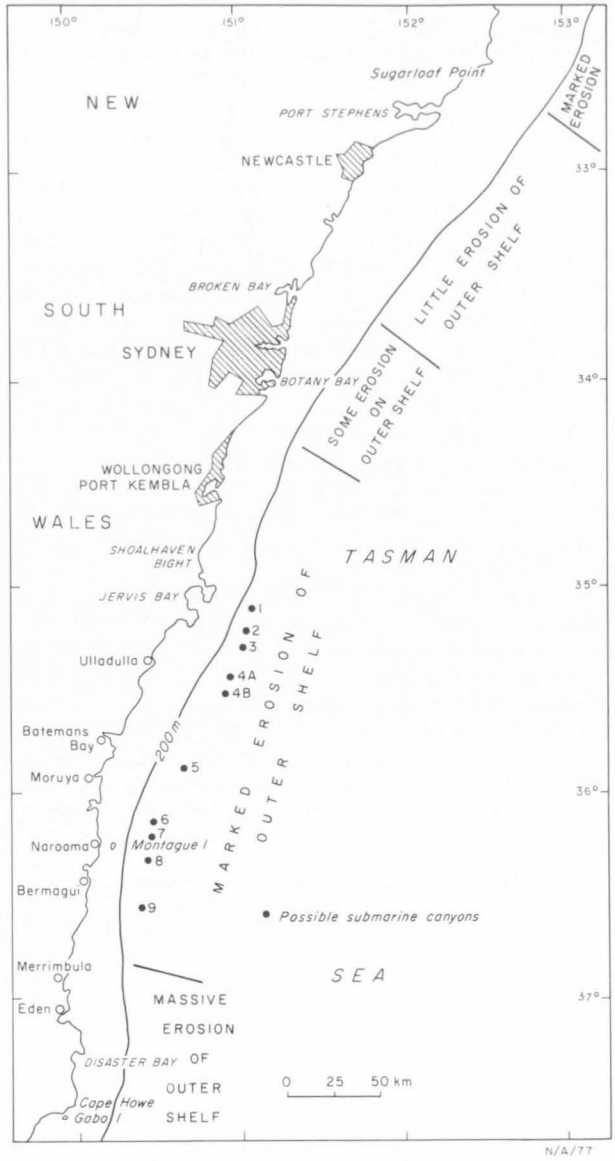

Fig. 23. Location of submarine canyons (indicated by numerals) and outer shelf areas affected by erosion or deposition. 1 = Perpendicular; 2 = Beecroft; 3 = St George; 4AB = Conjola; 5 = Batemans Bay; 6-8 = Tuross (A+B) and Moruya; 9 = Bermagui.

St George canyon (Fig. 25) is much smaller than the Beecroft and Perpendicular canyons. It is 1.0 km wide, and has its southern shoulder at a depth of 370 m and its floor at 448 m. The V-shaped cross-section is absent and the feature is probably a canyon head.

Conjola canyons A and B. Two canyon-like features were crossed to the east of Lake Conjola which is close to Ulladulla (Fig. 23-4A & B). Phipps (1963) has described a canyon east of Ulladulla but it is not known if his Ulladulla canyon is the same as either of the features described here.

Although both features are called canyons, Conjola A does not have the typical canyon section (Fig. 26A). However, both are figured because they occur in close proximity in an otherwise undissected continental slope. The shoulders of both canyons are at a depth of about 415 m. Conjola A is about 2.0 km wide, and Conjola B is only 0.5 km wide.

Batemans Bay canyon. The echo profile across the Batemans Bay canyon (Fig. 23-5) is shown in Figure 26. On the north side of the canyon the shelf break is

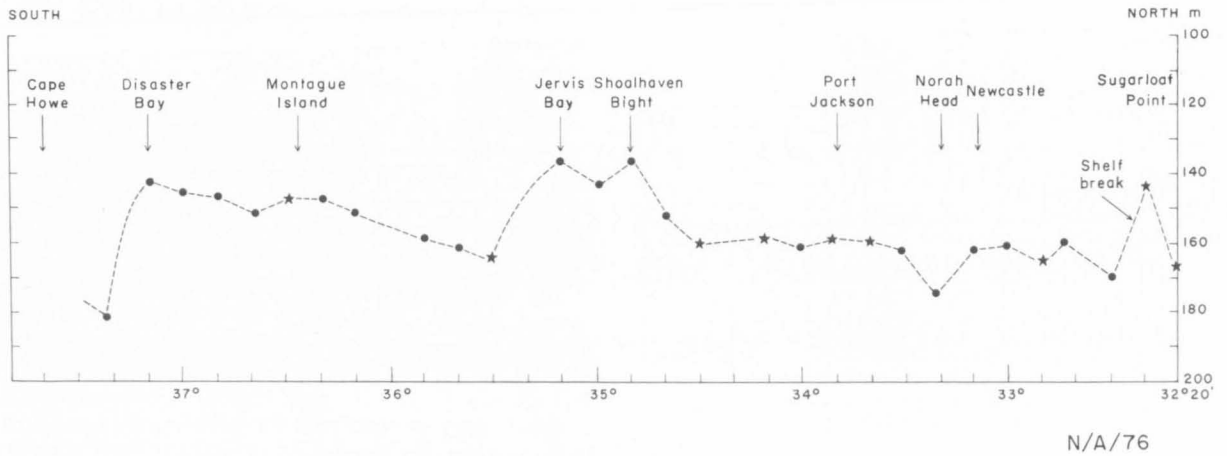

Fig. 22. South-to-north variation in the depth of the shelf break. Closed circles represent localities where the shelf break is easily identified. Stars represent localities where the shelf break is gradational.

followed by a steep descent down to at least 385 m. The canyon shoulder on the north side is at 440 m, and on the south side it is at 545 m. The canyon is 8.0 km wide and its floor is at a depth of 640 m. The deepest part of the canyon is beneath the southern wall. The floor to the north is irregular, possibly indicating that it is underlain by sediments which have slumped down the northern slope. The canyon walls, however, are relatively smooth. They are not stepped in the manner described by Phipps (1963). Although the north-south profile shows an atypical canyon shape, the probability that the feature forms part of a large canyon system is supported by the continental slope bathymetry which shows a canyon system extending down to 4500 m.

Moruya and Tuross canyons. Three canyon-like features (Fig. 23-6, 7, 8) crossed during seismic traverse 21 are shown in Figure 27. The depths to the canyon floors are 640 m (Moruya canyon), 585 m (Tuross A), and 695 m (Tuross B). Tuross B with the typical V-shaped cross-section is probably a true canyon, but the others are probably the heads of small tributary canyons. All three may merge to form a significant feature to the east. Tuross B canyon is about 3 km wide. The profile (Fig. 27A) shows a gentle, stepped southern slope; steps occur at 530, 570, and 636 m. The northern slope is steeper, and has steps at 530, 570, and 599 m. The lower part of the canyons forms a deeply incised V. It appears that the steps can be approximately correlated from canyon to canyon,

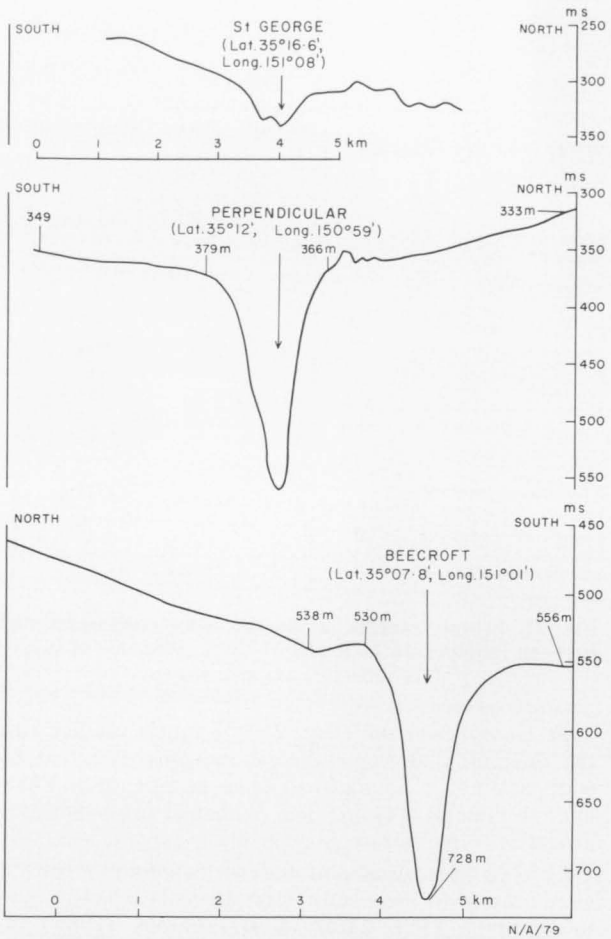

Fig. 25. Bathymetric profiles across St George, Perpendicular, and Beecroft canyons. The locations of the canyons are shown in Figure 23.

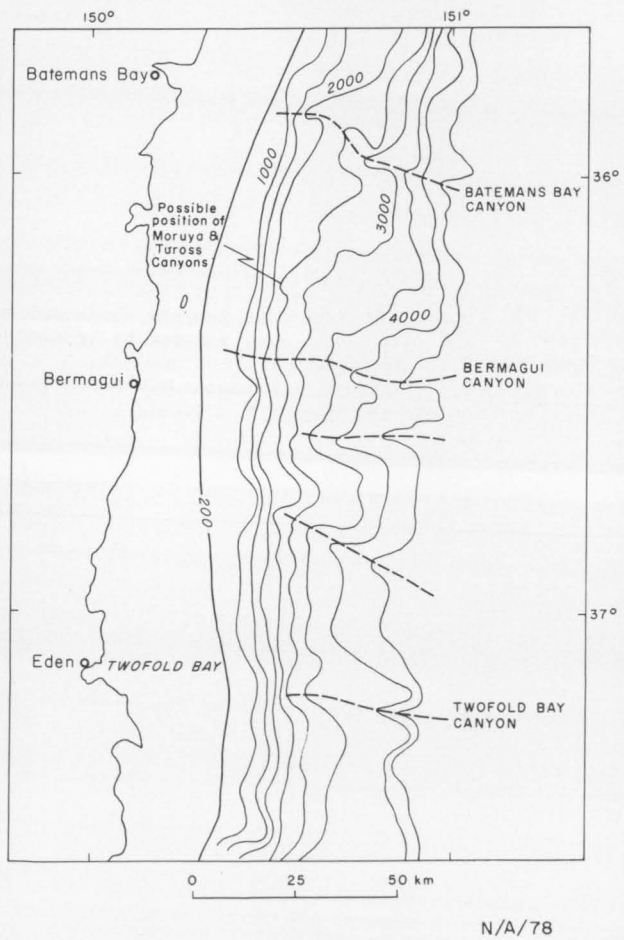

Fig. 24. Bathymetry of the outer continental margin south of 36°S. Depths are in metres.

suggesting that they form part of the same system and have been subject to similar conditions of formation.

Bermagui canyon. The position of the Bermagui canyon is shown in Figure 23-9 and a section across the canyon in Figure 27B. The canyon is 6.0 km wide between shoulders whose depths are both 472 m. It is symmetrical, with a flat floor 1.0 km wide at a depth of 695 m. Steps occur on the south side at 629 m, and on the north side at 644, 549, and 490 m. The canyon is cut into the prograding sediments forming the continental slope. Nowhere is it seen to cut into basement. It heads above 120 m, i.e. above the shelf break, which in this area is at a depth of 140 m.

Large canyon systems

Bathymetric contours on the continental slope (Fig. 24) indicate large canyon systems southeast of Batemans Bay, southeast of Bermagui, and east of Twofold Bay. Echo and seismic profiles at a depth of 300 m east of Twofold Bay did not reveal a canyon, so presumably it heads below this depth.

The Batemans Bay, Bermagui, and Twofold Bay canyon systems may extend to a depth of 4500 m (Fig. 24). Conolly (1969) reported coalescing sediment fans at the base of the continental rise south of Jervis Bay. It seems unlikely that erosion attributed wholly to Quaternary events could be sufficient to form such large features to depths of 4500 m. Both Conolly (1968) and Von der Borch (1968; 1972) suggest a pre-Pleistocene age for canyon initiation.

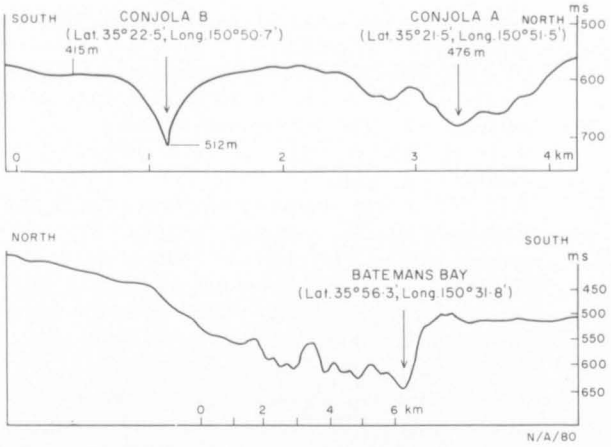

Fig. 26. Bathymetric profiles across Conjola A and B and Batemans Bay canyons. The locations of the canyons are shown in Figure 23.

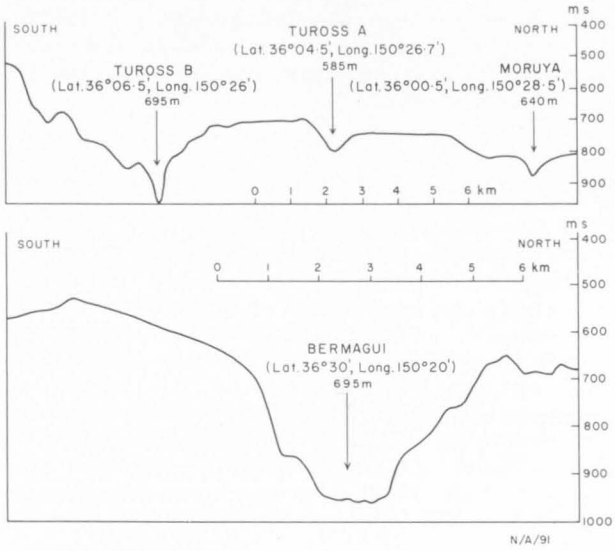

Fig. 27. Bathymetric profiles across Tuross A and B, Moruya, and Bermagui canyons. The locations of the canyons are shown in Figure 23.

Three major unconformities have been detected in the seismic sections in the area south of Jervis Bay. This suggests that erosion, slumping, and the formation of new slopes have occurred several times in the past. These are likely to be pre-Pleistocene.

On balance the evidence is thought to indicate a pre-Pleistocene age for the start of canyon formation although extensive downcutting is likely to have occurred during the Pleistocene, and in the case of the Bermagui canyon system to have continued after the Holocene transgression began.

Phipps (1963) postulated a Pleistocene age for the initial formation of canyons east of Jervis Bay and Ulladulla. The present work has produced little evidence bearing on their age of formation.

Shelf break, terracing, and eustatism

The classical theory of continental shelf development made use of the concept of the marine profile of equilibrium and envisaged an inner wave-cut terrace or abrasion platform merging seawards with a wave-built terrace of delta-like form. This concept of the marine profile of equilibrium and wave base at the shelf margin has since been challenged in a series of closely argued papers (Dietz & Menard, 1951; Dietz, 1952, 1963), and it is now generally believed that the gross morphology of the shelf and shelf-break are related to Pleistocene eustatic low sea levels and not to modern conditions (Curray, 1969).

While it has been recognized that the morphology of the outer shelf and shelf break may have been modified by local influences such as ice-scouring in high latitudes, deltaic deposition, and local current activity, the relatively constant depth of the shelf break around the continents has led most geologists to relate it to eustatic events, usually to the last glacial maximum, and to attribute variations in its depth to subsequent sedimentation, differential compaction of sediments, erosion, isostatic movements, and tectonism during the Holocene.

Assuming a eustatic origin for the shelf break off southeast Australia, Phipps (1966) postulated that variations in its depth are a result of tectonic warping since the late Pleistocene. Phipps (*in* Thom et al., 1972) has since revised his rate of warping, suggesting that it may date back to the Tertiary. This theory is based on the presumed eustatic / erosional origin for the shelf break and the suggestion that terraces at depths shallower than the shelf break are not depth-correlatable, i.e. they have been differentially warped. The recognition of the shelf break as a geological datum line owing its origin to one event at one time is crucial to the argument.

The relations between subsurface dips and outer-shelf morphology suggest that the shelf break may be both a depositional and an erosional feature. In eight of the west-to-east sections (Figs. 18-21) the sea-bottom and subsurface sediment reflectors are parallel, indicating that the shelf break is a transitory, depositional, prograding feature, precursors of which can be recognized in the subsurface. These concordant relations between subsurface reflectors and sea-floor are best seen between Newcastle and Sydney where the shelf-break is at its deepest and was probably unaffected by erosion during low stands of sea level. Twenty west-to-east sections indicate that erosion of subsurface units has occurred on the outer shelf. This may have affected only the outer shelf (Fig. 19A, B, C), only the upper slope (Fig. 20C, E), or may have been widespread, affecting all parts of the outer shelf and upper slope (Figs. 19A-E, 20A, F). Erosion of the outer shelf may be the result of surf action during a lower sea level, local current activity in the past or at present, or mass movement and slumping on unstable slopes. Erosion affecting only the outer-shelf zone is dominant between Sydney and Shoalhaven Bight, and suggests that while most of the outer shelf came within the influence of a lower sea level, it was below sea level, and the shelf break itself was outside the influence of surf-base erosion. Those parts of the shelf where erosion has affected the outer shelf, shelf break, and upper slope (north of Newcastle and south of Shoalhaven Bight) are also the areas where the shelf break is shallowest (Fig. 22) and probably represent areas which were well within the range of surf-base erosion during lower sea levels. South of Jervis Bay, the southward shallowing in the depth of the outer shelf, and the increase in the severity of erosion in the same direction are probably related. The area was probably markedly affected by surf-base erosion. It is clear that the outer-shelf zone and shelf break owe their formation to both depositional and erosional processes. These may be unrelated in time, and as such negate the assumption that the shelf break has

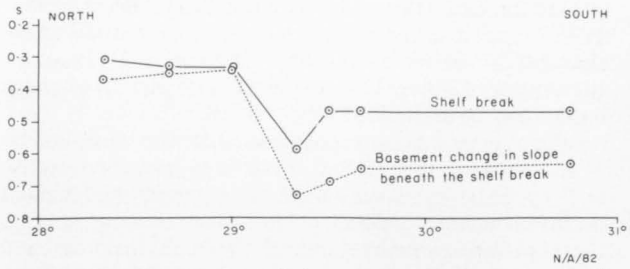

Fig. 28. North-to-south variations in the depth to the shelf break, and the basement change in slope beneath the shelf break (from Jones et al., 1975).

formed as a result of one process related to a single eustatic event.

The depth of the shelf break off southeast Australia is related to the depth of basement (Fig. 28), and the morphology of the outer shelf is related to morphological variations in a surface which is the little-modified Atlantic-type rift scar produced during sea-floor spreading in the Cretaceous (Jones et al., 1975). The same authors stated that where large volumes of sediment covered basement, the effect of basement on present-day morphology was obliterated. However, between Sugarloaf Point and Jervis Bay, the basement variations are still reflected in the present surface in spite of a thick sediment pile. The north-south variations in the depth of the shelf break (Fig. 22) show morphological highs southeast of Sugarloaf Point and northeast of Jervis Bay, and a low southeast of Newcastle. These correspond with similar basement features (Figs. 11, 13) described earlier. Therefore, in spite of progradation and surf-base erosion, basement morphology still has an affect on the present-day variations in the depth of the shelf break. To assign depth variations in the shelf break to warping is therefore incorrect.

Terraces over this part of the New South Wales shelf (Pl. 2) and farther north (Jones, 1973a and b) appear to be characterized by uniformity of depth over large distances, which suggests that they form part of a surface largely unaffected by major tectonic warping. It is likely, however, that differential compaction has affected the sediments, and that eastward tilting accompanying glacially controlled transgressions and regressions has affected both the rigid basement and the plastic sediment pile.

SEDIMENTOLOGY

Shirley (1964) studied sediment grab samples collected between Crowdy Head and Batemans Bay, and concluded that inshore sediments are coarse, middle-shelf sediments are muddy, and outer-shelf sediments are predominantly coarse and calcareous. He concluded also that the shells of the outer zone live in that depth at the present time; that mud to the east of Newcastle is derived from the Hunter River; and that sand to the east of Broken Bay is derived from the Hawkesbury River. Grainsize variations were considered only in terms of medium and coarse sands. The mineralogy and constitution of the sediments were not described. In the present work, grab samples were collected on an 18-km grid (Pl. 1), but closer sampling intervals were used in selected areas. Station data and sample descriptions are shown in Appendix 1. Two factors must be borne in mind during the interpretation of the sample data: *a.* the sampling pattern, and *b.* the samples represent a mixture of the top 5-10 cm of bottom sediment.

Methods. In the laboratory, samples were oxidized with hydrogen peroxide, washed, and air-dried at 50°C. A preliminary analysis of grainsize distribution was performed by wet sieving into three fractions, greater than 2 mm, 2.0-0.062 mm, and less than 0.062 mm. The calculated percentages of gravel, sand, and mud form the basis of an understanding of grainsize variation. The gravel fraction was further seived into 9 fractions (—5.25, —4.25, —3.25, —2.25, —2.0, —1.75, —1.25, and —1.0 ϕ) and the percentage of each fraction determined. Grainsize distribution within the sand fraction was derived with a settling tube, the design and mechanics of which have been described by Mayo (1972). The mud fraction was analysed by standard pipette analysis, and the total grainsize data were programmed through a CTC 3600 computer (Mayo, op. cit.). Final output consisted of standard parameters (mean, standard deviation, skewness, and kurtosis), percent sand, gravel, silt, and clay, and a graphical representation of the frequency distribution. Problems associated with the interpretation of frequency curves using composite data have been treated by Russell (1968) and Marshall (in press).

Statistical parameters used in the interpretation of the sediments are the sample mean (Pl. 3A) and the sample standard deviation (Pl. 3B). The sample mean was determined algebraically by the method of moments and used to give a better idea of sediment-size distribution compared to that shown in Plate 1. The inclusive graphic standard deviation has been shown by Folk (1968) to be a good measure of sorting (Pl. 3B).

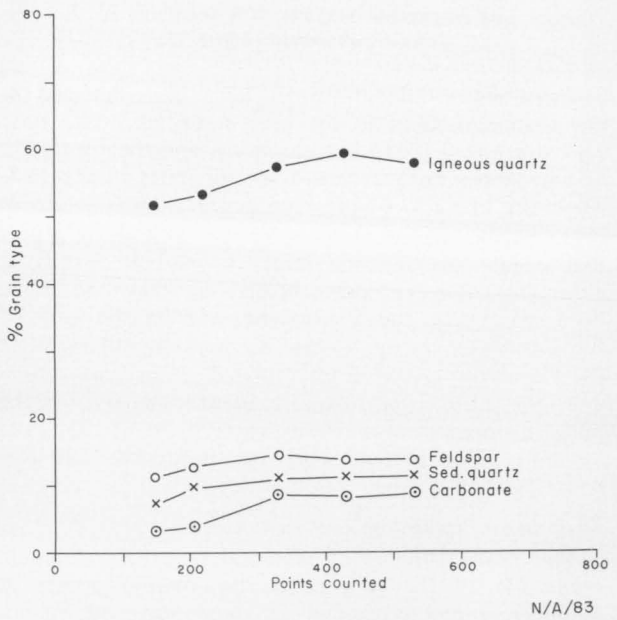

Fig. 29. Plot of number of points counted against percent grain types of the shelf sediments. The graph shows that the optimum number of point counts in medium to coarse sands is about 500.

The mineralogy of individual samples was described by means of impregnated thin sections viewed with a petrological microscope. An approximation of the volumetric percentages of individual components was obtained by use of a Swift Point Counter. The theory of point counting has been dealt with by Chayes (1956) and Demirmen (1971). In the present work 300 to 500 points per sample were counted. The accuracy of the result was not significantly increased by increasing the number of points counted (Fig. 29).

Terrigenous components

Quartz. Total quartz in the sediments ranges from 2 to 82 percent of the sample (Appendix 2). Five different quartz types were identified:

Igneous quartz. Normally large angular to subrounded grains (Fig. 30) with straight or slightly undulose extinction. When forming parts of composite grains they usually show a granitic or graphic texture.

Volcanic quartz. Large partly euhedral grains, zoned (Fig. 31).

Metamorphic quartz. Recognized either by strongly undulose extinction, or by the occurrence of composite grains intergrown with foliated micas.

Vein quartz. Identified by abundant inclusions and vacuole trains.

Sedimentary quartz. This falls into two major categories: either large rounded to subrounded polymictic grains (Fig. 32), or small axelike grains (Fig. 33). The first group commonly exhibit impact fractures and regular and irregular syntaxial rims.

The degree of roundness of the quartz grains varies greatly, even within one sample (Fig. 30). This is especially seen in samples collected between Broken Bay and Norah Head.

The proportion of quartz in the sediment decreases uniformly with distance from the present shoreline (Fig. 34B). This suggests that barriers to quartz migration did not exist. It further suggests that the offshore distribution of quartz is a function of distance from the source, and dilution by calcium carbonate. The distribution of major quartz types shows a marked provinciality in the inner-shelf zone (Appendix 2). Plutonic quartz is predominant over sedimentary quartz between Jervis Bay and Eden, whereas the reverse is true between Jervis Bay and Newcastle. The local influx of volcanic quartz east of Port Kembla is probably related to Permian volcanic rocks. Plutonic quartz also makes an important contribution between Newcastle and Crowdy Head. This provinciality suggests that at least in the inshore sediments there has been little longshore mixing. In the middle-shelf and outer-shelf zones, most quartz is sedimentary. However, plutonic quartz forms an appreciable part of total quartz on the outer shelf

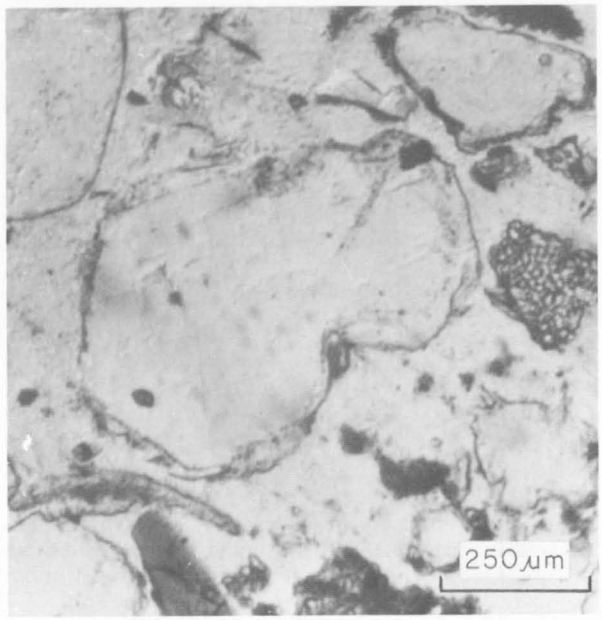

Fig. 31. Photomicrograph at station 1646, depth 86 m, showing subhedral volcanic quartz fragment. Ordinary light. (m 1623.)

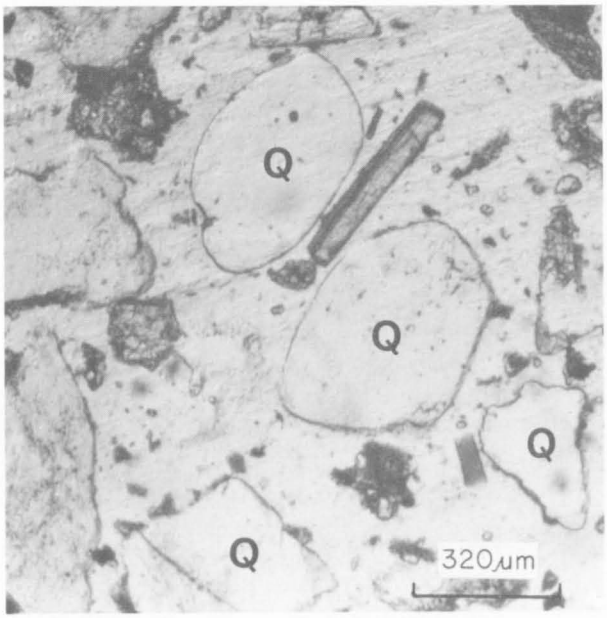

Fig. 30. Photomicrograph at station 1717, depth 124 m, showing well rounded, angular, and corroded quartz grains. Ordinary light. (m 1623.)

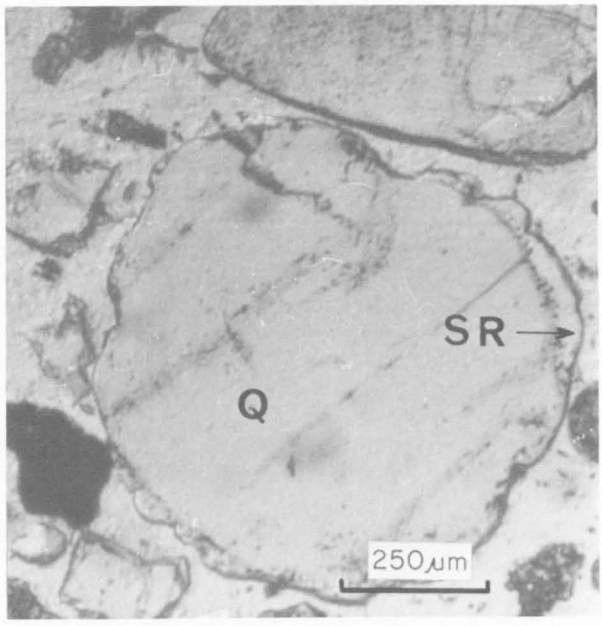

Fig. 32. Photomicrograph at station 1711, depth 60 m, with quartz grain showing irregular syntaxial rim. Ordinary light. (m 1623.)

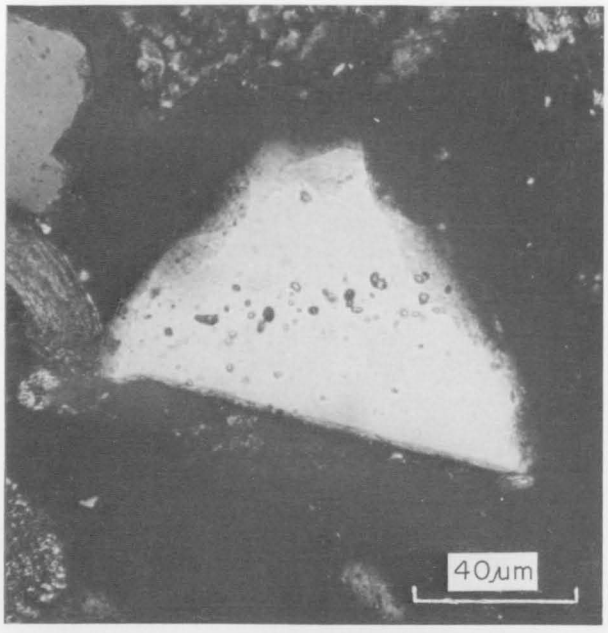

Fig. 33. Photomicrograph at station 1706, depth 115 m, showing axe-like quartz grain in the mid-shelf muds. Crossed nicols. (m 1664.)

east-southeast of Port Stephens, and east of Montague Island. Off Port Stephens, it is likely to have been derived from the nearby outcrop of the Port Stephens/Sugarloaf Point basement high; off Montague Island, the concentration of plutonic quartz was probably derived from the Montague Island granite. In the middle-shelf zone sediments between Port Kembla and Newcastle, distinction can be made between two types of sedimentary quartz (Fig. 62): sandstone quartz south of Sydney and southeast of Newcastle, and shale quartz between Newcastle and Sydney. The shale quartz probably relates to the onshore exposures of Wianamatta Group shale and the Narrabeen Group.

Rock fragments. Rock fragments occur in most samples. Five types are most common:

Igneous rocks. Granitic rock fragments occur most commonly, but a syenite occurred in one sample. Volcanic fragments are usually altered to a mixture of chlorite surrounding laths of andesine feldspar. Such volcanic fragments are undoubtedly basic, the included hornblende having undergone extensive alteration.

Sedimentary quartzite or slightly impure sandstone. In sedimentary quartzite, adjacent quartz grains have microstylolitic contacts suggesting burial and load pressure solution. In slightly impure sandstone, mud-grade material or some mica occurs between the quartz grains, which are usually in tangential contact.

Calcareous sandstone occurs rarely. Quartz grains are generally cemented by a poikilitic carbonate cement (Davies, 1971).

Limestone clasts are of two types: true intraclasts or extraclasts, in which the allochems are cemented by drusy or granular calcite; and silicified limestone fragments in which allochems are seen only as outlines.

Shale or siltstone, which sometimes show a trace of bedding.

The proportion of rock fragments in the sample ranges from 1 to 9 percent, except a single sample from south of Crowdy Head, which contained 32 percent. Rock fragments are most abundant in the inshore sediments, and almost everywhere diminish eastwards. The plot of rock fragments varying with depth shows a percentage decrease to about the 60-m mark, below which the proportion of rock fragments varies randomly (Fig. 34A).

Feldspars. Feldspars range from 1 to 14 percent and average about 4 percent of the sediments. Highest values occur in the close-inshore sediments between Merimbula and Montague Island, and decrease sharply seawards. It is noticeable that this increase occurs rapidly, so that in most of the middle-shelf and outer-shelf sediments feldspars form less than 1 percent of the total sediment. Throughout most of the area north of Jervis Bay, the middle-shelf and outer-shelf sediments have a much higher feldspar content than their southern counterparts. High values are noticeable in the close-inshore sediments northeast of Jervis Bay, east of Port Kembla, and east of Crowdy Head. Over much of the area between Sydney and Sugarloaf Point, feldspar values are lower in the close-inshore sediments than in the middle-shelf sediments.

Orthoclase, albite, and andesine are the three commonest feldspars (Figs. 35, 36). Most of the feldspars are fresh or only slightly altered, and round to subangular. Few feldspar clasts are sericitized. In one sample, carbonate partly replaces calcic feldspar (Fig. 36). The feldspars are of plutonic or volcanic origin. A zoned, partly rounded feldspar in samples east of Sydney suggests a volcanic source. Exceedingly fresh albite and orthoclase in sediments northeast of Sugarloaf Point suggest a plutonic source, possibly in the Lachlan Fold Belt, but more likely from granites intruding the Carboniferous volcanics west of Gloucester. Between Sydney and Port Stephens, low feldspar values generally occur in sediments whose quartz content suggests a shale source.

Carbonate components

The total carbonate in the sediments ranges from 3 to 96 percent. These values, obtained by modal analysis of thin sections, do not correlate well with values obtained by chemical analysis. The difference between the two methods varies from 2 to 21 percent, and is probably caused by the thin sections not being fully representative of the bulk sample. The distribution of carbonate, calculated by chemical analysis, is shown in Figure 65A. In general, the contours show an increase in carbonate away from the shore, the outer-shelf sediments containing more than 80 percent carbonate.

Molluscs. The proportions of molluscan material range from 1 to 39 percent of the total sample, and average 17 percent. Almost all are highly abraded (Figs. 37, 38), prismatic, or foliaceous. Mollusc fragments increase significantly with depth. Pelecypods are by far the most important group, scaphopods are rare, and gastropods almost absent (Fig. 39). Most molluscan fragments have undergone extensive algal boring (Fig. 38). Silicification has affected some clasts, but not to the same degree as other carbonate grains.

Echinoderms. Echinoderms constitute 1 to 9 percent of the sediments, and average 3.6 percent. No discernible variation with depth occurs. The highly porous echinoderm skeletal debris makes such fragments ideal sites for the precipitation of glauconite (Fig. 40) and silica.

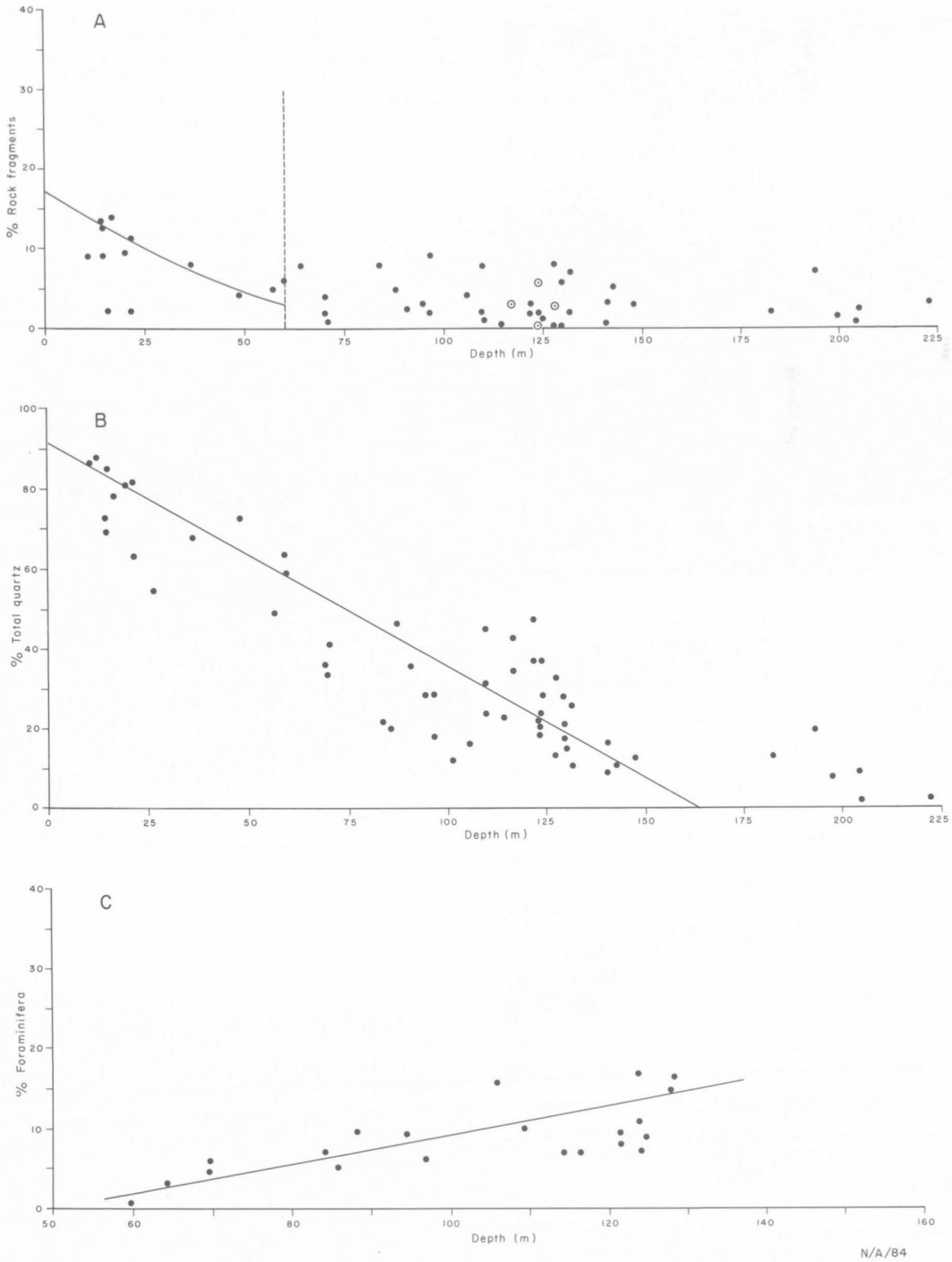

Fig. 34. Variation of percent rock fragments, total quartz, and foraminifera with depth.

Foraminifera. The proportion of foraminifera ranges from 0 to 35 percent of the total sample, and averages 12.6 percent. Most forms are benthonic, but planktonic forms are also present. Two samples contain arenaceous forms: *Globorotalia, Globigerina,* and *Reophax* are common genera. The proportion of foraminifera increases fairly regularly with depth (Fig. 34C). It also increases with depth when calculated as a percentage of total carbonate and not total rock, but to a lesser degree.

Bryozoa. Bryozoa form a small (0 to 21 percent, average 4.3 percent) but consistent fraction of the sediments, especially on the middle shelf and outer shelf (Fig. 39). Their distribution shows little relation to depth. Large autopores are commonly filled with glauconite or silica.

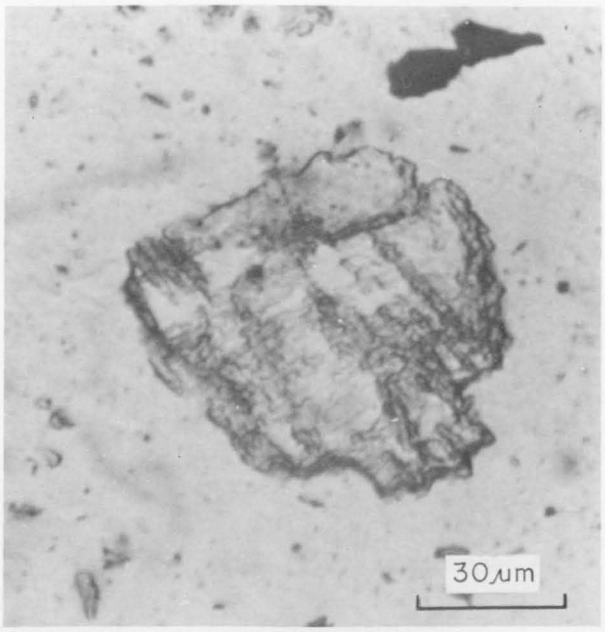

Fig. 35. Photomicrograph at station 1706, depth 115 m, showing albite being replaced by glauconite along cleavage traces. Ordinary light. (m 1664.)

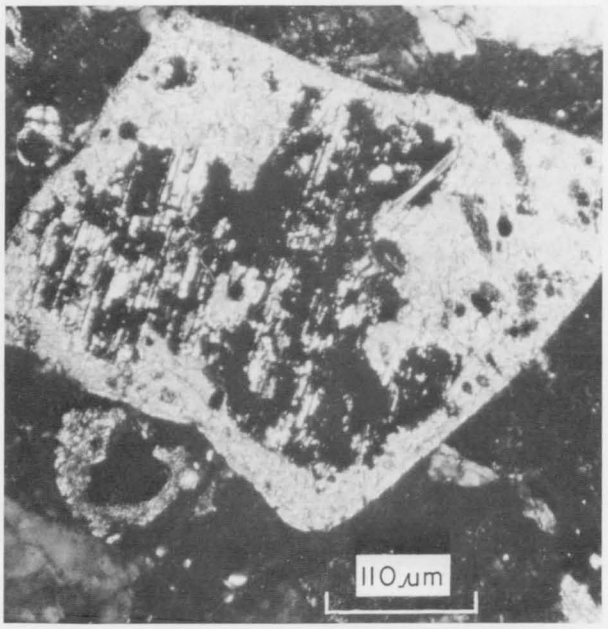

Fig. 36. Photomicrograph at station 1718, depth 117 m, showing calcite replacing calcic feldspar. Ordinary light. (m 1664.)

Unidentified carbonate. In almost all sediments there is a significant percentage of unidentified material made up of recrystallized or micritized fragments. Occasional grains of *Halimeda* and *Lithophyllum* fragments, and crystal rosettes were also noted.

Authigenic components

The only identifiable major authigenic component within the sediments is glauconite. It can form up to 7 percent of the sediment, but averages only 1.4 percent. It occurs most commonly infilling the chambers of foraminifera, or as discrete globular pellets (Figs. 41, 42). It also occurs infilling chambers within coralline algae and bryozoa, within micropores in echinoderm skeletons (Fig. 40), and replacing carbonate grains, quartz, and in one sample feldspar along the cleavage. The pellets (Fig. 41) are undoubtedly infills of the chambers of foraminifera (Fig. 42), the glauconite having been released after dissolution or disintegration of the test.

Heavy minerals

Fifty-six samples collected on a grid pattern over the shelf (Fig. 43) were chosen from the total sediment samples collected. Separation and weighing, followed by acidification and reweighing resulted in an expression of the percentage of heavy minerals free from $CaCO_3$. The samples were then analysed petrographically by grain mounts, 100-200 grains being ana-

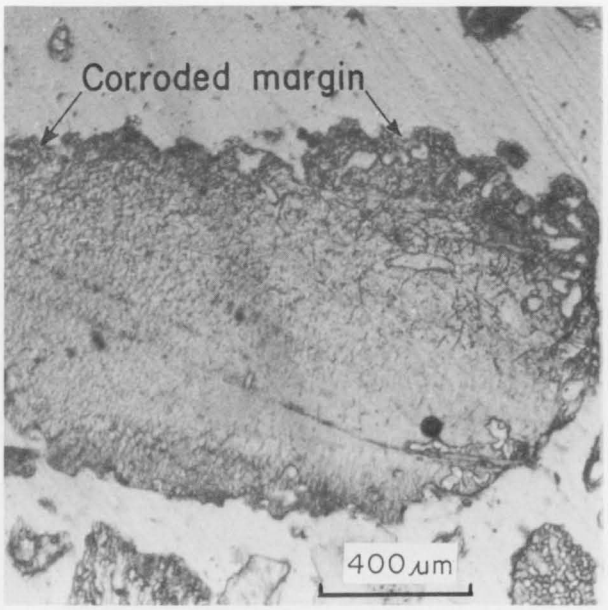

Fig. 37. Photomicrograph at station 1675, depth 110 m, showing the corroded margin of a mollusc fragment. Ordinary light. (m 1623.)

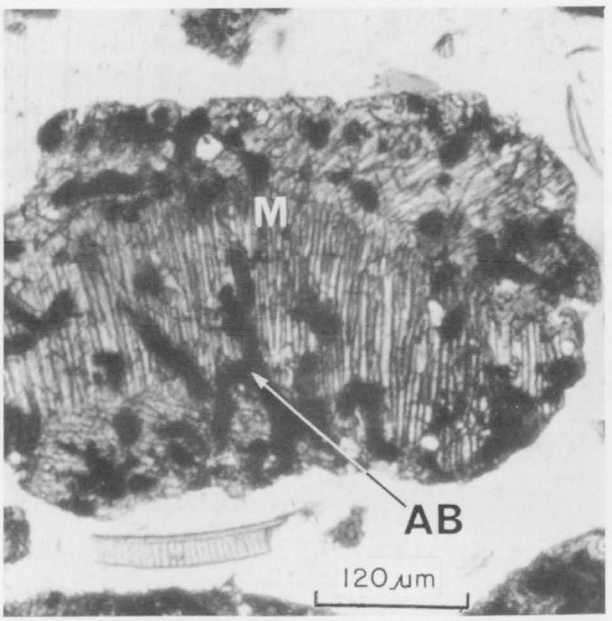

Fig. 38. Photomicrograph at station 1627, depth 124 m, showing algal borings (AB) within a prismatic mollusc fragment. Ordinary light. (m 1623.)

lysed per slide (Fig. 44). No detailed examination of the opaque fraction has been attempted except for the identification of leucoxene grains. The translucent fraction was examined in detail. The results are shown in Appendix 2.

Zircon usually occurs as rounded grains (Fig. 45), perfectly euhedral crystals, or partly water-worn crystals. Most grains are clear, but some are straw-yellow. Rutile in the translucent fraction occurs as well-rounded grains and partly-rounded crystals (Fig. 46). Colours range from pale orange to very dark red-brown. Tourmaline is almost exclusively grown and forms well-rounded grains or water-worn prismatic crystals (Fig. 45); occasional blue varieties occur. Garnet is rare, pink, and some grains have dodeca-

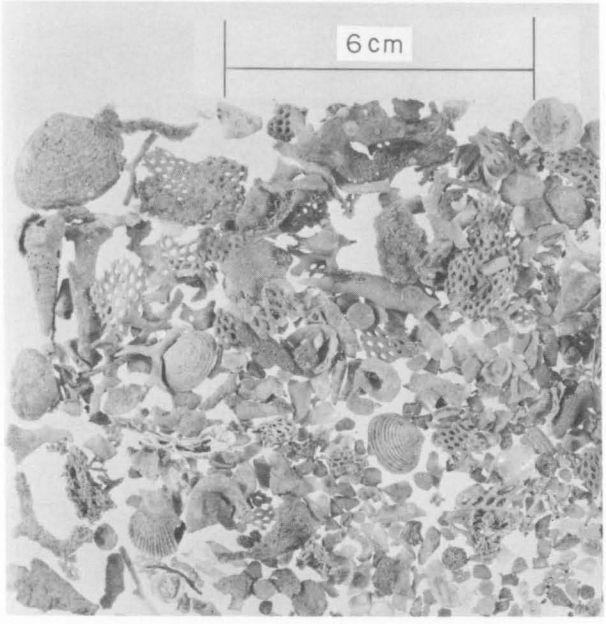

Fig. 39. Molluscan and bryozoan gravel from the shelf edge at station 1773, depth 192 m. (GA 8296.)

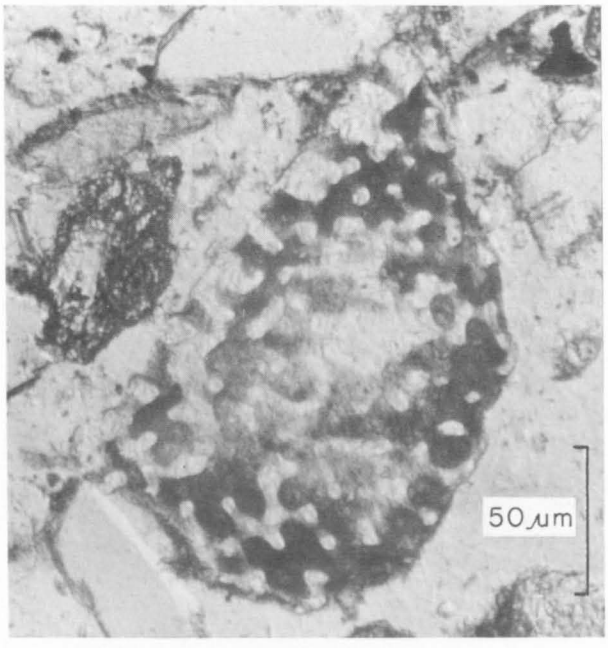

Fig. 40. Photomicrograph at station 1706, depth 115 m, showing glauconite infilling the micropores within an echinoderm fragment. Ordinary light. (m 1664.)

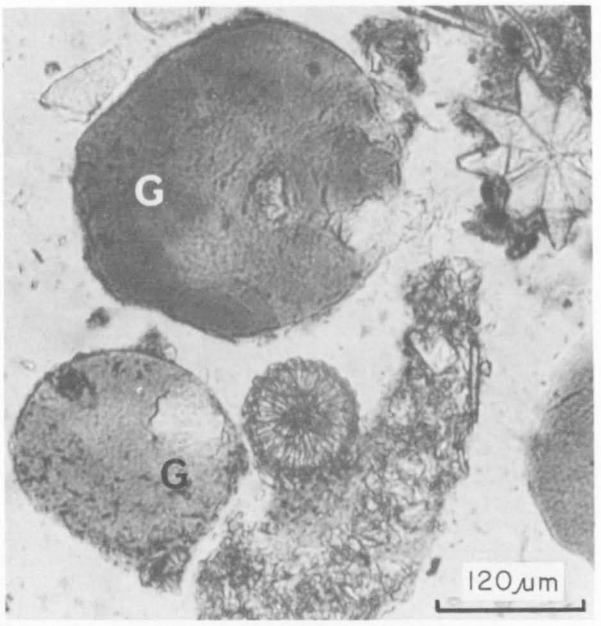

Fig. 41. Photomicrograph at station 1660, depth 124 m, showing discrete globules of glauconite (G), probably released after disintegration of the tests of foraminifera. (m 1623.)

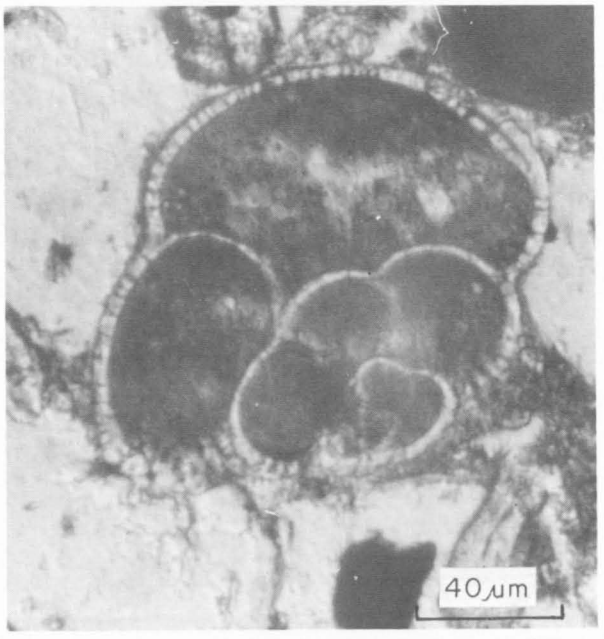

Fig. 42. Photomicrograph at station 1706, depth 115 m, showing glauconite infilling test of foraminifer. (m 1664.)

hedral faces. The most abundant of the translucent grains are amphiboles and the epidote group (Fig. 45). Amphiboles are almost entirely green hornblende, and the epidote minerals consist mainly of yellowish green, irregular epidote grains and colourless zoisite.

In shallow water, the sediments contain an average of 0.8 percent heavy minerals, while the middle-shelf and outer-shelf sediments contain 0.4 percent (Appendix 2). This seaward decrease is partly a result of diluent carbonate. The values can be markedly upgraded if the heavy minerals are calculated as a percentage of the terrigenous fraction. On this basis an average value of 0.9 percent is obtained for the middle-shelf and outer-shelf sediments. Recalculation of the

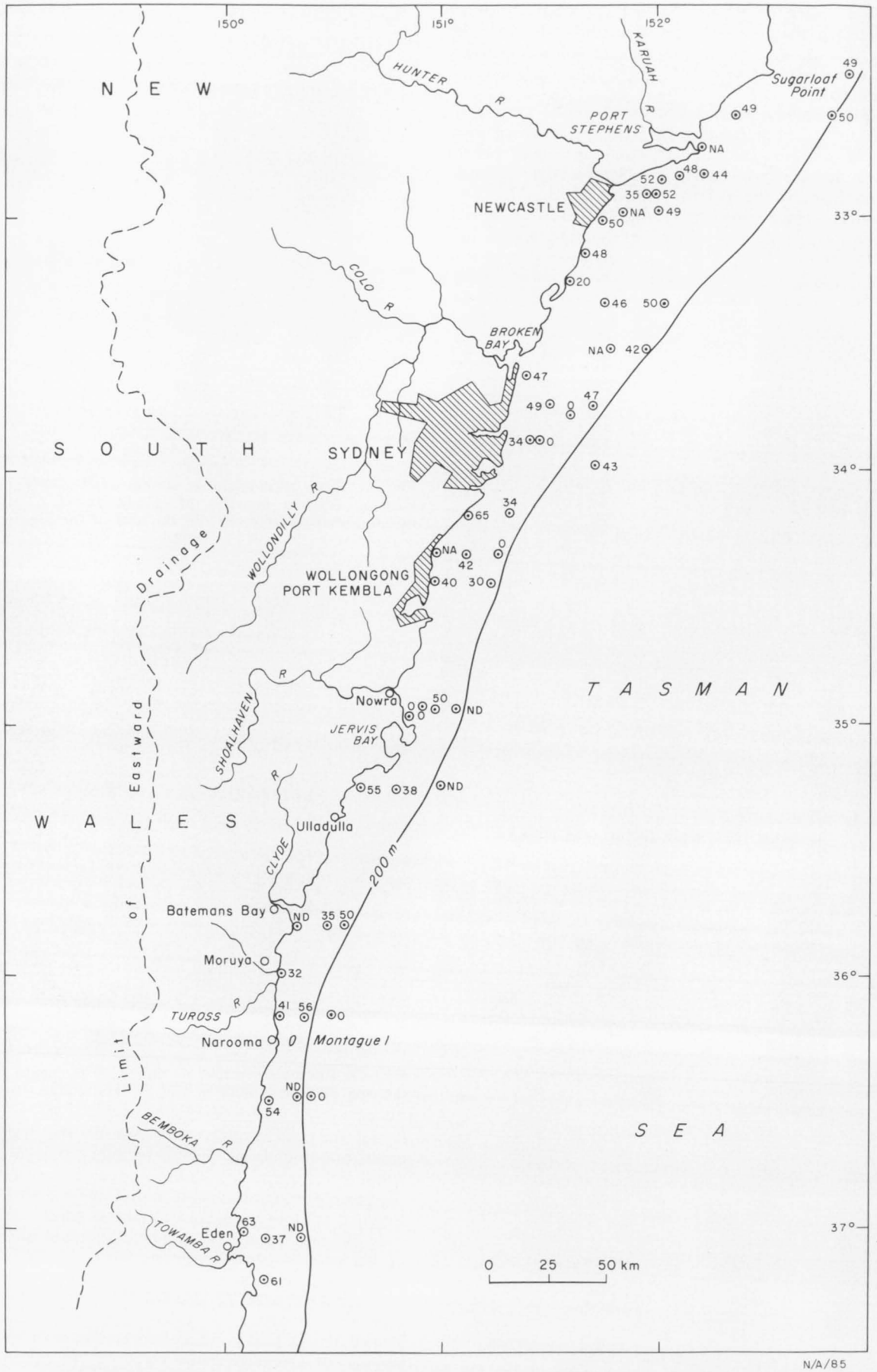

Fig. 43. Distribution of samples collected for heavy-mineral analysis. Figures with samples represent the percentage of opaques in the heavy-mineral fraction. No data are available for some samples (ND).

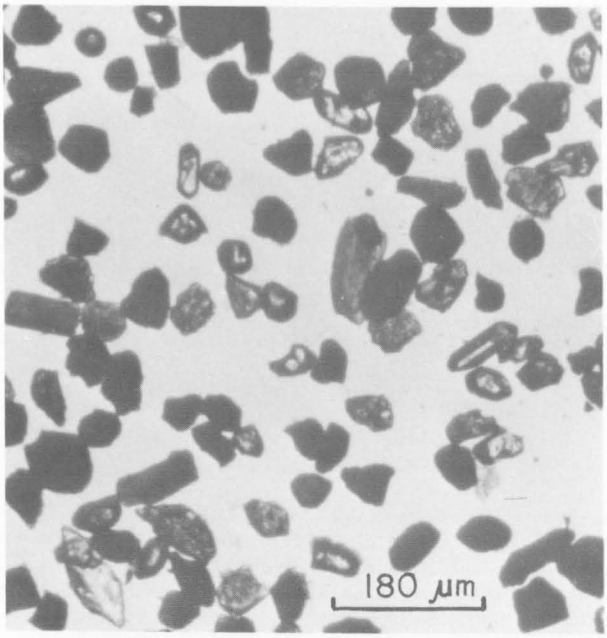

Fig. 44. Photomicrograph at station 1541, depth 18 m, showing heavy-mineral concentrate. Reflected light. (m 1664.)

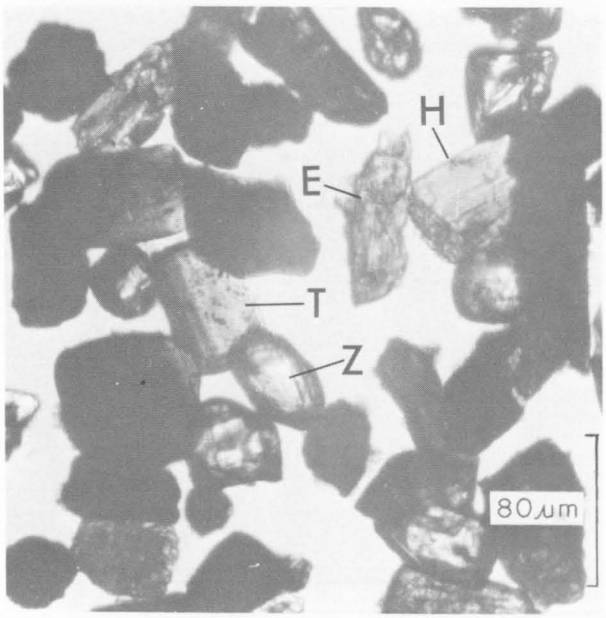

Fig. 45. Photomicrograph at station 1541, depth 18 m, showing rounded zircon (Z), prismatic tourmaline (T), epidote (E), and hornblende (H) in the heavy-mineral concentrate. Reflected light. (m 1664.)

values for the inshore sediments results in only a marginal increase in the total sediment figure because carbonate is low.

The spatial distribution of the opaques as a percentage of the total heavy-mineral fraction is shown in Figure 43 and a plot of total opaques against depth is shown in Figure 47. These data show that there is a marginal west-to-east decrease in total opaques both north and south of Jervis Bay; however, the reverse is true in the section northeast of Jervis Bay. Over the whole area, there is also a west-to-east reduction in the range percent of opaques. The widest range occurs in the close-inshore sediments. The latitudinal variation for these close-inshore sediments (Fig. 48D, E, F) shows a marked linear decrease in percent opaques from latitudes 37°S to 35°S, approaching zero near Shoalhaven Bight. It is not known how far the area of zero opaques extends. However, a significantly high value was obtained in sediments northeast of Wollongong.

The data in Figure 49 show that although the total percentage of translucents is highest in the outer shelf sediments, zircon, rutile, and tourmaline are more abundant on the inner shelf. North of Jervis Bay, a dominantly stable zircon-rutile-tourmaline assemblage occupies the inner shelf, and an unstable amphibole-epidote-pyroxene assemblage dominates the middle-shelf and outer shelf. South of Jervis Bay, mixed stable and unstable assemblages occur all over the shelf, the unstable amphibole-pyroxene-epidote assemblage increasing seawards.

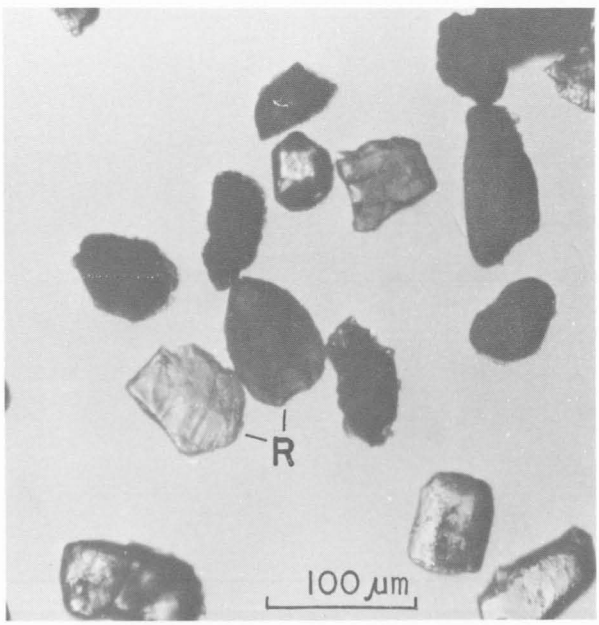

Fig. 46. Photomicrograph at station 1541, depth 18 m, showing rounded and angular rutile grains (R) in the heavy-mineral concentrate. Reflected light. (m 1664.)

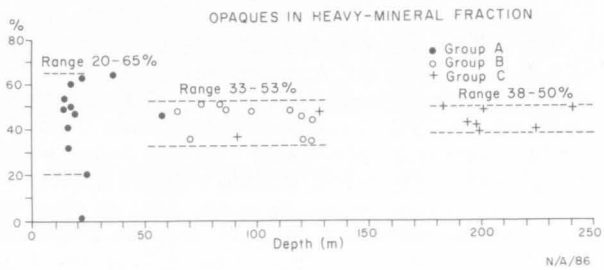

Fig. 47. Depth distribution of opaques in the heavy-mineral fraction. Groups A, B, and C refer to computer-delineated groupings.

TABLE 3. HEAVY-MINERAL DATA FOR ONSHORE LOCALITIES. DATA FROM WHITWORTH (1956) AND GARDNER (1955)

	Location	*Latitude*	*% Zircon*	*% Rutile*	*% Ilmenite*
1	Nelsons Reach	32°44′S	57	28	14
2	Caves Beach	33°00′S	33	44	22
3	Catherine Hill Bay	33°10′S	50	42	6
4	Tuggerah Caves	33°20′S	43	43	10
5	Terrigal	33°26′S	38	38	21
6	Botany Bay	34°00′S	23	67	6
7	Bellambi Beach	34°23′S	38	37	24
8	Port Kembla	34°30′S	38	29	17
9	Shellharbour	34°35′S	26	45	28
10	Shoalhaven River	34°50′S	22	18	50
11	Bawlee Point	35°45′S	7	4	80
12	Moruya	35°52′S	3	2	95
13	Narooma	36°12′S	12	7	80
14	Bega	36°40′S	5	3	80

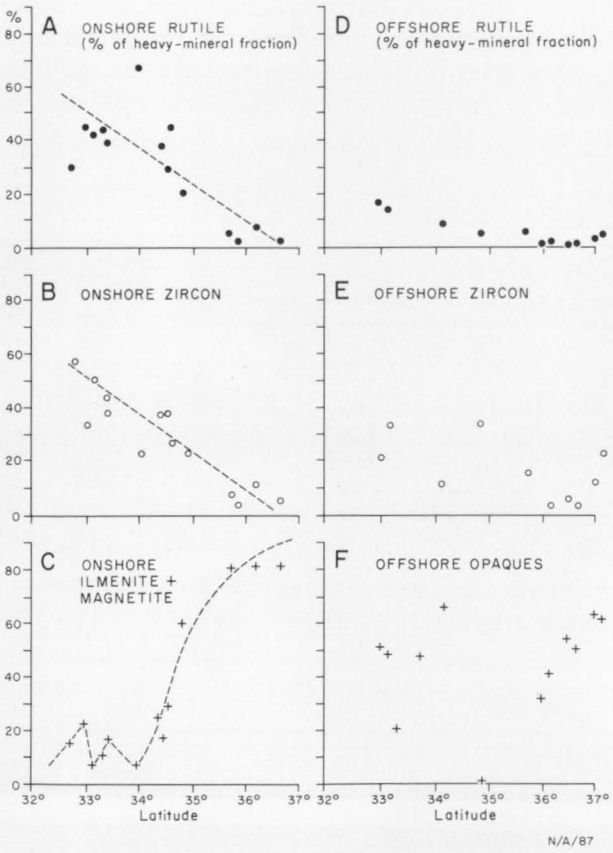

Fig. 48. Latitudinal variation in the percentage of onshore and offshore rutile and zircon, onshore ilmenite + magnetite, and offshore opaques. The offshore figures refer to sediments in the depth range 15-60 m.

The distribution of titanium on the continental shelf is shown in Figure 50. A comparison of the computed titanium values (Appendix 2) in the translucent fraction with the total titanium content indicates that most titanium occurs in the opaque fraction. Some of this occurs within leucoxene, a little may be present in dark rutile, but most will be in the form of ilmenite. The high percentage of opaques and the low rutile values south of Jervis Bay indicate that the high titanium values (Fig. 50) are related to ilmenite. Both rutile and zircon (Fig. 48) increase northwards in the close-inshore sediments.

The positions of onshore localities at which heavy minerals have been analysed are shown in Figure 50. Plots of the data (Table 3) from these localities against latitude (Fig. 48A, B, C) show a south-to-north increase in rutile and zircon, and a decrease in ilmenite and magnetite. The marked southerly increase of ilmenite and magnetite was previously indicated by Whitworth (1956). Similar variations can be seen in the opaque and translucent components in offshore sediments which occur in depths of 15 to 60 m. Zircon and rutile decrease in a southerly direction, while the percentage of opaques increases in this direction. While Figure 50 shows that titanium is high in the southerly sediments, Figure 48 shows that rutile is low: the titanium must therefore occur predominantly as ilmenite. The plot of percent opaques in Figure 48 therefore effectively shows the variation of ilmenite. The comparable onshore and offshore trends suggest a

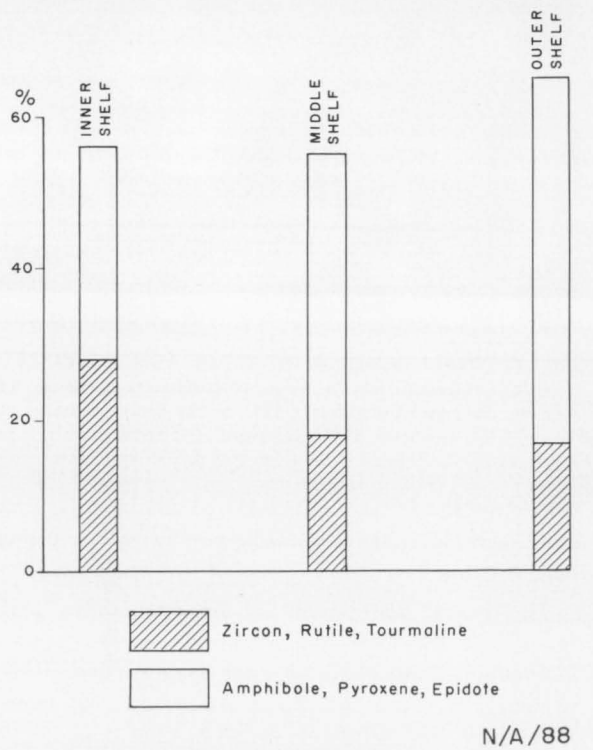

Fig. 49. Distribution of translucent heavy minerals on the inner, middle, and outer shelf north of Jervis Bay.

Fig. 50. Distribution of titanium values greater than 1000 ppm (stippled) on the continental shelf. Numbered onshore localities referred to in Table 3 are also shown.

similar provenance. Past workers have generally concluded that onshore the heavy minerals are locally derived. Culley (1933), Carroll (1940), Whitworth (1956), and Overstreet (1967) concluded that the source of quartz and heavy minerals along the New South Wales coast is the Mesozoic or Permo-Triassic sediments of the Sydney Basin. Carroll (op. cit.) and Culley (op. cit.) favoured the Permian and Triassic as a source for monazite in the Newcastle area, but Gardner (1955) suggested the Carboniferous sandstones as the main source. Whitworth (1956) concluded that heavy minerals near Sydney may have a provenance in the Hawkesbury Sandstone, but between Sydney and Newcastle the Narrabeen Group forms the major source. Whitworth (op. cit.) also considered that the relatively high ilmenite and magnetite around Wollongong can be traced to the nearby Permian volcanics, and suggested that the following general conclusions can be drawn on heavy-mineral provinces and their sources. North of Shellharbour is a province of high rutile and low ilmenite, especially between Sydney and Newcastle, where the source of rutile is the Narrabeen Group sediments; between Shoalhaven Bight and Shellharbour, rutile decreases, and black sands are contaminated by magnetite and ilmenite derived from the Permian volcanics of the hinterland; south of Shoalhaven Bight, the black sands are composed essentially of magnetite and ilmenite derived from Palaeozoic mafic and granitic intrusions. The scarcity of rutile and zircon is due to the scarcity of Permo-Triassic and Mesozoic rocks.

The similarity between the offshore and the onshore heavy-mineral suites suggests that the above conclusions may also apply to the offshore sediments in the zone 15-60 m.

Silt and clay

Surface sediments on the continental shelf contain either less than 2 percent or more than 10 percent silt and clay; therefore, there are either no fines or appreciable quantities. The quantities and types of clay minerals in the shelf sediments are shown in Appendix 4. Kaolinite, mica, chlorite, and illite are the dominant

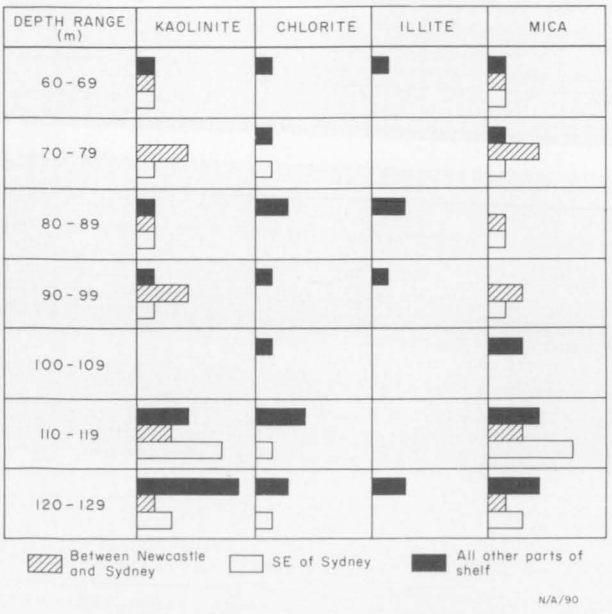

Fig. 51. Depth frequency distribution of clay types in shelf sediments. Horizontal percentage scale.

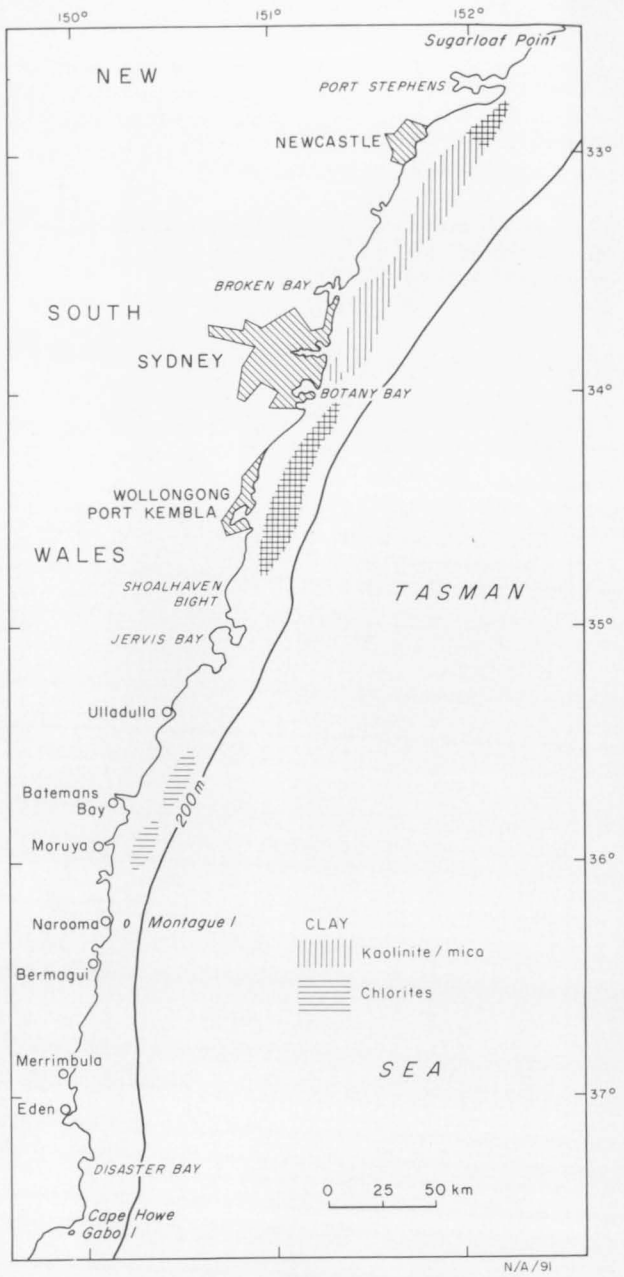

Fig. 52. Areal distribution of principal clay types on the continental shelf.

minerals in that order of abundance, confirming the conclusions of Loughnan & Craig (1962), who examined 15 samples collected between Moreton Island (south Queensland) and Sydney.

Granulometric analysis (Appendix 4) shows that sediments containing greater than 10 percent fines occur as zones orientated northeast to southwest (Pls. 1, 3a). By far the largest zone occurs between Sydney and Newcastle. Others occur farther south, east of Port Kembla and south of Jervis Bay. All occur in water depths of 60 to 130 m. The depth and spatial distribution of clay types are shown in Figures 51 and 52. The following conclusions may be drawn:

(a) The most widespread clay minerals are kaolinite and mica.

(b) East of Sugarloaf Point, the clays are essentially chlorite, and some chlorite also occurs east of Port

Kembla and northeast and southeast of Batemans Bay (Fig. 52).

(c) Illite is present in only a few samples, southeast of Port Stephens, southeast of Newcastle, and immediately north and south of Broken Bay.

(d) Clays are predominantly kaolinite/mica assemblages between Newcastle and Port Stephens.

(e) South of Jervis Bay, the clay mineralogy shows a fundamental change, chlorite replacing kaolinite in a dominantly chlorite assemblage.

(f) Clays are largely absent in the depth range 100 to 109 m, and are abundant in the range 110 to 130 m. The absence between 100 and 109 m may be the result of the sampling interval used.

The depth distributions of silt and clay shown in Figure 53A and B indicate a decrease of clay with increasing depth, and a broad scatter of silt.

The distribution of clay types shown in Figure 52 can be explained in terms of provenance. Ferguson & Hosking (1955), Loughnan (1958), and Loughnan & Craig (1962) have suggested that the Triassic shales are the likely source of clays on the continental shelf. These shales contain kaolinite and illite, but the illite weathers to kaolinite. The occurrence of predominantly kaolinitic clays directly offshore from the Triassic parts of the Sydney Basin (Fig. 52) is therefore in accord with the onshore geology. Grim & Loughnan (1962) showed that illite may be regenerated in the estuarine environment by uptake of potassium by interlayered minerals. The presence of illite offshore from the mouths of major rivers is therefore significant (samples 1644, 1646, 1647 off Broken Bay, and samples 1629, 1630 off the Hunter River). The chlorite/mica association occurs offshore from Palaeozoic igneous and sedimentary rocks, except east of Port Kembla where chlorite is probably related to the onshore Permian volcanics.

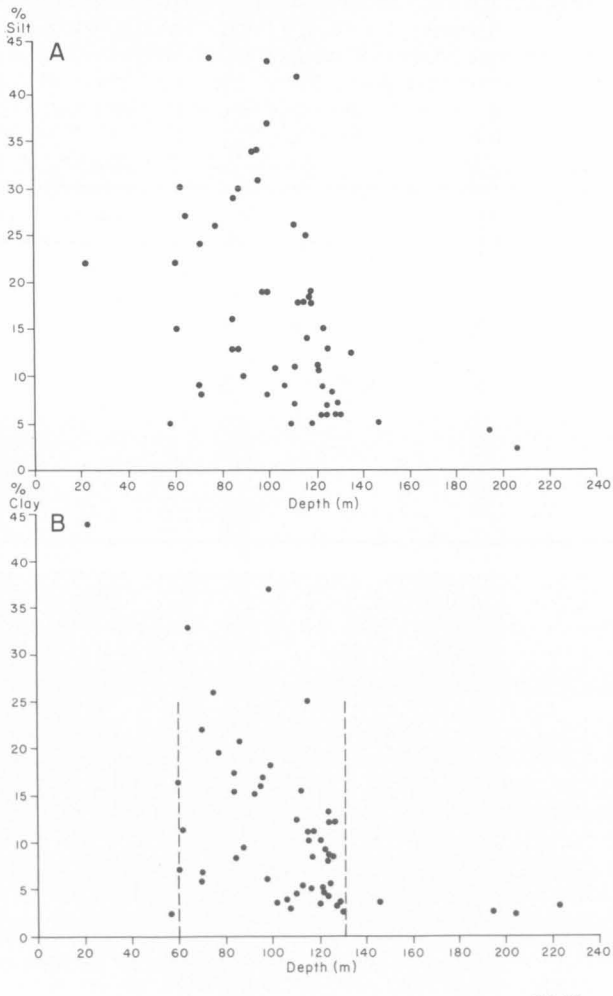

Fig. 53. Depth distribution of A. silt, B. clay.

Sediment types

Shepard's (1954) 10-compartment textural classification, with sand, silt, and clay end members has been used to describe the shelf sediments (Fig. 54). Over 100 samples, composed of 100 percent sand and gravel, are not plotted on the diagram. The distribution of sediment types is shown in Plate 1. Sand-size sediments (Fig. 55) dominate the southeast Australian continental shelf. Silty sands and sandy clays occur only as lenses on the middle shelf between Newcastle and Port

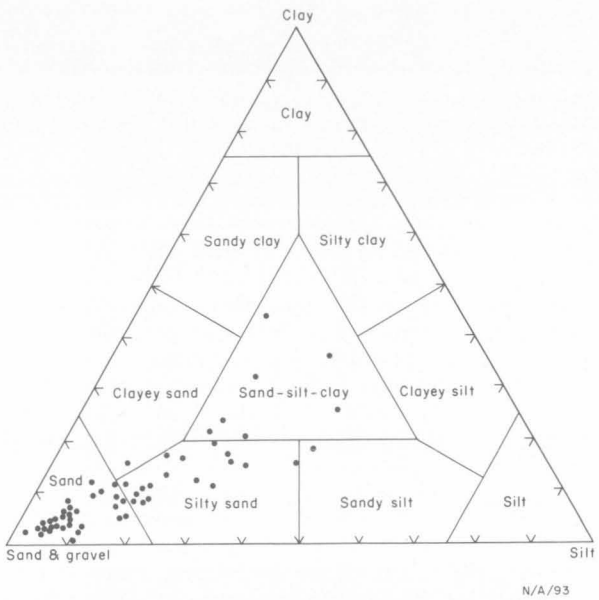

Fig. 54. Three-component textural classification of sediments on the continental shelf of southeast Australia. More than 100 samples of 100% sand and gravel plotting at the sand and gravel axis are not shown.

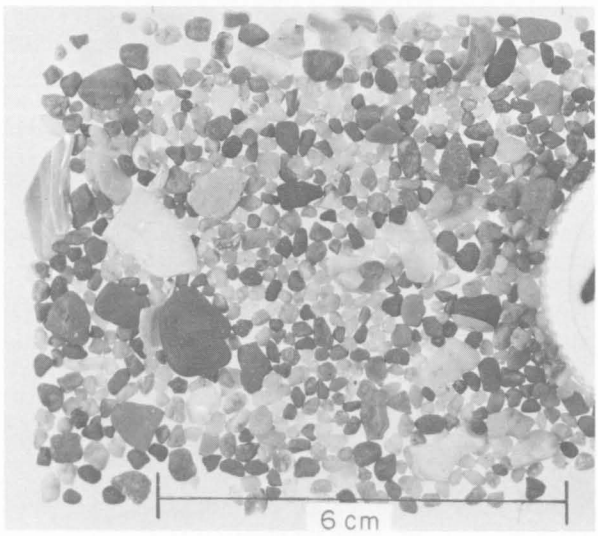

Fig. 55. Quartz sand from the inner shelf at station 1708, depth 27 m. (GA 8286.)

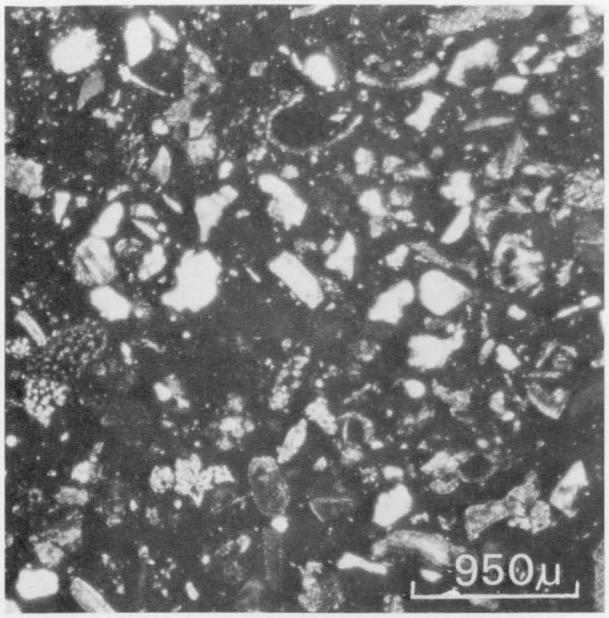

Fig. 56. Photomicrograph at station 1695, depth 110 m, showing silty fine sand from the mid-shelf. Crossed nicols. (m 1623.)

Kembla (Fig. 56). Quartz gravels (Pl. 1) occur almost wholly as patches on the inner shelf south of Crowdy Head, north of Newcastle, and south of Batemans Bay; they also occur on the outer shelf east of Montague Island, in association with cemented carbonate gravel. East and south of Jervis Bay, carbonate gravels occur as lenses on the outer shelf, the largest being north and south of Twofold Bay. These gravels are composed of fenestrate Bryozoa, bivalves (*Arca trapezia, Cardita*), solitary corals, gastropods, crinoids, and rare brachiopods (Fig. 57). All the fragments are extensively bored (Fig. 38) and either heavily iron-stained or grey and chalky. None of the shells has retained any vestige of original colour, and all are in differing stages of comminution, and present the appearance of an old fauna. It is extremely unlikely that they represent part of a living benthos and thereby representative of a modern sediment (Shirley, 1964). They are clearly out of equilibrium with the depositional regime of the present day.

It is clear that the Shepard (1954) classification does not adequately portray the sediment variation on the continental shelf because of the dominance of sands. Shirley (1964), recognizing this also, plotted the distribution of coarse and medium sands for the area between Crowdy Head and Batemans Bay. As most of the shelf sediments are sand, a better idea of the distribution can be obtained by plotting the distribution of mean grainsize and standard deviation (Pls. 3A, B). A large variation in both parameters is indicated. The inner part of the shelf from Port Stephens to south of Batemans Bay is composed of coarse to medium sand. In only a few places is the inner shelf mantled with sediments with a mean grainsize coarser than sand grade, e.g. between Sydney and Broken Bay. North of Port Stephens, and south of Batemans Bay, the close-inshore sediment is largely fine sand.

Sediments on the middle shelf and outer shelf north of Jervis Bay are very different from those of Jervis Bay (Pl. 3A). In the northern area, the middle shelf is mantled by belts of very fine sand, within which silt and clay-grade material dominate in places. These are especially seen between Newcastle and Broken Bay, east of Port Kembla, and an isolated patch east of Sydney. Northeast of Newcastle, and east of Wollongong, the mean grainsize contours are steep on the shoreward side of the clay/silt belts, indicating a relatively abrupt change from medium-sand to silt and clay-sized sediment. On the oceanward side, however, the contours suggest a more gradual decrease in grainsize. East and northeast of Newcastle, the outer-shelf sediments are predominantly medium to coarse sands. A tongue of coarse sand extends southwards from east of Crowdy Head. Farther south, however, east of Wollongong, the outer shelf sediments are largely of fine sand grade.

Near Jervis Bay is a ridge of northeasterly-coarsening sediment (Pl. 3A), with gravel occupying the outer shelf east of Shoalhaven Bight. South of Jervis Bay, the middle shelf is covered predominantly by medium-grade sands, with lenticles of fine sand southeast of Batemans Bay and east of Eden. The outer shelf between Jervis Bay and Montague Island is blanketed by medium and coarse sands, and south of Montague Island coarse sand and gravel cover the equivalent areas.

Major similarities in contour configuration can be seen between mean grainsize and standard deviation (Pls. 3A, B) in the middle shelf zone, and on the outer shelf northeast of Jervis Bay and south of Montague Island. That the inclusive graphic standard deviation is a good measure of sorting (Folk, 1968) is borne out by the data. Areas of well to moderately sorted sediments occur predominantly on the inner parts of the shelf. East of Newcastle, Sydney, and Batemans Bay, such sediments also occur on the outer shelf. Most of the shelf is covered by poorly sorted sediments, but sediment tongues exhibiting poor to extremely poor sorting occur in the middle shelf, coincident with areas of high silt and clay content. Close-inshore sediments south of Jervis Bay are also poorly sorted. The outer shelf and upper slope is generally characterized by poorly sorted sediments, but north of Port Stephens

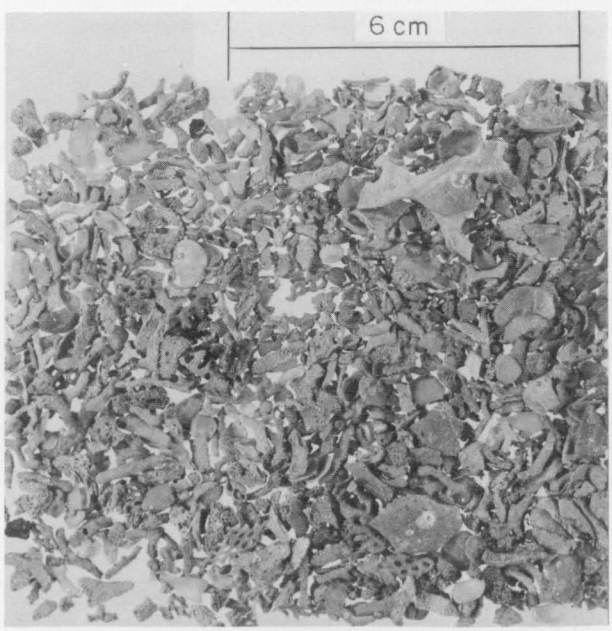

Fig. 57. Carbonate gravel from the outer shelf at station 1673, depth 200 m.

and south of Batemans Bay the outer shelf is composed of very poorly to extremely poorly sorted sediment.

Two principal sediment characteristics which influence the degree of sorting are the percentages of mud and carbonate. The relatively high proportion of mud in the middle shelf results in poor sorting, while high carbonate has a similar but much more widespread effect. The percentage of calcium carbonate generally increases with depth (Fig. 65A). Either mud or calcium carbonate percentage may act singly in determining the sorting coefficient, as occurs east of Newcastle and Port Kembla, or in unison east of Port Stephens and Shoalhaven. The areas of poor sorting east and northeast of Batemans Bay can be attributed wholly to the marked increase in the calcium carbonate in the sediments. A similar explanation accounts for the poor sorting on the outer shelf south of Montague Island and northeast of Jervis Bay.

Relations between sediment type and water depth

Over much of the shelf, three sedimentary zones are recognizable which coincide within broad limits with the three morphological zones described earlier (Fig. 58).

1. 15-60 m, a gently sloping area with few knick points or terraces. This area is covered generally by well to medium sorted quartz sands (Fig. 55).
2. 60-120 m, a steeply dipping (1-2°) highly terraced mid-shelf region covered by fine sands and extremely poorly sorted silts and clays (Fig. 56).
3. below 120 m, a flat outer plain with wide flat terraces at various depths, mantled by poorly sorted carbonates of varying grainsize (Fig. 57).

This threefold division is best seen on the shelf north of Jervis Bay, but also occurs to the south along latitudes 36°00′ and 36°20′ (Pl. 2). In some parts of the southern area, however, the shelf has a nearly smooth profile (Pl. 2, latitudes 36°40′ to 36°50′S) and in these areas the whole of the shelf is mantled by medium-grained poorly sorted sand, while silt and clay are rare.

Thus, a relation exists between the major morphological features of the shelf and the sediment types, particularly north of Jervis Bay.

Sample clustering

The continental shelf sediments have so far been classified into descriptive geological groupings using only two variables, i.e. mean grainsize and standard deviation. It is, however, desirable that as many variables as possible be taken into account when differentiating sediment groups, because only then will it be possible to suggest a genetic interpretation for the groupings. Q-mode factor analysis has been used to achieve this aim.

The results of Q-mode factor analysis of the data for continental shelf sediments are shown in Figures 59 and 60. Three factors account for 90.45 percent of the total sample variance. Increasing the number of factors to 6 explains only another 4 percent of variance. The three delineated groupings correspond to those previously described from grainsize data.

Group A. Group A sediments are described by Factor 1 variables, which are mean grainsize and the percentage sand. Total data for sediments which are affected largely by Factor 1 are given in Appendixes 3 and 5 which represent data used and not used in the

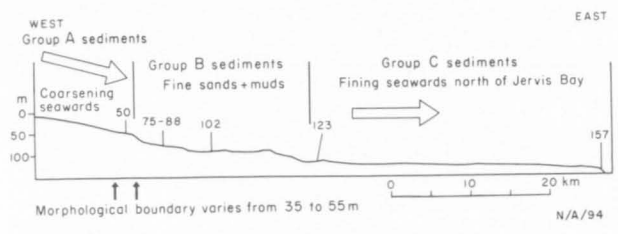

Fig. 58. West-to-east bathymetric profile along latitude 33°10′S, showing the co-occurrence of sediment groups and major morphological zones.

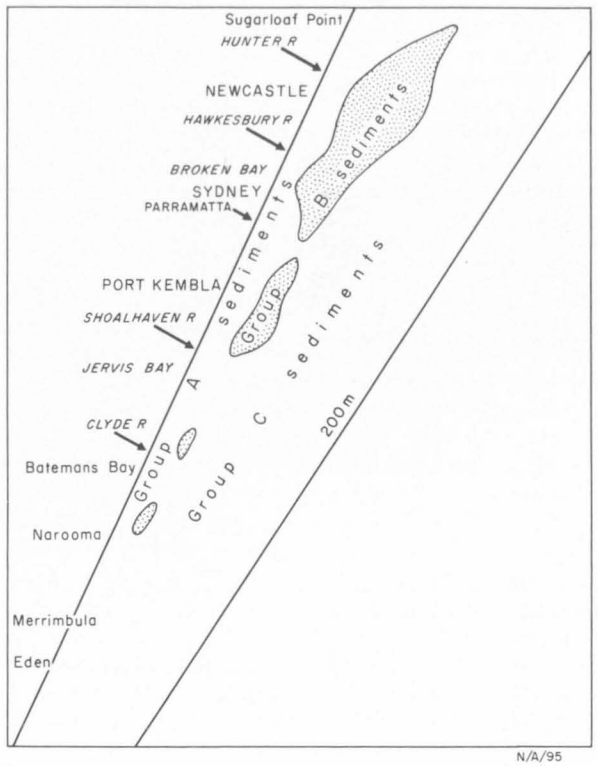

Fig. 59. Diagrammatic representation of the distribution of the computer-delineated sediment groups A, B, and C.

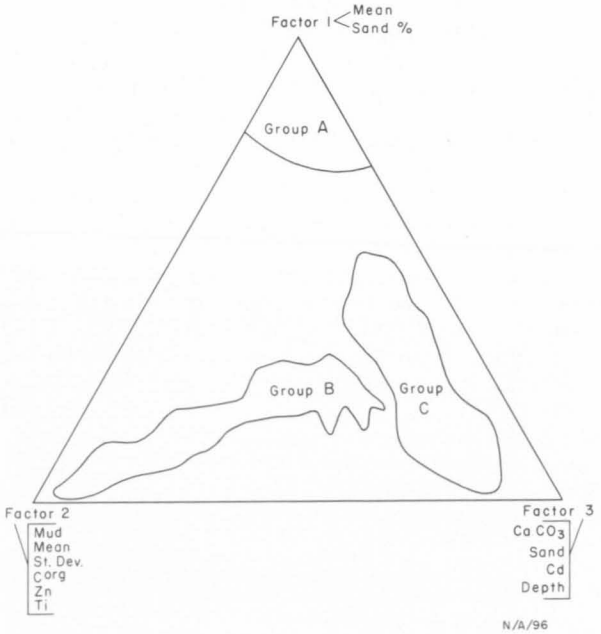

Fig. 60. Triangular plot showing the result of Q-mode factor analysis. The three factors, accounting for 90.45% of the total sample variance, indicate a subdivision of the shelf sediments into three groupings (A, B, C).

statistical grouping. The data not used confirm the specific character of the sediments shown by the clustering. The modal data especially show that the sediments contain high quartz (63-88%), but feldspar is either high or low depending on the provenance relations. Although sorting was not chosen as an important variable by the computer, all samples show good to moderate sorting. In addition, all samples occur within a limited depth range (15-60 m). Geochemical data (Appendix 4) show that the sediments exhibit a marked paucity in most cations, except iron. Petrographic work shows that the iron occurs almost entirely as oxide coatings on grains.

It is likely that the sediments separated by Factor 1 are a natural grouping with a probable common origin.

Group B. Group B sediments are described by Factor 2 variables, which are standard deviation, mud, mean grainsize, and zinc concentration. The inclusion of three granulometric variables is significant in aiding a geological interpretation. All samples separated by Factor 2 are poorly sorted silty and clayey sand in 60-130 m water depth. This group equates with the very poorly to extremely poorly sorted, very fine sand, silt, and clay described previously.

Group C. Group C sediments are described by Factor 3 variables, which are calcium carbonate, depth, cadmium concentration, and percentage sand, the increase of which corresponds with increasing factor loadings. Samples within this group occupy a mid-shelf to outer-shelf position, are high in calcium carbonate, and show highly variable sorting and grainsize characteristics. The relations within the group leading to a postulated origin are discussed later.

Origin of shelf sediments

The distribution and characteristics of bottom sediments on continental shelves give an integrated picture, from which inferences can be made regarding where sediments come from and how they get there. It is much more difficult to say when they arrived in their present position. Since Johnson (1919) suggested the concept of a size-graded continental shelf, many authors (especially Shepard, 1932) have shown that a non-graded condition at present exists. This has led to conclusions that sediments on shelves today may be modern, relict, or palimpsest. Palimpsest is the term suggested by Swift et al. (1971, p. 343) for a mixed sediment, i.e. sediments exhibiting both relict and modern characteristics. Sediments form part of either the near-shore modern sand blanket, the relict sand blanket, or the modern mud blanket. Swift (1970), while recognizing that the time of emplacement was the best criterion for identifying types of shelf sediment, concluded that grainsize is of most use in determining whether a sediment is in equilibrium with the present or with a former regime. In view of the above concepts of grade, facies, and depositional environment, the computer-delineated sediment groupings are examined to define their depositional environment, their time of deposition, and ultimately their classification as modern, relict, or palimpsest. Granulometry, major mineral components, heavy-mineral components, and relation to shelf morphology are examined specifically.

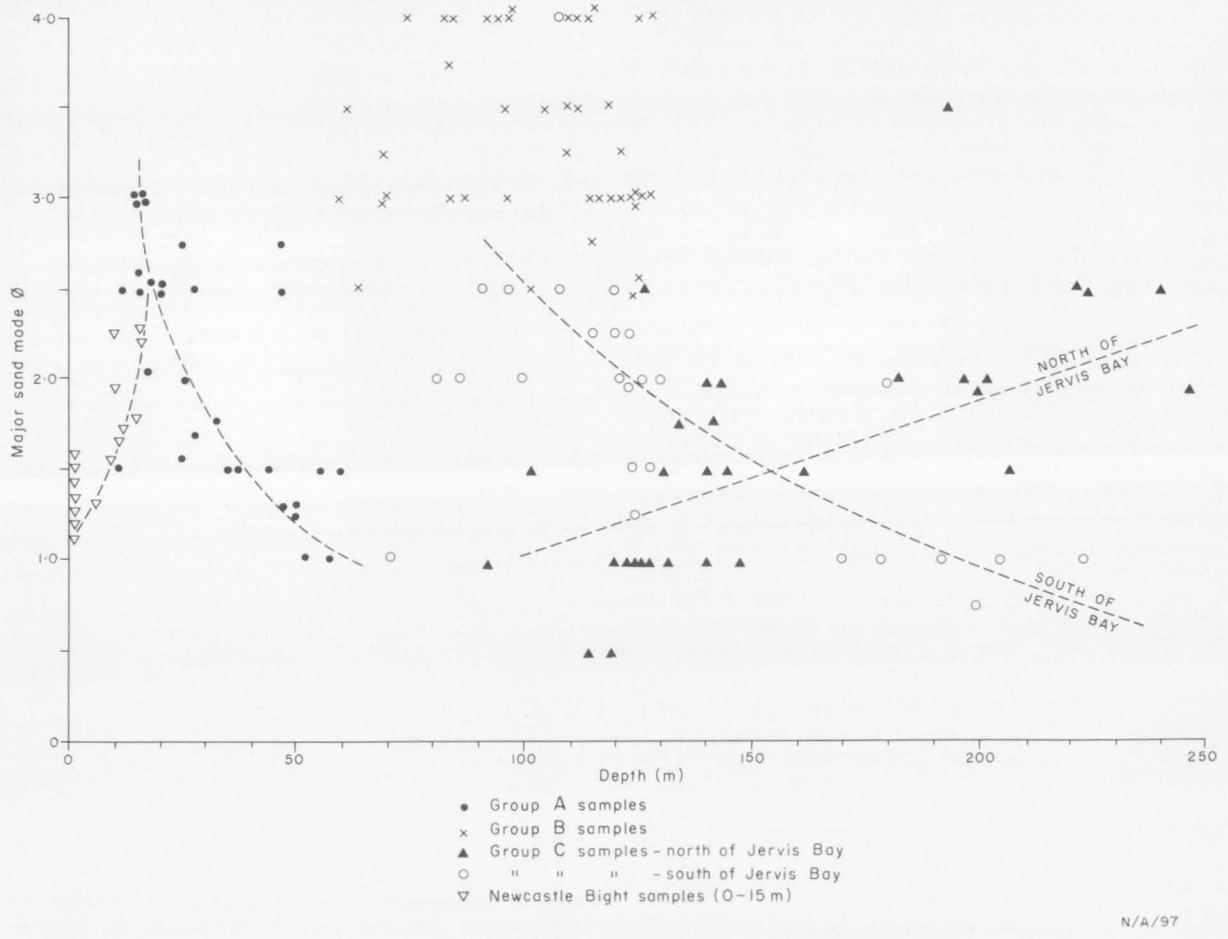

Fig. 61. Distribution of the major sand mode against depth. Data for the Newcastle Bight samples (depth 0.15 m) were supplied by R. Boyd (Sydney University.)

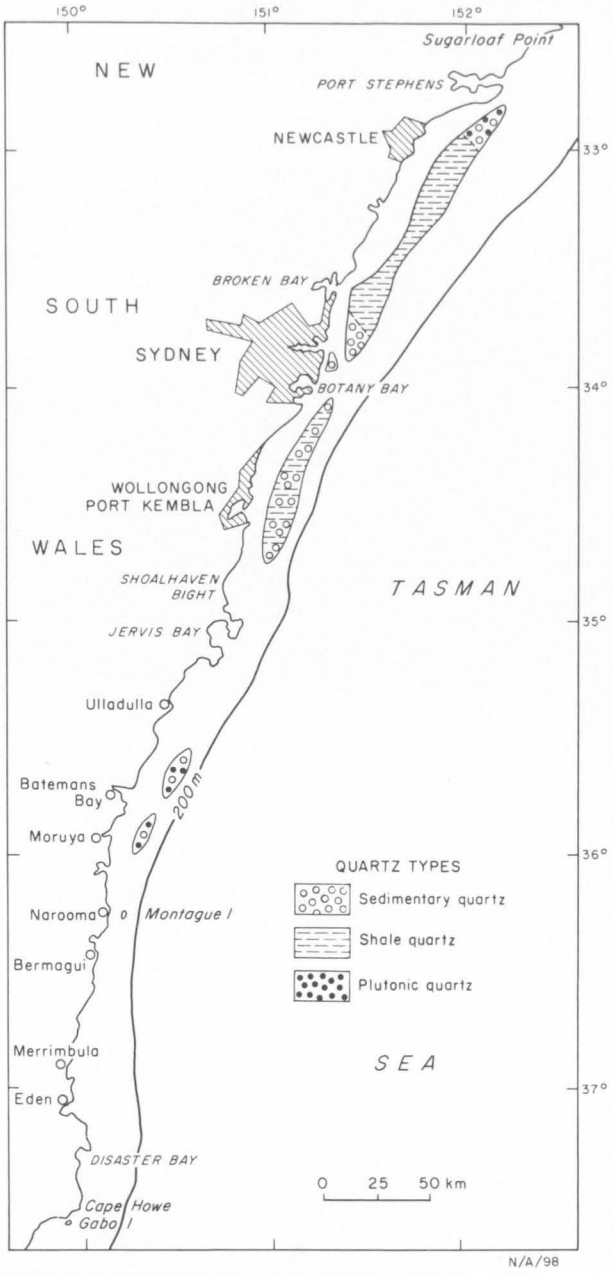

Fig. 62. Distribution of principal quartz types.

The sediments in the three computer-delineated groups are predominantly sands, and while their overall distribution can be adequately portrayed by a plot of mean grainsize (Pl. 3A), the position of the major sand mode is a more useful parameter in helping to solve problems of origin and time of deposition. The variation in the position of the major sand mode with depth is shown in Figure 61. This parameter was not used in the computer grouping and yet the same three groupings emerge when the major sand mode is plotted against depth. In Figure 61 the data for depth zone 0-15 m, supplied by R. Boyd of Sydney University, show that grainsize decreases away from the shore, an opposite trend to that of the sands in the 15-60 m zone.

Group A. The following appear to influence the origin of Group A sediments:

1. The sediments occur on a morphologically distinct part of the shelf in water depths of 15-60 m. They are bounded on the eastern side by sediments with a high mud content, and on the west by sediments with a different grainsize distribution.

2. Grainsize of the major sand mode increases with depth and is independent of calcium carbonate content. Grainsize variations in the sand populations seaward and landward of Group A sediments do not show this trend.

3. The average heavy-mineral content in the Group A sediments is higher than in other shelf sediments, and the north-south variation in abundance and type parallels the onshore variation. Within Group A sediments, heavy-mineral content decreases seawards.

The similarities between onshore and offshore heavy-mineral accumulations suggest that: onshore sediments were derived from offshore sediments by onshore transport; or both were derived from similar sources; or similar depositional environments to the present existed during Pleistocene sea level lows.

In view of the evidence previously put forward suggesting that existing onshore deposits are derived from the immediate hinterland, the obvious deduction to be made from the similarity in onshore and offshore heavy-mineral sands at the same latitude is that no significant movement of this fraction of the sediments parallel to the coastline is occurring at present, or has taken place in the immediate past. It seems likely that the bulk of the existing onshore heavy-mineral sands reached their present position as a result of the landward movement of the paralic sand wedge during the Holocene (and earlier) transgressions. The relatively high heavy-mineral content of Group A sediments suggests that one or more protracted stillstands occurred when sea level was 15-60 m below present datum, and that the existing onshore deposits were derived from beach sands which migrated landwards during the transgressions. The differences in grainsize trends which occur at the 15-m isobath indicate that this movement of Group A sediments is no longer taking place. Group A sediments are therefore relict.

The reversed textural gradient (Fig. 61) shown by Group A sediments is characteristic of intertidal zones (Swift, 1970), bounded seaward by a tidal current maximum induced by shoaling (Fleming, 1938), an example of which is Broken Bay (Albani, 1974). Group A sediments occur on a gently sloping platform bounded seawards by a marked change of slope at 50-70 m. It therefore approximates the condition described by Swift (1970) and Fleming (1938) for the production of reversed textural gradients in intertidal areas. The overall reversed gradient between 15 and 60 m may therefore represent a series of intertidal zones, with accompanying reversed gradient, which developed during a rapidly rising sea level. Short stillstands during this rise would probably lead to the formation of lag deposits. In this context it is relevant that along five traverses off Newcastle gravel occurred at a depth of 35 m. This may therefore represent either a beach deposit formed while sea level was lower, or a lag deposit formed during transgression.

Group B. The following factors need to be considered when postulating an origin for the Group B sediments:

1. The sediments occur on a morphologically distinct part of the shelf in water depths of 60-120 m.

2. They differ markedly from all other shelf sediments in their mud component, and in the grainsize of the major part of the sand component (2.5-4.0 ϕ).

3. The dominant type of clay in the sediments varies from north to south along the shelf (Fig. 52). Separate provinces of the main quartz varieties can also be delineated (Fig. 62).

4. Clay increases towards shallow water (Fig. 53B).

5. The grainsize of the major sand mode shows little dependence on depth (Fig. 61).

6. The titanium concentration varies directly with the silt content (Fig. 63), and inversely with depth.

7. The largest area of Group B sediments occurs in the northern part of the area where the major rivers enter the ocean (Fig. 59).

From the above, Group B sediments may owe their origin to very different processes acting on mud and sand separately, or to a single process acting on mud and sand simultaneously. The sediments may be wholly recent, palimpsest, or relict.

Any explanation of the origin of the Group B sediments must explain their bimodality, their granulometric uniqueness, and their position on the mid-shelf. An adequate interpretation at this stage is not possible because lines of evidence for or against a particular origin are negative. Close similarities in textural relations between the mid-shelf sediments and the muds of the Hunter Estuary (Boyd, 1974) are not direct evidence of a present-day provenance relation. It is just as likely to represent genetic similarities in the environments of deposition of the two sediment types. Similarly the position offshore from a major river system is not evidence of present-day sedimentation, because during periods of lower sea level, rivers most likely discharged in the mid-shelf position. A clear resolution of the problem is not forthcoming from the literature. Although Creager & Sternberg (1972) described a recent mid-shelf muddy sand from the shelf

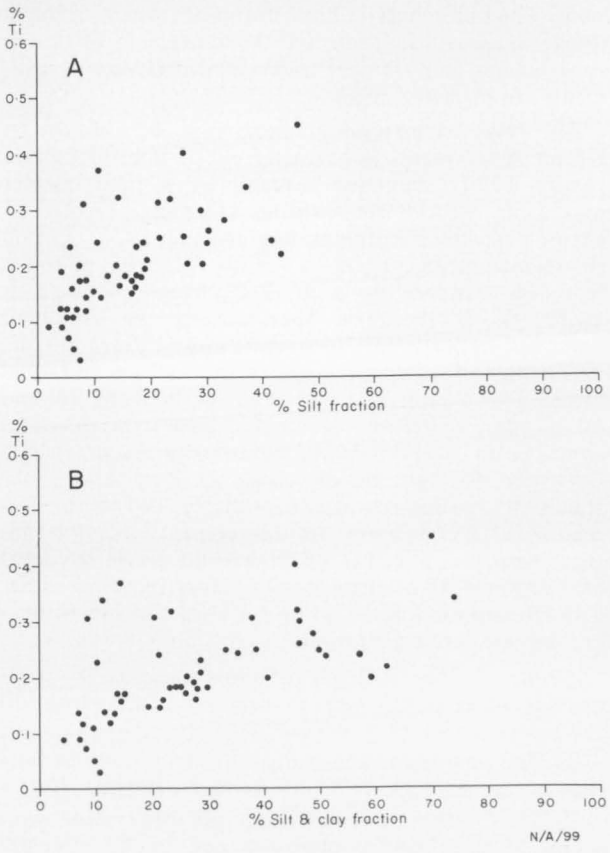

Fig. 63. Plot of titanium against A. silt, B. silt and clay.

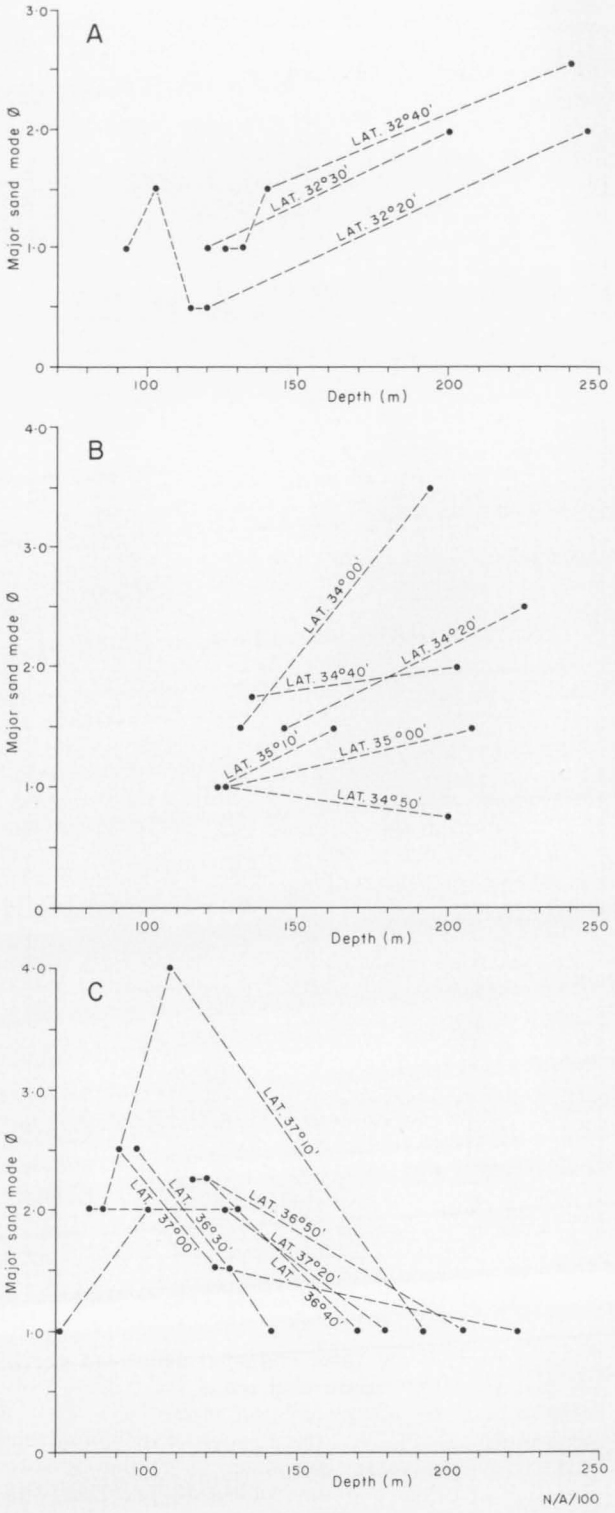

Fig. 64. Plots of the major sand mode against depth along individual west-to-east traverses in the A. northern, B. central, and C. southern parts of the area.

off northwest USA, the sand modes were finer than in the east Australian sediments. Sternberg (pers. comm.) has, in addition, expressed doubts that mid-shelf bottom current velocities are strong enough to transport 2-3 ϕ material. By inference, therefore, the sand component in the Australian samples may be relict, a conclusion also reached by Meade (1972) for similar mid-shelf deposits off eastern USA. This still leaves the problem of the mud. If the mud and sand are not

genetically related, then the question must be asked as to why they occupy identical positions on the shelf. Without according them both a relict origin, this is difficult to answer. Albani's conclusions (1974, and pers. comm.) that little sand or mud is at present being passed to the continental shelf from river input, together with the well-defined textural gradients in the close-inshore and Group A sediments (Fig. 61), the relatively sharp boundaries between Group A and Group B sediments, and the coincident morphological change suggest that Group B sediments are not recent. It is difficult to envisage the marked provincialism of the clay distribution resulting from present-day sedimentation. Mixing of clay types is sure to occur during the suspension period by bypassing Group A sediments. It is concluded, therefore, that both sand and mud components are likely to be relict. They may represent subaerially-mixed river and swamp deposits which formed during low sea levels, or mixed barrier flat/barrier dune/beach sand deposits. Jones (1973a, b) described shallow linear depressions parallel to the coast for a distance of 45 km on the Queensland Shelf, which may be remnants of coastal lagoons. The axes of these depressions occur in 60-m water depth. Shepard (1960), describing barrier systems, differentiated three major facies: beach sands with a mean grainsize of 3 ϕ; barrier dunes with the major sand mode in the range 2-3 ϕ, higher silt content than the beach sands, and heavy minerals concentrated in the silt fraction; and barrier flats behind the barrier dunes, with a mud content of about 20 percent. All three facies should form near a major change of slope. Characteristics of Group B sediments compare well with Shepard's descriptions of barrier system facies. Mixing of the facies during the last sea-level rise, and bioturbation since that rise would result in the poor sorting characteristics displayed by the sediments at the present time. The present relatively sharp facies are therefore explained as a function of the position of ancient sea levels, which are known to have oscillated between 50 and 100 m below existing level for a large part of the late Pleistocene. The sources of the quartz in the sand component are likely to be the Permo/Triassic sediments forming the mid-shelf ridge, the negligible transport explaining the marked provincialism in quartz type. The clay/silt would be derived from sluggish rivers crossing the relatively flat inner-shelf zone. The provincialism shown by the clays would therefore result from different river systems draining different hinterlands. Shepard (op. cit.) considered that barrier system facies best develop close to an area of subsidence. This is exactly the position where the Group B sediments occur on the shelf, straddling the mid-shelf basement hinge described on p. 7.

Group C. Group C sediments contain abundant carbonate and subordinate quartz, and are poorly or very poorly sorted. The plot of major sand modes against depth (Fig. 61) shows two different relations. North of Jervis Bay, the major sand mode changes with increasing depth from 1.0 to 2.5 ϕ. South of Jervis Bay the reverse relation is seen, the major sand mode coarsening from 2.5 to 1.0 ϕ with increasing depth. These trends are not the result of lumping all the data together. The plots of individual traverses shown in Figure 64 indicate that the reversal in grainsize trend is first noticeable east of Shoalhaven Bight, corresponding with the position of a basement and topographic high. North of Jervis Bay, therefore, an equilibrium coarse-to-fine profile occurs where fine sands and muds occupy the middle shelf; i.e. in about 120 m of water, coarse sediments occur adjacent to fine sands and muds. Where the coarse-to-fine profile ocurs, the outer shelf is wide, flat, and grades imperceptibly into the upper slope. The shelf break is at an average depth of 160 m. South of Jervis Bay, the outer shelf is narrow and shallow, with the shelf break at about 140-150 m. The continental slope is steep, and both slope and outer shelf show evidence of major erosion (Davies, 1973).

Isotopic dating (Phipps, 1970) and petrographic studies suggest that carbonates mantling the outer shelf are relict. The question then arises as to whether the sediments are reworked. South of Jervis Bay, the coarse shelf-edge gravels, the high shelf break, the abundant evidence of erosion, and the fine-to-coarse textural gradient point to the sediments being relict from at least the last sea level low. North of Jervis Bay, however, the equilibrium textural gradient, scant evidence of erosion, deeper shelf break, and gentle upper slope suggest that the area was not exposed during the Wisconsin, but formed a gently shelving sea which maintained sedimentation over a long period. These sediments are therefore also probably relict. They are unlikely to be palimpsest and the result of modern depositional processes. The textural gradient is most likely related to a shoreline at about 100 to 120 m.

GEOCHEMISTRY

The aims of the geochemical work undertaken in this study have been to determine and evaluate the concentration and distribution of certain selected elements and minerals, to suggest reasons for the variation, and to delineate problems which may require further study. Elements were chosen for analysis because of their geological, economic, and environmental importance. Both main group and transition metals and non-metals were studied. Chemical analysis was carried out by the Australian Mineral Development Laboratories. The results of the analysis are given in Appendix 4.

General distribution and concentration patterns

Data shown in Figures 65 and 66 are for elements and minerals whose analytical range facilitated contouring. Values for tin, copper, lead, nickel, and cadmium were too low. Maximum, minimum, and mean values together with comparative values from other locations are shown in Table 4.

Calcium carbonate. The data in Figure 65A show a general increase of calcium carbonate away from the coast, with more than 90 percent occurring on the outer shelf. Low values (less than 10%) occur in the close-inshore quartz sands. High values occur close inshore east of Batemans Bay.

Phosphate. Highest values (4000-5000 ppm) occur on the outer shelf (Fig. 65B), but a large portion of the sediments on the shelf between Port Kembla and Batemans Bay also have high values. There appears to be a strong positive relation with calcium carbonate. Values in the mid-shelf muddy sands are generally higher than those reported for the Scotian Shelf (Canada) in Table 4 (Phipps & King, 1969).

TABLE 4. METAL CONCENTRATIONS IN AUSTRALIAN SHELF SEDIMENTS AND OTHER AREAS

		$CaCO_3$	P_2O_5	*Sn*	*Cu*	*Pb*	*Zn*	*Mn*	*Ni*	*Fe*	*Co*	*Cd*	*As*	C^{org}	*Ti*
Southeast Australian Continental Shelf	Max.	53.8	7 500	10	5	10	35	80	10	1.4	10	3	180	0.25	0.78
	Min.	1.43	140	5	2.5	2.5	0	5	2.5	0.1	2.5	0.5	1.0	0.01	0.03
Inner shelf	Mean	15.1	653	5.5	4.1	3.3	12.6	30.6	5.2	0.38		1.0	10.6	0.07	0.16
Mid-shelf	Max.	56.6	3 500	20	20	20	140	180	35	3.6	25	4.0	50	1.4	0.45
	Min.	12.4	960	5	2.5	5	15	50	10	0.9	2.5	0.5	1	0.26	0.05
	Mean	38.3	1 573	6.3	8	10	50	95	21	1.86	9.3	2.3	9.0	0.7	0.21
Outer shelf	Max.	95.6	10 500	20	10	10	85	380	35	8.7	15	5	130	1.2	0.2
	Min.	8.6	200	5	2.5	2.5	5	25	3	0.2	3	1	10	0.04	0.03
	Mean	59.0	2 560	5.7	4.3	5.3	26	84	17	2.1	8.3	3	35.2	0.16	0.07
Sands—Gulf of Paria (1)	Av.				6.8	20.3		460	16.3	3.0	7.2				
	Min.				2.1	3.6		20	8.9	0.98	3.3				
	Max.				13	81		1 100	23	4.9	11				
	Detr. Av.				4.6	17.3			14.01		3.95				0.27
	N.D. Av.			1.3	1.4	0.5			3.1		3.08				0.62
Muds—Gulf of Paria (2)	Av.				18	22		1 420	29	5.15	11.3				
	Min.				15	13		400	22	4.21	9.8				
	Max.				23	32		2 900	32	6.41	13				
	Detr. Av.				15	24.8			24.4		9.27				0.47
	N.D. Av.			1.4	4.4	0.61			4.3		2.3				0.75
Sahara (3) Sand	Silt		1 800		78	62	130	605	108		16				
	Min.		1 200		34	46	25	53	41		3				
	Max.		2 000		61	53	160	467	79		24				
Morocco (3)	Silt		1 100		58	30	101	563	53		13				
	Sand		4 600		22	27	64	424	22		8				
World averages (4)	Shale		1 600	6	45	20	95	850	68	4.7	19	0.3	13		0.46
	SST					7	16		2	0.98	0.3		1.0		0.15
	LST				4	9	20	1 100	20	0.38	0.1	0.035	1.0		0.04
Average shale (5)					57	20	80	850	95	4.7	20	0.3	6.6	0.1	0.45
Cardigan Bay (6, 7)	Min.				2.5	5.4	3.8					0.2			
	Max.				43	240	144					3.4			
West Africa (8)	Min.				18	3	18		35					11	
	Max.				129	32	337		455					23	

Timor Sea (9)	Min.										0.31	
	Max.										1.9	
Broad Sound (10)	MNE	56.7	915	15.2	9.9	20.1	770	15.2	1.57	11	0.05 to 0.3	0.22
	SPT	4.5	842	21	16	57.1	551	32.6	3.9	17.4	0.4 to 0.9	0.47
	Int.	31.6	497	12.8	9.7	16.7	579	16.3	1.3	12.4	0.05 to 0.55	0.24
	Mch.	24.2	803	17.8	11.4	36.6	363	20.1	2.3	11	0.45 to 0.7	0.37
Saarich Inlet (11)	Min.			30	Tr	48		21			1	
	Max.			120	Tr	180		34			7.21	
Nearshore sediments (8)				48	20	95		55				
Caribbean (11)											0.5 to 1.0	
Black Sea (12)											0.52 to 0.87	
Scotian Shelf (13)	Grav.	0.34	500				90		0.58			0.054
	Sand	1.43	700				220		1.12			0.18
	Silt	3.97	1 200				320		1.99			0.35
	Clay	3.92	1 800				700		4.06			0.495

All values are in ppm except for $CaCO_3$, Fe, C^{org}, and Ti which are percentages. At Broad Sound, marine (MNE), supratidal (SPT), intertidal (INT), and mangrove channel (MCH) environments are delineated. Figures in parentheses refer to references from which the data were obtained:

1 and 2. Hirst, D. A., 1962a, b
3. Summerhayes, C. P., 1972
4. Turekian, K. K., & Wedepohl, K. H., 1961
5. Krauskopf, K., 1967
6. Jones, A. S. G., 1972
7. Jones, A. S. G., 1973
8. Calvert, S. E., & Price, N. B., 1970
9. Van Andel, T. H., & Veevers, J. J., 1967
10. Cook, P. J., & Mayo, W. (in prep.)
11. Richards, F. A., 1970
12. Berner, R. A., 1970
13. Phipps, C. V. G., & King, L. H., 1969

N.D. = non-detrital

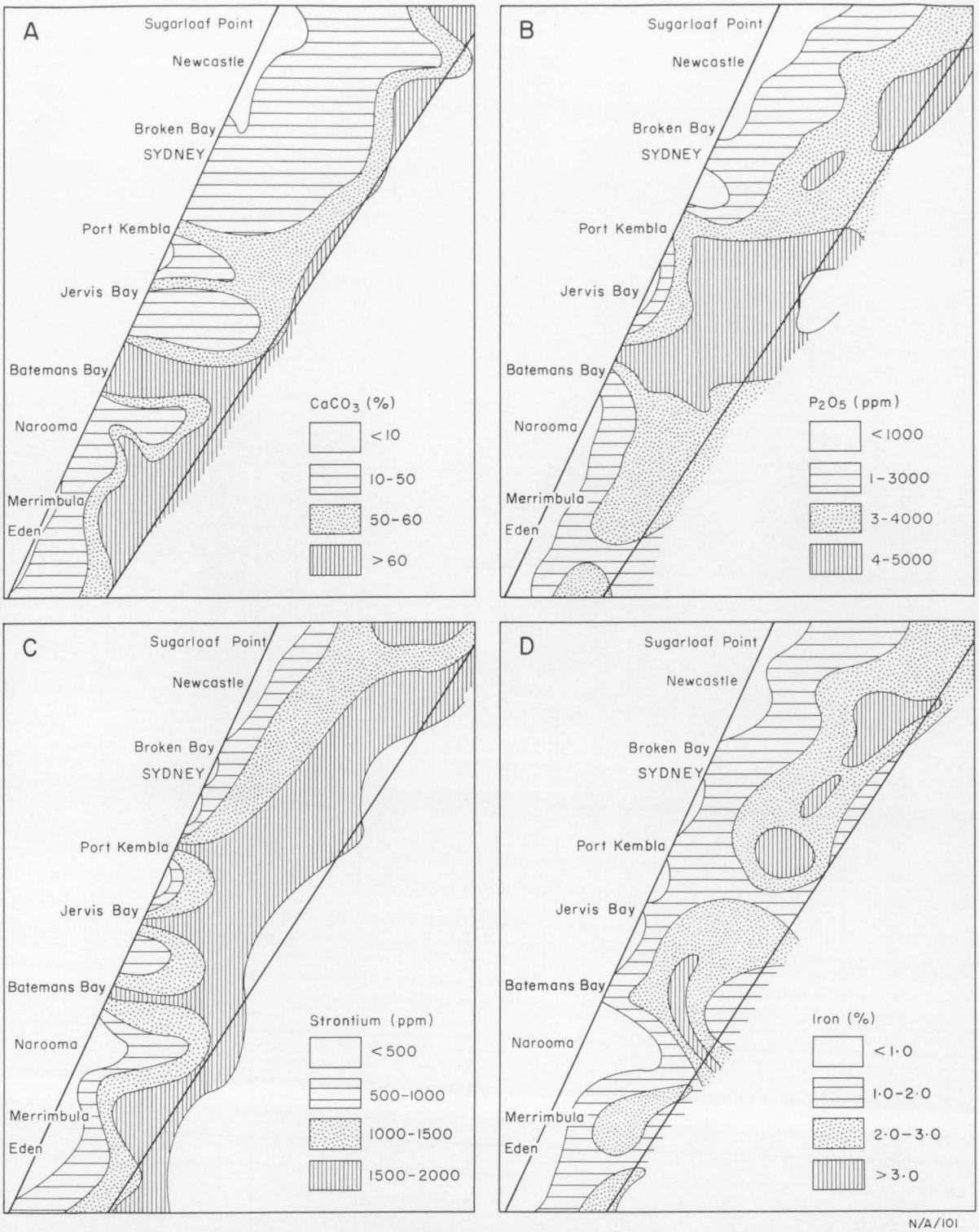

Fig. 65. Diagrammatic representation of the distribution of A. $CaCO_3$, B. P_2O_5, C. strontium, and D. iron.

Strontium. The distribution of strontium is shown in Figure 65C. Average outer-shelf values are in excess of 2000 ppm. In almost all places there is an increase in strontium away from the present coastline, essentially paralleling changes in calcium carbonate. The differences in the strontium and calcium carbonate distribution may be explained as due to variations in the relative proportions of aragonite and other carbonate species. The strontium values are much lower than values reported for recent reefal sediments (St John, 1970), but are similar to expected values in colder-water detrital carbonates (Conolly & Von der Borch, 1967; Wass, 1970; Lees & Buller, 1972).

Copper. Copper in the shelf sediments ranges from 2.5 to 20 ppm. Highest values occur in the mid-shelf muddy sands, where the mean value is higher than maximum values in most of the other shelf sediments. Comparisons of these values with the average shale (45 ppm—Table 4) and the average limestone (4 ppm—

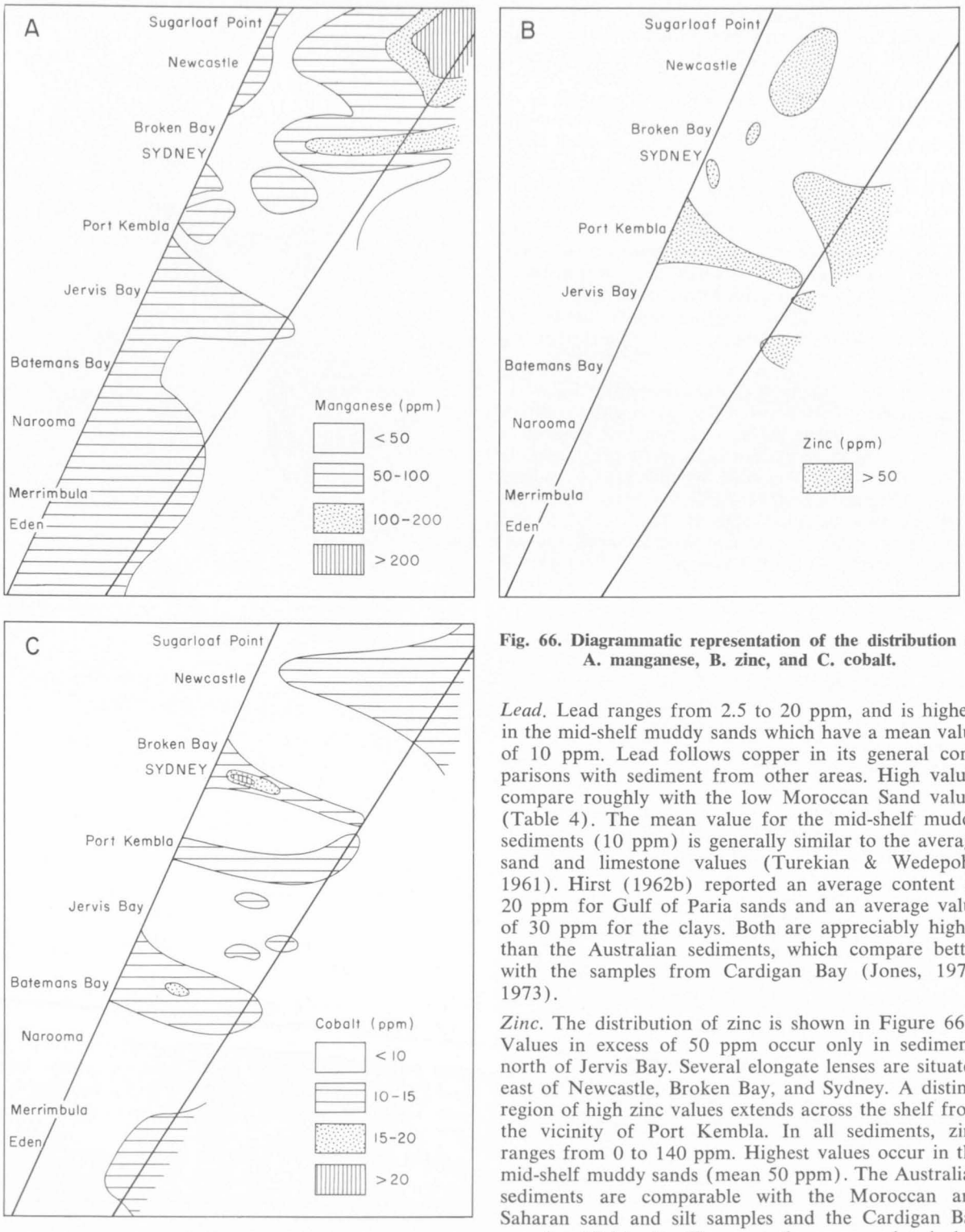

Fig. 66. Diagrammatic representation of the distribution of A. manganese, B. zinc, and C. cobalt.

Table 4) illustrates the relative influence of silt and carbonate in the shelf sediments. The mid-shelf sediment copper contents are comparable with values for Cardigan Bay, Wales (Jones, 1972, 1973). The highest values are comparable with some of the Moroccan Shelf sands analysed by Summerhayes (1972), but generally the Moroccan and Saharan Shelf sands are richer in copper than the Australian sediments. The average values for the mid-shelf muddy sands is closer to sand values from the Gulf of Paria (Hirst, 1962b), where the muds and clays show higher concentrations.

Lead. Lead ranges from 2.5 to 20 ppm, and is highest in the mid-shelf muddy sands which have a mean value of 10 ppm. Lead follows copper in its general comparisons with sediment from other areas. High values compare roughly with the low Moroccan Sand values (Table 4). The mean value for the mid-shelf muddy sediments (10 ppm) is generally similar to the average sand and limestone values (Turekian & Wedepohl, 1961). Hirst (1962b) reported an average content of 20 ppm for Gulf of Paria sands and an average value of 30 ppm for the clays. Both are appreciably higher than the Australian sediments, which compare better with the samples from Cardigan Bay (Jones, 1972, 1973).

Zinc. The distribution of zinc is shown in Figure 66B. Values in excess of 50 ppm occur only in sediments north of Jervis Bay. Several elongate lenses are situated east of Newcastle, Broken Bay, and Sydney. A distinct region of high zinc values extends across the shelf from the vicinity of Port Kembla. In all sediments, zinc ranges from 0 to 140 ppm. Highest values occur in the mid-shelf muddy sands (mean 50 ppm). The Australian sediments are comparable with the Moroccan and Saharan sand and silt samples and the Cardigan Bay samples (Table 4). However, the mean value is less than in the average shale. Mean values for the closer-inshore sands and the outer-shelf carbonates are higher than values reported for the average sandstone and limestone respectively (Table 4).

Manganese. The distribution of manganese is shown in Figure 66A. North of Port Kembla, values in excess of 150 ppm are common on the outer shelf, while to the south, values less than 50 ppm characterize most of the area. South of Port Kembla there appears little relation between manganese and iron. In all sediments manganese ranges from 5 to 380 ppm. The highest mean

values occur in the outer shelf carbonate (84 ppm). This is low compared with all reported analyses, except those from the continental shelf off eastern Canada (Phipps & King, 1969). Hirst (1962a) reported average values of 1000 ppm for sands and 2000 ppm for muds in the Gulf of Paria. Moroccan and Saharan sediments, although closer to the Australian samples, are still much higher in manganese. The average shale and limestone (Table 4) contain about 88 to 11 times more manganese. Australian shelf sediments are therefore unusually deficient in manganese. Only the Scotian Shelf samples compare with the east Australian samples. However, whereas in the Scotian samples increasing manganese content correlates with decreasing grainsize, the reverse is true in the Australian sample, the highest manganese occurring in the coarse carbonates of the outer shelf.

Nickel. Concentrations of nickel range from 2.5 to 35 ppm. Lowest values occur in the close inshore sands. Highest values occur in the mid-shelf and outer-shelf sediments. The highest mean value of 21 ppm occurs in the mid-shelf sands. This is higher than values reported for sands from the Gulf of Paria, but lower than muds from the same locality (Table 4). The values are also lower than most Moroccan and Saharan sands, and are much lower (X3) than the average shale (Turekian & Wedepohl, 1961; Krauskopf, 1967). They are, however, comparable with the average limestone.

Iron. It is noticeable (Fig. 65D) that iron values generally increase away from the shoreline, the highest values occupying the mid-shelf to outer-shelf area (2.1% mean value). It is noticeable also that iron values decrease away from the outer shelf down the continental slope. The axis of change coincides approximately with the 140-m isobath.

The mean outer-shelf value of 2.1 percent is lower than the average value for the Gulf of Paria sediments (Table 4). It is much lower than the average shale, but higher than the average sandstone and limestone (Table 4). It is similar to values reported by Phipps & King (1969) for sands and silts of the Scotian Shelf.

Cobalt. The distribution of cobalt is shown in Figure 66C. It ranges in concentration from 2.5 to 25 ppm, the highest mean value occurring in the mid-shelf and outer-shelf sediments (9.3-8.3 ppm). These averages fall midway between the averages for sand and mud samples in the Gulf of Paria, and are very similar to concentrations in the Moroccan and Saharan sediments. The average value for shale is nearly twice as high, but cobalt in the Australian sediments is 30 to 90 times more concentrated than in the average sandstone and limestone.

Cadmium. A range of 0.5-5 ppm occurs in the sediments, with highest mean values occurring in the mid-shelf (2.3 ppm) and outer-shelf (3 ppm) sediments. Compared with average rock types, the Australian sediments are an order of magnitude richer in cadmium than the average shale and sandstone, and two orders of magnitude richer than the average limestone (Table 4). Jones (1972) measured cadmium in comparable concentrations in the Cardigan Bay sediments.

Arsenic. Arsenic ranges in concentration from 1 to 180 ppm. Low values occur close inshore, while high values occur in sediments occupying the outer shelf between Port Kembla and Newcastle (Fig. 67). These values are two orders of magnitude higher than the values quoted for the average shale, sandstone and limestone

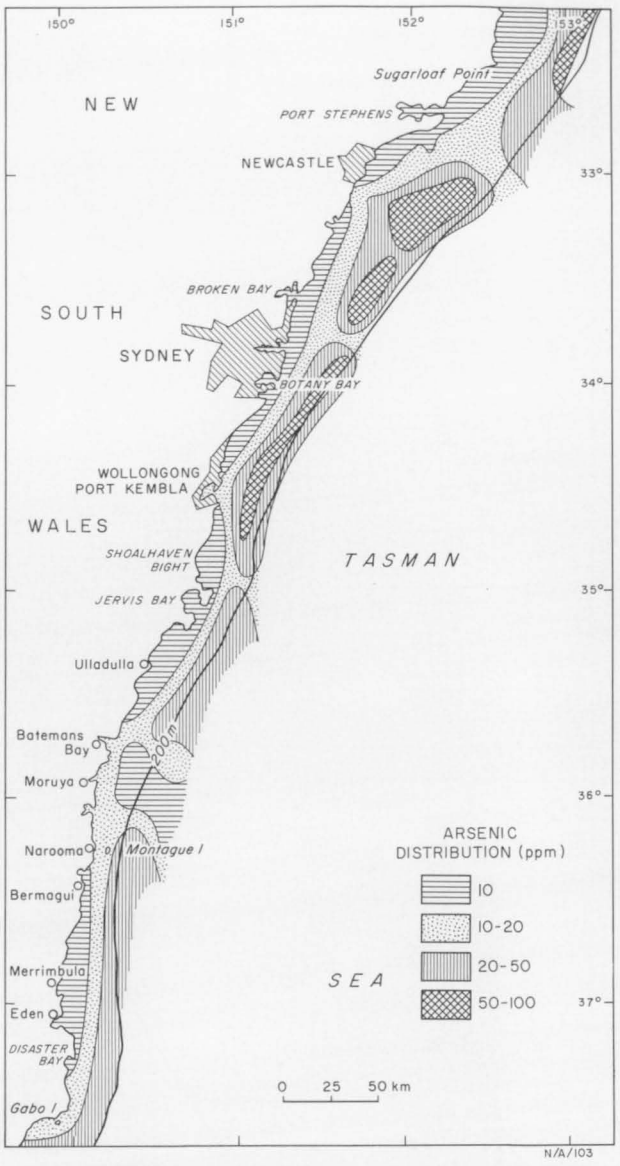

Fig. 67. Distribution of arsenic on the continental shelf.

(Table 5). Similarly the average value for crustal rocks (1.8 ppm) is markedly lower than values found in the Australian shelf sediments. Tooms et al. (1969) reported high arsenic contents (up to 188 ppm) in phosphorites, and Pilipchuk and Sevast'Yanov (1968) reported high arsenic contents (18 ppm) in Black Sea sediments.

TABLE 5. ARSENIC CONTENTS IN SEDIMENTS AND ROCKS

Average shale	1.3 ppm	Turekian & Wedepohl, 1961
Average sandstone	1.0 ppm	
Average limestone	1.0 ppm	
Crustal rocks	1.8 ppm	Mason, 1966
Sea water	2.6 ppb	Turekian, 1968
World-wide phosphorites	0.4-188 ppm	Tooms et al., 1969
Lake Michigan sediments	5.3 ppm	Ruch et al., 1970
Black Sea sediments	18 ppm	Pilipchuk & Sevast'Yanov, 1968
East Australian shelf sediments	1-180 ppm	

Variable	Factor I	Factor 2	Factor 3	Factor 4	Factor 5	Factor 6
$CaCO_3$	−			+++		
P_2O_5	−−−					
Sn		+			+	
Cu	+	−	+			
Pb					+	+
Zn		+				++
Mn					+++	
Ni				++		
Fe		+++			+	
Co						++
Cd				++		
As			−−−			
C_{org}		+++				
Ti	−		+		+	
S.D.	−−−					
Mean	+	+	+			+
Gravel	−−−					
Sand	+++					
Mud		+++				
Depth			−−			−

KEY TO FACTOR MATRIX

+++ −−− Positive and Negative Factor Loadings greater than 0·8

++ −− Positive and Negative Factor Loadings between 0·6 and 0·8

+ − Positive and Negative Factor Loadings between 0·3 and 0·6

N/A/104

Fig. 68. Varimax rotated factor matrix for Group A sediments.

Organic Carbon. Organic carbon is most abundant in the mid-shelf muddy sediments where it ranges from 0.26 to 1.4 percent (mean 0.7%). Van Andel & Veevers (1967) reported similar values for Timor Sea sediments. Krauskopf (1967) quoted a figure of 0.1 percent for the average shale.

Titanium. The distribution of titanium is shown in Figure 50. The highest value occurs in the close-inshore sediments (0.78%), but the highest mean occurs in the mid-shelf muddy sands (0.21%). Concentrations are comparable with those reported for the Gulf of Paria and the Moroccan and Saharan sands and silts (Table 4). However, higher concentrations occur in the average shale, whereas values reported for average sandstones and limestones compare well with their unlithified counterparts on the east Australian shelf. Scotian shelf sediments are also comparable in titanium content (Table 4).

Interpretation

R-mode factor analysis (Appendix 4B) has been used to examine relations between variables within the major groupings previously delineated by the Q-mode factor analysis.

Group A sediments. This represents the well sorted quartz sands which occupy the depth range 15-60 m. Six factors explain 75.3 percent of the sample variance. The varimax rotated factor matrix for these sediments is shown in Figure 68.

Factor 1. Eight variables make up factor 1 (Fig. 68) of which P_2O_5, standard deviation, and gravel vary directly with calcium carbonate and titanium, while percent sand varies directly with the mean grainsize and copper concentration. The mean grainsize, and percentages of titanium, copper, and calcium carbonate form only a small part of the factor. The significant correlation coefficients are shown in Figure 69. The highly significant inverse relation between sand and phosphate/gravel/standard deviation is a result of the closed-array structure of the granulometric data. However, a significant positive relation occurs between the granulometric (gravel, standard deviation) and chemical data.

The granulometric variables suggest that textural control largely influences the factor. Sedimentary evidence indicates that the sediments are relict and that car-

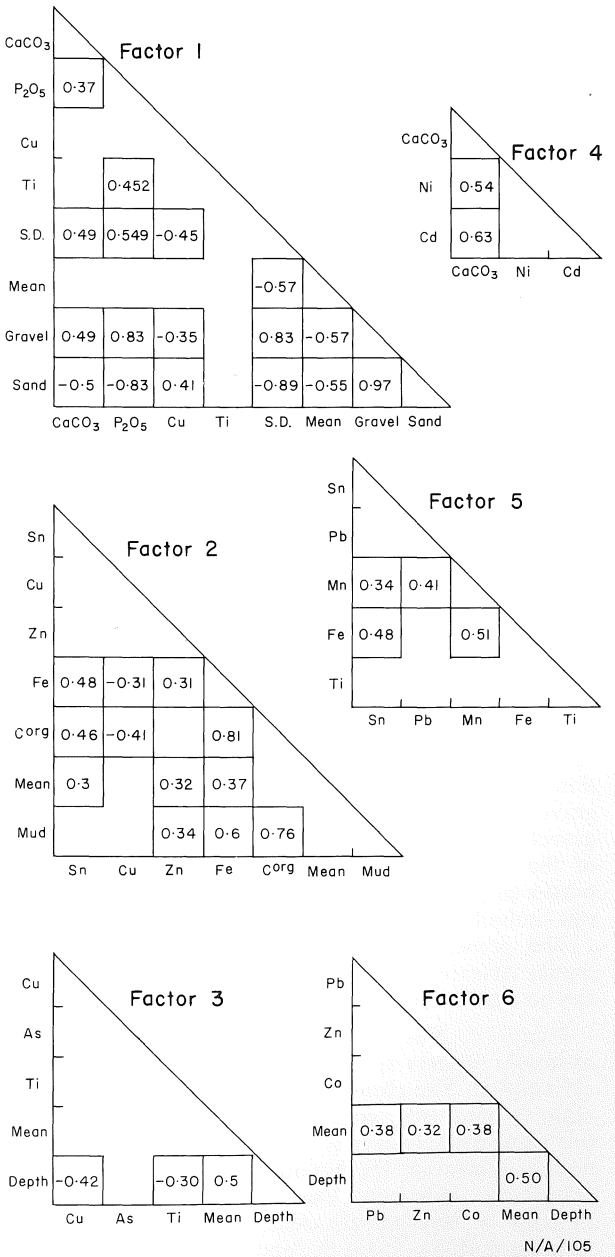

N/A/105

Fig. 69. Significant correlation coefficients for each factor (95% significance level) for Group A sediments.

bonate-shell lag gravels were left stranded in deeper water during the Holocene sea-level rise. This explains the significant carbonate/gravel association. The correlation coefficients for gravel: $CaCO_3$:P_2O_5 indicate that phosphate occurs primarily in association with gravel, i.e. sand-grade $CaCO_3$ is not associated with phosphate. The association of phosphate with carbonate gravel may be due to phosphatization of lag gravels close to a shoreline, i.e. diagenetic alteration, or organo/phosphatic layers on the shells related to the living organism. In both cases, the relation of phosphate is to a specific depositional regime, the shoreline zone. This also helps to explain the association of titanium with phosphate. At first glance, this correlation suggests a possible substitution of titanium during phosphatization. However, it is highly likely that titanium in these sediments occurs within heavy minerals which also concentrate within a shoreline environment. The non-association of titanium with gravel is therefore interpretable, as titanium probably forms part of the fine sand/silt fraction. It correlates with gravel only because it relates to the same depositional environment.

Factor 2. Six variables constitute factor 2, which is dominated by mud, organic carbon, and iron. The basis of this interpretation is therefore once again textural control. Tin, zinc, and copper form minor contributors to the factor. The significant correlation coefficients are shown in Figure 69. Iron, by virtue of its significant correlation with mud, is likely to be finely disseminated iron oxide and/or hydroxides onto which zinc has been adsorbed either during weathering or transport. The absence of metals other than tin, adsorbed on iron hydroxides or organic material, suggests that the critical basis to this factor is the modern depositional regime. Krauskopf (1956) has shown that lead is a readily adsorbed metal. It should therefore form a part of this factor if the oxides and/or organic material had a long residence time within the present environment.

Factor 3. The association of arsenic, depth, copper, titanium, and mean grainsize is thought to reflect the effect that depth has on its co-variables. The significant correlations between copper, titanium, mean grainsize, and depth indicate that copper and titanium decrease with depth and form part of the 2.0-3.0 $\emptyset$ sand fraction. The inverse relation between copper, titanium, and mean grainsize is opposite to that found by Jones (1973) for Cardigan Bay samples. However, the presence of copper within the medium to fine sand fraction explains the negative correlation of copper with gravel and mud in factors 1 and 2, and titanium with gravel in factor 1. The titanium undoubtedly forms part of the heavy-mineral fraction, while copper probably occurs as part of rock fragments or pyroxene which are size-limited.

The presence of arsenic within the factor is enigmatic. Arsenic and depth show positive factor loadings but no significant correlation.

Factor 4. The association of $CaCO_3$, nickel, and cadmium appears at first sight to be a simple geochemical relation. The close resemblance of cadmium to calcium in ionic size and charge would tend to support this view, while the ready substitution of nickel for magnesium reinforces the hypothesis. However, carbonate-producing organisms like molluscs and corals are thought to discriminate against cadmium and nickel (Mullin & Riley, 1956; St John, 1970), while in almost all reported cases, cadmium and nickel concentrations are exceptionally low in calcareous skeletons, and are lower in aragonite forms than in calcite. St John (1970) has suggested that boring algae are important agents for increasing trace metal contents. Kanwisher & Wainright (1967) reported that 12 percent by volume of the scleractinian coral *Montrastrea annularis* comprised boring algae. Almost all carbonate fragments on the continental shelf have been heavily bored by algae (Fig. 38). The relation of cadmium and nickel with $CaCO_3$ may therefore be due to halmyrolitic factors operative during and since the Holocene transgression. It is possible, however, that the relation indicates a specificity of cadmium and nickel for some particular carbonate-precipitating organism, as has been reported by Bowen & Sutton (1951) in the case of nickel in the sponge *Dysidae crawshayi* and by Stevenson & Ufret (1966), for nickel in the sea urchin *Echinometra lucunter.* In view of the almost ubiquitous association of boring algae with detrital carbonate material, the factor 4 associations are most likely to be the result of this underlying influence.

Factor 5. The association of manganese, tin, lead, iron, and titanium is thought to be a result of diagenetic-geochemical variables. The major component of the factor is manganese which shows significant positive correlations with tin, lead, and iron (Fig. 69). Manganese hydroxides and oxides form an important part of the particulate fraction in sea water, and form active scavengers of metals (Goldberg, 1954; Goldberg & Arrhenius, 1958; Krauskopf, 1956). Krauskopf (1956) stated that manganese dioxide and hydrated ferric oxides provide strongly adsorbent surfaces for lead, and the highly significant correlation coefficients for manganese, iron, and lead (Fig. 69) support the contention.

Petrographic studies show that most sedimentary particles in Group A sediments are partly covered by brown oxidation coatings. It is impossible to state whether these coatings are a result of colloidal precipitation from sea water or were formed on the grains during a previous depositional cycle. The lead association suggests that the oxide coatings have surrounded the grains for some time. This would be consistent with the present-day hydraulic regime in the inshore zone where colloidal particles are more likely to remain in suspension owing to agitated conditions.

Factor 6. Zinc, cobalt, lead, mean grainsize and depth form the important variables in factor 6. All variables correlate with mean grainsize which suggests that some sediment component may be the underlying cause of the association. Lead, zinc, and cobalt may occur within rock or mineral fragments, e.g. augites and hornblendes. It is also possible that micas form sites for all three metals.

Group B sediments. The varimax rotated factor matrix for Group B sediments is shown in Figure 70. Six factors explain 80 percent of the sample variance. The correlation half-matrixes showing significant correlations for each factor show a large number of statistically significant correlations which are due to the closed array structure of some of the data. This is especially the case in factor 1 (Fig. 71).

Factor 1. This is composed of organic carbon, mud, silt, clay, standard deviation, sand, mean grainsize, copper, nickel, zinc, manganese, iron, titanium, and $CaCO_3$. All variables except $CaCO_3$ and sand correlate negatively (Fig. 71).

The geochemical variation can be explained almost wholly on the basis of the fine-grained components of

Variable	Factor 1	Factor 2	Factor 3	Factor 4	Factor 5	Factor 6
$CaCO_3$	+	−		−	−	+
P_2O_5		−−−				
Sn				+++		
Cu	−−					
Pb					++	
Zn	−			++		
Mn	−	−				−
Ni	−−	−				
Fe	−	−−−				−
Co			+++			
Cd						+++
As		−−				−
Corg	−−−		+			
Ti	−				+	
S.D	−−−					
Mean	−−				+	
Gravel					−−	
Sand	+++				−	
Mud	−−−				+	
Silt	−−				+	
Clay	−−−		+		+	
Depth		−		−	−	

KEY TO FACTOR MATRIX

+++ −−− Positive and Negative Factor Loadings greater than 0·8

++ −− Positive and Negative Factor Loadings between 0·6 and 0·8

+ − Positive and Negative Factor Loadings between 0·3 and 0·6

N/A/106

Fig. 70. Varimax rotated factor matrix for Group B sediments.

the sediments. The correlation coefficients suggest that copper is likely to occur in three sites: adsorbed on the surfaces of clay minerals; within or on organic material; and within detrital minerals of clay grade.

Revelle et al. (1955) reported copper mainly associated with the soft parts of organisms, and Hirst (1962b) concluded that copper forms part of clay minerals. Zinc, like copper, occurs in the same three sites, but nickel only occurs in clay minerals of the finest fraction, where it is associated with zinc and manganese. Hirst (1962b) and Nicholls & Loring (1962) also showed nickel intimately associated with clay minerals. It is likely to occur adsorbed on or within the lattice of degraded clays. Goldberg (1954) pointed to the co-variance of nickel and manganese, both of which correlate significantly with themselves and with clay minerals in the mid-shelf sediments. A plot of titanium against silt or clay (Fig. 63) suggests that titanium probably occurs in silt-grade heavy minerals, and in lattice positions in clay.

The critical variables in this factor are undoubtedly those indicating a depositional environment, i.e. the granulometric variables. This has previously been suggested as relict. Also the significant association of manganese with nickel and iron suggests that precipitation of manganese and iron hydroxides, with concomitant scavening of other trace metals from the overlying water column, has occurred since deposition.

The occurrence of calcium carbonate and sand in this factor is due entirely to the closed-array nature of the granulometric data, and the intimate association of calcium carbonate with sand-grade material.

Factor 2. The variables within this factor are P_2O_5, iron, arsenic, manganese, nickel, depth, and $CaCO_3$. The significant relation between P_2O_5 and $CaCO_3$ (Fig. 71) suggests that phosphate occurs either as part of originally phosphatic shells, or as a diagenetic replacement of shell debris. The strong association of iron with phosphate, and the poor relation of iron with

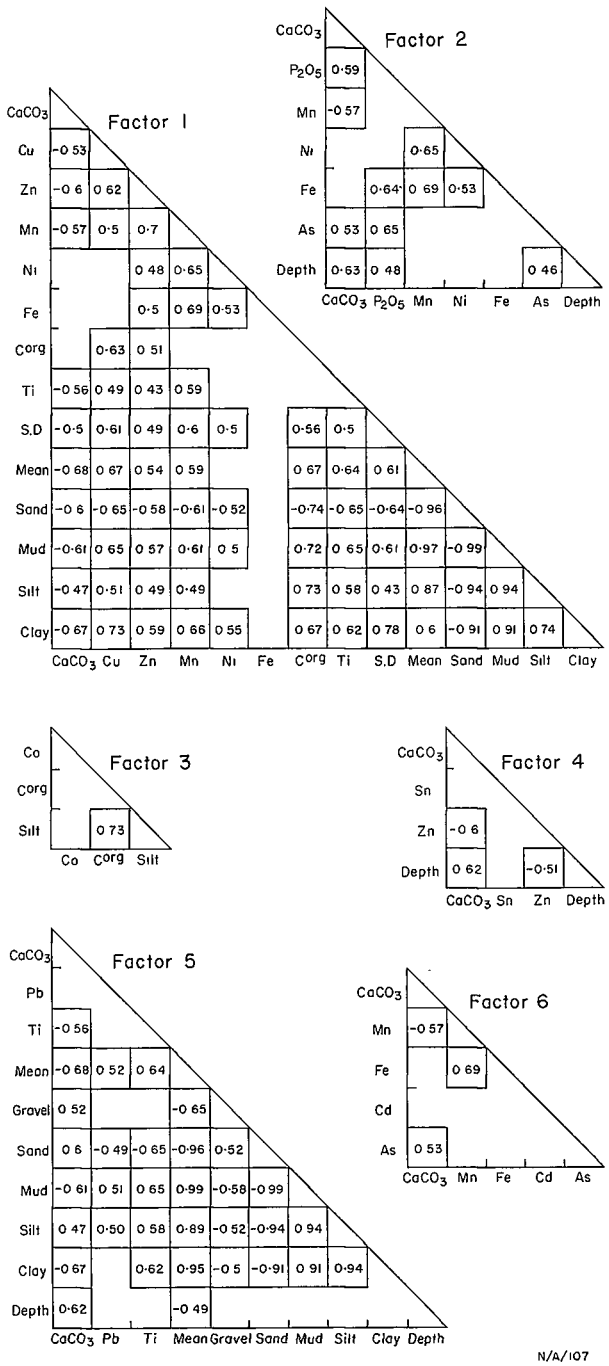

Fig. 71. Significant correlation coefficients for each factor (95% significance level) for Group B sediments.

calcium carbonate imply that iron and phosphate may owe their origin to related processes. This is more likely to be the result of phosphatization and ferruginization related to low sea levels rather than to oxidation of discrete parts of phosphatic carbonate shells.

Arsenic shows significant positive relations with phosphate and calcium carbonate. The generally poor chemical relations between arsenic and calcium, the close affinities between arsenic and phosphorus, and the high arsenic values associated with marine phosphorites (Tooms et al., 1969) support the view that arsenic in these sediments is associated with the phosphate and probably second-order correlation induced by the close association of phosphate and calcium carbonate. McConnell (1970) supported the contention in reporting that arsenic substitutes for phosphates in apatite lattices.

It is suggested that the underlying causes relating the elemental and mineralogic correlations are diagenetic phosphatization and ferruginization associated with past low sea levels.

Factor 3. The variables in factor 3, in order of importance, are cobalt, organic carbon, and silt. The correlation matrix shows only one significant relation—that between organic carbon and silt. Cobalt does not correlate significantly with either carbon or silt, suggesting that it may occur associated with only a part of the organic/silt fraction. A close association of cobalt with organic material has been suggested by many workers (Hirst, 1962b; Nicholls & Loring, 1962; Hogdahl, 1963); Riley & Chester (1971) considered that cobalt is essential to the growth of some marine organisms. However, El Wakeel & Riley (1961) concluded that one-half to one-third of cobalt occurring in deep-sea sediments is sited in ferromanganese minerals. Smithells (1962) concluded that cobalt substitutes for iron in igneous rocks, especially basic igneous rocks, and that there is a strong relation between cobalt and nickel. In the east Australian Group B sediments, the poor correlation between cobalt and nickel and their presence in different factors preclude any possibility of cobalt occurring in silt-sized igneous-derived minerals like pyroxene or amphiboles. It is more likely therefore that cobalt occurs associated with a particular part of the organic fraction, either adsorbed on surfaces which have specific chelation properties or internally situated as a result of incorporation during growth of the organic material. The basic reason for the distribution of cobalt may therefore be either organic genesis or diagenesis.

Factor 4. Tin, zinc, calcium carbonate, and depth are the four variables within factor 4 (Fig. 70). Both tin and zinc correlate negatively against each other (Fig. 71). This must indicate that zinc and tin occur within different components of the detrital non-carbonate fraction. The absence of granulometric variables within the factor suggests that tin and zinc are housed somewhere within the accessory part of the non-carbonate fraction.

Factor 5. The principal variables within factor 5 are lead, titanium, mud, silt, and clay. Other less important variables are a result of the closed array granulometric data (Fig. 70). Lead correlates significantly with silt, and titanium with clay and silt (Fig. 71). Amphiboles and pyroxenes comprise an important part of the silt fraction. The titanium and lead might well occur within augites and hornblendes (Deer et al., 1972). They are unlikely to occur within epidotes which are also accessory minerals within the silt-grade fraction. The underlying cause of this factor is therefore discrete mineralogic components within the silt fraction.

Factor 6. Cadmium, calcium carbonate, manganese, iron, and arsenic are the major variables in factor 6 (Fig. 70). Cadmium correlates positively, but not significantly, with calcium carbonate (Fig. 71), and the other variables correlate negatively with cadmium and calcium carbonate. The origin of the association is obscure, and may involve a combination of diagenetic and geochemical criteria.

Group C sediments. The varimax rotated factor matrix for Group C is shown in Figure 72. Six factors explain 72 percent of the sample variance. The correlation half-matrixes showing the significant correlations for each factor are shown in Figure 73. In factors 4 and 5, no significant correlation coefficients occur.

Factor 1. Phosphate, copper, zinc, nickel, iron, cobalt, titanium, and depth comprise the major variables in factor 1. The highly significant relation between phosphate and iron is similar to that seen in Group B sediments. Phosphatization and oxidation may therefore be related processes during shallow-water diagenesis. The highly significant phosphate:zinc association suggests substitution of zinc for calcium during phosphatization. However, zinc and nickel may occur as adsorbed ions on the iron oxide coatings surrounding grains. The significant zinc:titanium association is puzzling and may represent a heavy-mineral association which could also include iron. If this is the case, then the underlying cause of this association may be shallow-water deposition close to the edge of the continental shelf, facilitating diagenetic phosphatization and heavy-mineral accumulation. Oxidation of grains is likely to accompany the phosphatization, a phenomenon also reported by Summerhayes (1972).

Factor 2. Factor 2 is geochemically unimportant and is a function of the closed-array nature of the granulometric data.

Factor 3. The association of manganese, nickel, iron, and arsenic is significant because of the absence from this factor of variables suggesting diagenesis (phosphate), sedimentation (granulometry), or mineralogy (calcium carbonate). The extremely significant arsenic:manganese correlation supports previous contentions (Bostrom & Valdes, 1969; Pilipchuk & Sevast'Yanov, 1968) that arsenic migrates in the colloidal form adsorbed on metal complexes. In the present case it is suggested that arsenic is being transported adsorbed on manganese colloids, a conclusion which is reinforced by the less significant arsenic:iron correlation, and the highly significant arsenic:nickel and nickel:manganese correlations. Goldberg (1954) suggested scavening of nickel by hydrous manganese dioxide, and Krauskopf (1956) showed that other adsorbents were ineffective in removing nickel. It is further suggested that the arsenic-nickel-manganese colloids are being deposited in the deeper, quieter waters of the outer shelf. The abnormally high concentrations and the localized occurrences point to a modern source and explanation. This is likely to be urban and industrial pollution.

Factor 4. Calcium carbonate, cobalt, cadmium, tin, and titanium constitute factor 4. The first three variables correlate positively and the last two negatively (Fig. 72). No statistically significant correlations occur (Fig. 73). However, a plot of percent calcium carbonate against the factor scores shows a significant rela-

Variable	Factor 1	Factor 2	Factor 3	Factor 4	Factor 5	Factor 6
$CaCO_3$				+		+
P_2O_5	− − −					
Sn				− −		
Cu	−				−	
Pb						+
Zn	− − −					
Mn			− − −			
Ni	− −		− −			
Fe	− −		−			
Co	−			+	+	
Cd				+ +		
As			− − −			
C_{org}					+	+ +
Ti	−			−	+	
S.D.		+ + +				
Mean		− −			+	
Gravel		+ + +				
Sand		− − −				
Mud					+ +	
Depth	−				+	

KEY TO FACTOR MATRIX

+++ − − − Positive and Negative Factor Loadings greater than 0·8

++ − − Positive and Negative Factor Loadings between 0·6 and 0·8

+ − Positive and Negative Factor Loadings between 0·3 and 0·6

N/A/108

Fig. 72. Varimax rotated factor matrix for Group C sediments.

tion, suggesting that mineralogy may be the underlying cause of the association (Fig. 74). This may be a result of an inherent carbonate trace element chemistry, or halmyrolitic algal boring similar to that suggested for Group A (factor 4) sediments.

Factor 5. Cobalt, organic carbon, titanium, mean grainsize, mud, and depth are the major positive variables in the factor, and copper correlates negatively with all. Very few of the variables correlate significantly. The presence of granulometric variables suggests a causal relation with the deposition of mud. However, the relations are unclear and the conclusion is highly speculative.

Factor 6. Three variables, calcium carbonate, lead, and organic carbon make up factor 6 (Fig. 72). No significant correlations occur (Fig. 73), but the most likely relation is between lead and organic material which still persists in relation to some shell material. The lead may be genetically related to the biology or may have been adsorbed from sea water after deposition of the shell and related organic material.

Controls on chemical distribution and concentration

The principal controls on chemical distribution and concentration are shown in Figure 75. By far the most important is the depositional environment, which affects 24 percent of the sample variance in Group A, 45 percent in Group B, and 24 percent in Group C. The control effected by the depositional environment is seen in two ways:

(a) grainsize variations reflect the chemical imprint of the sediments from both an inherent and an induced chemical viewpoint, and

(b) the depositional environment markedly affects early diagenetic overprints (algal boring and phosphatization/oxidation).

Provenance has also played a part in determining the trace-metal chemistry. The largest area of Group B muds occurs in the northern part of the area where the major rivers enter the ocean. In addition, specific mineralogy (pyroxenes and amphiboles) relates to the onshore geology. The effluent input into the system from areas of major industrial/urban conurbations represents a recent provenance effect. This is especially seen in the case of zinc, arsenic, and cobalt.

Pollutants

Zinc, arsenic, cobalt, and cadmium occur in concentrations which are high compared with standard rocks,

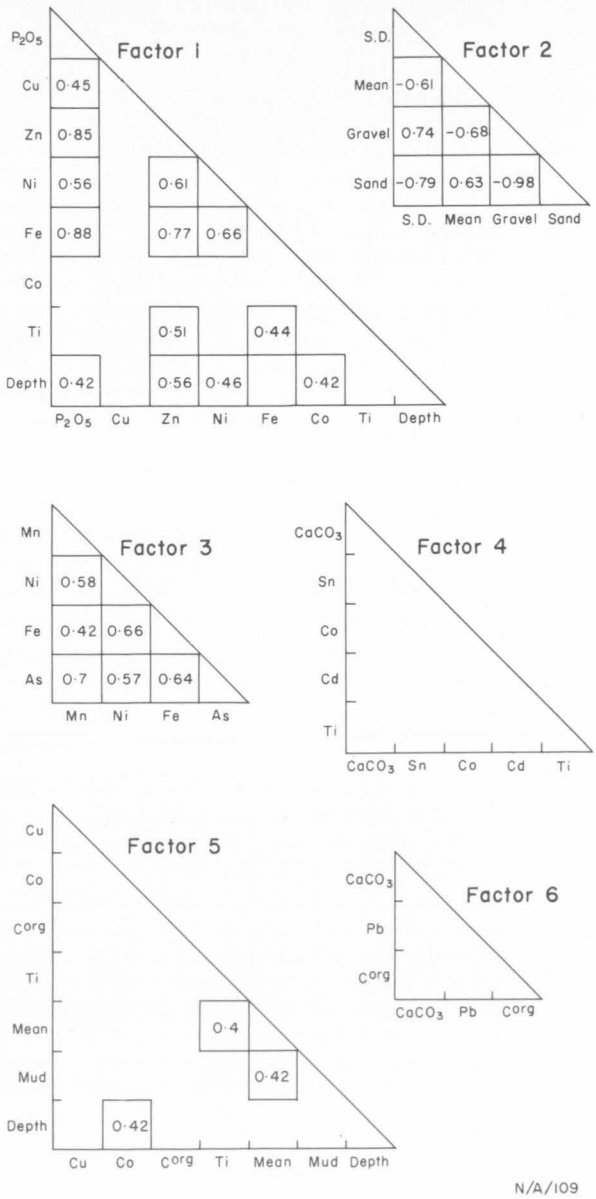

Fig. 73. Significant correlation coefficients for each factor (95% significance level) for Group C sediments.

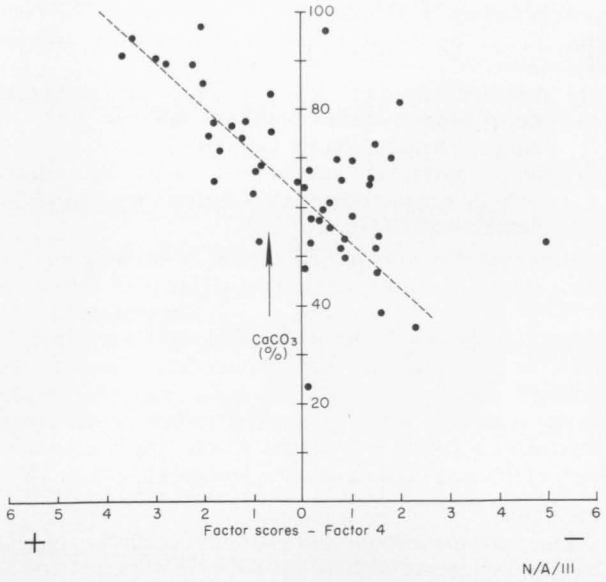

Fig. 74. Plot of percent calcium carbonate against the factor scores in Group C sediments.

and with sediments from other continental shelves. High concentrations are most likely to result from a combination of high input and minimum dilution. It has been previously noted that the sediments of the continental shelf are relict, and that little modern diluent is being added. The shelf surface is therefore one on which metals may accumulate, unhindered by sediment dilution. The major sources of input may be: natural weathering of rocks; natural weathering of soils enriched artificially by metals in fertilizers; and effluent input from urban and industrial conurbations. The distribution of metals on the shelf could therefore point to a distinction between agricultural and industrial derivation.

Zinc. The distribution map (Fig. 66B) shows zinc occurring in concentrations greater than 50 ppm only on those parts of the shelf adjacent to areas of major industrial/urban conurbations. The plume of high zinc values off Port Kembla is unlikely to be a coincidence as a copper smelter occurs onshore.

Arsenic. Possible natural sources of arsenic in the sediments (Fig. 67) are normal sea water, sea water enriched in arsenic in solution derived by natural erosive processes, and arsenic contained in sediment deposited on the shelf. Artificial sources of arsenic are industrial, urban, and agricultural wastes, which may be transported in solution and concentrated in the shelf sediments by organic or inorganic processes, or transported in solid form with sediment particles.

Sea water containing normal amounts of arsenic (2.6 ppb—Table 6) could be a source of metal enrichment in the sediments only if extreme inorganic or organic concentration occurred. Both processes would be aided by the fact that there has been little sedimentation on the outer continental shelf since the last sea level low. While some inorganic mechanism aided by minimal sediment dilution is a possibility, it does not readily explain the distribution shown in Figure 70. Relict sediments occur on the outer continental shelf throughout the area studied, but high arsenic concentrations are only present locally. Organic concentration from sea water is also possible, but there is not a close relation between arsenic and organic carbon in the sediments. Figures 68, 70, and 72 show that arsenic and organic carbon occur in different statistical factors, and are therefore unlikely to be controlled by the same environmental parameters.

Tooms et al. (1969) have shown that high arsenic concentrations occur in many phosphorites. In the southeast Australia area, the phosphate content of the sediments increases towards the edge of the shelf, and phosphate and arsenic appear therefore to be genetically correlated. However, the R-mode factor analysis separates arsenic and phosphate into different factors, suggesting that they are not related and that they are likely to have been controlled by different parameters. This indicates that the arsenic content of the shelf sediments is not a function of a mineralogic characteristic, like phospate. Also, the fact that arsenic does not occur within any factor related to mineralogic or depositional variables supports the conclusion that arsenic in the shelf sediments is not part of an inherent sedimentary characteristic. The arsenic is likely therefore to be entering the system from an external source.

Natural erosion of rock and soil in the hinterland may be a source of arsenic, although the major rock types contain very little arsenic. Brown & Swaine (1964) and Swaine (pers. comm.) reported only small arsenic concentrations in the coals of the Sydney Basin (3 ppm). This is low compared with coals from other parts of the world. Swaine (1955) also reported arsenic concentrations of 1-50 ppm in soils of various countries. If one assumes similar levels for Australian soils, the arsenic is likely to be derived from underlying rocks, and from pesticides and fertilizers used in agriculture. Ammonium sulphate (114 ppm), phospates (100 ppm), and superphosphates (hundreds of ppm) contain arsenic in various proportions (Swaine, 1962). Much of this will remain in the soil because the pH of the system renders it insoluble. It is therefore unlikely to reach the ocean unless it moves attached to other particles. As mentioned above, however, very little sedimentation is occurring on the continental shelf. An agricultural source for the arsenic seems also to be precluded by its distribution (Fig. 67): the maximum arsenic concentrations occur offshore from areas of major urban and industrial development, and not offshore from agricultural areas. This points to an external source of arsenic linked to the major industrial centres, i.e. the arsenic may be a pollutant discharged on the continental shelf either as a result of industrial activities (industrial effluent) or as a by-product of urban development (urban effluent). For example, Angino et al. (1970) reported increasing concentrations of arsenic in the Kansas River owing to pollution by detergents used in household washing.

Cobalt and cadmium. The distribution of cobalt shown in Fig. 66C shows relatively high levels east of Newcastle, Sydney, and Port Kembla; between Wreck Bay and Batemans Bay, and east of Eden. It is noticeable that the plumes east of Newcastle, Sydney, and Port Kembla transgress surface lithofacies and mineralogic boundaries, but the high concentrations between Wreck Bay and Batemans Bay and east of Eden coincide with areas of high calcium carbonate (Fig. 65A). The three plumes east of Newcastle, Sydney, and Port Kembla differ in shape; east of Newcastle the plume broadens eastwards, but east of Sydney and Port Kembla the plumes either narrow or maintain their width eastwards. It is unlikely to be accident that such plumes occur offshore from three major industrial/urban conurbations.

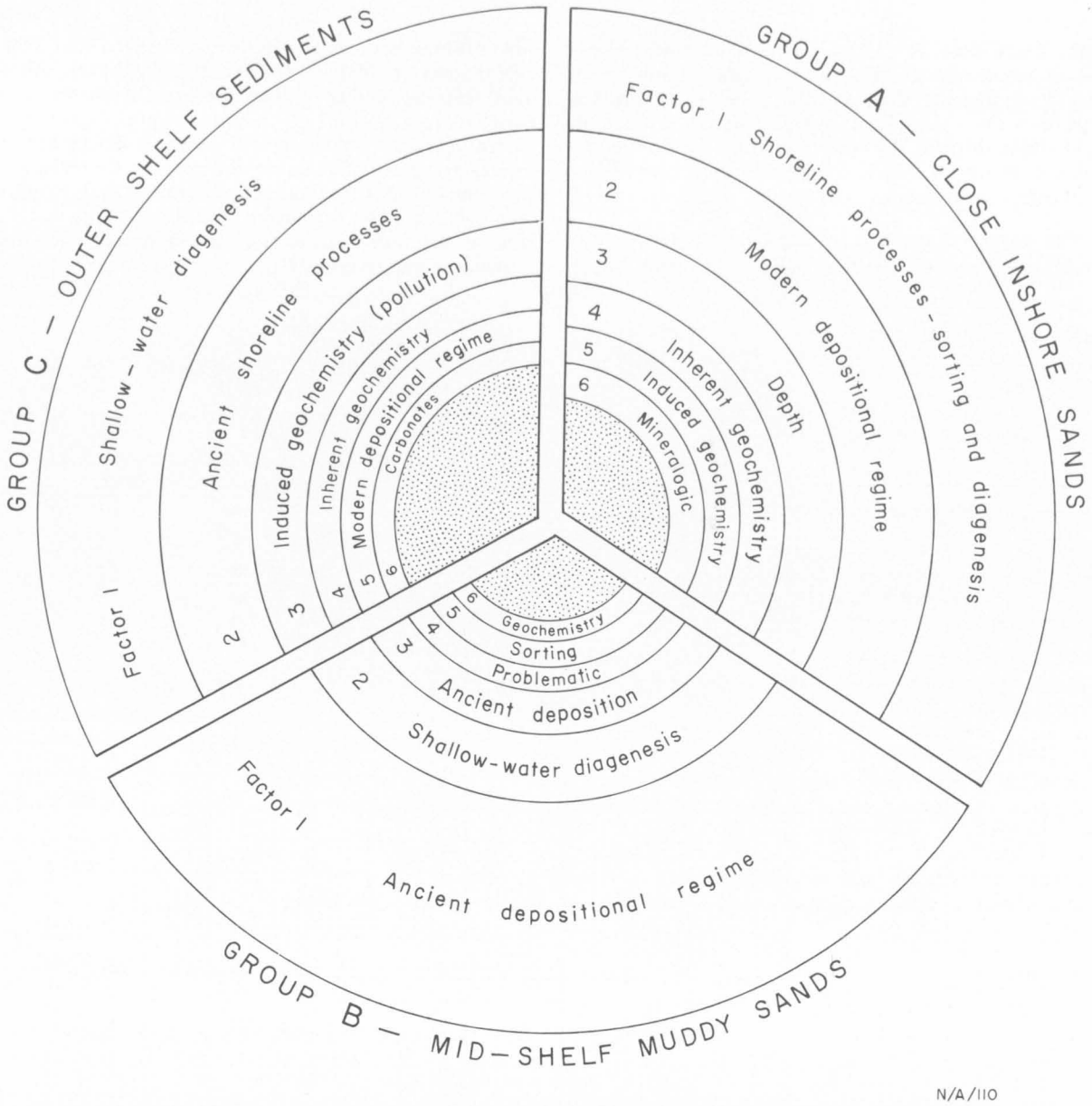

Fig. 75. Principal controls on chemical distribution and concentration in the groups of shelf sediments delineated by factor analysis. The circle radii represent 100% variance. The percentage variance explained by each factor is therefore a proportion of the radius, e.g. in Group C sediments, shallow-water diagenesis (Factor 1) explains a higher percentage of sample variance than does inherent geochemistry (Factor 4).

These are areas where cobalt is most likely to be produced (as a by-product of smelting processes) and used (paint, glass, ceramic manufacture). The eastward-broadening plume east of Newcastle suggests air transport, the cobalt having been derived from smoke stacks, while the eastward thinning plumes east of Sydney and Port Kembla suggest direct input into seawater.

The association of high cobalt and high calcium carbonate between Wreck Bay and Batemans Bay, and east of Eden is difficult to explain. Difficulties in pinpointing the position of cobalt, and in suggesting mechanisms for the association have already been described.

Cadmium is enriched in the surface shelf sediments compared with standard rocks and sea water. The analytical techniques were not of a sufficient standard to allow contouring of results. Little can therefore be said of its distribution. However it is a sufficiently toxic and dangerous metal to require a more thorough study, especially in view of its likely source from zinc and copper smelting.

ECONOMIC POTENTIAL

Reworking and redistribution of the superficial sediments during the Holocene transgression must have resulted in the destruction of near-surface heavy-mineral seams which may have been present on fossil bodies now submerged. More deeply buried seams may, however, have escaped reworking and may still be preserved offshore. Areas where there is evidence of terracing, mainly on the middle shelf, might be expected to hold the best prospects for accumulations of this sort.

On the middle shelf and inner shelf the average titanium content of the surface grab samples is 0.3 per-

cent. There may be places where significantly higher values occur, and if these values persist to any depths they may indicate that potentially mineable blanket-type deposits exist. Such deposits would presumably have been formed by the redistribution of heavy-mineral seams in beach dunes destroyed during the Holocene transgression.

The increasing demand for sand and gravel for constructional purposes, and the depletion of readily accessible onshore sources of supply are likely to lead to the exploitation of offshore resources in the future. Abundant reserves of quartz sand are present on the inner shelf between 15 and 60 m water depth. High-quality coarse aggregate, however, will probably not be easy to locate; gravels found during the present survey are of very limited distribution and unsuitable composition, although the wide spacing of sample stations, and the lack of any sub-surface information makes a reliable assessment impossible.

REFERENCES

ALBANI, A. D., 1974—Sedimentary environments in Broken Bay, N.S.W. *J. geol. Soc. Aust.*, 21, 279-90.

ANGINO, E. E., MAGNUSON, L. M., WAUGH, T. C., GALLE, O. K., & BREDFELDT, J., 1970—Arsenic in detergents: possible danger and pollution hazard. *Science*, 168(3929), 389-90.

BERNER, R. A., 1970—Pleistocene sea levels indicated by buried black sediments in the Black Sea. *Nature*, 227, 700.

BLOOM, A. L., 1967—Pleistocene shorelines: A new test of isostasy. *Bull. geol. Soc. Am.*, 78, 1477-93.

BOLAND, F. M., & HAMON, B. V., 1970—The East Australian Current, 1965-1968. *Deep Sea Res.*, 17, 777-94.

BOSTRAM, K., & VALDES, S., 1969—Arsenic in ocean floors. *Lithos*, 2, 351-60.

BOWEN, V. T., & SUTTON, D., 1951—Comparative studies of mineral constituents of marine sponges: I. The Genera *Dysidea, Chondrilla, Terpios. J. mar. Res.*, 10, 153-67.

BOYD, R., 1974—Marine geological investigation of the N.S.W. coast between Port Stephens and Nora Head. *Hons. Thesis, Univ. Sydney* (unpubl.).

BRITISH ADMIRALTY, 1956—Australia Pilot, II, 4th Edn. *London, Hydrographer of the Navy.*

BRITISH ADMIRALTY, 1960—Australia Pilot, III, 5th Edn. *London, Hydrographer of the Navy.*

BROWN, H. R., & SWAINE, D. J., 1964—Inorganic constituents of Australian coals. *J. Inst. Fuel*, 37, 422-40.

BROWNE, W. R., 1969—Geomorphology. *In* PACKHAM, G. H. (Ed.)—The geology of New South Wales. *J. geol. Soc. Aust.*, (16)1, 654.

CALVERT, S. E., & PRICE, N. B., 1970—Minor metal contents of Recent organic rich sediments off South West Africa. *Nature*, 227, 593-95.

CARROLL, D., 1940—Possibilities of heavy mineral correlation of some Permian sedimentary rocks of New South Wales. *Bull. Am. Ass. Petrol. Geol.*, 24(4), 636-48.

CHAPPELL, J., 1974a—Upper mantle rheology in a tectonic region. *J. geophys. Res.*, 79, 390-98.

CHAPPELL, J., 1974b—Late Quaternary glacio and hydro-isostasy, on a layered earth. *Quatern. Res.*, 4, 429-40.

CHAYES, F., 1956—PETROGRAPHIC MODAL ANALYSIS: AN ELEMENTARY STATISTICAL APPROACH. *N.Y., Wiley.*

CONOLLY, J. R., & VON DER BORCH, C. C., 1967—Sedimentation and physiography of the sea floor south of Australia. *Sediment. Geol.*, 1, 181-220.

CONOLLY, J. R., 1968—Submarine canyons of the continental margin, east Bass Strait (Australia). *Marine Geol.*, 6, 449-61.

CONOLLY, J. R., 1969—Western Tasman sea floor. *N.Z. J. Geol. Geophys.*, 12, 310-43.

COOK, P. J., & MAYO, W., in prep.—Geochemistry of a tropical estuary—Broad Sound, Queensland. *Bur. Miner. Resour. Aust. Bull.* 182.

CREAGER, J. S., & STERNBERG, R. W., 1972—Specific problems in understanding bottom sediment distribution and dispersal on the Continental Shelf, 347-362. *In* SWIFT, D. J. P., DUANE, D. B., & PILKEY, O. H. (Eds.)—SHELF SEDIMENT TRANSPORT, PROCESS AND PATTERN. *Strondsburg, Penn., Dowden, Hutchinson, & Ross.*

CULLEY, A. G., 1933—Notes on the mineralogy of the Narrabeen Series of New South Wales. *Roy. Soc. N.S.W. J. & Proc.*, 66(2), 344-77.

CURRAY, J. R., 1969—History of continental shelves. *In* New concepts of continental margin sedimentation: *AGI short course lecture notes*, 7-9 Nov. Philadelphia.

CURRAY, J. R., & MOORE, D. G., 1964—Pleistocene deltaic progradation of continental terrace, Costa de Nayaret, Mexico, 193-215. *In* VAN ANDEL, T. H., & SHOR, G. G. (Eds.)—Marine geology of the Gulf of California. *Am. Ass. Petrol. Geol. Mem.*, 3, 496

DAVIES, P. J., 1971—Calcite precipitation and recrystallization fabrics—their significance in Jurassic limestones of Europe. *J. Geol. Soc. Aust.*, 18, 279-92.

DAVIES, P. J., 1973—Submarine canyons on the continental margin of S.E. Australia. *Bur. Miner. Resour. Aust. Rec.* 1973/147 (unpubl.).

DAVIS, R. C., 1973—STATISTICS AND DATA ANALYSIS IN GEOLOGY. *N.Y., Wiley.*

DEMIRMEN, F., 1971—Counting error in petrographic point-count analysis: A theoretical and experimental study. *Mathematical Geol.*, 3, 15-41.

DEER, W. A., HOWIE, R. A., & ZUSSMAN, J., 1972—ROCK FORMING MINERALS, 2, Chain Silicates. *London, Longman.*

DIETZ, R. S., 1952—Geomorphic evolution of the continental terrace (continental shelf and slope). *Bull. Am. Ass. Petrol. Geol.*, 36, 1802-20.

DIETZ, R. S., 1963—Wave base, marine profile of equilibrium, and wave-built terraces: a critical appraisal. *Ibid.*, 74, 971-90.

DIETZ, R. S., & MENARD, H. W., 1951—Origin of abrupt change in slope at continental shelf margin. *Bull. Am. Ass. Petrol. Geol.*, 35(9), 1994-2016.

DU PLESSIS, A., SCRUTTON, R. A., BARNABY, A. M., & SIMPSON, E. S. W., 1972—Shallow structure of the continental margin of South West Africa. *Marine Geol.*, 77-89.

EMERY, K. O., & MILLIMAN, J., 1968—Sea levels during the past 35,000 years. *Science*, 162, 1121-3.

EL WAKEEL, S. K., & RILEY, J. P., 1961—Chemical and mineralogical studies of deep sea sediments. *Geochim. cosmochim. Acta*, 25, 110.

FALVEY, D., 1974—The development of continental margins in plate tectonic theory. *APEA J.*, 14, 95-106.

FERGUSON, J. A., & HOSKING, J. S., 1955—Industrial clays of the Sydney area, N.S.W., 1. Geology and Mineralogy. *Aust. J. appl. Sci*, 6, 380-407.

FLEMING, R. H., 1938—Tides and tidal currents in the Gulf of Panama. *J. Marine Res.*, 1, 192-206.

FOLK, R. L., 1968—PETROLOGY OF SEDIMENTARY ROCKS. *Austin, Texas, Hemphill.*

GARDNER, D. E., 1955—Beach sand heavy mineral deposits of eastern Australia. *Bur. Miner. Resour. Aust. Bull.* 28.

GARY, M, MCAFEE, R., & WOLF, C. L., (Eds.), 1973—GLOSSARY OF GEOLOGY. *Washington, Am. geol. Inst.*

GILL, E. D., & HOPLEY, D., 1972—Holocene sea levels in eastern Australia—a discussion. *Mar. Geol.*, 12, 223-33.

GOLDBERG, E. D., 1954—Marine Geochemistry, 1. Chemical scavengers of the sea. *J. Geol.*, 62, 249-65.

GOLDBERG, E. D., & ARRHENIUS, G. O. S., 1958—Chemistry of Pacific pelagic sediments. *Geochim. cosmochim. Acta*, 13, 153-212.

GRIFFITH, B. R., & HODGSON, E. A., 1971—Offshore Gippsland Basin fields. *APEA J.*, 11(1), 85-9.

GRIM, R. E., & LOUGHNAN, F. C., 1962—Clay minerals in sediments from Sydney Harbour, Australia. *J. sediment. Petrol.*, 32, 240-8.

HAMON, B. V., 1965—The East Australian Current 1960-1964. *Deep Sea Res.*, 12, 899-921.

HAMON, B. V., 1968—Temperature structure in the cyper 250M in the East Australian current area. *Aust. J. marine freshwater Res.*, 69, 91-9.

HARBAUGH, J. W., & DEMIRMEN, F., 1964—Application of factor analysis to petrologic variations of Americus Limestone (Lower Permian), Kansas and Oklahoma. *Kansas Univ. spec. Publ.* 15.

HAYES, D. E., & RINGIS, J., 1973—Seafloor spreading in the Tasman Sea. *Nature*, 243, 454-8.

HIRST, D. M., 1962a—The geochemistry of modern sediments from the Gulf of Paria—I. The relationship between the mineralogy and the distribution of major elements. *Geochim. cosmochim. Acta*, 26, 309-34.

HIRST, D. M., 1962b—The geochemistry of modern sediment from the Gulf of Paria—II. The location and distribution of trace elements. *Ibid.*, 26, 1147-87.

HOGDAHL, O. T., 1963—THE TRACE ELEMENTS IN THE OCEAN: A BIBLIOGRAPHIC COMPILATION. *Oslo, Central Inst. Ind. Res.*

JAMES, E. A., & EVANS, P. R., 1971—The stratigraphy of the offshore Gippsland Basin. *APEA J.*, 11(1), 71-4.

JOHNSON, D. W., 1919—SHORE PROCESSES AND SHORELINE DEVELOPMENT. *N.Y., Wiley.*

JONES, A. S. G., 1973—The concentration of copper, lead, zinc, and cadmium in shallow sediments, Cardigan Bay, Wales. *Marine Geol.*, 14, M1-M9.

JONES, A. S. G., 1972—A partial geochemical study of shallow marine sediments, Cardigan Bay (Wales). *Ibid.*, 12, 313-33.

JONES, H. A., 1973a—Submerged shorelines and channels on the east Australian continental shelf between Sandy Cape and Cape Moreton: heavy-mineral prospects. *Bur. Miner. Resour. Aust. Rec.* 1973/46 (unpubl.).

JONES, H. A., 1973b—Morphology of the east Australian continental shelf between Cape Moreton and Tweed Heads in relation to offshore heavy-mineral prospects. *Bur. Miner. Resour. Aust. Rec.* 1973/123 (unpubl.).

JONES, H. A., DAVIES, P. J., & MARSHALL, J. F., 1975—Origin of the shelf break off southeast Australia. *J. geol. Soc. Aust.*, 22(1), 71-8.

KAMERLING, P., 1966—Sydney Basin offshore. *APEA J.*, 6, 76-9.

KANWISHER, J. W., & WAINWRIGHT, S. A., 1967—Oxygen balance in some reef corals. *Biol. Bull. Mar. Biol. Lab., Woods Hole*, 133, 378-90.

KLOVAN, J. E., 1966—The use of factor analysis in determining depositional environments from grainsize distributions. *J. sediment. Petrol.*, 36, 115-25.

KNOTT, S. T., & HOSKINS, H., 1968—Evidence of Pleistocene events in the structure of the continental shelf off the northeastern United States. *Marine Geol.*, 6, 5-26.

KRAUSKOPF, K. B., 1956—Factors controlling the concentration of thirteen rare metals in sea water. *Geochim. cosmochim. Acta*, 9, 1-32.

KRAUSKOPF, K. B., 1967—INTRODUCTION TO GEOCHEMISTRY. *N.Y., McGraw-Hill.*

LAMBERT, I. B., & WHITE, A. J. R., 1965—The Berridale wrench fault: A major structure in the Snowy Mountains of New South Wales. *J. geol. Soc. Aust.*, 12, 25-34.

LEES, A., & BULLER, A. T., 1972—Modern temperate-water and warm-water shelf carbonate sediments contrasted. *Marine Geol.*, 13, M67-M73.

LEWIS, K. B., 1973—Erosion and deposition on a tilting continental shelf during Quaternary oscillations of sea level. *N.Z. J. Geol. Geophys.*, 16, 281-301.

LOUGHNAN, F C., 1958—The origin, mineralogy and some physical properties of the commercial clays of N.S.W. *Geol. Ser. No. 2 Univ. N.S.W*

LOUGHNAN, F. C., & CRAIG, D. C., 1962—A preliminary investigation of the Recent sediments off the east coast of Australia. *Aust. J. marine freshwater Res.*, 13, 48-56.

MARSHALL, J. F., 1977—Marine geology of the Capricorn Channel area. *Bur. Miner. Resour. Aust. Bull.* 163.

MASON, B., 1966—PRINCIPLES OF GEOCHEMISTRY, 3rd edn. *N.Y., Wiley.*

MAYO, W., 1972—A computer programme for calculating statistical parameters of grainsize distributions derived from various analystical methods. *Bur. Miner. Resour. Aust. Rec.* 1972/140 (unpubl.).

MCCONNELL, D., 1970—Arsenic in phosphorite and apatite. *Econ Geol.*, 65(1), 64-5.

MEADE, R. H., 1972—Sources and sinks of suspended matter on continental shelves, 249-262. *In* SWIFT, D. J. P., DUANE, D. B., & PILKEY, O. H. (Eds.)—SHELF SEDIMENT TRANSPORT, PROCESS AND PATTERN. *Strondsburg, Penn., Dowden, Hutchison & Ross.*

MULLIN, J. B., & RILEY, J. P., 1956—The occurrence of cadmium in seawater and in marine organisms and sediments. *J. Mar. Res.*, 15, 103-22.

NICHOLLS, G. D., & LORING, D. H., 1962—The geochemistry of some British Carboniferous sediments. *Geochim. cosmochim. Acta.*, 26, 181-223.

OVERSTREET, W. C., 1967—The geological occurrence of monazite. *U.S. geol. Surv. Prof. Pap.*, 530, 327.

PHIPPS, C. V. G., 1963—Topography and sedimentation of the continental shelf and slope between Sydney and Montague Island, N.S.W. *Aust. Oil Gas J.*, 12, 40-6.

PHIPPS, C. V. G., 1966—Evidence of Pleistocene warping of the New South Wales continental shelf. *Geol. Surv. Canad. Pap.*, 6(15), 280-93.

PHIPPS, C. V. G., 1966—Evidence of Pleistocene warping of the New South Wales continental shelf. *Geol. Surv. Canad. Pap.*, 66(15), 280-93.

PHIPPS, C. V. G., 1967—The character and evolution of the Australian continental shelf. *APEA J*, 7(2), 44-9.

PHIPPS, C. V. G., 1970—Dating of eustatic events from cores taken in the Gulf of Carpentaria, and samples from the New South Wales continental shelf. *Aust. J. Sci.*, 32, 329-330.

PHIPPS, C. V. G., & KING, L. H., 1969—Chemical, mineralogical and textural variations in sediments from the Scotian Shelf. *Maritime Sediments*, 5(3), 101-12.

PILIPCHUK, M. F., & SEVAST'YANOV, V. F., 1968—Arsenic in recent Black Sea sediments. *Dokl. Acad. Sci. USSR*, 179, 194-97. Transl. from *Dokl. Acad. Nauk. SSSR*, 179, 697-700.

REVELLE, R., BRAMLETTE, M., ARRHENIUS, G., & GOLDBERG, E. D., 1955—Pelagic sediments of the Pacific, 221-236. *In* POLDERVAART, A. (Ed.)—CRUST OF THE EARTH. *Geol. Soc. Am. spec. Pap.* 62.

RICHARDS, F. A., 1970—The enhanced preservation of organic matter in anoxic marine environments, 399-411. *In* HOOD, D. W., (Ed.)—ORGANIC MATTER IN NATURAL WATERS. *Inst. Marine Sci., Alaska, Occas. Pub.* 1.

RILEY, J. P., & CHESTER, R., 1971—INTRODUCTION TO MARINE CHEMISTRY. *Academic Press.*

RONA, P. A., 1969—Middle Atlantic continental slope of the United States: Deposition and erosion. *Bull. Am. Ass. Petrol. Geol.*, 53, 1453-65.

RONA, P. A., 1973—Relations between rates of sediment accumulation on continental shelves, sea-floor spreading, and eustacy inferred from the central north Atlantic. *Bull. geol. Soc. Am.*, 84, 2851-72.

RUCH, R. R., KENNEDY, E. J., & SHIMP, N. F., 1970—Distribution of arsenic in unconsolidated sediments from southern Lake Michigan. *Illinois State Geol. Surv. envir. geol. Notes*, 37.

RUSSELL, R. J., 1968—Where most grains of very coarse sand and fine gravel are deposited. *Sedimentology*, 11, 31-8.

SHEPARD, F. J., 1932—Sediments of the continental shelves. *Bull. geol. Soc. Am.*, 43, 1017-39.

SHEPARD, F. P., 1954—Nomenclature based on sand-silt-clay ratios. *J. Sedim. Petrol.*, 24, 151-8.

SHEPARD, F. P., 1960—Gulf Coast barriers, 197-270, *In* SHEPARD, F. P., PHLEGAR, F. B., & VAN ANDEL, T. H. Eds.)—RECENT SEDIMENTS, NORTH WEST GULF OF MEXICO, 1951-1958. *Tulsa, Am. Assoc. Petrol. Geol.*

SHIRLEY, J., 1964—An investigation of the sediments on the continental shelf of New South Wales. *J. geol. Soc. Aust.*, 11(2), 331-42.

SMITHELLS, C. J., 1962—METALS REFERENCE BOOK, 1, 206-213. *London, Butterworths.*

STANLEY, D. J., 1969—THE NEW CONCEPTS OF CONTINENTAL MARGIN SEDIMENTATION. *Am. geol. Inst. Publ.*

STEVENSON, R. A., UFRET, S. L., 1966—Iron, manganese and nickel in skeletons and food of sea urchins *Tripneustus esculenteus* and *Echinometra lucunter. Limnol. Oceanogr.*, 11, 11-7.

ST JOHN, B. E., 1970—Trace elements in corals of the Coral Sea. *Ph.D. Thesis, Univ. Qld* (unpubl.).

SUMMERHAYES, C. P., 1972—Geochemistry of continental margin sediments from northwest Africa. *Chem. Geol.*, 10, 137-56.

SWAINE, D. J., 1955—The trace element content of soils. *Comm. Bur. Soil Sci. tech. Commun.* 48, 157.

SWAINE, D. J., 1962—The trace element content of fertilizers. *Comm. Bur. Soil. Sci. tech. Commun.* 52, 306.

SWIFT, D. J. P., 1969—Outer shelf sedimentation: Processes and products. *In* STANLEY, D. J. (Ed.)—THE NEW CONCEPTS OF CONTINENTAL MARGIN SEDIMENTATION. *Am. geol. Inst. Publ.*

SWIFT, D. J. P., 1970—Quaternary shelves and the return to grade. *Marine Geol.*, 8, 5-30.

SWIFT, D. J. P., STANLEY, D. J., & CURRAY, J. R., 1971—Relict sediments on continental shelves: A reconstruction. *J. geol.*, 79, 322-46.

SYMONDS, P. A., 1973—The structure of the north Tasman Sea. *Bur. Miner. Resour. Aust. Rec.* 1973/167 (unpubl.).

TAYLOR, D. J., 1966—Esso Gippsland Shelf No. 1: The mid-Tertiary foraminiferal sequence. *Bur. Miner. Resour. Aust. Petrol. Search Subs. Acts Publ.*, 76, 31-4.

THOM, B. G., HAILS, J. R., MARTIN, A. R. H., & PHIPPS, C. V. G., 1972—Postglacial sea levels in eastern Australia—a reply. *Marine Geol.* 12, 233-42.

TOOMS, J. S., SUMMERHAYES, C. P., & CRONAN, D. S., 1969—Geochemistry of marine phosphate and manganese deposits. *Oceanogr. Marine Biol. Ann. Rev.*, 7, 49-100.

TUREKIAN, K. K., 1968—OCEANS. *Englewood Cliffs, N.J., Prentice-Hall.*

TUREKIAN, K. K., & WEDEPOHL, K. H., 1961—Distribution of the elements in some major units of the earth's crust. *Bull. geol. Soc. Am.*, 72, 175-92.

VAN ANDEL, J. H., & CALVERT, S. E., 1971—Evolution of sediment wedge, Walvis Shelf, south west Africa. *J. Geol.*, 79, 585-602.

VAN ANDEL, T. H., & VEEVERS, J. J., 1967—Morphology and sediments of the Timor Sea. *Bur. Miner. Resour. Aust. Bull.* 83.

VON DER BORCH, C. C., 1972—Marine geology of the Huon Gulf region, New Guinea. *Bur. Miner. Resour. Aust. Bull.* 127.

VON DER BORCH, C. C., 1968—Southern Australian submarine canyons: their distribution and ages. *Marine Geol.*, 6, 267-79.

WALCOTT, R. I., 1972—Past sea levels, eustasy and deformation of the earth. *Quatern. Res.*, 2, 1-14.

WASS, R. E., CONOLLY, J. R., & MACINTYRE, R. J., 1970—Bryozoan carbonate sand continuous along southern Australia. *Marine Geol.*, 9, 63-73.

WELLMAN, P., & MCDOUGALL, I., 1974—Potassium-argon ages on the Cainozoic volcanic rocks of New South Wales. *J. geol. Soc. Aust.*, 21, 247-72.

WHITWORTH, H. F., 1956—The zircon-rutile deposits on the beaches of the east coast of Australia with special reference to their mode of occurrence and the origin of the minerals. *Dep. Mines N.S.W., tech. Rep.*, 4, 7-60.

R76/1687(2) Cat. no. 78 7637 1

PLATE 1

149°00′ 150°00′ 151°00′ 152°00′ 153°00′ 153°30′

31°30′ 32°00′ 33°00′ 34°00′ 35°00′ 36°00′ 37°00′ 38°00′

TAREE
Gloucester
MUSWELLBROOK
SINGLETON
MAITLAND
CESSNOCK
KURRI KURRI
NEWCASTLE
THE ENTRANCE
GOSFORD
SYDNEY
CAMDEN
WOLLONGONG
BOWRAL
PORT KEMBLA
Coal Cliff
Bulli
ORANGE
BATHURST
LITHGOW
KATOOMBA
MUDGEE
GOULBURN
CANBERRA
QUEANBEYAN
A.C.T
Ulladulla
Nowra
Narooma
COOMA
Tathra
Merimbula
Eden
BURRENDONG RESERVOIR
BURRAGORANG LAKE
LAKE GEORGE
LAKE MACQUARIE
Manning River
Hunter River
Goulburn River
Williams River
Macdonald River
Capertree River
Colo River
Wollondilly River
Shoalhaven River
Clyde River
Moruya River
Tuross River
Towamba River
Crowdy Head
Sugarloaf Point
Norah Head
Broken Bay
Port Jackson
Botany Bay
Port Hacking
Jervis Bay
Beecroft Head
Bowen Island
Wreck Bay
Bateman's Bay
Montague Island
Brush Island
Bass Point
Shoalhaven Bight
Disaster Bay
Gabo Island
RANGE
DIVIDING
GREAT
NEW ENGLAND HIGHWAY
PACIFIC HIGHWAY
GREAT WESTERN HIGHWAY
MID WESTERN HIGHWAY
HUME HIGHWAY
FEDERAL HIGHWAY
SNOWY MOUNTAINS HIGHWAY
MONARO HIGHWAY
PRINCES HIGHWAY
N S W
VIC
TASMAN SEA

CONTINENTAL SHELF SEDIMENTS

CENTRAL AND SOUTHERN N.S.W. SHELF

NEW SOUTH WALES

1978

Scale 1:1000000

10 0 10 20 30 40 50 60 70 80 KILOMETERES

10 0 10 20 30 40 50 NAUTICAL MILES

Lambert Conformal Conic Projection

CLAY

SAND — SILT

75/25 50/50 25/75 PERCENTAGES

* Absent from this sheet

SEDIMENT CLASSIFICATION

Note: The triangular diagram classifies the sediments according to the proportion of sand–, silt–and clay–sized particles they contain. The Wentworth scale is used. The corners of the inner triangle represent 60/20/20 percentages.

Sand
Silty sand
Sand/silt/clay
Gravel

> 90% carbonate
60–90% carbonate
30–60% carbonate
0–30% carbonate

Sea bed sample station
200 Bathymetric contour in metres
Contour intervals 20 m (0–200 m)
100 m (> 200 m)
Swamp
Highway

Published by the Bureau of Mineral Resources, Geology and Geophysics, Department of National Resources.
Issued under the authority of the Minister for National Resources.

Geology 1972 by P.J. Davies, J.F. Marshall, H.A. Jones
Compiled 1972 by P.J. Davies
Cartography by Geological Branch, B.M.R.
Drawn by Vera Shepherd
Printed by Mercury-Walch, Hobart, Australia.

Bibliographic reference: P.J. Davies 1978. Marine Geology of the Continental Shelf of S.E. Australia. Bur. Miner. Resour. Aust. Bull. 195

Geological reliability: The distribution of sediments is based on analysis of sea bed samples from stations whose positions are marked. Extrapolation between stations has been guided by bathymetry

Bathymetric reliability; Bathymetric contours have been compiled from published and unpublished RAN Hydrographic Service and National Mapping charts

NOT TO BE USED FOR NAVIGATION

N.T.
W.A.
QLD.
S.A.
N.S.W.
VIC.
T.

Copies of this map may be obtained from the Bureau of Mineral Resources, Geology and Geophysics, Canberra, A.C.T.

PLATE 2

TERRACES ON THE CONTINENTAL SHELF

Depth in metres

S.B. = Shelf break

SCALE 1:1 000 000

0 10 20 30 40 50 60 70 80 90 100 KILOMETRES

0 10 20 30 40 50 NAUTICAL MILES

149°30′ 150°00′ 151°00′ 152°00′ 153°00′ 153°30′

31°30′ 32°00′ 33°00′ 34°00′ 35°00′ 36°00′ 37°00′ 38°00′

MUDGEE
MUSWELLBROOK
SINGLETON
MAITLAND
CESSNOCK
KURRI KURRI
NEWCASTLE
TAREE
Crowdy Head
Sugarloaf Point
PORT STEPHENS
LAKE MACQUARIE
THE ENTRANCE
GOSFORD
WOY WOY
BROKEN BAY
BATHURST
LITHGOW
KATOOMBA
SYDNEY
CAMDEN
BURRAGORANG LAKE
BOTANY BAY
PORT HACKING
WOLLONGONG
BOWRAL
PORT KEMBLA
Shellharbour
GOULBURN
NOWRA
JERVIS BAY
WRECK BAY
Ulladulla
Batemans Bay
BATEMANS BAY
Narooma
Montague Island
Bermagui
Bega
Eden
Mallacoota
Gabo Island

Manning River
Hunter River
NEW ENGLAND HIGHWAY
HUNTER RIVER
GOULBURN RIVER
GREAT WESTERN HIGHWAY
DIVIDING RANGE
Capertree River
COLO RIVER
MACDONALD RIVER
WILLIAMS RIVER
PACIFIC HIGHWAY
NEPEAN RIVER
GREAT SOUTHERN RIVER
WOLLONDILLY RIVER
HUME HIGHWAY
SHOALHAVEN RIVER
CLYDE RIVER
PRINCES HIGHWAY
Moruya River
Tuross River
Towamba River

TASMAN SEA

NEW SOUTH WALES
VICTORIA

PORT STEPHENS
0 | 40 | 124 | S.B.=141 | LATITUDE 32°45′
150 | 70 | 117 | 130-141

NEWCASTLE
0 | 48 | 91 | 115 | 130-140 | LATITUDE 32°55′
150 | 40 | 70 | 115 | 121 | 124 | 124 | 130 | S.B.=150 | LATITUDE 33°00′
117 | 132 | 140

LAKE MACQUARIE
0 | 102 | 113-119 | 157 | LATITUDE 33°10′
150 | 50 | 104 | 123

THE ENTRANCE
0 | 40 | 86 | 124-126 | 130 | 170 | S.B.=150-174 | LATITUDE 33°20′
150 | 104

WOY WOY
0 | 100 | 115 | 135 | S.B.=160 | LATITUDE 33°30′
150 | 125

BROKEN BAY
0 | 50 | 113-117 | 130-140 | S.B. at 33°40′=157 | LATITUDE 33°42·5′
150 | 102

SYDNEY
0 | 63 | 81 | 110-115 | 122 | 125 | 135 | LATITUDE 33°45′
150 | 72-77

0 | 100 | 117 | 121 | S.B.=157 | LATITUDE 33°50′
29

0 | 82 | 79 | 101 | 117 | 117 | 132 | 138 | 144 | LATITUDE 33°52·5′
63 | 77
49 | 74 | 110
33 | 100 | 132 | 123 | 136 | 147 | 139

BOTANY BAY
0 | 128 | 135 | 146 | S.B.=160 | LATITUDE 34°00′
150

PORT HACKING
0 | 44 | 66 | 113 | 132 | 146 | S.B.=157 | LATITUDE 34°10′
150 | 127

0 | 31 | 44 | 56 | 90 | 122 | 135 | 148 | S.B.=157 | LATITUDE 34°20′
150 | 50 | 74 | 115 | 131

WOLLONGONG
0 | 40 | 80 | 130 | 140 | S.B.=160 | LATITUDE 34°30′
150

PORT KEMBLA
0 | 48 | 92 | 119 | 145 | 158 | 199 | S.B.=150(?) | LATITUDE 34°40′
150 | 105 | 134

NOWRA
0 | 24 | 48 | 89 | 115 | 130 | 163 | S.B.=130 | LATITUDE 34°50′
150 | 97

JERVIS BAY
0 | 48 | 60 | 97 | 128 | 144 | S.B.=142 | LATITUDE 35°00′
150 | 50 | 71 | 108

WRECK BAY
0 | 48 | 104 | 118 | 130 | S.B.=135 or 168 | LATITUDE 35°10′
150 | 111

Ulladulla
0 | 97 | 116 | 126 | 134 | 146 | S.B.=141 | LATITUDE 35°20
150

0 | 48 | 110 | 118 | 130 | 144 | S.B.=157-165 | LATITUDE 35°30′
150 | 126 | 132

0 | 58 | 114 | 121 | 129 | 152 | S.B.=154 | LATITUDE 35°40′
150

Batemans Bay
BATEMANS BAY
0 | 100-110 | S.B.=157 | LATITUDE 35°50′
150 | 113-117

0 | 64 | 81 | 104 | 124 | 126 | S.B.=123(?) | LATITUDE 36°00′
150 | 73 | 91 | 122

0 | 116 | 142 | S.B.=146 | LATITUDE 36°10′
150 | 130

Narooma
Montague Island
0 | 97 | 122 | 124 | 142 | S.B.=142 | LATITUDE 36°20′
150 | 31 | 53 | 129 | 130

Bermagui
0 | 62 | 82 | 89 | 130 | 141 | S.B.=143 | LATITUDE 36°30′
150

Bega
0 | 146 | S.B.=150 | LATITUDE 36°40′
150

0 | 35 | 115 | 123 | 127 | S.B.=157 | LATITUDE 36°50′
150

Eden
0 | 46 | 128 | 143 | S.B.=143 | LATITUDE 37°00′
150 | 124

0 | 17 | 73 | 99 | 110 | 124 | 146 | LATITUDE 37°10′
150 | 88

0 | 13 | 73 | 97 | 106 | 124 | S.B.=126-161 | LATITUDE 37°20′
150

Mallacoota
Gabo Island

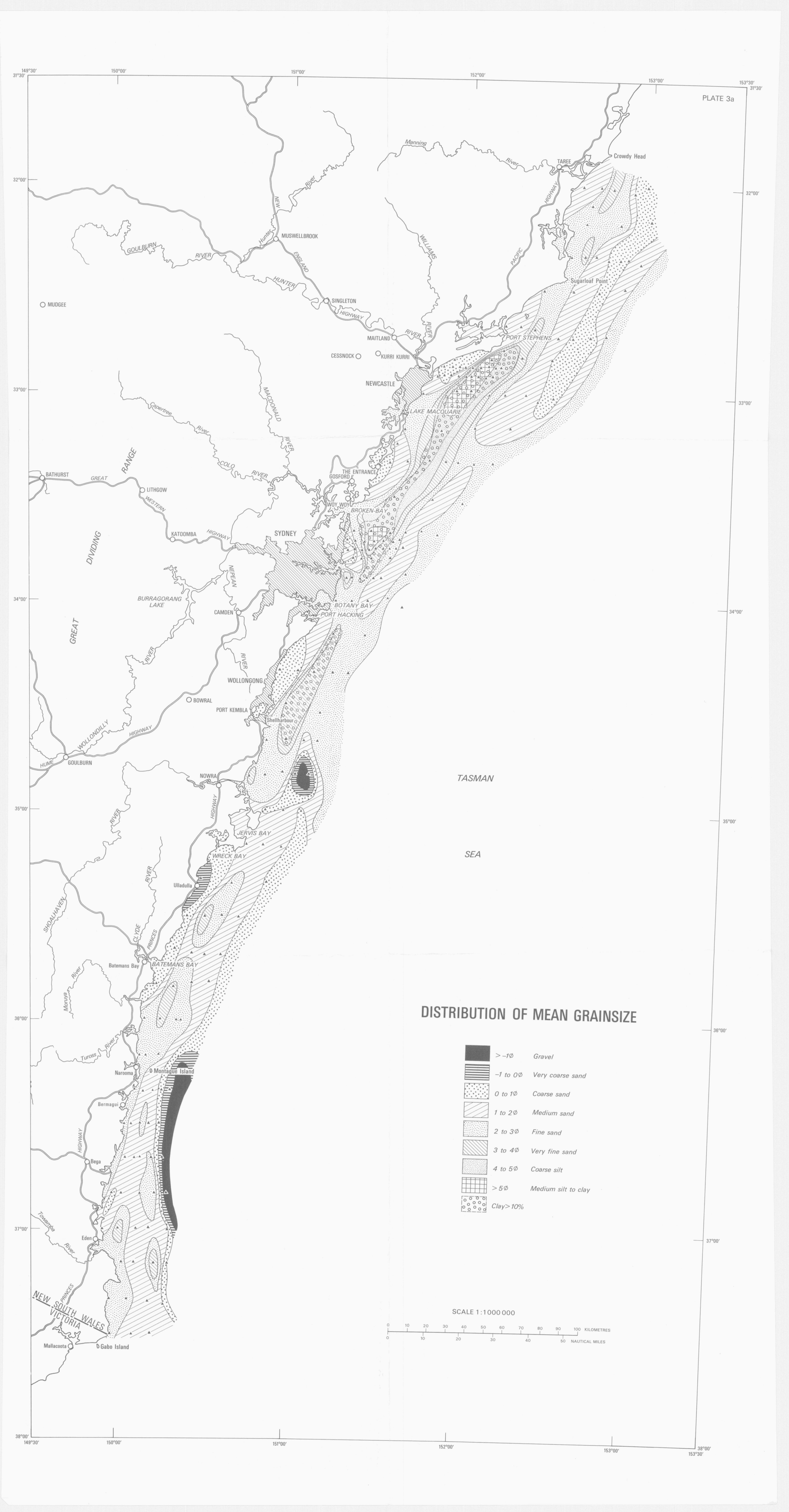

DISTRIBUTION OF MEAN GRAINSIZE

> −1Ø	Gravel
−1 to 0Ø	Very coarse sand
0 to 1Ø	Coarse sand
1 to 2Ø	Medium sand
2 to 3Ø	Fine sand
3 to 4Ø	Very fine sand
4 to 5Ø	Coarse silt
> 5Ø	Medium silt to clay
Clay > 10%	

SCALE 1:1000000

0 10 20 30 40 50 60 70 80 90 100 KILOMETRES

0 10 20 30 40 50 NAUTICAL MILES

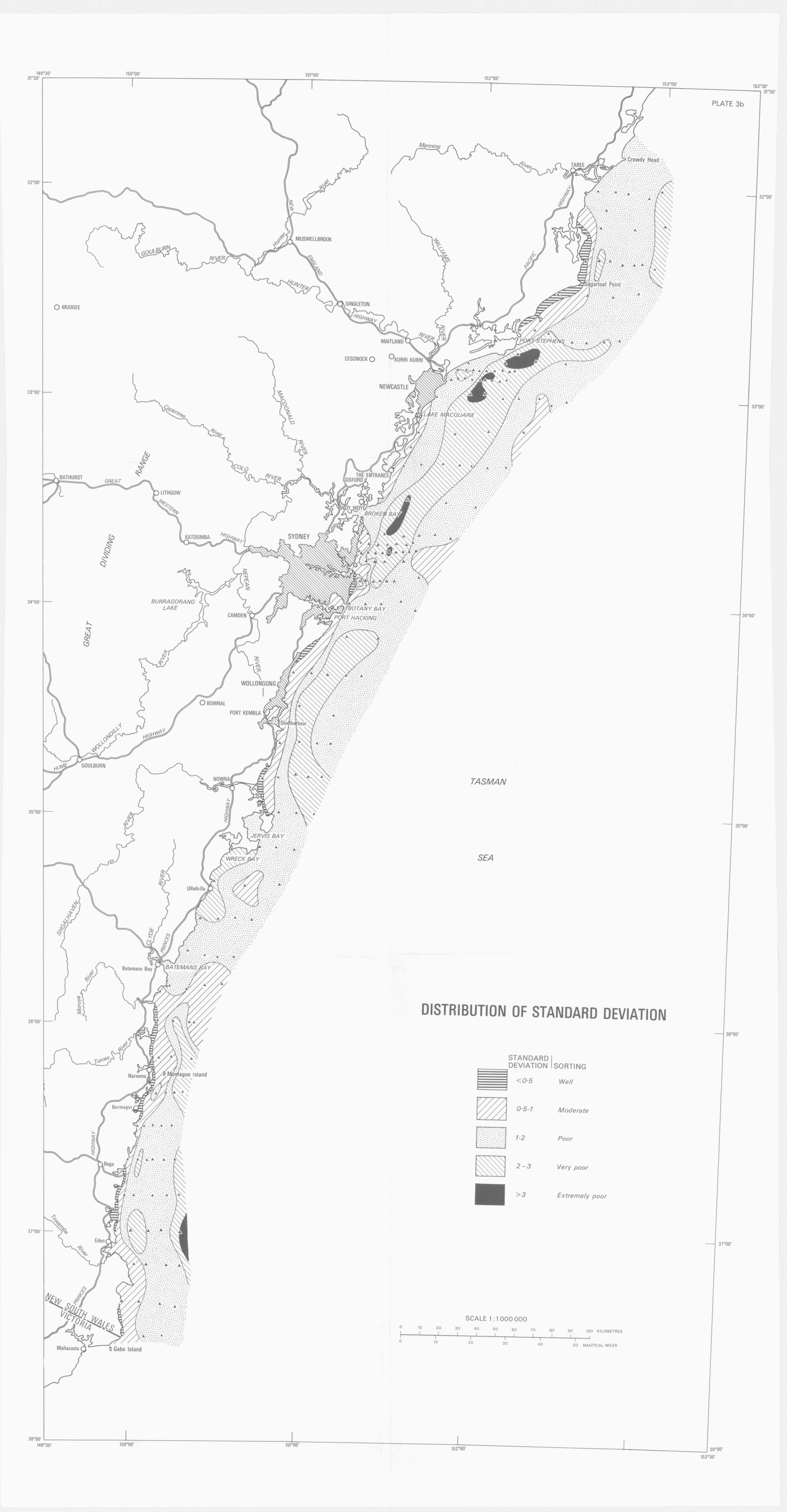
PLATE 3b
DISTRIBUTION OF STANDARD DEVIATION
STANDARD DEVIATION | SORTING
<0·5 Well
0·5-1 Moderate
1-2 Poor
2-3 Very poor
>3 Extremely poor
SCALE 1:1 000 000
0 10 20 30 40 50 60 70 80 90 100 KILOMETRES
0 10 20 30 40 50 NAUTICAL MILES
TASMAN SEA
NEW SOUTH WALES
VICTORIA
SYDNEY
NEWCASTLE
WOLLONGONG
MUSWELLBROOK
SINGLETON
MAITLAND
CESSNOCK
KURRI KURRI
THE ENTRANCE
GOSFORD
LITHGOW
BATHURST
KATOOMBA
CAMDEN
BOWRAL
PORT KEMBLA
Shellharbour
GOULBURN
NOWRA
Ulladulla
Batemans Bay
BATEMANS BAY
JERVIS BAY
WRECK BAY
Narooma
Montague Island
Bermagui
Bega
Eden
Mallacoota
Gabo Island
TAREE
Crowdy Head
Sugarloaf Point
PORT STEPHENS
LAKE MACQUARIE
BROKEN BAY
BOTANY BAY
PORT HACKING
MUDGEE
BURRAGORANG LAKE
GREAT DIVIDING RANGE
GREAT WESTERN HIGHWAY
HUME HIGHWAY
PRINCES HIGHWAY
NEW ENGLAND HIGHWAY
PACIFIC HIGHWAY
Manning River
Hunter River
GOULBURN RIVER
HUNTER RIVER
WILLIAMS RIVER
MACDONALD RIVER
Colo River
Nepean River
Shoalhaven River
Clyde River
Moruya River
Tuross River
Towamba River
149°30′
150°00′
151°00′
152°00′
153°00′
153°30′
31°30′
32°00′
33°00′
34°00′
35°00′
36°00′
37°00′
38°00′

BUREAU OF MINERAL RESOURCES, GEOLOGY AND GEOPHYSICS

BULLETIN 195

BMR MICROFORM MF23

MARINE GEOLOGY OF THE CONTINENTAL SHELF OFF SOUTHEAST AUSTRALIA

P.J. DAVIES

APPENDICES

APPENDIX 1

STATION DATA

Sample No. (prefix S72)	Latitude S	Longitude E	Fix*	Depth (m)	Sampling method	Date (mth/day)	Time (EST)	Colour
1530	36°40.0	150°00.2	A	15	Pipdred	02/13	0835	10 YR5/4
1531	36°30.0	150°03.8	A	15		02/13	1015	5 YR6/1
1532	36°20.0	150°07.2	A	15		02/13	1120	10 YR7/4
1533	36°10.0	150°08.2	A	16		02/13	1325	5 YR6/1
1534	35°59.8	150°10.0	A	16		02/13	1435	5 YR6/1
1535	35°50.0	150°14.2	A	24		02/13	1510	10 YR5/4
1536	35°37.0	150°20.0	A	16		02/13	1730	10 YR5/4
1537	33°10.0	151°38.2	A	20		02/16	1040	5 YR7/2
1538	33°00.0	151°44.1	A	17		02/16	1150	5 YR7/2
1539	32°50.0	151°54.5	A	15		02/16	1335	10 YR5/4
1540	32°40.3	152°12.0	A	11		02/16	1600	10 YR6/2
1541	32°30.0	152°24.6	A	18		02/16	1745	10 YR6/2
1542	32°20.3	152°33.3	A	20		02/16	1920	10 YR6/2
1595	32°00.0	152°36.8	A	27		02/26	0732	
1596	32°00.0	152°42.8	A	51		02/26	0810	10 YR5/4
1597	32°01.4	152°54.3	A	115		02/26	0915	10 YR5/4
1598	31°59.5	152°58.8	A	124		02/26	0955	10 YR5/4
1599	32°09.6	153°00.3	A	161	Boxdred+ Camera	02/26	1055	
1600	32°10.7	152°49.8	A	113	Pipdred	02/26	1245	10 YR5/4
1601	32°10.6	152°38.1	A	59		02/26	1355	5 YR5/2
1602	32°09.8	152°30.8	A	16		02/26	1436	10 YR6/2
1603	32°02.8	152°40.0	A	47	Boxdred	02/26	1545	10 YR5/4
1604	32°00.5	152°47.0	A	86	Pipdred	02/26	1650	5 YR5/2
1605	32°29	152°52	A	201		02/27	0845	10 YR6/2
1606	32°22	152°57	B	247		02/27	1007	10 YR6/2

Sample No. (prefix S72)	Latitude S	Longitude E	Fix*	Depth (m)	Sampling method	Date (mth/day)	Time (EST)	Colour
1607	32°20.5	152°52.6	A	120		02/27	1050	10 YR5/4
1608	32°21.0	152°49.8	A	115		02/27	1115	10 YR5/4
1609	32°21.0	152°46.0	A	102		02/27	1145	10 YR5/4
1610	32°19.8	152°42.0	A	93		02/27	1215	10 YR6/2
1611	32°20.0	152°38.0	A	88		02/27	1242	5 YR5/2
1612	32°30.0	152°34.6	A	102		03/02	1014	10 YR4/2
1613	32°30.0	152°43.0	B	121		03/02	1110	10 YR5/4
1614	32°40.1	152°46.8	C	241		03/02	1204	10 YR4/2
1615	32°43.2	152°40.8	B	139		03/02	1245	10 YR4/2
1616	32°43.6	152°35.0	B	132		03/02	1320	10 YR5/4
1617	32°43.5	152°29.7	B	126		03/02	1356	5 Y 5/2
1618	32°40.7	152°21.5	B	98		03/02	1440	5 Y 5/2
1619	32°40.7	152°15.3	B	50		03/02	1520	10 YR5/4
1620	33°11.0	151°50.6	B	115		03/03	1007	5 Y 5/2
1621	33°10.0	152°02.0	C	128		03/03	1121	10 Y 4/2
1622	33°10.0	152°14.0	D	144		03/03	1235	10 YR5/4
1623	33°01.2	152°29.0	B	225		03/03	1504	
1624	33°02.2	152°23.7	B	148		03/03	1614	10 YR5/4
1625	33°00.2	152°19.4	A	143		03/03	1625	10 YR5/4
1626	32°59.9	152°12.4	A	132	Pipdred	03/03	1735	10 YR4/2
1627	33°00.5	152°07.0	A	124		03/03	1811	5 Y 4/4
1628	32°59.3	152°00.7	A	115		03/03	1825	5 Y 4/4
1629	32°59.1	151°55.6	B	99		03/03	1932	5 Y 4/4
1630	32°49.8	152°07.4	A	64		03/03	0810	5 Y 4/1
1631	32°49.5	152°17.8	A	126		03/03	0920	5 Y 5/2

Sample No. (prefix S72)	Latitude S	Longitude E	Fix*	Depth (m)	Sampling method	Date (mth/day)	Time (EST)	Colour
1632	32°50.1	152°28.3	A	137		03/05	1050	10 YR4/2
1635	33°20.4	151°33.0	A	33	Boxdred	03/06	0930	10 YR5/4
1636	33°20.0	151°39.4	A	60		03/11	1200	10 YR5/4
1637	33°19.6	151°46.6	A	120		03/11	1252	5 Y 5/2
1638	33°20.0	151°52.5	A	125	Pipdred	03/11	1345	10 Y 4/2
1639	33°20.0	151°56.5	A	132		03/11	1415	5 Y 5/2
1640	33°20.5	152°01.8	B	141		03/11	1445	5 Y 5/2
1641	33°20.5	152°06.6	C	183		03/11	1520	5 Y 5/2
1642	33°31.8	151°58.0	C	198		03/11	1708	5 Y 5/2
1643	33°30.7	151°48.1	B	140		03/11	1825	5 Y 5/2
1644	33°30.0	151°35.0	A	84		03/11	1934	5 Y 5/2
1645	33°40.0	151°21.3	A	37	Boxdred	03/12	1150	
1646	33°40.2	151°27.0	A	86	Pipdred	03/12	1240	5 Y 5/2
1647	33°40.4	151°33.7	A	124		03/12	1328	5 Y 5/2
1648	33°40.2	151°39.0	B	128		03/12	1354	5 Y 5/2
1649	33°40.0	151°44.5	B	141		03/12	1430	5 Y 5/2
1650	33°40.8	151°49.8	C	225		03/12	1503	5 Y 5/2
1651	33°52.3	151°40.0	B	200		03/12	1654	5 Y 5/2
1652	33°49.6	151°30.3	A	122		03/12	1806	5 Y 5/2
1653	33°49.8	151°19.5	A	48	Boxdred	03/12	1920	
1654	34°00.00	151°15.6	A	31		03/13	0743	10 YR5/4
1655	34°00.1	151°21.5	A	108	Pipdred	03/13	0825	5 Y 5/2
1656	34°00.1	151°27.1	A	130		03/13	0901	5 Y 5/2
1657	33°59.4	151°33.8	A	194		03/13	0940	5 Y 5/2
1658	34°01.9	151°39.0	B	404	Boxdred	03/13	1136	
1659	34°09.6	151°26.3	A	205	Pipded	03/13	1453	5 Y 5/2
1660	34°09.9	151°15.2	A	124		03/13	1605	5 Y 5/2
1661	34°10.0	151°06.0	A	37		03/13	1712	10 YR5/4
1662	34°20.0	150°56.8	A	18	Boxdred	03/14	0622	10 YR5/4
1663	34°20.0	151°03.0	A	57	Pipdred	03/14	0705	10 YR5/4

Sample No. (prefix S72)	Latitude S	Longitude E	Fix*	Depth (m)	Sampling method	Date (mth/day)	Time (EST)	Colour
1664	34°20.4	151°08.4	A	124		03/14	0742	5 Y 5/2
1665	34°20.2	151°15.1	A	146		03/14	0820	5 Y 5/2
1666	34°20.5	151°20.5	B	225		03/14	0852	5 Y 5/2
1667	34°31.9	151°11.1	A	148		03/14	1109	10 YR4/2
1668	34°29.6	150°59.2	A	60		03/14	1313	5 Y 4/2
1669	34°40.0	150°52.6	A	27	Boxdred	03/16	0812	10 YR4/2
1670	34°39.9	150°59.2	A	115	Pipdred	03/16	0910	5 Y 5/2
1671	34°40.0	151°05.3	A	135		03/16	0949	5 Y 5/2
1672	34°40.0	151°10.5	C	203	Boxdred	03/16	1040	5 Y 5/2
1673	34°49.6	151°06.9	C	201	Pipdred	03/16	1247	10 YR6/2
1674	34°49.5	151°02.6	B	126	Pipdred	03/16	1318	10 YR5/4
1675	34°49.3	150°58.1	A	110		03/16	1400	5 Y 5/2
1676	34°50.2	150°52.2	A	57		03/16	1448	5 Y 5/2
1677	34°50.4	150°46.6	A	22		03/16	1520	5 Y 5/2
1678	35°00.1	150°52.8	A	55		03/17	0708	10 YR5/4
1679	35°00.0	150°58.8	A	124		03/17	0746	10 YR5/4
1680	35°00.2	151°04.6	B	208	Boxdred	03/17	0821	5 Y 6/2
1681	35°10.4	150°58.2	B	162		03/17	1040	10 YR4/2
1682	35°09.7	150°51.9	A	124	Pipdred	03/17	1151	10 YR5/4
1683	35°09.6	150°46.1	A	47	Boxdred	03/17	1225	5 Y 7/2
1684	35°20.0	150°30.0	A	30		03/17	1410	10 YR6/2
1685	35°20.9	150°40.5	A	121	Pipdred	03/17	1522	5 Y 5/2
1686	35°20.3	150°52.3	B	179	Boxdred	03/17	1628	
1687	35°30.3	150°24.9	A	25		03/18	0802	5 Y 7/2
1688	35°30.7	150°31.0	A	106	Pipdred	03/18	0840	5 Y 5/2

Sample No. (prefix S72)	Latitude S	Longitude E	Fix*	Depth (m)	Sampling method	Date (mth/day)	Time (EST)	Colour
1689	35°30.5	150°39.6	B	122		03/18	0925	10 YR4/2
1690	35°30.8	150°42.8	B	146		03/18	1004	10 YR4/2
1691	35°41.5	150°37.0	C	159		03/18	1126	10 YR5/4
1692	35°41.5	150°31.0	B	128		03/18	1200	10 YR5/4
1693	35°41.2	150°26.6	A	115		03/18	1241	5 Y 5/2
1694	35°39.7	150°20.7	A	46	Boxdred	03/18	1318	5 Y 7/2
1695	35°50.7	150°20.5	A	110	Pipdred	03/19	0700	5 Y 5/2
1696	35°49.5	150°26.8	A	124		03/19	0742	5 Y 5/2
1697	35°49.7	150°33.1	B	252		03/19	0823	5 Y 5/2
1698	32°55.1	151°49.2	A	22		03/27	0825	5 Y 4/1
1699	32°54.7	151°51.4	A	23		03/27	0842	10 YR6/2
1700	32°54.6	151°33.8	A	37		03/27	0857	10 YR5/4
1701	32°54.9	151°56.1	A	44		03/27	0914	10 YR5/4
1702	32°55.1	151°58.6	A	70		03/27	0934	10 Y 4/2
1703	32°55.2	152°00.5	A	84		03/27	0955	10 Y 4/2
1704	32°55.1	152°03.2	A	95		03/27	1015	10 Y 4/2
1705	32°55.4	152°05.6	A	110		03/27	1042	10 Y 4/2
1706	32°55.1	152°08.0	A	115		03/27	1101	10 Y 4/2
1707	32°52.0	151°51.2	A	22		03/27	1344	10 YR5/4
1708	32°52.0	151°54.0	A	27		03/27	1400	10 YR7/4
1709	32°52.0	151°56.3	A	31		03/27	1418	10 YR5/4
1710	32°53.2	151°58.6	A	48		03/27	1427	10 YR5/4
1711	32°53.2	152°01.5	A	60		03/27	1457	5 Y 4/1
1712	32°53.2	152°04.0	A	75		03/27	1517	5 Y 4/1
1713	32°52.0	152°06.8	A	93		03/27	1544	5 Y 4/1

Sample No. (prefix S72)	Latitude S	Longitude E	Fix*	Depth (m)	Sampling method	Date (mth/day)	Time (EST)	Colour
1714	32°52.3	152°09.0	A	97		03/27	1606	5 Y 4/1
1715	32°52.2	152°10.7	A	124		03/27	1628	5 Y 5/2
1716	33°42.2	151°37.8	A	128		03/28	1810	5 Y 5/2
1717	33°43.2	151°34.5	A	124		03/28	1842	5 Y 5/2
1718	33°42.8	151°31.3	A	117		03/28	1903	5 Y 5/2
1719	33°43.0	151°28.2	A	112		03/28	1925	5 Y 5/2
1720	33°42.7	151°25.2	A	84		03/28	1947	5 Y 5/2
1721	33°42.8	151°21.8	A	58		03/28	2008	10 YR6/2
1722	33°42.8	151°19.2	A	21	Pipdred	03/28	2025	10 YR7/4
1723	33°45.0	151°20.0	A	21	Boxdred	03/29	1323	
1724	33°45.4	151°21.6	A	40		03/29	1346	10 YR5/4
1725	33°45.6	151°24.2	A	70	Pipdred	03/29	1413	5 Y 5/2
1726	33°45.6	151°26.2	A	99		03/29	1432	5 Y 5/2
1727	33°45.2	151°28.5	A	117		03/29	1453	5 Y 5/2
1728	33°45.0	151°31.4	A	122		03/29	1513	5 Y 5/2
1729	33°45.0	151°33.4	A	122		03/29	1535	5 Y 5/2
1730	33°44.8	151°35.9	A	128		03/29	1559	5 Y 5/2
1731	33°44.6	151°38.0	A	135	Boxdred	03/29	1623	10 YR4/2
1732	33°47.5	151°33.8	A	128	Pipdred	03/29	1721	5 Y 5/2
1733	33°47.8	151°27.3	A	117		03/29	1754	5 Y 5/2
1734	33°48.0	151°24.2	A	97		03/29	1823	5 Y 5/2
1735	33°47.9	151°21.6	A	79		03/29	1842	10 YR4/2
1736	33°53.0	151°17.3	A	27	Boxdred	03/30	0745	5 Y 6/1
1737	33°53.1	151°19.7	A	62	Pipdred	03/30	0807	5 Y 5/2
1738	33°53.1	151°21.9	A	77		03/30	0845	5 Y 5/2

Sample No. (prefix S72)	Latitude S	Longitude E	Fix*	Depth (m)	Sampling method	Date (mth/day)	Time (EST)	Colour
1739	33°53.4	151°24.3	A	113		03/30	0906	5 Y 5/2
1740	33°53.0	151°26.8	B	120		03/30	0927	5 Y 5/2
1741	33°53.2	151°29.2	B	124		03/30	0950	5 Y 5/2
1742	33°53.0	151°31.6	B	139	Boxdred	03/30	1027	10 YR4/2
1743	36°00.1	150°15.8	A	102	Pipdred	03/31	0905	5 Y 5/2
1744	36°00.1	150°22.0	A	119		03/31	0938	5 Y 5/2
1745	36°00.2	150°23.1	B	123		03/31	1030	5 Y 5/2
1746	36°10.4	150°22.6	B	124	Pipdred	03/31	1235	10 YR5/4
1747	36°09.8	150°15.6	A	108		03/31	1323	5 Y 5/2
1748	36°10.2	150°10.9	A	75		03/31	1404	5 Y 5/2
1749	36°20.2	150°10.7	A	53		03/31	1539	10 YR5/4
1750	36°20.3	150°14.8	A	91		03/31	1601	10 YR4/2
1751	36°19.9	150°16.9	B	124		03/31	1624	5 Y 5/2
1752	36°19.9	150°18.5	B	388		03/31	1649	
1753	36°30.2	150°06.7	A	57		04/01	0855	10 YR5/4
1754	36°30.2	150°103	A	97		04/01	0900	5 Y 5/2
1755	36°30.2	150°13.1	A	128		04/01	0938	10 YR4/2
1756	36°30.0	150°16.9	B	141	Boxdred	04/01	1010	10 YR5/4
1757	36°40.1	150°18.2	B	170	Pipdred	04/01	1228	5 Y 6/4
1758	36°40.3	150°14.2	A	119	Pipdred	04/01	1255	5 Y 5/6
1759	36°40.0	150°10.0	A	115		04/01	1323	5 Y 5/2
1760	36°39.5	150°07.8	A	86		04/01	1353	5 Y 5/6
1761	36°39.9	150°04.7	A	70		04/01	1423	5 Y 5/6
1762	36°49.9	149°56.6	A	13	Boxdred	04/01	1538	10 YR6/2
1763	36°50.0	150°00.0	A	49	Pipdred	04/01	1605	10 YR5/4

Sample No. (prefix S72)	Latitude S	Longitude E	Fix*	Depth (m)	Sampling method	Date (mth/day)	Time (EST)	Colour
1764	36°50.2	150°03.6	A	71		04/01	1630	10 YR5/4
1765	36°50.1	150°09.6	A	102		04/01	1706	5 Y 5/6
1766	36°50.0	150°15.4	B	130		04/01	1740	5 Y 5/6
1767	36°50.0	150°19.4	B	205		04/01	1812	5 Y 5/6
1768	37°00.3	149°56.1	A	22		04/02	0921	10 YR6/2
1769	37°00.3	150°02.1	A	70		04/02	0955	5 [illegible] 5/2
1770	37°00.3	150°08.3	A	91	Pipdred	04/02	1030	5 [illegible] 5/2
1771	37°00.3	150°13.4	B	124		04/02	1110	10 [illegible]YR4/2
1772	37°00.4	150°19.6	B	223		04/02	1152	5 [illegible] 5/2
1773	37°10.6	150°20.1	B	192		04/02	1305	10 [illegible]YR5/4
1774	37°10.5	150°14.9	A	108		04/02	1349	10 [illegible]YR5/4
1775	37°10.2	150°07.8	A	86		04/02	1426	10 [illegible]YR4/2
1776	37°10.0	150°00.3	A	17		04/02	1505	10 [illegible]YR6/2
1777	37°19.8	149°58.4	A	15	Boxdred	04/02	1630	5 Y 7/2
1778	37°20.4	150°05.4	A	91	Pipdred	04/02	1715	5 Y 5/2
1779	37°21.0	150°12.6	B	126		04/02	1800	10 YR4/2
1780	37°22.8	150°18.2	C	179		04/02	1848	5 Y 5/6
1781	37°29.8	149°59.0	A	22		04/03	1435	5 Y 7/2
1782	37°30.5	150°06.4	A	112		04/03	1513	10 YR4/2
1783	37°30.0	150°13.2	B	168		04/03	1601	[illegible] Y 6/4
1860	32°47.4	152°11.6	A	77	Pipdred Camera	05/02	1302	[illegible] Y 3/2

POSITION GRADING

A. Accurate: Error less than one n mile. Fixed by direct references to charted position.

B. Good: Error less than n miles. Short D.R. run from 'A'-class fix or first-class celestial fix.

C. Fair: Error probably less than three n miles. Standard celestial fix or short to moderate D.R. run from 'B'-class fix.

D. Approximate: Error may be as much as five to eight n miles. Interpolation between widely spaced 'B'-class or 'C'-class fixes.

APPENDIX 2

HEAVY-MINERAL VALUES FOR THE CONTINENTAL SHELF SEDIMENTS

Sample No.	% heavies in total sample	% heavies in sand fraction	% heavies in sand minus carbonate	PETROGRAPHIC ANALYSIS - SAND FRACTION: TRANSLUCENT FRACTION: % Opaques	% Leucoxene in opaques	% Zircon	% Rutile	% Amphiboles	% Epidotes	% Pyroxenes	% Tourmaline	% Garnet	% Others	% opaques in sand minus carbonate	% translucents in sand minus carbonate	% rutile in translucents	ppm titanium in translucents	ppm total titanium in sample	% zircon in translucents	ppm zirconium in translucents
1530	1.18	2.22	1.33	50	12	7	-	42	41	2	4	-	4	.665	.665	-	-	2100	.047	231
1531	1.71	.2	.2	54	15	14	-	25	42	11	5	2	1	.108	.092	-	-	2700	.013	64
1533	.92	2.59	1.02	41	11	7	2	34	36	5	11	-	5	.42	.6	.012	70	1300	.042	209
1534	1.12	.21	.17	32	15	-	-	43	18	7	24	4	4	.054	.116	-	-	2800	-	-
1535	.81	-	.17	-	-	coarse ferruginous grains only														
1537	1.46	2.44	2.27	48	6	63	28	1	-	-	4	-	4	1.52	1.18	.33	1980	7800	.743	3702
1538	.17	.74	.53	50	13	41	34	10	4	-	11	-	-	.265	.265	.09	539	2200	.109	541
1605	.96	.34	.23	49	12	6	12	26	24	19	7	1	5	.113	.117	.014	84	700	.007	35
1614	1.33	.74	.67	50	18	21	5	21	18	2	18	1	4	.335	.335	.017	100	1400	.104	517
1618	.31	-	-	49	25	25	18	20	23	7	1	1	5					2000		

NOTES ON PETROGRAPHIC ANALYSIS

1. Percentages calculated from counts of 100-200 grains. Translucent grains counted range from 60 to 120. 2. White grains in the opaque fraction were counted as leucoxene. 3. The opaque fraction may include some rutile, particularly in the coarser samples. 4. Amphiboles are almost entirely green hornblende. 5. Zoisite and other members of the epidote group were counted as epidote. 6. Pyroxenes are mainly augite, but include orthorhombic pyroxenes. 7. Tourmalines are predominantly brown varieties; occasional blue varieties occur. 8. The 'others' group includes indeterminate grains, monazite, andalusite, rare topaz, brookite, anatase, and apatite. 9. The petrographic analysis was conducted by Dr H.A. Jones.

APPENDIX 2 (cont'd).

Sample No.	% heavies in total sample	% heavies in sand fraction	% heavies in sand minus carbonate	PETROGRAPHIC ANALYSIS - SAND FRACTION: TRANSLUCENT FRACTION: % Opaques	% Leucoxene in opaques	% Zircon	% Rutile	% Amphiboles	% Epidotes	% Pyroxenes	% Tourmaline	% Garnet	% Others	% opaques in sand minus carbonate	% translucents in sand minus carbonate	% rutile in translucents	ppm titanium in translucents	ppm total titanium in sample	% zircon in translucents	ppm zirconium in translucents
1628	.13	.72	.29	49	39	11	-	31	34	14	-	-	10	.14	.15	-	-	2500	.016	82
1629	-	-					n o t	e n o u g h	s a m p l e											
1630	.09	.87	.39	48	31	30	16	33	16	2	2	-	1	.187	.203	.033	194	2000	.061	303
1631	.18	1.28	.52	44	18	26	8	24	20	15	3	-	4	.229	.290	.023	139	3100	.075	376
1634	.37	.09	.14	20	15	1	-	52	28	-	15	2	2	.028	.112	-	-	1500	.001	6
1637	.86	.87	.73	46	17	35	7	15	25	4	11	-	3	.336	.394	.027	165	2400	.138	687
1641	.6	.65	.4	50	22	10	6	24	26	18	4	4	8	.2	.2	.012	72	1300	.012	60
1642	.38	.52	.42	42	19	27	3	23	23	13	6	-	5	.176	.244	.007	44	1300	.066	328
1643	1.55	1.41	.49	-	-		c o a r s e	l i m o n i t i c	g r a i n s									800		
1646	-	1.01	.51	49	19	21	4	34	22	3	8	-	8	.25	.26	.01	62	2400	.06	272
1648	.23	.91	.21	47	8	19	1	35	24	16	4	-	1	.99	.11	.001	7	800	.021	105
1650	.23	.32	.21	40	25	13	6	37	18	21	1	2	2	.084	.126	.008	46	1000	.016	8
1651	.23	.5	.14	39	12	14	5	46	12	16	4	-	3	.06	.085	.004	26	1000	.01	60
1657	.57	.49	.39	43	20	14	6	46	12	16	3	1	2	.168	.222	.018	86	1400	.003	16
1660	.32	1.21	.69	34	12	21	1	30	30	2	2	1	13	.235	.455	.005	27	2100	.096	476

APPENDIX 2 (cont'd).

Sample No.	% heavies in total sample	% heavies in sand fraction	% heavies in sand minus carbonate	PETROGRAPHIC ANALYSIS - SAND FRACTION: TRANSLUCENT FRACTION % Opaques	% Leucoxene in opaques	% Zircon	% Rutile	% Amphiboles	% Epidotes	% Pyroxenes	% Tourmaline	% Garnet	% Others	% opaques in sand minus carbonate	% translucents in sand minus carbonate	% rutile in translucents	ppm titanium in translucents	ppm total titanium in sample	% zircon in translucents	ppm in zirconium in translucents
1661	2.13	2.35	2.11	65	6	31	25	12	7	-	22	-	3	1.372	.739	.185	1106	6000	.229	1141
1662	1.33		.64	-	-	s a m p l e	c o n t a m i n a t e d	w i t h	i r o n	o x i d e	c o a t i n g s									
1664	.11		.10	42	15	25	-	24	25	5	3	3	15	.042	.058	-	-	1900	.015	75
1665	1.72		.62	-	-	6	-	30	25	5	30	-	4	-	.062	-	-	1000	.04	186
1667	.78	-	.3	30	25	25	3	32	20	10	5	-	5	.09	.21	.006	-	600	.53	-
1668	.33	-	.29	40	30	18	-	30	24	8	12	2	6	.116	.174	-	-	1600	.031	155
1673	.23	-	.015	-	-	c o a r s e	f e r r u g i n o u s	g r a i n s	o n l y											
1675	.54	-	.38	50	26	22	6	30	30	5	5	-	2	.19	.19	.011	-	1200	.042	210
1676	.43	-	.31	-	-	17	-	34	19	14	4	-	12	-	.31	-	-	900	.053	265
1677	.67	.91	.75	-	-	35	5	25	15	20	-	-	-	-	.075	.038	224	2800	.263	1307
1684	.48	-	.02	55	40	11	1	30	25	2	23	-	8	.011	.009	-	-	400	-	-
1685	.91	-	.37	38	25	12	-	36	32	-	14	1	5	.14	.23	-	-	700	.028	140
1686	1.06	-	.29	-	c o n t a m i n a t i o n	b y	i r o n	o x i d e	c o a t i n g s											
1695	.74	-	.61	35	25	17	-	22	42	6	2	2	9	.214	.4	-	-	1400	.068	340
1696	.85	-	.3	50	50	18	2	40	23	6	10	2	9	.15	.15	-	-	600	.027	135

APPENDIX 2 (cont'd).

Sample No.	% heavies in total sample	% heavies in sand fraction	% heavies in sand minus carbonate	PETROGRAPHIC ANALYSIS - SAND FRACTION: TRANSLUCENT FRACTION: % Opaques	% Leucoxene in opaques	% Zircon	% Rutile	% Amphiboles	% Epidotes	% Pyroxenes	% Tourmaline	% Garnet	% Others	% opaques in sand minus carbonate	% translucents in sand minus carbonate	% rutile in translucents	ppm titanium in translucents	ppm total titanium in sample	% zircon in translucents	ppm in zirconium in translucents
1702	.16	.43	.22	35	26	9	4	58	21	4	2	2	-	.077	.143	.006	34	3200	.013	64
1703	.04	.09	.09	52	18	13	8	28	30	21	-	-	-	.047	.043	.003	21	3000	.006	28
1712	-	.13	.13	52	10	47	7	22	22	-	-	2	-	.067	.062	.004	26	4500	.029	146
1721	.27	.34	.13	47	21	32	11	19	18	3	14	-	3	.06	.068	.008	45	1100	.022	108
1730	.54	.61	.69	-	-	15	-	35	35	5	5	-	5	-	.69	-	-	1800	.104	515
1740	.22	.8	.36	34	21	9	3	45	25	9	4	-	5	.122	.238	.007	43	3700	.021	107
1741	.43	2.38	.81	-	-	20	2	35	35	-	-	-	8	-	.810	.016	97	400	.162	807
1746	.52	-	.12	-	-	8	-	32	30	10	10	-	10	-	.12	-	-	400	.01	5
1747	.53	-	.25	56	14	9	-	18	24	9	21	3	16	.14	.11	-	-	800	.01	5
1753	.51	-	.42	45	30	10	-	35	30	-	13	2	10	.19	.23	-	-	500	.023	115
1755	1.19	-	.46	-	s a m p l e c o n t a m i n a t e d w i t h i r o n o x i d e c o a t i n g s															
1756	.72	-	.10	-	-	15	-	40	18	8	9	-	10	-	.1	-	-	-	-	-
1768	.2	.24	.17	63	17	37	7	-	15	-	30	4	7	.107	.063	.004	26	1400	.023	116
1770	.31	.48	.14	37	50	10	5	47	26	-	5	7	-	.051	.088	.004	26	1800	.009	44
1772	.07	-	.005	-	-	a m p h i b o l e s > e p i d o t e s > z i r c o n s > t o u r m a l i n e														

APPENDIX 2 (cont'd).

Sample No.	% heavies in total sample	% heavies in sand fraction	% heavies in sand minus carbonate	PETROGRAPHIC ANALYSIS - SAND FRACTION: TRANSLUCENT FRACTION % Opaques	% Leucoxene in opaques	% Zircon	% Rutile	% Amphiboles	% Epidotes	% Pyroxenes	% Tourmaline	% Garnet	% Others	% opaques in sand minus carbonate	% translucents in sand minus carbonate	% rutile in translucents	ppm titanium in translucents	ppm total titanium in sample	% zircon in translucents	ppm in zirconium in translucents
1776	1.17	.81	.71	61	18	60	9	7	9	-	11	4	-	.43	.277	.025	149	1600	.167	828
1860	.24	.02	-	n o t e n o u g h s a m p l e																
GROUP 'A' SEDIMENTS																				
AVERAGE	.95	1.09	.79	44	12	27	10	23	19	4	13	1	3	.420	.41	.05	345	2775	.14	750
GROUP 'B' SEDIMENTS																				
AVERAGE	.25	.74	.38	45	22	23	7	31	24	7	3	< 1	4	.18	.24	.026	86	2946	.051	254
GROUP 'C' SEDIMENTS																				
AVERAGE			.4	36	17	16	5	34	23	12	5	1	4	.116	.275	.01	58	1000	.047	226

APPENDIX 3

MODAL ANALYSIS OF SHELF SEDIMENTS

Sample No.	% Igneous quartz	% Metamorphic quartz	% Sedimentary quartz	% Total quartz	% Rock fragments	% Feldspars	% Augite/ hornblende	% Echinoderms	% Glauconite	% Molluscs	% Foraminifera	% Bryozoa	% Unidentified carbonate	% Unidentified	% Total carbonate	% Carbonate by analysis	% Total clastics	Depth (m)
1530	51	7	11	69	7	14	-	-	-		9			-	9	7	90	15
1532	57	4	11	72	3	13	-	-	-	-	-	-	-	-	10	8.4	88	15
1537	7	-	74	81	9	1	-	-	-		9			-	9	7.9	91	20
1538	13	3	62	78	14	3	-	-	-		8			-	8	9.8	92	11
1539	33	-	51	84	9	3	-	-	-		6			-	6	-	95	11
1540	36	1	49	86	9	3	-	-	-		4			-	4	4	92	11
1595	15	6	33	54	32	2	-	-	-		11			-	11	-	89	27
1611	9.6	2	35	47	5	8	-	2.5	2.0	20	9.6	2.5	-	-	35	21	61.6	88
1620	-	-	23	23	< 1	< 1	-	3	< 1	19	7	< 1	-	-	30	44.7	25	115
1624	9.9	1	1.7	13	3.4	2.3	1.7	5.4	1.4	12.5	15.9	5.4	28	11.3	68.9	64.5	18.4	148
1625	6.2	1	3.6	11	5.3	5.6	0.3	4	0.3	21.1	11.9	4	31	5.6	72.3	70.7	21.7	143
1626	7	1.6	2.5	11	2.2	2.5	-	5.7	1.9	25.2	19.2	3.2	27.8	1.3	81.1	68.3	15.7	132
1627	2.3	0.7	18	21	0.3	2.6	-	5.2	3.9	19.6	17.4	3	25.2	2.3	69.8	56.6	24	124
1630	2.6	1.3	56	60	7.7	3.9	-	2.9	1.3	1.0	3.5	0.3	13.2	6.4	20.9	17.6	71.4	64
1638	0.9	1.5	25.2	28	1.2	2.4	-	4.7	1.2	16	9.2	5	30	2.7	64.9	46	31.2	125

APPENDIX 3 (cont'd).

Sample No.	% Igneous quartz	% Metamorphic quartz	% Sedimentary quartz	% Total quartz	% Rock fragments	% Feldspars	% Augite/ hornblende	% Echinoderms	% Glauconite	% Molluscs	% Foraminifera	% Bryozoa	% Unidentified carbonate	% Unidentified	% Total carbonate	% Carbonate by analysis	% Total clastics	Depth (m)
1639	8.9	1.6	15.2	26	6.6	2.1	1.8	5.2	1.3	17.8	14.7	3.4	17.8	3.4	60.7	51.7	34.4	132
1640	6.5	.4	9.9	17	3	1.3	.4	7.4	.4	24.7	33.3	.4	4.3	7.8	70.5	57.8	21.1	141
1641	5.8	.6	6.4	13	2.3	3.8	-	7.9	2.6	21.3	19.3	.3	26.3	3.2	75.1	63.3	18.9	183
1642	-	-	8.6	9	.7	1.0	-	3.8	.3	16.6	19.3	10.6	39.2	.7	88.7	67.8	10.3	198
1646	.3	-	19.7	20	-	2.4	-	2	-	8.5	5.1	-	22.4	39.7	38	34	22.4	86
1648	3.2	1.3	28.1	33	3.2	2.9	2.3	3.5	.6	3.2	10.3	2.3	35.5	3.5	57.1	51	38.7	128
1656	10.3	.3	6.4	17	6.1	2.7	8.8	3	1.8	12.2	17	1.5	27.4	2.4	69.9	61.4	25.8	130
1657	3.9	.5	15.7	20	1.5	6.9	-	6.4	2	30.4	22.1	1.0	.5	9.3	60.4	60.7	28	194
1659	1.5	-	7.3	9	3.0	2.4	1.8	5.8	1.2	18.5	17.9	1.2	33.6	5.8	78.8	67	14.2	205
1660	-	.6	23.5	24	2.0	2.6	-	1.7	2.9	14.6	7.2	-	21.8	23.2	45.3	42.4	28.7	124
1661	27.3	4.3	36	68	10.8	7.9	.7	-	-	1.4	-	-	5.8	5.8	7.9	5.7	86.3	32
1675	-	5.0	40	45	1.8	5.4	-	0.5	4.1	16.2	9.5	1.8	5	10.4	33	54.3	52.7	110
1677	46	13	4	63	11	11	-	-	-	-	-	-	-	-	7	5	85	22
1688	-	-	16.4	16	4.3	5	-	4	6.8	24.1	15.8	1.9	13.6	8	59.4	55.1	25.7	106
1695	.3	-	23.7	24	7.8	1.9	-	2.5	2.2	9.7	9.7	.6	25.9	9.0	48.4	47.4	84.3	110

APPENDIX 3 (cont'd).

Sample No.	% Igneous quartz	% Metamorphic quartz	% Sedimentary quartz	% Total quartz	% Rock fragments	% Feldspars	% Augite/ hornblende	% Echinoderms	% Glauconite	% Molluscs	% Foraminifer	% Bryozoa	% Unidentified carbonate	% Unidentified	% Total carbonate	% Carbonate by analysis	% Total clastics	Depth (m)
1702	-	-	36.3	36.3	2	5.6	-	7.5	1	9.8	5.9	.3	8.2	22.9	31.7	24	44.6	70
1703	-	-	22	22	7.7	2.2	-	7.7	1.9	12.9	7.4	.3	12.1	25.6	40.4	30	31.9	84
1704	-	-	28.9	28.9	2.7	2.7	-	4.7	1.2	9.4	8.8	.3	17.1	24.2	40.3	31.4	34.3	95
1706	-	-	30.7	30.7	1.0	3.2	-	7.7	3.8	7.7	8.6	-	22.4	15	46.4	34.3	34.9	110
1711	-	-	58.8	58.8	6.2	4	-	2.2	.3	3.1	.6	.3	6.8	17.5	13	12.4	69.3	60
1714	-	-	28.8	28.8	9.2	2.5	-	8.6	2.1	6.4	5.8	-	20.6	15.6	41.4	32.1	41.8	97
1716	-	-	27.7	27.7	7.9	3.1	-	3.1	2.5	12.5	14.5	1.3	23	4.4	54.4	49.7	38.7	128
1717	-	-	36.8	36.8	5.6	1.9	-	1.9	.3	4	10.6	2.3	33	3.3	51.8	33.3	44.3	124
1718	-	-	34	34	3.2	5.0	-	2.3	2.9	7.9	6.7	-	26.8	14	43.7	35.5	42.2	117
1725	-	-	34.4	34.4	4.2	2.8	-	2.5	-	5.8	5.8	13.6	23.9	6.9	51.6	37.1	41.4	70
1728	-	-	47.1	47.1	1.6	6.6	-	3.6	1.6	10.8	8.5	-	16.1	3.9	39	41.2	55.3	122
1729	-	-	37	37	3.4	4.6	-	3.4	2.5	13.3	9	1	23.7	2.1	50.4	50.7	45	122
1732	-	-	21.2	21.2	1.4	2.1	-	8.6	2.1	15.1	16.8	1.4	27.7	3.8	69.6	54.3	24.7	128
1733	-	-	43	43	2.7	6.3	-	-	.6	12	7	-	20.3	3.3	39.3	37.4	57	117
1751	3.2	.9	16.8	20	-	6.4	.3	3.5	1.5	15.6	10.4	2.3	35.7	3.5	67.8	35.9	26.4	124

APPENDIX 3 (cont'd).

Sample No.	% Igneous quartz	% Metamorphic quartz	% Sedimentary quartz	% Total quartz	% Rock fragments	% Feldspars	% Augite/ hornblende	% Echinoderms	% Glauconite	% Molluscs	% Foraminifera	% Bryozoa	% Unidentified carbonate	% Unidentified	% Total carbonate	% Carbonate by analysis	% Total clastics	Depth (m)
1753	13.2	3.1	32.6	48.9	5	10.5	-	1.6	-	9.3	12.4	-	14.7	3.1	38	18	64.4	57
1754	5.8	.6	12.8	18	2	3.8	-	2.6	1.2	17.1	7.8	.9	30.4	3.8	62.6	68.3	23.8	97
1755	6.3	1.3	5.9	13.5	3.3	2.6	5.3	3.6	.3	16.1	9.5	19.1	24	2.6	77.6	70	19.4	128
1756	-	-	10.2	10.2	.5	.5	2.2	3.5	-	18.5	17.5	13.7	32	1.3	88.7	88	11.2	141
1763	23.3	8.6	41.1	73	4.3	10.4	-	-	-	3.7	1.8	-	5.5	1.2	11.0	16.7	87.7	49
1764	15.7	2.5	22.5	40.7	.9	6.8	-	3.4	.3	14.5	3.1	1.2	26.8	2.5	49	45	48.4	71
1765	1.3	1.3	9	11.6	.3	1	3.5	3.5	.3	39.2	9	-	29.9	1.6	85.1	74	12.9	102
1766	1.9	.9	11.9	14.7	.3	.6	-	3.8	.6	18.6	17	.9	40.4	2.9	80.7	73	15.6	130
1767	.2	.2	2.2	2.2	.3	.8	2.5	3.0	-	24.6	16.9	21.3	27.9	.6	96.2	93	3.3	205
1768	10	-	72	82	1.9	6.5	-	-	-	1.9	-	-	7.5	-	9.4	6.4	90.4	22
1770	6.5	1	28.1	35.6	4.5	7.9	1.4	3.1	.3	15.4	5.5	3.4	21.9	1	50.4	50.2	48	91
1771	2.1	-	16.4	18.5	6.1	4.3	1.4	1.4	1.8	25.4	8.9	1.7	27.5	3.9	66.3	65.2	29.2	124
1772	-	-	2.1	2.1	3	-	7.2	4.3	-	17.4	12.8	17.7	32	.9	93	89	5.1	223

APPENDIX 4

GEOCHEMICAL, X-RAY AND GRANULOMETRIC DATA

Sample No.	% Calcium carbonate	Phosphate ppm	Tin ppm	Copper ppm	Lead ppm	Zinc ppm	Manganese ppm	Nickel ppm	% Iron	Cobalt ppm	Cadmium ppm	Arsenic ppm	% Organic carbon	Titanium ppm	Standard Deviation ø	Mean ø	Kurtosis	Skewness	% Gravel	% Sand	% Silt	% Clay	Depth (m)	Clay minerals
1530	7.02	<500	<10	5	<5	10	30	5	0.4	5	<1	5	0.04	0.21	0.6	2.6	-0.5	0.4	0.0	100.0	0.0	0.0	15	
1531	19.4	1500	<10	5	5	10	40	5	0.4	5	1	10	-	0.27	0.6	2.7	22.3	1.6	0.1	99.9	0.0	0.0	15	
1532	8.4	<500	<10	<5	5	10	20	<5	0.3	5	<1	12	-	0.10	0.5	2.2	0.2	0.7	0.0	100.0	0.0	0.0	15	
1533	18.8	<500	<10	5	<5	10	35	5	0.3	5	<1	10	-	0.13	0.5	2.7	62.4	5.0	0.2	99.8	0.0	0.0	16	
1534	9.3	<500	<10	5	5	5	30	5	0.3	5	1	12	0.04	0.28	0.5	2.6	48.0	-3.0	0.1	99.9	0.0	0.0	16	
1535	60.2	500	20	5	10	20	90	20	0.8	10	6	15	0.15	0.04	1.2	0.5	9.0	-2.6	7.9	92.1	0.0	0.0	24	
1537	7.9	<500	<10	5	5	10	40	5	0.3	5	1	3	0.04	0.78	0.6	2.5	0.4	-0.3	0.0	100.0	0.0	0.0	20	
1538	9.8	<500	10	5	<5	10	35	5	0.3	5	1	2	0.08	0.22	1.4	2.0	11.3	3.1	5.6	94.4	0.0	0.0	17	
1540	4.1	<500	<10	5	<5	5	20	<5	0.1	<5	<1	10	-	0.11	0.7	1.5	22.0	-2.1	0.3	99.7	0.0	0.0	11	
1541	2.14	<500	<10	5	<5	5	15	<5	0.1	<5	1	12	-	0.08	0.4	2.0	15.5	0.1	0.02	99.98	0.0	0.0	18	
1542	1.43	<500	<10	5	<5	5	20	<5	0.1	5	1	5	0.02	0.13	0.4	2.1	4.8	1.7	0.0	100.0	0.0	0.0	20	
1605	21.3	2500	<10	5	5	35	190	25	3.5	15	3	80	-	0.07	1.4	1.7	10.3	-2.6	3.7	96.3	0.0	0.0	201	
1606	51.9	10500	<10	5	5	85	130	35	8.7	15	4	130	0.12	0.17	2.0	1.5	3.4	-2.0	9.8	90.2	0.0	0.0	247	
1607	75.0	2000	<10	5	5	25	220	25	2.3	10	4	50	0.10	0.06	1.9	1.0	2.9	-1.7	9.9	90.1	0.0	0.0	120	
1608	69.7	2000	<10	<5	5	20	220	25	1.9	10	4	70	0.12	0.04	1.9	0.5	2.4	-1.6	11.6	88.4	0.0	0.0	115	

APPENDIX 4 (cont'd).

Sample No.	% Calcium carbonate	Phosphate ppm	Tin ppm	Copper ppm	Lead ppm	Zinc ppm	Manganese ppm	Nickel ppm	% Iron	Cobalt ppm	Cadmium ppm	Arsenic ppm	% Organic carbon	Titanium ppm	Standard Deviation ø	Mean ø	Kurtosis	Skewness	% Gravel	% Sand	% Silt	% Clay	Depth (m)	Clay minerals
1609	64.5	1500	<10	<5	<5	15	110	20	1.4	5	3	35	0.08	0.05	1.6	1.0	4.2	-2.0	9.6	90.4	0.0	0.0	102	
1610	36.7	1500	<10	<5	5	15	110	10	1.4	5	2	12	0.07	0.04	1.4	1.5	7.2	-2.4	5.3	94.7	0.0	0.0	93	
1611	20.7	1000	<10	5	10	30	65	10	1.3	5	<1	<2	0.39	0.15	2.6	3.6	3.2	1.7	1.0	79.4	10.0	9.6	88	Chlorite
1612	17.6	500	<10	<5	<5	10	40	5	0.8	<5	<1	5	0.07	0.06	1.0	1.8	20.6	-3.7	1.7	98.3	0.0	0.0	102	
1613	63.6	1000	10	5	5	15	120	15	1.1	10	3	5	0.07	0.03	1.3	0.9	8.8	-2.5	4.5	95.5	0.0	0.0	121	
1614	49.3	2000	<10	5	<5	35	90	20	2.2	10	3	25	0.14	0.14	1.8	2.1	6.0	-2.3	5.7	94.3	0.0	0.0	241	
1615	58.5	2000	<10	5	5	20	310	20	2.1	10	3	70	0.07	0.05	2.0	0.3	1.4	1.5	15.4	84.6	0.0	0.0	139	
1616	49.5	1500	<10	5	<5	20	180	15	1.5	10	3	35	0.07	0.03	1.4	0.9	7.4	-2.0	4.9	95.1	0.0	0.0	132	
1617	56.6	2000	<10	5	<5	25	120	20	2.0	10	3	35	0.24	0.07	1.8	1.2	3.1	-1.8	9.9	90.1	0.0	0.0	126	
1618	34.0	1000	<10	5	5	40	90	20	1.6	10	3	<2	0.29	0.20	2.1	3.4	6.4	2.2	0.6	85.7	7.6	6.1	98	Chlorite
1619	5.8	500	<10	5	<5	10	25	5	0.3	5	<1	<2	0.03	0.05	0.8	1.3	13.9	-1.4	0.7	99.3	0.0	0.0	50	
1620	44.7	2400	10	5	10	35	85	35	1.4	5	1	15	0.55	0.16	2.5	4.3	3.0	1.0	2.2	70.0	17.7	10.0	115	Chlorite
1621	51.4	3200	20	5	<5	35	85	25	2.7	10	2	10	0.23	0.10	2.3	1.6	2.4	-1.9	11.9	88.1	0.0	0.0	128	
1622	66.2	3400	<10	5	5	35	140	25	3.1	5	3	70	0.12	0.06	1.0	1.9	11.9	-2.1	0.9	99.1	0.0	0.0	144	
1624	64.5	3300	<10	5	5	35	270	30	3.7	10	1	110	0.11	0.05	1.5	1.0	5.8	-2.2	6.8	93.2	0.0	0.0	148	

APPENDIX 4 (cont'd).

Sample No.	% Calcium carbonate	Phosphate ppm	Tin ppm	Copper ppm	Lead ppm	Zinc ppm	Manganese ppm	Nickel ppm	% Iron	Cobalt ppm	Cadmium ppm	Arsenic ppm	% Organic carbon	Titanium ppm	Standard Deviation ø	Mean ø	Kurtosis	Skewness	% Gravel	% Sand	% Silt	% Clay	Depth (m)	Clay minerals
1625	70.7	3300	<10	5	5	30	180	30	3.5	5	1	80	0.12	0.05	0.9	1.6	15.7	-2.6	1.1	98.9	0.0	0.0	143	
1626	68.3	3300	<10	5	5	35	150	30	3.1	10	1	50	0.22	0.07	1.9	1.3	2.7	-1.8	10.7	89.3	0.0	0.0	132	
1627	56.6	3500	<10	5	5	65	150	35	3.6	15	1	30	0.41	0.12	2.4	2.8	5.2	1.6	3.1	84.2	7.2	5.5	124	Kaolinite
1628	37.4	1350	<10	15	10	50	120	35	2.0	5	1	4	0.80	0.25	3.1	5.7	-0.5	0.9	0.0	53.1	26.1	25.3	115	Kaolinite
1629	28.1	1600	<10	20	15	70	140	35	2.6	5	<1	10	1.20	0.34	3.1	6.8	0.4	-1.1	0.0	26.1	37.1	36.8	99	Kaolinite/ illite
1630	17.6	1450	<10	20	15	120	180	30	2.7	<5	1	2	1.25	0.20	3.7	5.9	-1.2	0.4	0.0	40.6	26.6	32.8	64	Kaolinite/ illite
1631	41.9	2100	10	15	10	65	150	35	2.8	5	1	12	0.72	0.31	3.1	3.4	1.8	1.2	2.9	76.7	8.4	12.0	126	Kaolinite
1632	56.4	2600	<10	5	<5	25	380	30	3.1	5	3	100	0.09	0.04	1.3	1.0	8.8	-1.2	4.0	96.0	0.0	0.0	137	
1634	3.3	220	<10	5	<5	5	15	5	0.2	<5	<1	<2	-	0.15	0.6	1.8	15.0	-0.4	0.2	99.8	0.0	0.0	24	
1635	36.4	600	<10	5	<5	10	55	15	0.3	<5	<1	12	-	0.08	1.4	0.9	5.9	-2.2	9.2	90.8	0.0	0.0	33	
1636	9.8	410	<10	<5	<5	10	20	5	0.4	5	<1	180	0.10	0.05	1.2	1.2	10.2	-2.5	2.9	97.1	0.0	0.0	60	
1637	41.7	1150	<10	10	10	35	65	20	1.3	5	1	25	0.46	0.24	2.5	4.1	3.6	1.8	0.5	78.3	11.0	10.2	120	Kaolinite/ mica
1638	46.0	1850	<10	5	<5	40	110	25	2.0	5	2	<2	0.39	0.16	2.8	3.3	2.9	0.9	4.1	81.2	6.4	8.3	125	
1639	51.7	2400	<10	5	5	35	110	15	2.4	5	3	25	0.31	0.11										
1640	57.8	3500	<10	5	5	35	120	15	3.0	10	3	45	0.18	0.10	1.2	2.1	10.2	-2.3	1.7	98.3	0.0	0.0	141	

APPENDIX 4 (cont'd).

Sample No.	% Calcium carbonate	Phosphate ppm	Tin ppm	Copper ppm	Lead ppm	Zinc ppm	Manganese ppm	Nickel ppm	% Iron	Cobalt ppm	Cadmium ppm	Arsenic ppm	% Organic carbon	Titanium ppm	Standard Deviation ø	Mean ø	Kurtosis	Skewness	% Gravel	% Sand	% Silt	% Clay	Depth (m)	Clay minerals
1641	63.3	4400	<10	5	5	40	100	20	2.8	5	2	45	0.17	0.13	1.4	2.2	7.8	-2.4	4.4	95.6	0.0	0.0	183	
1642	67.8	2300	10	5	5	25	65	20	1.8	5	3	30	0.19	0.13	1.5	2.2	9.8	-2.9	4.4	95.6	0.0	0.0	198	
1643	54.0	4400	<10	5	5	40	160	25	4.5	5	3	80	0.21	0.08	1.3	1.8	6.1	-1.5	2.2	97.8	0.0	0.0	140	
1644	27.6	960	10	10	10	35	55	10	1.2	<5	2	3	0.61	0.18	3.0	4.2	0.9	1.4	0.2	71.6	12.7	15.5	84	Illite/ chlorite
1646	34.0	1300	<10	15	20	60	80	25	1.7	10	3	4	1.20	0.24	2.9	5.5	0.02	1.1	0.0	48.9	30.3	20.8	37	Kaolinite/ illite
1647	39.8	1400	<10	15	15	35	70	20	1.7	10	1	2	0.65	0.18	2.7	4.1	2.1	1.6	0.2	75.0	12.9	11.8	85	Illite/ kaolinite
1648	50.5	2600	<10	5	5	25	95	15	2.5	10	3	25	0.20	0.08	1.1	1.6	5.9	-1.2	1.5	98.5	0.0	0.0	128	
1649	53.3	2900	10	5	<5	40	85	15	2.6	10	3	50	0.18	0.10	1.4	2.1	7.2	-2.0	2.8	97.2	0.0	0.0	141	
1650	62.8	2400	<10	5	10	35	70	15	1.5	10	3	15	0.24	0.10	1.1	2.7	24.8	-4.0	1.3	98.7	0.0	0.0	225	
1651	63.8	2600	10	5	5	35	70	15	2.3	10	3	25	-	0.10	1.1	2.5	14.5	-2.7	1.0	98.9	0.0	0.0	200	
1652	49.7	2100	<10	5	5	25	80	10	2.0	15	3	15	0.45	0.14	2.6	2.8	3.5	0.8	3.5	82.9	8.7	4.9	122	Mica/ chlorite
1653	22.6	760	<10	25	35	50	20	5	1.7	5	1	2	0.10	0.22										
1655	30.0	1150	<10	5	15	25	35	10	1.1	10	3	10	0.38	0.12	1.6	2.7	13.4	2.8	0.5	91.7	5.1	2.7	108	
1656	61.4	3900	<10	5	5	35	120	15	4.1	15	4	90	0.23	0.06	1.4	1.7	6.8	-2.0	4.0	96.0	0.0	0.0	130	
1657	60.7	2300	<10	5	5	35	50	10	1.5	15	4	10	0.26	0.14	1.9	3.0	9.1	0.8	3.4	89.6	4.3	2.8	194	

APPENDIX 4 (cont'd).

Sample No.	% Calcium carbonate	Phosphate ppm	Tin ppm	Copper ppm	Lead ppm	Zinc ppm	Manganese ppm	Nickel ppm	% Iron	Cobalt ppm	Cadmium ppm	Arsenic ppm	% Organic carbon	Titanium ppm	Standard Deviation Ø	Mean Ø	Kurtosis	Skewness	% Gravel	% Sand	% Silt	% Clay	Depth (m)	Clay minerals
1658	95.9	470	<10	<5	<5	30	55	20	0.2	15	5	<2	-	0,02										
1659	67.1	2200	<10	<5	<5	35	65	25	1.8	15	3	20	0.24	0,09	2,0	2,7	9.0	0.4	4.5	91.0	2.2	2.3	205	
1660	42.4	1750	<10	5	10	50	65	25	2.0	10	3	5	0,90	0,21	2,4	3,9	2,6	1.5	0.3	71.0	19.9	8.8	124	Kaolinite/ mica
1661	5.7	360	<10	<5	5	5	55	5	0.6	<5	1	10	0.04	0,60	0,6	1,8	38.9	-3,5	0.3	99.7	0.0	0.0	37	
1662	51.9	2300	<10	25	10	140	260	25	2.2	15	3	20	1.10	0,22										
1663	54.5	2000	<10	<5	5	15	120	20	1.5	15	3	35	0,32	0,04	1,1	0,9	9,2	-1,7	3,3	96,7	0.0	0.0	57	
1664	47.8	1550	<10	10	5	40	55	25	1.7	10	1	5	0,82	0,19	2,6	3.4	2.5	1.3	1.2	71,4	19.5	8.0	124	Mica/ kaolinite/ chlorite
1665	65.9	4200	<10	<5	5	35	80	20	4.1	15	3	80	0.31	0,10	2,0	2,4	7.8	1,9	1.2	90,1	4.9	3.8	146	
1666	67.8	4200	<10	<5	<5	65	65	25	2.6	5	3	10	0,24	0,10	0,6	2.9	0.9	0,0	0.0	100.0	0.0	0.0	225	
1667	72.6	5000	<10	<5	5	50	80	30	4,0	15	4	70	0,23	0,06	1,1	2,2	11.2	-2,3	2.2	97.8	0.0	0.0	148	
1668	29.8	1100	20	15	15	140	85	20	1.8	5	3	5	0.7	0,16	2.3	3.6	3.7	1.3	1.3	76.6	14.9	7.2	60	Mica/ chlorite
1670	43.6	1550	<10	<5	5	40	65	20	1.5	5	3	8	0,76	0.20	2,1	3.9	1.7	0.8	0,8	73.2	14.4	11,6	115	Mica/ kaolinite/ chlorite
1671	64.7	3200	10	<5	5	35	70	25	3.3	10	4	65	1.22	0.07	1.3	1.8	8.4	-2.1	2.4	97.6	0.0	0.0	135	
1672	67.4	8700	<10	85	5	75	70	30	3.8	10	4	48	0,24	0,06	1.3	2.1	10.1	-2,8	4.5	95.5	0.0	0.0	203	
1673	89.7	1800	<10	5	<5	30	55	25	1.5	10	5	20	0.13	0.04	2.5	-0.5	-1.1	-0.6	33.5	66.5	0.0	0.0	201	

APPENDIX 4 (cont'd).

Sample No.	% Calcium carbonate	Phosphate ppm	Tin ppm	Copper ppm	Lead ppm	Zinc ppm	Manganese ppm	Nickel ppm	% Iron	Cobalt ppm	Cadmium ppm	Arsenic ppm	% Organic carbon	Titanium ppm	Standard Deviation ϕ	Mean ϕ	Kurtosis	Skewness	% Gravel	% Sand	% Silt	% Clay	Depth (m)	Clay minerals
1674	64.7	1500	<10	5	<5	10	45	20	1.2	5	4	25	0.08	0.03	2.7	-0.9	-1.4	-0.4	38.3	61.7	0.0	0.0	126	
1675	54.3	1800	<10	5	<5	35	50	20	1.8	15	3	12	0.34	0.12	2.5	2.6	4.2	0.8	5.1	83.5	7.0	4.4	110	Mica/ kaolinite
1676	23.3	1050	<10	<5	<5	30	30	10	1.2	5	1	<2	0.25	0.09	1.6	2.8	13.7	2.8	0.2	92.7	4.8	2.3	57	
1677	5.0	760	10	<5	5	35	80	5	1.4	5	<1	<2	0.23	0.28	0.6	3.1	2.0	-1.2	0.0	100.0	0.0	0.0	22	
1678	53.8	990	<10	<5	<5	10	20	10	0.5	5	3	<2	0.20	0.03	1.6	0.9	4.7	-2.1	9.9	90.1	0.0	0.0	55	
1679	38.1	1500	<10	<5	10	15	40	10	1.3	10	3	20	0.08	0.07	1.5	1.3	5.6	-2.2	7.5	92.5	0.0	0.0	124	
1680	72.8	3100	<10	<5	<5	35	50	20	1.6	10	4	15	0.08	0.06	2.3	0.8	-0.4	-0.8	29.0	71.0	0.0	0.0	208	
1681	48.6	2500	<10	<5	<5	55	55	10	2.1	10	3	25	0.10	0.05	1.5	1.2	5.1	-1.8	8.2	91.8	0.0	0.0	162	
1682	41.9	2000	<10	<5	<5	15	45	10	2.0	10	3	25	0.10	0.08	1.0	1.2	13.6	-2.4	2.0	98.0	0.0	0.0	124	
1683	35.7	400	<10	<5	<5	5	5	5	0.1	5	1	<2	0.05	0.03	1.8	1.5	3.4	-1.9	12.4	87.6	0.0	0.0	47	
1684	94.3	780	<10	<5	<5	25	10	5	0.1	15	4	<2	0.20	0.04	2.0	-0.9	-0.5	-0.2	55.5	44.5	0.0	0.0	30	
1685	39.7	4000	20	<5	10	25	45	10	2.6	5	1	25	0.18	0.07	0.8	2.2	28.4	-3.8	0.9	99.1	0.0	0.0	121	
1686	60.7	3700	<10	<5	5	25	50	15	1.7	5	3	25	0.08	0.05	2.1	0.8	-0.2	-0.8	28.1	71.9	0.0	0.0	179	
1687	35.2	7500	<10	<5	<5	10	10	5	0.1	10	1	<2	0.01	0.03	2.1	0.8	-0.1	-0.8	27.5	72.5	0.0	0.0	25	
1688	55.7	3200	<10	5	<5	40	55	10	2.7	10	3	15	0.49	0.12	2.0	3.0	7.6	2.0	0.8	86.5	8.8	3.9	106	Mica/ chlorite

APPENDIX 4 (cont'd).

Sample No.	% Calcium carbonate	Phosphate ppm	Tin ppm	Copper ppm	Lead ppm	Zinc ppm	Manganese ppm	Nickel ppm	% Iron	Cobalt ppm	Cadmium ppm	Arsenic ppm	% Organic carbon	Titanium ppm	Standard Deviation ø	Mean ø	Kurtosis	Skewness	% Gravel	% Sand	% Silt	% Clay	Depth (m)	Clay minerals
1689	53.8	3900	<10	<5	<5	25	55	10	2.5	5	4	35	0.13	0.04	1.1	2.2	15.9	3.1	1.9	98.1	0.0	0.0	122	
1690	84.01	3200	<10	<5	<5	20	80	10	2.3	5	5	45	0.13	0.04	1.1	1.3	15.4	-3.1	2.2	97.8	0.0	0.0	146	
1691	88.3	2200	<10	5	<5	20	45	10	1.5	10	5	30	0.20	0.04	1.4	1.2	4.9	-1.8	8.2	91.8	0.0	0.0	159	
1692	60.7	3400	<10	<5	10	25	40	15	2.0	10	4	35	0.15	0.05										
1693	63.8	4400	<10	5	10	40	50	15	3.4	15	4	40	0.20	0.08	1.1	1.8	12.7	-2.6	2.0	98.0	0.0	0.0	115	
1695	47.4	1700	<10	5	<5	25	50	10	1.3	10	3	<2	0.46	0.14	1.0	3.2	28.5	-1.2	0.8	87.7	11.2	0.3	110	Mica/ chlorite
1696	58.3	3600	<10	<5	5	25	45	10	2.2	10	3	30	0.14	0.06	0.9	2.1	10.6	-2.0	0.8	99.2	0.0	0.0	124	
1698	5.7	2400	<10	30	20	170	470	65	4.4	25	1	<2	1.27	0.60	3.5	7.0	-1.4	0.1	0.0	33.6	22.4	44.0	22	
1699	9.3	290	<10	<5	5	10	50	<5	0.3	5	1	<2	0.11	0.05	2.3	-0.2	-0.9	-0.7	32.3	67.7	0.0	0.0	23	
1700	3.8	180	<10	<5	<5	5	45	<5	0.2	<5	1	<2	0.08	0.05	0.8	1.2	22.0	-3.6	1.9	98.1	0.0	0.0	37	
1701	4.3	270	<10	<5	<5	<5	5	45	0.3	<5	1	<2	0.08	0.04	0.8	1.3	27.0	-3.5	1.0	99.0	0.0	0.0	44	
1702	24.0	1300	<10	15	15	70	110	20	2.1	10	2	<2	0.87	0.32	3.0	5.3	-0.2	1.0	0.0	54.2	23.8	22.0	70	Kaolinite/ mica
1703	30.0	1300	10	15	10	65	140	20	2.1	5	1	<2	0.83	0.30	2.7	5.3	0.4	1.1	0.0	53.4	29.1	17.5	84	"
1704	31.4	1300	10	15	10	55	120	20	1.9	5	1	<2	0.82	0.26	2.6	5.1	1.1	1.4	0.0	53.5	30.5	16.0	95	"
1705	31.65	1300	<10	15	10	50	120	20	1.9	5	1	<2	0.82	0.25	2.4	4.8	2.1	1.7	0.0	61.4	26.2	12.4	110	"

APPENDIX 4 (cont'd).

Sample No.	% Calcium carbonate	Phosphate ppm	Tin ppm	Copper ppm	Lead ppm	Zinc ppm	Manganese ppm	Nickel ppm	% Iron	Cobalt ppm	Cadmium ppm	Arsenic ppm	% Organic carbon	Titanium ppm	Standard Deviation ø	Mean ø	Kurtosis	Skewness	% Gravel	% Sand	% Silt	% Clay	Depth (m)	Clay minerals
1706	34.3	1450	20	5	10	50	120	10	2.1	10	2	<2	0.66	0.23	2.5	4.2	2.3	1.7	0.0	71.5	17.6	11.0	115	Kaolinite/ mica
1707	3.1	340	<10	<5	<5	50	180	<5	0.5	<5	1	3	0.06	0.05	2.1	-0.1	0.2	-1.3	21.9	78.1	0.0	0.0	22	
1708	2.6	180	<10	<5	<5	5	45	<5	0.2	<5	<1	<2	0.5	0.06	1.9	0.4	1.9	-1.7	14.5	85.5	0.0	0.0	27	
1709	4.5	250	<10	<5	<5	5	85	<5	0.3	<5	<1	<2	0.04	0.06	2.0	-0.4	-0.4	-1.0	30.8	69.2	0.0	0.0	31	
1710	3.09	270	<10	<5	<5	5	50	<5	0.4	<5	<1	<2	0.03	0.07	1.3	1.0	8.7	-2.5	5.1	94.9	0.0	0.0	48	
1711	12.4	1250	<10	10	15	80	150	30	2.0	10	1	<2	0.81	0.31	2.9	4.8	0.7	1.1	0.4	61.5	21.6	16.5	60	Kaolinite/ mica
1712	21.9	1650	<10	15	20	100	180	40	2.7	15	2	8	1.12	0.45	2.9	6.1	-0.4	0.7	0.0	29.9	44.0	26.1	75	"
1713	27.6	1300	<10	10	10	65	150	30	2.0	15	2	5	0.78	0.28	2.6	5.2	1.1	1.4	0.0	51.2	33.5	15.3	93	Kaolinite
1714	32.1	1250	<10	5	10	50	120	25	1.9	15	2	5	0.63	0.24	2.8	4.9	1.0	1.5	0.0	64.4	18.5	17.1	97	Mica/ kaolinite
1715	35.7	1850	10	<5	15	65	150	30	2.7	15	3	12	0.69	0.25	2.9	4.2	1.3	1.2	0.8	65.8	20.2	13.3	124	Kaolinite/ mica
1716	49.7	2300	<10	5	5	35	80	20	2.1	15	2	50	0.26	0.11	2.1	2.5	7.0	2.2	0.2	89.9	6.3	3.5	128	Mica/ kaolinite
1717	33.3	1700	<10	<5	5	40	75	15	1.6	15	2	20	0.34	0.11	2.2	2.7	6.3	1.3	3.5	86.9	5.5	4.1	124	
1718	35.5	1350	<10	5	5	40	80	15	1.4	10	2	5	0.31	0.17	2.5	3.7	3.2	1.7	0.3	73.7	17.5	8.5	117	Kaolinite/ mica
1719	40.9	1350	<10	5	15	50	95	25	1.7	15	2	8	1.02	0.24	2.5	5.3	1.3	1.4	0.0	43.7	41.7	15.5	112	"
1720	40.0	1150	<10	5	10	45	85	20	1.2	10	3	4	0.73	0.18	2.2	4.1	4.8	2.0	0.3	75.7	15.8	8.3	84	"

APPENDIX 4 (cont'd).

Sample No.	% Calcium carbonate	Phosphate ppm	Tin ppm	Copper ppm	Lead ppm	Zinc ppm	Manganese ppm	Nickel ppm	% Iron	Cobalt ppm	Cadmium ppm	Arsenic ppm	% Organic carbon	Titanium ppm	Standard Deviation ø	Mean ø	Kurtosis	Skewness	% Gravel	% Sand	% Silt	% Clay	Depth (m)	Clay minerals
721	44.7	910	10	5	5	20	45	10	0.7	10	2	12	0.13	0.11	0.6	2.4	0.2	0.4	0.0	100.0	0.0	0.0	58	
722	36.9	590	<10	5	5	10	100	10	0.5	10	2	8	0.08	0.04	0.7	1.4	38.5	-4.2	0.7	99.3	0.0	0.0	21	
723	76.2	1550	<10	15	15	85	470	20	3.2	25	4	15	0.16	0.12	0.9	-1.7	4.3	-1.1	96.0	4.0	0.0	0.0	21	
724	66.9	1450	<10	5	10	30	140	20	1.2	20	4	40	0.19	0.06	2.1	-0.2	-0.5	-0.9	34.4	65.6	0.0	0.0	40	
725	37.1	1200	<10	10	10	35	75	15	1.2	20	3	10	0.54	0.17	2.2	3.6	5.8	2.3	0.1	84.4	8.6	6.7	70	Chlorite/ kaolinite/ mica
726	40.5	1350	10	10	15	60	100	20	1.6	25	4	5	1.06	0.22	2.6	5.7	0.5	1.2	0.0	37.9	43.5	18.5	99	Mica/ kaolinite
727	44.7	1300	<10	15	5	40	80	20	1.5	20	4	10	1.40	0.18	3.0	3.9	1.8	1.0	2.4	67.6	18.9	11.2	117	Mica/ chlorite/ kaolinite
728	41.2	1420	<10	5	5	35	65	15	1.5	5	1	4	0.45	0.32	2.7	3.6	2.7	1.4	1.1	75.2	14.7	9.0	122	Mica/ kaolinite
729	50.7	1850	<10	5	5	25	80	20	1.6	5	3	15	0.37	0.23	2.4	2.7	5.2	1.4	2.4	87.0	5.8	4.8	122	Chlorite
730	56.6	2600	<10	5	5	30	95	20	2.4	5	3	35	0.27	0.18	1.2	1.5	4.9	-0.9	1.4	98.6	0.0	0.0	128	
731	63.3	4000	<10	5	5	40	120	20	3.6	10	3	65	0.16	0.08	1.0	1.9	9.4	-1.6	1.5	98.5	0.0	0.0	135	
732	54.3	2600	<10	5	5	35	80	20	2.6	5	3	40	0.32	0.05	2.0	2.5	6.9	1.8	1.3	88.6	6.8	3.3	128	
733	37.4	1150	<10	5	10	35	65	15	1.2	5	3	5	0.65	0.15	2.1	3.6	5.2	1.6	0.9	76.9	17.1	5.1	117	Kaolinite/ mica
734	35.2	920	<10	5	10	30	65	10	0.7	<5	3	<2	0.38	0.09	1.1	1.8	4.0	-0.7	0.9	99.1	0.0	0.0	97	
735	75.7	1800	<10	5	15	20	95	15	1.4	10	4	40	0.20	0.04	2.0	0.1	1.1	-1.5	17.9	82.1	0.0	0.0	79	

APPENDIX 4 (cont'd).

Sample No.	% Calcium carbonate	Phosphate ppm	Tin ppm	Copper ppm	Lead ppm	Zinc ppm	Manganese ppm	Nickel ppm	% Iron	Cobalt ppm	Cadmium ppm	Arsenic ppm	% Organic carbon	Titanium ppm	Standard Deviation ø	Mean ø	Kurtosis	Skewness	% Gravel	% Sand	% Silt	% Clay	Depth (m)	Clay minerals
1736	20.9	450	<10	5	10	30	35	<5	0.4	<5	1	2	0.04	0.11	0.5	2.4	0.2	0.7	0.0	100.0	0.0	0.0	27	
1737	43.1	1300	<10	5	10	40	75	15	1.4	5	3	2	0.63	0.20	2.5	4.6	2.3	1.4	0.3	58.9	29.5	11.3	62	Mica/ kaolinite
1738	21.8	920	<10	5	10	15	45	15	0.8	<5	1	8	0.04	0.12	0.8	2.3	26.5	-3.8	1.0	99.0	0.0	0.0	70	
1739	46.6	1300	<10	10	20	55	70	15	1.4	5	3	12	0.65	0.18	2.2	3.6	4.8	1.3	1.3	75.7	17.6	5.4	113	Kaolinite/ mica
1740	44.5	2100	<10	5	15	35	75	15	2.4	5	3	20	0.32	0.37	2.2	2.7	4.5	0.9	3.4	82.3	11.1	3.3	120	"
1741	45.5	2800	<10	5	10	35	100	20	3.2	5	3	55	0.04	0.20	1.3	1.7	5.1	-1.4	3.1	96.1	0.0	0.0	124	
1742	61.2	3700	<10	5	10	35	130	20	3.9	5	3	80	0.04	0.15	1.3	1.7	5.8	-1.4	2.6	97.4	0.0	0.0	139	
1743	44.0	1300	<10	5	10	30	55	15	1.2	5	3	4	0.42	0.10	2.0	3.1	6.3	1.6	0.9	85.6	11.1	3.5	102	Mica
1744	50.7	2000	<10	5	5	25	65	15	1.2	<5	4	12	0.25	0.09	0.6	2.9	0.1	-0.5	0.0	100.0	0.0	0.0	119	
1745	51.6	2100	<10	<5	<5	30	45	15	1.2	5	3	10	0.15	0.08	0.8	2.7	15.6	-2.4	0.5	99.5	0.0	0.0	123	
1746	46.2	1600	10	<5	5	15	40	10	1.2	10	3	30	0.04	0.04	2.5	-0.3	-0.9	-0.6	32.5	67.5	0.0	0.0	124	
1747	79.7	880	<10	<5	10	10	45	10	0.5	5	1	3	0.04	0.08	0.7	2.7	30.8	-3.7	0.5	99.5	0.0	0.0	108	
1748	31.4	760	<10	5	<5	15	40	10	0.5	5	1	2		0.06										
1749	7.9	330	<10	5	<5	5	20	<5	0.4	<5	1	12	0.04	0.03	1.2	0.9	9.7	-1.9	2.7	97.3	0.0	0.0	53	
1750	26.7	850	<10	<5	<5	5	45	<5	0.4	<5	1	15	0.04	0.06	0.7	2.8	59.6	-5.9	0.6	99.4	0.0	0.0	91	

APPENDIX 4 (cont'd).

Sample No.	% Calcium carbonate	Phosphate ppm	Tin ppm	Copper ppm	Lead ppm	Zinc ppm	Manganese ppm	Nickel ppm	% Iron	Cobalt ppm	Cadmium ppm	Arsenic ppm	% Organic carbon	Titanium ppm	Standard Deviation ø	Mean ø	Kurtosis	Skewness	% Gravel	% Sand	% Silt	% Clay	Depth (m)	Clay minerals
1751	35.9	1600	<10	5	5	15	45	5	1.4	5	1	3	0.1	0.09	2.2	0.4	-0.2	-0.8	19.3	80.7	0.0	0.0	124	
1753	18.3	760	<10	5	5	10	35	<5	0.7	<5	1	10	0.06	0.05	1.8	1.1	3.0	-1.6	8.6	91.4	0.0	0.0	57	
1754	68.3	1550	<10	<5	10	15	40	15	1.0	5	3	12	0.15	0.06	1.8	2.1	4.1	-2.2	10.2	89.8	0.0	0.0	97	
1755	69.7	3500	<10	5	10	25	50	15	2.3	5	3	55	0.15	0.04	1.8	1.3	2.8	-1.7	9.9	90.1	0.0	0.0	128	
1756	87.8	2400	<10	5	10	30	55	15	1.6	10	4	40	0.2	0.03	1.6	1.0	4.0	-1.9	10.8	89.2	0.0	0.0	141	
1757	95.6	1050	<10	5	5	15	55	15	0.5	5	4	4	0.24	0.04	2.2	-1.1	-1.0	0.2	61.8	38.2	0.0	0.0	170	
1758	44.7	2100	<10	5	10	20	45	15	1.9	5	3	5	0.24	0.07	1.4	2.0	5.7	-2.0	4.8	95.2	0.0	0.0	119	
1759	73.8	2300	<10	<5	10	20	40	15	2.0	5	4	30	0.20	0.05	1.6	1.9	6.2	-2.3	5.9	94.1	0.0	0.0	115	
1760	75.5	1300	<10	5	10	15	35	10	0.8	5	4	10	0.14	0.03	1.8	1.6	2.6	-1.8	11.8	88.2	0.0	0.0	86	
1761	27.6	1050	<10	<5	5	10	25	<5	0.9	5	2	8	0.08	0.04	2.2	1.1	1.9	-1.7	12.8	87.2	0.0	0.0	70	
1762	4.8	190	<10	<5	<5	10	5	<5	0.4	<5	1	<2	0.04	0.07	0.5	2.1	2.0	1.3	0.0	100.0	0.0	0.0	13	
1763	16.7	570	<10	5	<5	5	20	<5	0.5	<5	1	8	0.04	0.02	1.0	1.0	12.7	-2.3	2.6	97.4	0.0	0.0	49	
1764	45.0	1300	<10	<5	<5	10	35	10	1.0	5	3	12	0.1	0.03	1.2	1.6	8.3	-1.9	3.1	96.9	0.0	0.0	71	
1765	74.0	1900	<10	5	10	15	45	15	1.4	10	3	20	0.2	0.05	1.5	2.0	5.5	-2.1	6.0	94.0	0.0	0.0	102	
1766	73.3	2000	<10	5	<5	20	45	20	2.0	10	4	20	0.2	0.07	1.8	2.9	10.7	1.6	1.7	90.2	5.9	2.3	130	

APPENDIX 4 (cont'd).

Sample No.	% Calcium carbonate	Phosphate ppm	Tin ppm	Copper ppm	Lead ppm	Zinc ppm	Manganese ppm	Nickel ppm	% Iron	Cobalt ppm	Cadmium ppm	Arsenic ppm	% Organic carbon	Titanium ppm	Standard Deviation ϕ	Mean ϕ	Kurtosis	Skewness	% Gravel	% Sand	% Silt	% Clay	Depth (m)	Clay minerals
1767	92.8	1400	<10	5	<5	15	25	15	0.7	15	4	5	0.2	0.04	2.3	-0.3	-0.9	-0.7	33.9	66.1	0.0	0.0	205	
1768	6.4	170	<10	5	<5	<5	5	5	0.2	<5	1	<2	0.06	0.14	0.6	1.6	14.4	1.9	0.1	99.9	0.0	0.0	22	
1769	50.2	1250	<10	5	5	15	45	15	0.9	5	4	10	0.39	0.17	2.2	3.4	6.2	1.9	0.9	85.2	8.0	5.9	70	Mica/ chlorite
1770	48.3	1400	<10	5	5	15	40	10	1.1	5	3	15	0.14	0.10	2.0	1.4	6.2	-2.0	2.5	97.5	0.0	0.0	91	
1771	65.2	2400	<10	10	5	20	40	15	2.2	10	4	30	0.14	0.04	1.5	1.4	4.3	-2.0	7.4	92.6	0.0	0.0	124	
1772	89.0	1200	<10	5	<5	10	25	15	0.6	10	4	4	0.17	0.03	3.0	1.1	1.9	0.6	22.6	66.3	7.9	3.1	223	
1773	68.5	1500	<10	5	5	15	45	15	1.4	10	3	30	0.09	0.04	1.7	0.3	1.7	-1.4	17.0	83.0	0.0	0.0	192	
1774	56.2	2000	<10	5	5	10	45	15	1.8	5	3	40	0.10	0.03	1.4	3.4	13.9	-3.7	3.7	96.3	0.0	0.0	108	
1775	46.2	1300	<10	5	<5	10	35	10	1.0	10	3	15	0.11	0.03	1.4	1.7	6.6	-2.1	3.3	96.7	0.0	0.0	86	
1776	33.8	500	<10	5	5	5	20	5	0.3	5	<2	<2	0.06	0.16	0.6	2.5	-0.3	0.2	0.0	100.0	0.0	0.0	17	
1777	4.3	140	<10	5	<5	<5	5	<5	0.3	<5	2	<2	0.02	0.05	0.6	2.3	0.4	0.6	0.0	100.0	0.0	0.0	15	
1778	44.5	1250	<10	5	5	10	45	10	0.9	5	2	5	0.1	0.04	0.9	2.3	19.8	-3.2	1.0	99.0	0.0	0.0	91	
1779	63.3	2000	10	5	5	10	45	15	1.4	10	3	20	0.1	0.04	1.4	1.7	11.2	-3.0	3.4	96.6	0.0	0.0	126	
1780	81.9	2500	<10	5	5	20	40	15	2.1	10	3	50	0.2	0.03	1.8	1.1	4.2	-1.9	7.3	92.7	0.0	0.0	179	
1781	8.6	200	<10	5	<5	<5	15	<5	0.2	<5	1	12	0.01	0.09	0.5	2.6	0.8	0.2	0.0	100.0	0.0	0.0	22	

APPENDIX 4 (cont'd).

Sample No.	1782	1783	1860
% Calcium carbonate	60.5	72.6	20.7
Phosphate *ppm*	1300	2400	1350
Tin ppm	<10	<10	<10
Copper ppm	5	5	15
Lead ppm	5	5	10
Zinc ppm	5	20	85
Manganese ppm	40	40	160
Nickel ppm	10	20	10
% Iron	0.9	2.3	2.5
Cobalt ppm	10	20	10
Cadmium ppm	3	3	1
Arsenic ppm	20	45	3
% Organic carbon	0.1	0.20	1.06
Titanium ppm	0.03	0.04	0.40
Standard Deviation ϕ	1.4	1.6	2.9
Mean ϕ	1.3	1.3	5.2
Kurtosis	6.8	4.7	0.2
Skewness	-2.1	-2.0	1.2
% Gravel	4.0	5.6	0.0
% Sand	96.0	94.4	54.3
% Silt	0.0	0.0	26.0
% Clay	0.0	0.0	19.7
Depth (m)	112	168	77
Clay minerals			Kaolinite/mica

TABLE 1. GROUP A SEDIMENTS

MEANS

15.10545	653.33333	5.45455	5.09091	3.33333	12.57576	30.60606	5.21212	
0.37879	10.30303	1.00000	10.63636	0.06515	0.16000	0.85455	1.86970	
2.53636	97.24848	0.87303	31.06061					

STANDARD DEVIATIONS

14.29741	1248.82111	1.45969	1.22126	1.61374	13.49891	21.20427	3.45740	
0.27924	16.99905	0.58630	30.76302	0.05751	0.18076	0.45006	0.67892	
5.49465	5.53913	1.27826	17.30054					

CORRELATION COEFFICIENTS

ROW 1 - $CaCO_3$

1.00000	0.36556	0.10619	-0.05201	0.11459	0.00490	0.14171	0.54015	0.13802	0.05155
0.63243	-0.06181	0.32755	-0.05556	0.49227	-0.17005	0.49111	-0.51013	0.24188	0.25775

ROW 2 - P_2O_5

0.36556	1.00000	0.00943	-0.25305	-0.06267	0.02700	-0.11449	0.07691	-0.05983	-0.00325
0.06850	-0.05834	-0.03523	0.45215	0.54866	-0.26098	0.82458	-0.83068	0.02789	0.00481

ROW 3 - Sn

0.10619	0.00943	1.00000	0.01992	0.16583	0.21627	0.34429	0.13510	0.48441	-0.06869
0.09129	-0.05884	0.45520	0.07698	0.00865	0.29814	-0.03914	0.05130	0.02436	0.02362

ROW 4 - Cu

-0.05201	-0.25305	0.01992	1.00000	0.09910	0.06355	-0.05348	0.10261	-0.31031	0.07954
0.05455	-0.17335	-0.40957	-0.04247	-0.44709	0.23899	-0.35816	0.40747	-0.27693	-0.41884

ROW 5 - Pb

0.11459	-0.06267	0.16583	0.09910	1.00000	0.38255	0.40716	-0.03967	0.26584	0.26106
0.04129	-0.06767	0.03648	0.27586	-0.34422	0.38031	-0.23525	0.25404	-0.06565	-0.15857

ROW 6 - Zn

0.00490	0.02700	0.21627	0.06355	0.38255	1.00000	0.16906	0.03396	0.31340	0.25354
-0.20236	-0.00614	0.29033	0.09029	-0.09200	0.31908	-0.13813	0.08531	0.34436	-0.17832

ROW 7 - Mn

0.14171	-0.11449	0.34420	-0.05348	0.40716	0.16906	1.00000	0.28272	0.50627	0.05258
-0.00628	-0.06768	0.32155	0.13534	-0.108366	0.07621	-0.17212	0.17189	-0.02935	0.07230

ROW 8 - Ni

0.54015	0.07691	0.13510	0.10261	-0.03967	0.03396	0.28272	1.00000	0.24110	-0.05962
0.19656	-0.01042	0.35348	0.00525	0.26646	-0.08238	0.15832	-0.21252	0.24649	0.15939

ROW 9 - Fe

0.13802	-0.05983	0.48441	-0.31031	0.26584	0.31340	0.50627	0.24110	1.00000	-0.04304
0.08589	-0.00238	0.80880	0.03529	0.05425	0.36574	-0.22128	0.10171	0.60244	0.27455

ROW 10 - Co

0.05155	-0.00325	-00.06869	0.07954	0.26106	0.25354	0.05258	0.24110	-0.04304	1.00000
-0.19205	0.01307	-0.12872	0.10526	-0.23403	0.37787	-0.11421	0.12579	-0.12092	-0.32548

ROW 11 - Cd

0.63243	0.06850	0.09129	0.05455	0.04129	-0.20236	-0.00628	0.19656	0.08589	-0.19205
1.00000	-0.17153	0.29196	-0.10468	0.11251	-0.05496	0.10331	-0.10248	0.19077	0.09551

ROW 12 - As

-0.06181	-0.05834	-0.05884	-0.17335	-0.06767	-0.00614	-0.06768	-0.01042	-0.00238	0.01307
-0.17153	1.00000	0.07016	-0.11127	0.08973	-0.15989	-0.02194	0.03431	0.05485	0.27319

ROW 13 - Organic Carbon

0.32755	-0.03523	0.45520	-0.40957	0.03648	0.29033	0.32155	0.35348	0.80880	-0.12872
0.29196	0.07016	1.00000	-0.13949	0.25202	0.20423	-0.06865	-0.06065	0.76024	0.39607

ROW 14 - Ti

-0.05556	0.45215	0.07698	-0.04247	0.27586	0.09029	0.13534	0.00525	0.03529	0.10526
-0.10468	-0.11127	-0.13949	1.00000	0.00960	0.22052	0.24412	-0.22665	-0.16281	-0.29878

ROW 15 - Standard Deviations

0.49227	0.54866	0.00865	-0.44709	-0.34422	-0.09200	-0.10836	0.26646	0.05425	-0.23403
0.11251	0.08973	0.25202	[illegible]	1.00000	-0.56817	0.82802	-0.14423	0.31826	0.49524

ROW 16 - Mean

-0.17005	-0.26098	0.29814	0.23899	0.38031	0.31908	0.07621	-0.02238	0.36574	0.37787
-0.05496	-0.15989	0.20423	0.22052	-0.56817	1.00000	-0.54689	0.08888	0.25052	-0.49524

ROW 17 - % Gravel

0.49111	0.82458	-0.03914	-0.35816	-0.23525	-0.13813	-0.17212	0.15832	-0.22128	-0.11421
0.10331	-0.02194	-0.06865	0.24412	0.82802	-0.54689	1.00000	-0.97494	-0.04933	0.17496

ROW 18 - % Sand

-0.51013	-0.83068	0.05130	0.40747	0.25404	0.08531	0.17189	-0.21252	0.10171	0.12579
-0.10248	0.03431	-0.06065	-0.22665	-0.88772	0.48761	-0.97494	1.00000	-0.14620	-0.23362

ROW 19 - % Clay

0.24188	0.02789	0.02436	-0.27693	-0.06565	0.34436	-0.02935	0.24649	0.60244	-0.12092
0.19077	0.05485	0.76024	-0.16281	0.31286	0.25052	-0.04933	-0.14620	1.00000	0.28096

ROW 20 - Depth

0.25775	0.00481	0.02362	-0.41884	-0.15857	-0.17832	0.07230	0.15939	0.27455	-0.32548
0.09551	0.27319	0.39607	-0.29878	0.49000	-0.49524	0.17496	-0.23362	0.28096	1.00000

Eigen Values

4.30062	3.68093	2.36141	1.74134	1.33898	1.15496	0.94614	0.79670	0.76394	0.74053
0.42424	0.32749	0.30946	0.24033	0.14551	0.10966	0.06308	0.03912	0.01367	0.00186

Cumulative Proportion of Total Variance

0.24003	0.42408	0.54215	0.62922	0.69616	0.75391	0.90122	0.84106	0.87925	0.91628
0.93749	0.95387	0.96934	0.98136	0.98863	0.99411	0.99727	0.99922	0.99991	1.00000

Rotated Factor Matrix

Variable 1

-0.38974	0.11145	-0.03676	0.85738	0.06947	0.08217

Variable 2

-0.89623	-0.03214	0.16336	0.03247	0.00628	0.09658

Variable 3

0.01522	0.32718	0.24034	0.04107	0.59440	-0.09908

Variable 4

0.45399	-0.42524	0.36239	0.27840	-0.08718	0.17599

Variable 5	0.14919	-0.04464	0.09691	0.07211	0.54889	0.51000
Variable 6	0.01414	0.38840	0.02856	-0.07242	0.12698	0.63934
Variable 7	0.11832	0.05754	-0.13621	0.15684	0.84743	0.06855
Variable 8	-0.10891	0.12746	-0.12427	0.67028	0.20736	0.04895
Variable 9	0.08049	0.78100	-0.02727	0.05209	0.51039	0.04279
Variable 10	0.05380	-0.13488	-0.04062	0.00790	-0.03956	0.79010
Variable 11	0.00215	0.12910	0.28959	0.71755	-0.04577	-0.26085
Variable 12	0.02961	0.02867	-0.70655	-0.12307	-0.05915	0.13466
Variable 13	-0.00492	0.88703	-0.10785	0.25369	0.25845	-0.06349
Variable 14	-0.44279	-0.13996	0.40100	-0.26920	0.37722	0.25954
Variable 15	-0.78930	0.22375	-0.28807	0.22831	-0.12180	-0.24389
Variable 16	0.41740	0.34757	0.51432	-0.13871	0.11553	0.49322
Variable 17	-0.95062	-0.12368	-0.05032	0.16455	-0.08718	-0.11338

Variable 18	0.95831	-0.04508	0.05746	-0.17798	0.12693	0.09314
Variable 19	-0.04744	0.89594	-0.05149	0.18532	-0.21328	0.09237
Variable 20	-0.14725	0.29810	-0.64178	0.16914	0.06825	-0.43404

Original and Successive Variances

Cycle No.	Variances
0	0.2789044
1	0.4231086
2	0.4477729
3	0.4506568
4	0.4508491

TABLE 2. GROUP B SEDIMENTS

MEANS										
	38.29082	1573.06122	6.32653	8.72449	10.15306	50.20408	95.00000	20.71429		
	1.85918	9.28571	2.34694	8.95918	0.68980	0.21327	2.52653	4.07959		
	1.00204	69.31837	29.67939	18.32204	11.60224	102.97959				
STANDARD DEVIATIONS										
	10.37724	523.14037	3.35030	4.97709	5.13891	23.76007	36.44345	7.63763		
	0.55035	5.17908	1.49026	10.08290	0.29746	0.08181	0.42464	1.07335		
	1.28314	16.32186	17.01041	10.29862	7.75879	21.19010				
CORRELATION COEFFICIENTS										
ROW 1 - $CaCO_3$										
	1.00000	0.59110	-0.16084	-0.52642	-0.43410	-0.59914	-0.56593	-0.18273	-0.05409	0.09339
	0.33868	0.52957	-0.35611	-0.56309	-0.53127	-0.67725	0.51759	0.59826	-0.61094	-0.47477
	-0.67125	0.62482								
ROW 2 - P_2O_5										
	0.59110	1.00000	-0.09151	-0.29032	-0.30047	-0.10338	0.06338	0.17724	0.64265	0.11443
	-0.10721	0.65045	-0.26003	-0.26421	-0.19609	-0.42653	0.46652	0.31201	-0.33457	-0.32296
	-0.29599	0.47512								
ROW 3 - Sn										
	-0.16084	-0.09151	1.00000	0.11920	0.13922	0.38910	0.15357	-0.07851	0.06952	-0.07933
	-0.05237	-0.15254	0.04209	0.02947	0.06993	0.07431	-0.07334	-0.05322	0.05697	0.06465
	0.02633	-0.12726								
ROW 4 - Cu										
	-0.52642	-0.29032	0.11920	1.00000	0.41506	0.61664	0.49820	0.38755	0.26391	-0.12701
	-0.24104	-0.29270	0.63306	0.49266	0.61025	0.67067	-0.35598	-0.64931	0.64710	0.50858
	0.73031	-0.40520								
ROW 5 - Pb										
	-0.43410	-0.30047	0.13922	0.41506	1.00000	0.43270	0.25864	0.18957	0.02435	-0.00559
	-0.02748	-0.30445	0.33768	0.40636	0.06016	0.52180	-0.42184	-0.49363	0.50523	0.50016
	0.40363	-0.35104								

ROW 6 - Zn										
	-0.59914	-0.10338	0.38910	0.61664	0.43270	1.00000	0.69954	0.48422	0.50411	-0.00091
	-0.24621	-0.20824	0.50583	0.43210	0.48572	0.54014	-0.25900	-0.57557	0.57088	0.48592
	0.58940	-0.51061								
ROW 7 - Mn										
	-0.56593	0.06338	0.15357	0.49820	0.25864	0.69954	1.00000	0.64557	0.69231	0.10348
	-0.41141	-0.12643	0.37841	0.59289	0.60310	0.59438	-0.21875	-0.61888	0.60827	0.48595
	0.65908	-0.26101								
ROW 8 - Ni										
	-0.18273	0.17724	-0.07851	0.38755	0.18957	0.48422	0.64557	1.00000	0.53493	0.09217
	-0.23729	0.06802	0.39667	0.37128	0.50471	0.45417	-0.04373	-0.51559	0.49952	0.40774
	0.55093	0.00975								
ROW 9 - Fe										
	-0.05409	0.64265	0.06952	0.26391	0.02435	0.50411	0.69231	0.53493	1.00000	0.09737
	-0.34435	0.30718	0.18320	0.30332	0.35150	0.14457	0.11931	-0.25527	0.23502	0.14226
	0.32394	0.12301								
ROW 10 - Co										
	0.09339	0.11443	-0.07933	-0.12701	-0.00559	-0.00091	0.10348	0.09217	0.09737	1.00000
	0.12050	0.15801	0.23555	-0.05092	-0.03620	0.01700	0.04098	-0.09855	0.09065	0.20511
	-0.04833	0.06726								
ROW 11 - Cd										
	0.33868	-0.10721	-0.05237	-0.24104	-0.02748	-0.24621	-0.41141	-0.23729	-0.34435	0.12050
	1.00000	0.26370	-0.13213	-0.19488	-0.31607	-0.23383	0.06390	0.27411	-0.26594	-0.19317
	-0.31972	0.08830								
ROW 12 - As										
	0.52957	0.65045	-0.15254	-0.29270	-0.30445	-0.20824	-0.12643	0.06802	0.30718	0.15801
	0.26370	1.00000	-0.36628	-0.33977	-0.26541	-0.49288	0.31948	0.40105	-0.40871	-0.39836
	-0.36344	0.45516								
ROW 13 - Organic Carbon										
	-0.35611	-0.26003	0.04209	0.63306	0.33768	0.50583	0.37841	0.39667	0.18320	0.23555
	-0.13213	-0.36628	1.00000	0.40624	0.55851	0.67130	-0.19830	-0.73906	0.72255	0.73155
	0.67413	-0.31416								

ROW 14 - Ti

-0.56309	-0.26421	0.02947	0.49266	0.40636	0.43210	0.59289	0.37128	0.30332	-0.05092
-0.19488	-0.33977	0.40624	1.00000	9.49818	0.63754	-0.31303	-0.65202	0.64737	0.57846
0.62326	-0.28777								

ROW 15 - Standard Deviations

-0.53127	-0.19609	0.06993	0.61025	0.06016	0.48572	0.60310	0.50471	0.35150	-0.03620
-0.31607	-0.26541	0.55851	0.49818	1.00000	0.61004	-0.11901	-0.63502	0.61932	0.43412
0.77828	-0.24211								

ROW 16 - Mean

-0.67725	-0.42653	0.07431	0.67067	0.52180	0.54014	0.59438	0.45417	0.14457	0.01700
-0.23383	-0.49288	0.67130	0.63754	0.61004	1.00000	-0.65117	-0.95823	0.96724	0.87340
0.92785	-0.49245								

ROW 17 - % Gravel

0.51759	0.46652	-0.07334	-0.35598	-0.42184	-0.25900	-0.21875	-0.04373	0.11931	0.04098
0.06390	0.31948	-0.19830	-0.31303	-0.11901	-0.65117	1.00000	0.52424	-0.57699	-0.51500
-0.49986	0.44602								

ROW 18 - % Sand

0.59826	0.31201	-0.05322	-0.64931	-0.49363	-0.57557	-0.61888	-0.51559	-0.25527	-0.09855
0.27411	0.40105	-0.73906	-0.65202	-0.63502	-0.95823	0.52424	1.00000	-0.99777	-0.94398
-0.91379	0.40818								

ROW 19 - % Clay

-0.61094	-0.33457	0.05697	0.64710	0.50523	0.57088	0.60827	0.49952	0.23502	0.09065
-0.26594	-0.40871	0.72255	0.64737	0.61932	0.96724	-0.57699	-0.99777	1.00000	0.94237
0.91488	-0.42509								

ROW 20 - Depth

-0.47477	-0.32296	0.06465	0.50858	0.50016	0.48592	0.48595	0.40774	0.14226	0.20511
-0.19317	-0.39836	0.73155	0.57846	0.43412	0.87340	-0.51500	-0.94398	0.94237	1.00000
0.73937	-0.36997								

ROW 21

-0.67125	-0.29599	0.02633	0.73031	0.40363	0.58940	0.65908	0.55093	0.32394	-0.04833
-0.31972	-0.36344	0.67413	0.62326	0.77828	0.92785	-0.49986	-0.91379	0.91488	0.73937
1.00000	-0.43022								

ROW 22

0.62482	0.47512	-0.12726	-0.40520	-0.35104	-0.51061	-0.26101	0.00975	0.12301	0.06726
0.08830	0.45516	-0.31416	-0.28777	-0.24211	-0.49245	0.44602	0.40818	-0.42509	-0.36997
-0.43022	1.00000								

Eigen Values

9.79470	3.06427	1.61362	1.24067	1.00237	0.89248	0.80422	0.68065	0.67072	0.48331
0.44634	0.30143	0.26607	0.23249	0.16381	0.12110	0.09967	0.05645	0.05314	0.00962
0.00268	0.00018								

Cumulative Proportion of Total Variance

0.44521	0.58450	0.65785	0.71424	0.75980	0.80037	0.83692	0.86786	0.89835	0.92032
0.94061	0.95431	0.96640	0.97697	0.98422	0.98992	0.99445	0.99702	0.99943	0.99987
0.99999	1.00000								

Rotated Factor Matrix

Variable 1	0.44191	-0.36392	0.16054	-0.30257	-0.43167	0.40459
Variable 2	0.20546	-0.84642	0.10130	-0.06740	-0.27137	-0.08666
Variable 3	0.05103	0.07114	0.02611	0.83553	0.01361	-0.00749
Variable 4	-0.74867	0.07237	-0.22698	0.25515	0.20226	0.00315
Variable 5	-0.22456	0.04134	0.00134	0.22914	0.73136	0.12881
Variable 6	-0.54205	-0.16312	-0.03555	0.66158	0.28273	-0.15424
Variable 7	-0.59444	-0.35964	0.01472	0.29151	0.24519	-0.45725
Variable 8	-0.65397	-0.47686	0.00897	-0.02849	0.07194	-0.11242

Variable 9	-0.34829	-0.79130	0.01240	0.21592	-0.01396	-0.32741
Variable 10	-0.03520	-0.11360	0.91097	0.00001	-0.01416	0.04489
Variable 11	0.17170	0.04125	0.03398	-0.02231	0.01570	0.88557
Variable 12	0.26586	-0.72773	0.01371	-0.12862	-0.16666	0.31633
Variable 13	-0.81556	0.17542	0.32664	0.12607	0.05156	0.08932
Variable 14	-0.58023	-0.00652	-0.12442	0.02843	0.39798	-0.21501
Variable 15	-0.84861	0.05845	-0.13140	0.10790	-0.16147	-0.24652
Variable 16	-0.76565	0.20077	0.05863	0.02415	0.54472	-0.14718
Variable 17	0.17021	-0.26174	0.03093	0.02696	-0.78854	0.07858
Variable 18	0.82158	-0.08863	-0.16701	-0.01191	-0.46990	0.14933
Variable 19	-0.80096	0.10479	0.15685	0.00914	0.50875	-0.14743
Variable 20	-0.68701	0.13656	0.34716	-0.00854	0.51386	-0.07083
Variable 21	-0.86454	0.06413	-0.07267	0.03242	0.35064	-0.20549
Variable 22	0.23895	-0.42865	0.07227	-0.38166	-0.40662	0.11872

TABLE 3. GROUP C SEDIMENTS

MEANS									
	57.35926	2588.39506	5.74074	5.27778	5.80370	26.35802	84.56790	16.91358	
	2.13086	8.48765	3.13580	34.48148	0.17975	0.06790	1.54198	1.54568	
	8.26049	91.24198	3.09198	140.90123					
STANDARD DEVIATIONS									
	21.39756	1512.80159	2.63523	9.06573	5.71149	14.31809	65.17859	6.81533	
	1.23061	3.68016	0.87683	25.13718	0.18185	0.03704	0.49063	0.81915	
	10.47352	10.64632	2.47740	41.53451					
CORRELATION COEFFICIENTS									
ROW 1 - $CaCO_3$									
	1.00000	0.13803	-0.11318	0.05991	0.05649	0.05714	-0.23962	0.18717	0.01251	0.09659
	0.36313	0.05561	0.24744	-0.14433	0.12039	-0.00424	0.25306	-0.28259	0.11936	0.22176
ROW 2 - P_2O_5									
	0.13803	1.00000	0.07116	0.44620	0.06529	0.84646	0.17796	0.56367	0.87578	0.25501
	0.11118	0.40485	0.03893	0.37145	-0.17699	0.23171	-0.21384	0.21794	-0.00883	0.42047
ROW 3 - Sn									
	-0.11318	0.07116	1.00000	-0.03488	-0.02967	0.03926	-0.06179	0.02449	0.05453	-0.01193
	-0.26047	-0.10735	0.13994	0.10578	-0.05819	0.11731	-0.09562	0.10715	0.04831	-0.01303
ROW 4 - Cu									
	0.05991	0.44620	-0.03488	1.00000	-0.00286	0.37503	-0.00508	0.23027	0.16309	0.05958
	0.12100	0.06070	0.03435	-0.01220	-0.04270	0.06307	-0.03566	0.04080	-0.01280	0.17950
ROW 5 - Pb									
	0.05649	0.06529	-0.02967	-0.00286	1.00000	0.04954	0.00949	-0.09572	0.07174	-0.03095
	-0.05951	0.05378	0.01904	0.15414	-0.13049	0.11081	-0.10785	0.12411	0.01691	-0.12904
ROW 6 - Zn									
	0.05714	0.84646	0.03926	0.37503	0.04954	1.00000	0.22332	0.61032	0.77157	0.28262
	0.10958	0.32567	0.11943	0.51458	-0.19683	0.28543	-0.22207	0.22263	0.04017	0.55724

ROW 7 - Mn

-0.23962	0.17796	-0.06179	-0.00508	0.00949	0.22332	1.00000	0.58367	0.42125	0.04935
-0.16300	0.70398	-0.11259	0.05477	-0.08288	-0.15953	-0.12680	0.14889	-0.21105	0.04932

ROW 8 - Ni

0.18717	0.56367	0.02449	0.23027	-0.09572	0.61032	0.58367	1.00000	0.66355	0.27568
0.04487	0.57024	0.12797	0.23771	0.03549	0.01325	-0.02283	0.01886	-0.02075	0.45783

ROW 9 - Fe

0.01251	0.87578	0.05453	0.16309	0.07174	0.77157	0.42125	0.66355	1.00000	0.32301
0.01808	0.64189	0.02478	0.44325	-0.17753	0.17938	-0.29997	0.30078	-0.00782	0.33496

ROW 10 - Co

0.09659	0.25501	-0.01193	0.05958	-0.03095	0.28262	0.04935	0.27568	0.32301	1.00000
0.26781	0.20559	0.04566	-0.00524	0.21906	-0.07735	0.00946	-0.05969	0.08496	0.41648

ROW 11 - Cd

0.36313	0.11118	-0.26047	0.12100	-0.05951	0.10958	-0.16300	0.04487	0.01808	0.26781
1.00000	-0.04837	0.21815	-0.10274	0.23356	-0.17582	0.26833	-0.29173	0.05851	0.25196

ROW 12 - As

0.05561	0.40485	-0.10735	0.06070	0.05378	0.32567	0.70398	0.57024	0.64189	0.20559
-0.04837	1.00000	-0.01840	0.06272	-0.13849	-0.06549	-0.22355	0.23304	-0.11236	0.06580

ROW 13 - Organic Carbon

0.24744	0.03893	0.13994	0.03435	0.01904	0.11943	-0.11259	0.12797	0.02478	0.02566
0.21815	-0.01840	1.00000	0.04428	0.01763	0.13274	0.25622	-0.26443	0.29115	0.12544

ROW 14 - Ti

-0.14433	0.37145	0.10578	-0.01220	0.15414	0.51458	0.05477	0.23771	0.44325	-0.00574
-0.10274	0.06272	0.04428	1.00000	-0.17325	0.39501	-0.30599	0.28236	0.27064	0.31075

ROW 15 - Standard Variations

0.12039	-0.17699	-0.05819	-0.04270	-0.13049	-0.19683	-0.08288	0.03549	-0.17753	0.21906
0.23356	-0.13849	0.01763	-0.17325	1.00000	-0.61070	0.73932	-0.79094	0.04464	0.17938

ROW 16 - Mean

0.00424	0.23171	0.11731	0.06307	0.11081	0.28453	-0.15953	0.01325	0.17938	-0.07735
0.17532	-0.06549	0.13274	0.39501	-0.61070	1.00000	-0.67906	0.62640	0.41678	0.05091

ROW 17 - % Gravel

0.25306	-0.21384	-0.09562	-0.03566	-0.10785	-0.22207	-0.12680	-0.02283	-0.29997	0.00946
0.26833	-0.22355	0.25622	-0.30599	0.73932	-0.67906	1.00000	-0.98251	-0.22020	0.19054

ROW 18 - % Sand

-0.28259	0.21794	0.10715	0.04080	0.12411	0.22263	0.14889	0.01886	0.30078	-0.05969
-0.29173	0.23304	-0.26443	0.28236	-0.79094	0.62640	-0.98251	1.00000	0.11614	-0.23041

ROW 19 - % Clay

0.11936	-0.00883	0.04831	-0.01288	0.01691	0.04017	-0.21105	-0.02075	-0.00782	0.08496
0.05851	-0.11236	0.29115	0.27064	0.04464	0.41678	-0.22020	0.11614	1.00000	0.11251

ROW 20 - Depth

0.22176	0.42047	-0.01303	0.17950	-0.12904	0.55724	0.04932	0.45783	0.33496	0.41648
0.25196	0.06580	0.12544	0.31075	0.17938	0.05091	0.19054	-0.23041	0.11251	1.00000

Eigen Values

4.86320	3.53109	2.23032	1.33326	1.22427	1.11268	1.04233	0.89498	0.78792	0.69449
0.58858	0.48584	0.31073	0.28095	0.21114	0.14899	0.12610	0.09894	0.02674	0.00745

Cumulative Proportion of Total Variance

0.24316	0.41971	0.53123	0.59789	0.65911	0.71474	0.76686	0.81161	0.85100	0.88573
0.91516	0.93945	0.95498	0.96903	0.97959	0.98704	0.99334	0.99829	0.99963	1.00000

Rotated Factor Matrix

Variable 1

-0.13131	0.18509	0.06585	0.47374	0.07235	0.58109

Variable 2

-0.88097	-0.18081	-0.20712	0.03052	-0.10615	0.09284

Variable 3

-0.12590	0.03619	0.10169	-0.70996	0.11061	0.09434

Variable 4

-0.57023	-0.05909	0.21063	0.11711	-0.46879	0.11368

Variable 5	0.04793	-0.23370	-0.06622	-0.01477	-0.10872	0.39563
Variable 6	-0.89621	-0.16780	-0.18652	-0.02083	0.05374	0.04171
Variable 7	-0.06603	-0.01775	-0.87802	-0.10880	-0.10967	-0.11184
Variable 8	-0.59507	0.11235	-0.61855	0.00198	0.08007	0.10298
Variable 9	-0.71510	-0.20709	-0.54000	-0.02096	0.07036	0.00727
Variable 10	-0.35404	0.16622	-0.16171	0.39172	0.37594	-0.28189
Variable 11	-0.19352	0.25277	0.15149	0.67792	0.09917	0.16198
Variable 12	-0.19867	-0.13986	-0.87305	0.13438	-0.05521	0.07804
Variable 13	-0.09992	0.21390	0.03528	-0.09378	0.33535	0.72290
Variable 14	-0.47054	-0.26870	-0.01425	-0.33080	0.40501	-0.04786
Variable 15	0.07241	0.84883	0.04371	0.08977	0.13103	-0.13998
Variable 16	-0.20736	-0.74269	0.21087	-0.11453	0.34020	0.19414
Variable 17	0.07226	0.93944	0.10906	0.05619	-0.12340	0.16026

Variable 18

-0.06170	-0.94274	-0.13022	-0.09228	0.02241	-0.15153

Variable 19

-0.02811	-0.18244	0.19554	0.03687	0.73448	0.21524

Variable 20

-0.68067	0.29159	0.01657	0.13738	0.32845	-0.10766

Original and Successive Variances

Cycle No.	Variances
0	0.2241703
1	0.4078271
2	0.4383346

APPENDIX 5. Q AND R-MODE FACTOR ANALYSIS

APPENDIX 5A. Q-MODE

Klovan (1966) showed that an ideal method for analysing large amounts of data, with a view to sample clustering, is Q-mode factor analysis, which examines sample to sample relations. Factor analysis does not assume a knowledge of the distributions, nor independence of the variables, but in Q-mode the original data must be transformed so that changes in all the variables have equal weighting (Harbaugh & Demiran, 1964). The conceptual reasoning within Q-mode analysis is given in Davis (1973). The principal objective of the technique is to identify the lowest number of factors which explain the maximum population variance. A factor is a mathematical computation (square root of the eigen value times each element in each eigenvector), and is composed of all the variables, graded (factor scores) in terms of their effect on the factor. While the factors need not necessarily represent geological processes, it is hoped that intuitive interpretation of factor-separated groupings will lead to geological deductions.

The effect the factor has on the sample is determined by the factor loadings and the most important variables within each factor are determined by means of the scaled factor scores.

APPENDIX 5B. R-MODE

The mathematical reasoning underly the R-mode factor analysis is given in Davis (1973). Means, standard deviations, correlation coefficients, and a varimax rotated factor matrix (Appendix 3) for a nominated number of factors are computed, from which the factor loadings may be used to determine the relative importance of variables within the factor. Each factor may represent a geological process, and the absolute size of the loadings in each factor for each variable reflects the degree to which each variable is controlled by that factor. In conjunction with the correlation matrix, the rotated factor matrix can be used to unravel the inter-relations between the variables measured in each sample.